RADIOLOGY AND ONCOLOGY

vol.52 no.4
december 2018

NOVO

CABOMETYX®
(kabozantinib) tablete
60 mg | 40 mg | 20 mg

- PFS[2]
- OS[2]
- ORR[2]

CABOMETYX® pomembno izboljša PFS, OS in ORR v drugi liniji zdravljenja napredovalega karcinoma ledvičnih celic[1]

RAZŠIRITEV INDIKACIJE:

Sedaj tudi za zdravljenje napredovalega karcinoma ledvičnih celic (KLC) pri predhodno nezdravljnenih odraslih bolnikih s srednje ugodnim ali slabim prognostičnim obetom.[2]

ORR: objektivna stopnja odziva; OS: celokupno preživetje; PFS: preživetje brez napredovanja bolezni

Referenci:
1. Choueiri TK, Escudier B, Powles T, *et al*. Cabozantinib versus everolimus in advanced renal cell carcinoma (METEOR): final results from a randomised, open-label, phase 3 trial. The Lancet Oncology. 2016;17(7):917-27.
2. Povzetek glavnih značilnosti zdravila Cabometyx.

Skrajšan povzetek glavnih značilnosti zdravila

CABOMETYX 20 mg filmsko obložene tablete
CABOMETYX 40 mg filmsko obložene tablete
CABOMETYX 60 mg filmsko obložene tablete
(kabozantinib)

TERAPEVTSKE INDIKACIJE Zdravljenje napredovalega karcinoma ledvičnih celic (KLC) pri predhodno nezdravljenih odraslih bolnikih s srednje ugodnim ali slabim prognostičnim obetom ter pri odraslih bolnikih po predhodnem zdravljenju, usmerjenem v vaskularni endotelijski rastni faktor (VEGF). **ODMERJANJE IN NAČIN UPORABE** Priporočeni odmerek je 60 mg enkrat na dan. Zdravljenje je treba nadaljevati tako dolgo, dokler bolnik več nima kliničnih koristi od terapije ali do pojava nesprejemljive toksičnosti. Pri sumu na neželene reakcije na zdravilo bo morda treba zdravljenje začasno prekiniti in/ali zmanjšati odmerek. Če je treba odmerek zmanjšati, se priporoča zmanjšanje na 40 mg na dan in nato na 20 mg na dan. Prekinitev odmerka se priporoča pri obravnavi toksičnosti 3. ali višje stopnje po CTCAE (*common terminology criteria for adverse events*) ali nevzdržni toksičnosti 2. stopnje. Zmanjšanje odmerka se priporoča za dogodke, ki bi lahko čez čas postali resni ali nevzdržni. V primeru pojava neželenih učinkov 1. in 2. stopnje, ki jih bolnik prenaša in jih je možno enostavno obravnavati, prilagoditev odmerjanja običajno ni potrebna. Treba je razmisliti o dodatni podporni oskrbi. V primeru pojava neželenih učinkov 2. stopnje, ki jih bolnik ne prenaša in jih ni mogoče obravnavati z zmanjšanjem odmerka ali podporno oskrbo, je treba zdravljenje prekiniti, dokler neželeni učinki ne izzvenijo do ≤ 1. stopnje, uvesti podporno oskrbo in razmisliti o ponovni uvedbi zdravljenja z zmanjšanim odmerkom. V primeru pojava neželenih učinkov 3. stopnje je treba zdravljenje prekiniti, dokler neželeni učinki ne izzvenijo do ≤ 1. stopnje, uvesti podporno oskrbo in ponovno uvesti zdravljenje z zmanjšanim odmerkom. V primeru pojava neželenih učinkov 4. stopnje je treba zdravljenje prekiniti, uvesti ustrezno zdravniško oskrbo, in če neželeni učinki izzvenijo do ≤ 1. stopnje, ponovno uvesti zdravljenje z zmanjšanim odmerkom. Če neželeni učinki ne izzvenijo, je treba trajno prenehati z uporabo zdravila. Pri bolnikih z blago ali zmerno ledvično okvaro je treba kabozantinib uporabljati previdno. Uporaba se ne priporoča pri bolnikih s hudo ledvično okvaro. Pri bolnikih z blago ali zmerno jetrno okvaro je priporočeni odmerek kabozantiniba 40 mg enkrat na dan. Pri teh bolnikih je treba spremljati neželene dogodke in po potrebi razmisliti o prilagoditvi odmerka ali prekinitvi dajanja. Uporaba se ne priporoča pri bolnikih s hudo jetrno okvaro. Način uporabe: Tablete je treba pogoltniti cele in jih ni dovoljeno drobiti. Bolnikom je treba naročiti, naj vsaj 2 uri pred uporabo zdravila in 1 uro po tem ničesar ne jedo. **KONTRAINDIKACIJE** Preobčutljivost na učinkovino ali katero koli pomožno snov. **POSEBNA OPOZORILA IN PREVIDNOSTNI UKREPI** Večina dogodkov se lahko pojavi zgodaj v teku zdravljenja, zato mora zdravnik bolnika v prvih 8 tednih zdravljenja skrbno spremljati, da oceni, ali je treba odmerek prilagoditi. Dogodki, ki se običajno pojavijo zgodaj, vključujejo hipokalciemijo, hipokaliemijo, trombocitopenijo, hipertenzijo, sindrom palmarno-plantarne eritrodisestezije (PPES), proteinurijo in gastrointestinalne dogodke (bolečine v trebuhu, vnetje sluznice, zaprtje, driska, bruhanje). Bolnike, ki imajo vnetno bolezen črevesja (npr. Crohnovo bolezen, ulcerozni kolitis, peritonitis, divertikulitis ali apendicitis), ki imajo tumorsko infiltracijo prebavil ali so imeli pred posegom na prebavilih zaplete (zlasti v povezavi z zapoznelim ali nepopolnim celjenjem), je treba pred uvedbo zdravljenja skrbno oceniti, nato pa natančno spremljati za pojav simptomov perforacij in fistul, vključno z abscesi in sepso. Trajna ali ponavljajoča se driska med zdravljenjem je lahko dejavnik tveganja za nastanek analne fistule. Uporabo kabozantiniba je treba pri bolnikih, pri katerih se pojavi gastrointestinalna perforacija ali fistula, ki je ni možno ustrezno obravnavati, prekiniti. Kabozantinib je treba uporabljati previdno pri bolnikih, pri katerih obstaja tveganje za pojav venske trombembolije, vključno s pljučno embolijo, in arterijske trombembolije ali imajo te dogodke v anamnezi. Z uporabo je treba prenehati pri bolnikih, pri katerih se razvije akutni miokardni infarkt ali drugi klinično pomembni znaki zapletov arterijske trombembolije. Kabozantiniba se ne sme dajati bolnikom, ki hudo krvavijo, ali pri katerih obstaja tveganje za hudo krvavitev. Zdravljenje s kabozantinibom je treba ustaviti vsaj 28 dni pred načrtovanim kirurškim posegom, vključno z zobozdravstvenim, če je mogoče. Kabozantinib je treba ukiniti pri bolnikih z zapleti s celjenjem rane, zaradi katerih je potrebna zdravniška pomoč. Pred uvedbo kabozantiniba je treba dobro obvladati krvni tlak. Med zdravljenjem je treba vse bolnike spremljati za pojav hipertenzije in jih po potrebi zdraviti s standardnimi antihipertenzivi. V primeru trdovratne hipertenzije, kljub uporabi antihipertenzivov, je treba odmerek kabozantiniba zmanjšati. Z uporabo je treba prenehati, če je hipertenzija resna ali trdovratna kljub zdravljenju z antihipertenzivi in zmanjšanemu odmerku kabozantiniba. V primeru hipertenzijske krize je treba zdravljenje prekiniti. Pri resni PPES je treba razmisliti o prekinitvi zdravljenja. Nadaljevanje zdravljenja naj se začne z nižjim odmerkom, ko se PPES umiri do 1. stopnje. V času zdravljenja je treba redno spremljati beljakovine v urinu. Pri bolnikih, pri katerih se razvije nefrotični sindrom, je treba z uporabo kabozantiniba prenehati. Pri uporabi kabozantiniba so opazili sindrom reverzibilne posteriorne levkoencefalopatije (RPLS), znan tudi kot sindrom posteriorne reverzibilne encefalopatije (PRES). Na ta sindrom je treba pomisliti pri vseh bolnikih s številnimi prisotnimi simptomi, vključno z epileptičnimi napadi, glavobolom, motnjami vida, zmedenostjo ali spremenjenim mentalnim delovanjem. Pri bolnikih z RPLS je treba zdravljenje prekiniti. Kabozantinib je treba uporabljati previdno pri bolnikih s podaljšanjem intervala QT v anamnezi, pri bolnikih, ki jemljejo antiaritmike, in pri bolnikih z relevantno obstoječo boleznijo srca, bradikardijo ali elektrolitskimi motnjami. Bolniki z redko dedno intoleranco za galaktozo, laponsko obliko zmanjšane aktivnosti laktaze ali malabsorpcijo glukoze/galaktoze ne smejo jemati tega zdravila. Plodnost, nosečnost in dojenje: Ženskam v rodni dobi je treba svetovati, da v času zdravljenja s kabozantinibom ne smejo zanositi. Zanositev morajo preprečiti tudi ženske partnerice moških bolnikov, ki uporabljajo kabozantinib. Med zdravljenjem in še vsaj 4 mesece po končanju terapije morajo tako bolniki in bolnice kot tudi njihovi partnerji uporabljati zanesljiv način kontracepcije. Kabozantiniba se ne sme uporabljati med nosečnostjo, razen če zdravljenje ni nujno potrebno zaradi kliničnega stanja ženske. Matere med zdravljenjem s kabozantinibom in še 4 mesece po končanju terapije ne smejo dojiti. Zdravljenje s kabozantinibom lahko predstavlja tveganje za plodnost pri moških in ženskah. **INTERAKCIJE** Kabozantinib je substrat za CYP3A4. Pri sočasni uporabi močnih zaviralcev CYP3A4 (npr. ritonavirja, itrakonazola, eritromicina, klaritromicina, soka grenivke) je potrebna previdnost. Kronični sočasni uporabi močnih induktorjev CYP3A4 (npr. fenitoina, karbamazepina, rifampicina, fenobarbitala ali pripravkov zeliščnega izvora iz šentjanževke) se je treba izogibati. Razmisliti je treba o sočasni uporabi alternativnih zdravil, ki CYP3A4 ne inducirajo in ne zavirajo ali pa inducirajo in zavirajo le neznatno. Pri sočasni uporabi zaviralcev MRP2 (npr. ciklosporin, efavirenz, emtricitabin) je potrebna previdnost, saj lahko povzročijo povečanje koncentracij kabozantiniba v plazmi. Učinka kabozantiniba na farmakokinetiko kontraceptivnih steroidov niso preučili, vendar pa se priporoča dodatna kontracepcijska metoda (pregradna metoda). Zaradi visoke stopnje vezave kabozantiniba na plazemske beljakovine je možna interakcija z varfarinom v obliki izpodrivanja s plazemskih beljakovin, zato je treba spremljati vrednosti INR. Kabozantinib morda lahko poveča koncentracije sočasno uporabljenih substratov P-gp v plazmi. Osebe je treba opozoriti na uporabo substratov P-gp (npr. feksofenadina, aliskirena, ambrisentana, dabigatran eteksilata, digoksina, kolhicina, maraviroka, posakonazola, ranolazina, saksagliptina, sitagliptina, talinolola, tolvaptana) sočasno s kabozantinibom. **NEŽELENI UČINKI** Za popolno informacijo o neželenih učinkih, prosimo, preberite celoten povzetek glavnih značilnosti zdravila Cabometyx. Najpogostejši resni neželeni učinki zdravila so hipertenzija, driska, PPES, pljučna embolija, utrujenost in hipomagneziemija. Najpogostejši neželeni učinki katere koli stopnje (ki so se pojavili pri vsaj 25 % bolnikov) so bili driska, hipertenzija, utrujenost, zvišanje vrednosti AST, zvišanje vrednosti ALT, navzea, zmanjšanje apetita, PPES, disgevzija, zmanjšanje števila trombocitov, stomatitis, anemija, bruhanje, zmanjšanje telesne mase, dispepsija in konstipacija. O hipertenziji so pogosteje poročali pri predhodno nezdravljeni populaciji bolnikov s KLC (67 %), v primerjavi z bolniki s KLC po predhodnem zdravljenju, usmerjenem v VEGF (37 %). *Zelo pogosti (≥ 1/10):* anemija, limfopenija, nevtropenija, trombocitopenija, hipotiroidizem, dehidracija, zmanjšan apetit, hiperglikemija, hipoglikemija, hipofosfatemija, hipoalbuminemija, hipomagneziemija, hiponatriemija, hipokaliemija, hiperkaliemija, hipokalciemija, hiperbilirubinemija, periferna senzorična nevropatija, disgevzija, glavobol, omotica, hipertenzija, disfonija, dispneja, kašelj, driska, navzea, bruhanje, stomatitis, konstipacija, bolečine v trebuhu, dispepsija, bolečina v ustih, suha usta, PPES, akneiformni dermatitis, izpuščaj, makulopapulozni izpuščaj, suha koža, alopecija, sprememba barve las oz. dlak, bolečine v okončinah, mišični spazmi, artralgija, proteinurija, utrujenost, vnetje sluznice, astenija, zmanjšanje telesne mase, zvišanje vrednosti ALT, AST in ALP v serumu, zvišanje vrednosti bilirubina v krvi, zvišanje vrednosti kreatinina, zvišanje vrednosti triglyceridov, zmanjšanje števila belih krvnih celic, povečana vrednost GGT, povečana vrednost amilaze, povečana vrednost holesterola v krvi, povečana vrednost lipaze. *Pogosti (≥ 1/100, < 1/10):* absces, tinitus, venska tromboza, arterijska tromboza, pljučna embolija, pankreatitis, bolečina zgornjega dela trebuha, gastroezofagealna refluksna bolezen, hemoroidi, pruritus, periferni edem, zapleti z ranami. *Občasni (≥ 1/1.000, < 1/100):* konvulzije, analna fistula, holestatični hepatitis, osteonekroza čeljusti. *Neznana pogostnost (ni mogoče oceniti iz razpoložljivih podatkov):* možganska kap, miokardni infarkt. **Vrsta ovojnine in vsebina:** Plastenka vsebuje 30 filmsko obloženih tablet. **Režim izdaje:** Rp/Spec. **Imetnik dovoljenja za promet z zdravilom:** Ipsen Pharma, 65 quai Georges Gorse, 92100 Boulogne-Billancourt, Francija **Pred predpisovanjem, prosimo, preberite celoten povzetek glavnih značilnosti zdravila!**
CAB-082018

▼Za to zdravilo se izvaja dodatno spremljanje varnosti. Tako bodo hitreje na voljo nove informacije o njegovi varnosti. Zdravstvene delavce naprošamo, da poročajo o katerem koli domnevnem neželenem učinku zdravila.

IPSEN
Innovation for patient care

SAMO ZA STROKOVNO JAVNOST

CAB1018-07, oktober 2018

PharmaSwiss
Choose More Life

Odgovoren za trženje v Sloveniji:
PharmaSwiss d.o.o., Brodišče 32, 1236 Trzin
telefon: +386 1 236 47 00, faks: +386 1 283 38 10

RADIOLOGY AND ONCOLOGY

December 2018
Vol. 52 No. 4
Pages 233-352
ISSN 1318-2099
UDC 616-006
CODEN: RONCEM

Publisher
Association of Radiology and Oncology

Affiliated with
Slovenian Medical Association – Slovenian Association of Radiology, Nuclear Medicine Society,
Slovenian Society for Radiotherapy and Oncology, and Slovenian Cancer Society
Croatian Medical Association – Croatian Society of Radiology
Societas Radiologorum Hungarorum
Friuli-Venezia Giulia regional groups of S.I.R.M.
Italian Society of Medical Radiology

Aims and scope
Radiology and Oncology is a journal devoted to publication of original contributions in diagnostic and interventional radiology, computerized tomography, ultrasound, magnetic resonance, nuclear medicine, radiotherapy, clinical and experimental oncology, radiobiology, radiophysics and radiation protection.

Editorial office

Radiology and Oncology
Zaloška cesta 2
P. O. Box 2217
SI-1000 Ljubljana
Slovenia
Phone: +386 1 5879 369
Phone/Fax: +386 1 5879 434
E-mail: gsersa@onko-i.si

Reader for English
Vida Kološa

Secretary
Mira Klemenčič
Zvezdana Vukmirović

Design
Monika Fink-Serša, Samo Rovan, Ivana Ljubanović

Layout
Matjaž Lužar

Printed by
Tiskarna Ozimek, Slovenia

Published quarterly in 400 copies

Beneficiary name: DRUŠTVO RADIOLOGIJE IN ONKOLOGIJE
Zaloška cesta 2
1000 Ljubljana
Slovenia

Beneficiary bank account number: SI56 02010-0090006751
IBAN: SI56 0201 0009 0006 751
Our bank name: Nova Ljubljanska banka, d.d.,
Ljubljana, Trg republike 2,
1520 Ljubljana; Slovenia

SWIFT: LJBASI2X

Subscription fee for institutions EUR 100, individuals EUR 50

The publication of this journal is subsidized by the Slovenian Research Agency.

Indexed and abstracted by:

- *Baidu Scholar*
- *Case*
- *Chemical Abstracts Service (CAS) - CAplus*
- *Chemical Abstracts Service (CAS) - SciFinder*
- *CNKI Scholar (China National Knowledge Infrastructure)*
- *CNPIEC*
- *Dimensions*
- *DOAJ (Directory of Open Access Journals)*
- *EBSCO (relevant databases)*
- *EBSCO Discovery Service*
- *Embase*
- *Genamics JournalSeek*
- *Google Scholar*
- *Japan Science and Technology Agency (JST)*
- *J-Gate*
- *Journal Citation Reports/Science Edition*
- *JournalGuide*
- *JournalTOCs*
- *KESLI-NDSL (Korean National Discovery for Science Leaders)*
- *Medline*
- *Meta*
- *Microsoft Academic*
- *Naviga (Softweco)*
- *Primo Central (ExLibris)*
- *ProQuest (relevant databases)*
- *Publons*
- *PubMed*
- *PubMed Central*
- *PubsHub*
- *ReadCube*
- *Reaxys*
- *SCImago (SJR)*
- *SCOPUS*
- *Sherpa/RoMEO*
- *Summon (Serials Solutions/ProQuest)*
- *TDNet*
- *Ulrich's Periodicals Directory/ulrichsweb*
- *WanFang Data*
- *Web of Science - Science Citation Index Expanded*
- *WorldCat (OCLC)*

This journal is printed on acid- free paper

On the web: ISSN 1581-3207
https://content.sciendo.com/raon
http://www.radioloncol.com

contents

review

State of the art in magnetic resonance imaging of hepatocellular carcinoma

Natally Horvat[1,2,3], Serena Monti[4], Brunna Clemente Oliveira[2,3], Camila Carlos Tavares Rocha[3], Romina Grazia Giancipoli[5], Lorenzo Mannelli[1]

[1] Department of Radiology, Memorial Sloan Kettering Cancer Center, New York, USA
[2] Department of Radiology, Hospital Sírio-Libanês, São Paulo, Brazil
[3] Department of Radiology, Hospital das Clínicas da Faculdade de Medicina da Universidade de São Paulo, Dr. Enéas de Carvalho Aguiar, São Paulo, Brazil
[4] IRCCS SDN, Naples, Italy
[5] Department of Nuclear Medicine, Sapienza University of Rome, Roma, Itália

Radiol Oncol 2018; 52(4): 353-364.

Received 2 October 2018
Accepted 19 October 2018

Correspondence to: Lorenzo Mannelli, M.D., Ph.D., Department of Radiology, Memorial Sloan Kettering Cancer Center. 300 East 66th Street, New York, NY, 10021, USA. Phone: +1 646-888-541; Fax: +1 929-321-5013; E-mail: mannellilorenzo@yahoo.it

Disclosure: No potential conflicts of interest were disclosed.

Background. Liver cancer is the sixth most common cancer worldwide and the second leading cause of cancer mortality. Chronic liver disease caused by viral infection, alcohol abuse, or other factors can lead to cirrhosis. Cirrhosis is the most important clinical risk factor for hepatocellular carcinoma (HCC) whereby the normal hepatic architecture is replaced by fibrous septa and a spectrum of nodules ranging from benign regenerative nodules to HCC, each one of them with different imaging features.

Multiple studies have demonstrated that magnetic resonance imaging (MRI) has excellent sensitivity and specificity for the detection and characterization of HCC in comparison with computed tomography (CT) and ultrasound. Beyond the standard protocol, the use of hepatobiliary contrast agents and the acquisition of additional sequences such as diffusion weighted imaging (DWI) with apparent diffusion coefficient mapping, subtraction imaging, multiplanar acquisition, and hepatobiliary phase, have been proposed to improve the detection of HCC, especially in the case of small, well-differentiated, and post-treatment HCC.

Conclusions. Furthermore, advanced techniques including the quantification of hepatic and intralesional fat and iron, magnetic resonance elastography, radiomics, radiogenomics, and positron emission tomography (PET)-MRI are highly promising for the extraction of new imaging biomarkers that reflect the tumor microenvironment and, in the future, may add decision-making value in the management of patients with HCC.

Key words: hepatocellular carcinoma; hepatic nodule; liver; cirrhosis; magnetic resonance imaging.

Introduction

Liver cancer is the sixth most common cancer worldwide and the second leading cause of cancer mortality.[1,2] In the United States, approximately 42220 new cases of liver cancer will be diagnosed and 30200 deaths will occur in 2018.[3] The incidence in men is three times higher than in women. Over a third of liver cancer consists of hepatocellular carcinoma (HCC). In recent years, five-year survival rates of HCC have considerably improved due to earlier detection and curative therapies.[4] However, the incidence is still rising in women while it has reached a plateau in men since 2010.[3]

The two most common risk factors of HCC are chronic infection from hepatitis B and/or hepatitis C virus and alcohol abuse.[3] Other important risk factors include consumption of aflatoxin (toxin

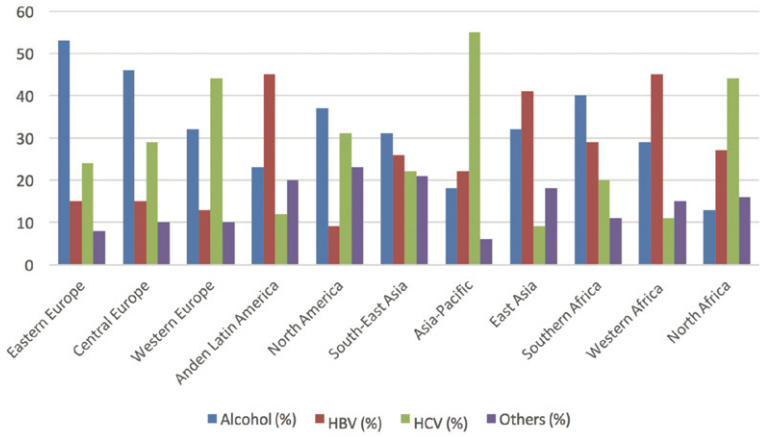

FIGURE 1. Geographical distribution of main risk factors for hepatocellular carcinoma (HCC) worldwide.

produced by a fungus that can infects grains, soybeans and peanuts) which occurs mainly in less developed countries and nonalcoholic fatty liver disease which occurs mainly in Western countries.[2] Figure 1 demonstrates the geographical distribution of the main risk factors for HCC worldwide.

Chronic liver disease caused by viral infection, alcohol abuse, or other factors can lead to cirrhosis. Cirrhosis is the most important clinical risk factor for HCC whereby the normal hepatic architecture is replaced by fibrous septa and a spectrum of nodules ranging from benign regenerative nodules to HCC.[5] The cirrhotic liver gives way to HCC via hepatocarcinogenesis, an anaplastic complex process characterized by stepwise accumulation of epigenetic and genetic alterations at the molecular and cellular level[6,7] and changes in the hepatic architecture seen at the histologic level. While initially hepatocarcinogenesis involves the replacement of normal hepatic architecture with regenerative nodules, this subsequently progresses to replacement with dysplastic nodules and then HCC. HCC itself progresses from well-differentiated to poorly differentiated HCC.[6]

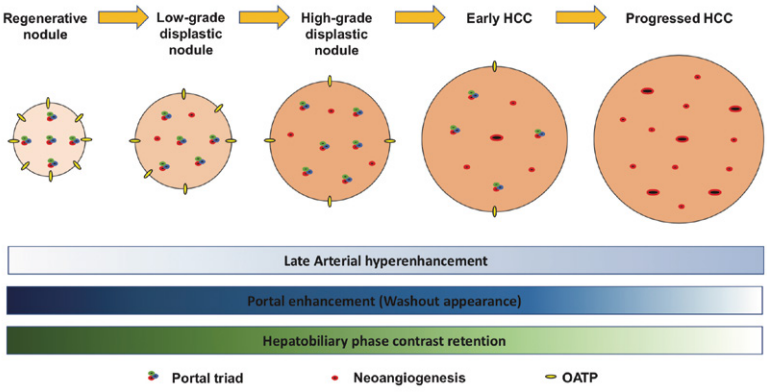

FIGURE 2. Graphic demonstrating hepatocarcinogenesis from regenerative nodules to progressed hepatocellular carcinoma (HCC), emphasizing the proportion of portal triad, neoangiogenesis, and organic anionic transporting polypeptides, and, consequently, the pattern of enhancement on late arterial, portal, and hepatobiliary phases.

The liver has a dual blood supply, *i.e.*, the hepatic portal vein and the hepatic artery. In the normal liver, approximately 75% of the liver is supplied by the hepatic portal vein. However, during hepatocarcinogenesis, neoangiogenesis decreases the portal blood supply and increases the arterial supply relative to the degree of malignancy within the nodules. This allows lesions to be detected on imaging. Emerging evidence also suggests that in hepatocarcinogenesis, the expression levels of organic anionic transporting polypeptides (OATP), a bile salt transporter protein on hepatocytes membranes, diminishes even before neoangiogenesis, which may have implications for earlier radiological detection of lesions using hepatobiliary agents (Figure 2).[7]

Magnetic resonance imaging

Magnetic resonance imaging (MRI) has rapidly evolved as a superior imaging technique in the oncologic field in the past few decades, having undergone improvements in its acquisition time and imaging quality. Multiple studies have demonstrated that MRI has excellent sensitivity and specificity for the detection and characterization of HCC compared with computed tomography (CT) and ultrasound.[8-11] However, mainly because of its high cost and limited availability especially in underdeveloped countries which bear a disproportionately high risk of HCC, its large-scale use for HCC screening is still restricted. Table 1 summarizes the main indications of MRI for HCC as recommended by the European Association (EASL) and American Association for the Study od Liver Diseases (AASLD) guidelines. [9,12]

MRI protocol

Standardized MRI protocols for HCC surveillance must be developed to allow clinicians and technologists to perform repeatable and reproducible high-quality examinations.[11] The minimum magnetic field strength of 1.5 Tesla (T) provides acceptable temporal, spatial, and contrast resolution that enable adequate assessment of hepatic lesions.[12]

The following sequences are essential for the diagnosis of HCC: T2-weighted imaging (WI); unenhanced T1WI opposed and in-phase; and multiphase T1WI (pre-contrast, late arterial, portal venous, and delayed or transitional phases). Slice thickness should be 5 mm or less for dynamic series and 8 mm or less for other imaging.[13,14]

Other sequences have been proposed to improve the detection of HCC, especially in cases of well-differentiated HCC or HCC post-treatment. These include diffusion weighted imaging (DWI) with apparent diffusion coefficient mapping, subtraction imaging, multi-planar acquisition, and hepatobiliary phase.[14,15] Table 2 summarizes these MRI sequences.

DWI improves the characterization of liver nodules without requiring contrast media injection.[15,17] Currently, DWI is used to increase the sensitivity of other sequences for the detection and characterization of HCC. Studies investigating the utility of DWI have demonstrated promising results for assessing prognosis, predicting response, distinguishing tumor from treatment effect, and monitoring response to therapy in patients with HCC.[18-22]

TABLE 1. Main indications of MRI for hepatocellular carcinoma (HCC)

Main indications of MRI for HCC evaluation
Nodules larger than 1.0 cm identified on ultrasound
For patients on the orthotopic liver transplantation waiting list
When the imaging features of the nodule on CT are not elucidative
History of allergy to iodinated contrast agent used on CT scans
After locoregional therapy

Contrast media agents

Dynamic contrast-enhanced sequences are routinely performed with gadolinium-based extracellular contrast agents (ECA) or hepatobiliary contrast agents (HBA). They allow the diagnosis of HCC by exploiting the physiologic changes in blood flow that accompany hepatocarcinogenesis. Following administration of the contrast agent, the dual vascular supply of the liver is opacified in the following sequential order: the hepatic arteries, the portal veins, and finally the hepatic veins.[7,14]

Typically, contrast agents are administered at rates of 2 mL/sec followed by saline infusion. The dose is usually based on body weight (ranging from 0.025 to 0.1 mmol gadolinium per kg) as well as on the agent and other factors.[7]

ECAs include gadoterate meglumine (Gd-DOTA) and gadopentate dimeglumine (Gd-DTPA) which are excreted primarily through glomerular filtration. The pattern of contrast enhancement can be studied in dynamic T1WI in the following phases: late arterial, portal venous, and delayed phases. HBAs include gadoxetate disodium (Gd-EOB-DTPA) and gadobenate dimeglumine (Gd-BOPTA) which are excreted through glomerular filtration but are also taken up by hepatocytes and excreted into the biliary system. As such, HBAs provide additional information regarding the presence of hepatocytes with OATP, which decrease in hepatocarcinogenesis.[23] With HBA administration,

TABLE 2. MRI sequences and hepatocellular carcinoma (HCC) features that can be assessed in each sequence

MRI sequences	HCC imaging features
T2WI	Usually hyperintense
T1WI opposed and in-phase	Intralesional microscopic fat (lower signal on opposed-phase) or iron (lower signal on in-phase)
T1WI with fat saturation pre-contrast	Demonstrates the presence of macroscopic fat and blood products After locoregional therapies, hyperintensity indicates coagulative necrosis
Dynamic late arterial phase	Hyperenhancement
Dynamic portal venous phase	Washout and capsule appearance
Dynamic delayed phase	Washout and capsule appearance
Diffusion weighted imaging	Restricted diffusion (helps to identify small lesions)
Subtraction imaging	Characterizes contrast enhancement in spontaneously hyperintense nodules on T1WI pre-contrast (especially important for lesions with blood products and after locoregional treatment)
Multi-planar acquisition	Helps to differentiate HCC from mass-like lesions or extra-hepatic lesions
Hepatobiliary phase	Generally hypointense

T1W1 = T1 weighted image; T2WI = T2 weighted image

the pattern of contrast enhancement can be studied in the late arterial, portal venous, transitional, and hepatobiliary phases.

Recently, in Europe, the use of intravenous linear agents such as gadodiamide and intravenous gadopentate dimeglumine have been suspended or restricted in response to the retention of gadolinium in the brain and in other tissues as reported in a scientific review. [24] However, there is still no evidence that this deposition causes any harm to patients. Hepatobiliary linear contrast agents continue to be available as their properties allow the recognition of poorly vascularized hepatic lesions which cannot be studied with other agents. The macrocyclic agents (gadobutrol, gadoteric acid, and gadoteridol) have a lower propensity to release gadolinium than linear agents and can continue to be used in their current indications.[24]

Advanced techniques

Quantification of fat and iron

Liver biopsy is the gold standard for quantifying iron and fat in the liver. However, this method is invasive and susceptible to sampling variability. MRI is a non-invasive, alternative method to quantify iron and fat within the liver. There are several sequences that can be used to quantify iron and fat within the liver. Regarding iron, the following techniques can be employed: signal intensity ratio techniques based on T2WI or T2*WI, quantitative relaxometry (based mainly on T2WI but also on T1WI), and MR susceptometry.[25-26] In regards to fat, post-processing of T1WI in- and opposed-phase provides quantification from a scale of 0–50% while the proton density fat fraction allows quantification of a full fat fraction from 0–100%.[27] Iron and fat content may contribute to differential diagnosis and may be a potential prognostic biomarker of HCC.[28] However, the evidence is still limited and this method is not used in the daily practice.

Magnetic resonance elastography

Magnetic Resonance Elastography (MRE) is an imaging modality used to stage liver fibrosis.[29,30] Recent studies have demonstrated the use of MRE for the evaluation of HCC with promising results for the prediction of tumor grade[31] and assessment of treatment response.[32] Well/moderately differentiated tumors demonstrated increased stiffness compared to poorly differentiated ones and there was a correlation between the percentage of tumor necrosis and tumor stiffness, particularly in HCCs treated with radioembolization.[31] However, the evidence is still limited and MRE is not yet routinely implemented.

Imaging features on MRI

Regenerative nodules

Regenerative nodules correspond to an area of parenchyma surrounded by fibrosis. These nodules are usually similar to background liver parenchyma but some may exhibit a fine area of peripheral late-phase enhancement corresponding to fibrosis. Regenerative nodules may present accumulation of iron which results in low signal intensity on T1- and T2-weighted imaging.[6,32]

Dysplastic nodules

Dysplastic nodules contain atypical cells but without malignancy on histological analysis. The radiological pattern of dysplastic nodules is variable and can be similar to regenerative nodules (in those with low-grade dysplasia) or well-differentiated HCC (in those with high-grade dysplasia).[33-35] These lesions often present as iso- or hypointense on T2-weighted imaging and are frequently hypovascular. Occasionally, a mildly elevated signal intensity may occur within a low signal-intensity nodule on T2-weighted imaging. This represents foci of HCC (the foci of high signal intensity) within a dysplastic nodule (the area with low signal intensity). The foci of HCC may also enhance in the arterial phase.[35]

HCC

HCC has a wide spectrum of radiological characteristics depending on its size and degree of histological differentiation. HCC can be classified as early or progressed HCC.

Early HCC often measures less than 2.0 cm and sometimes appears similar to high-grade dysplastic nodules on imaging. Histologically, it differs from dysplastic nodules because of stromal invasion. Radiologically, it has higher T2WI signal intensity, hypo- or iso- vascularization in the arterial phase, and washout appearance in the delayed phase.[7] Mild restricted diffusion has improved the sensitivity for HCC detection, mostly for small HCC, especially well-differentiated HCC with atypical postcontrast imaging patterns.[36]

Progressed HCCs are malignant lesions with the ability to invade vascular planes and metastasize. The radiological pattern is variable, but frequently a mosaic pattern is exhibited due to nodular areas' being interspersed by areas of hemorrhage, arteriovenous shunting, fibrosis, and necrosis. The main findings are: high signal intensity on T2-weighted imaging (Figures 3–4), hyperenhancement on arterial phase (Figures 3–7), washout appearance on delayed phase (Figures 3–5), and nodules that are surrounded by a capsule / pseudocapsule (more evident in the delayed phase) (Figure 3).

HCC may also be classified according to its growth patterns / macroscopic appearance into: single nodular type, well-defined, encapsulated with better prognosis; or multifocal type (multiple nodules in several hepatic segments), with a diffuse pattern, usually extensive, heterogeneous, with variable enhancement, usually better detected in the delayed phase (hypoenhancement), and often associated with vascular invasion (Figure 4).[35-37] Table 3 summarizes the main imaging features of HCC.

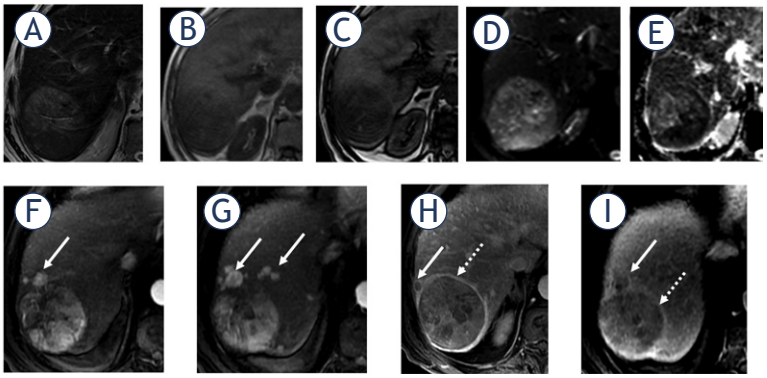

FIGURE 3. 53-year-old man with cirrhosis due to hepatitis B and hepatocellular carcinoma. Hepatic nodule in segment VII with high signal intensity on T2 weighted image (T2WI) **(A)**; with fat content **(B, C)** demonstrated by reduction of signal intensity on T1 weighted image (T1WI) opposite phase **(C)** when compared with T1WI in-phase **(B)**; restriction on diffusion **(D, E)** characterized by high signal on diffusion weighted imaging (DWI) **(D)** and low signal on the apparent diffusion coefficients (ADC) map **(E)**. On dynamic phases **(F-I)**, the nodule showed arterial hypervascular enhancement in the late arterial phase **(F)**; mosaic architecture **(F-I)**; washout appearance in the portal venous **(H)** and delayed **(I)** phases; and capsule (dashed arrows) **(H-I)** and satellites nodules (arrows) with the same pattern of enhancement **(F-I)**.

Atypical HCC

A minority of HCC presents atypical imaging features and awareness of these is important for early

TABLE 3. Main imaging features of hepatocellular carcinoma (HCC)

Imaging features	Description
Arterial hyperenhancement	Increased enhancement in the arterial phase. Reflects tumor neoangiogenesis.
Washout appearance	Hypoenhancement of the lesion compared with background liver tissue. Secondary to HCC extracellular reduced volume, rapid venous drainage and reduced intranodular portal venous supply.
Capsule appearance	Observed in approximately 80% of HCCs, detected on delayed phase, secondary to the lack of portal supply to malignant nodules. Corresponds to a pseudocapsule consisting of compressed adjacent liver parenchyma with occasional nonspecific inflammatory cells on histology.
Portal vein tumoral thrombosis	HCC invades and grows within the lumen. The vein appears dilated and with the same pattern of enhancement observed in the nodule.
T2 hyperintensity	The elevated signal intensity on T2WI can be useful to differentiate HCC from dysplastic nodules.
Restricted diffusion	Mildly elevated signal relative to the surrounding liver parenchyma on diffusion weighted imaging (DWI) and low signal intensity on apparent diffusion coefficients (ADC) map.
Corona enhancement	Enhancement of the peritumoral parenchyma after enhancement of the tumor itself, because of the passage of contrast through the draining sinusoids and portal venules into the surrounding sinusoids.
Intralesional fat	Loss of signal on the opposed-phase T1WI compared with the in-phase images.
Lesion iron sparing	Siderotic nodule is likely to be a dysplastic nodule. Development of an iron-free around the nodule suggests HCC foci.
Mosaic architecture	Nodular areas interspersed by areas of fibrosis, hemorrhage, arteriovenous shunting and necrosis. Characteristic of progressed HCCs.
Nodule-in-nodule architecture	Mildly elevated signal intensity on T2WI within nodule with low signal intensity, representing the focus of HCC within the low density dysplastic nodule, that may also enhance in the arterial phase.
Transitional phase hypointensity	Hypointensity compared with background liver following administration of a hepatobiliary contrast agent (2–5 minutes after contrast media administration).
Hepatobiliary phase hypointensity	Hypointensity compared with background liver following administration of a hepatobiliary contrast agent (20 minutes after).

T1W1 = T1 weighted image; T2WI = T2 weighted image

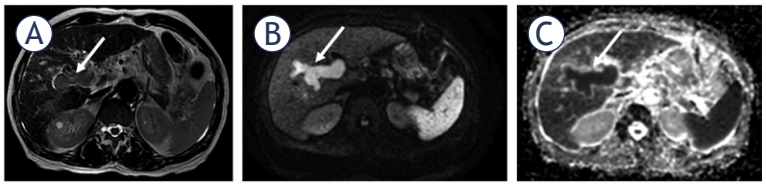

FIGURE 4. 63-year-old man with chronic hepatitis C and HCC with tumor invasion within the portal vein. Main and right portal veins demonstrate dilation (arrows), high signal intensity on T2 weighted image (T2WI) **(A)**, restriction on diffusion weighted imaging (DWI) **(B,C)**.

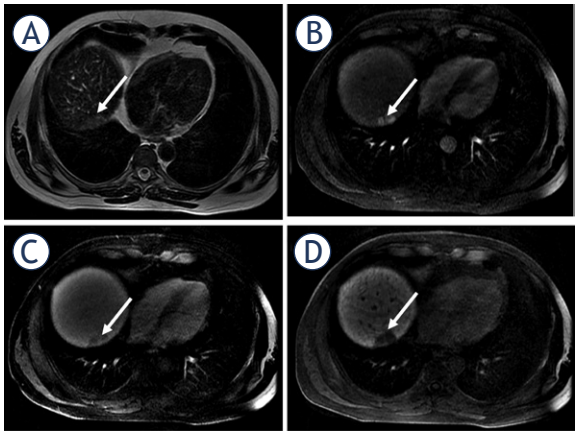

FIGURE 5. 49-year-old woman with cirrhosis due to chronic hepatitis C had a new hepatic nodule detected on screening ultrasound which was confirmed as HCC on MRI with hepatobiliary contrast agent. Hepatic nodule in segment VII (arrows) with high signal intensity on T2 weighted image (T2WI) **(A)**, hyperenhancement in the late arterial phase **(B)**, washout appearance **(C)**, and hypointense appearance in the hepatobiliary phase.

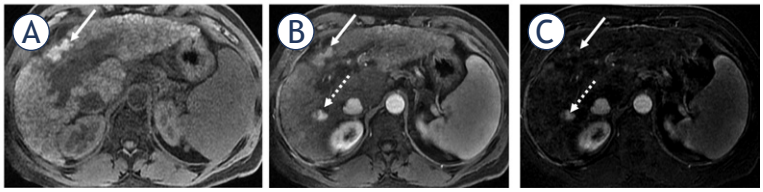

FIGURE 6. 62-year-old man with cirrhosis due to alcohol with a history of percutaneous radiofrequency ablation of a nodule in segment IV. On pre-contrast T1 weighted image (T1WI) with fat suppression **(A)** there is high signal intensity within the treated area (arrows) that was maintained in the arterial phase **(B)**; however, on subtraction no enhancement is detected **(C)**, which is compatible with no viable tumor. New HCC appeared during the follow-up in the segment VI (dashed arrow) with a true arterial hyperenhancement.

diagnosis and improving patient outcomes. Most of these cases are challenging and biopsy may be needed for confirmatory diagnosis.

Atypical enhancement patterns

Hypervascular nodules without washout appearance: Well-differentiated and small HCC lesions may

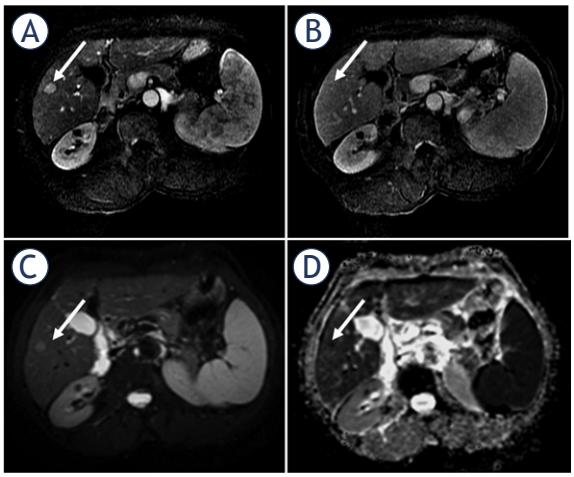

FIGURE 7. 59-year-old woman with cirrhosis due to chronic hepatitis B and small HCC. Small nodule (arrows) in segment V with arterial phase hyperenhancement **(A)**, without washout appearance **(B)**, and with diffusion restriction **(C, D)**. The patient underwent percutaneous biopsy with the diagnosis of well-differentiated HCC.

show atypical patterns of enhancement with lack of or poor arterial phase enhancement and persistent enhancement in the venous and delayed phases (Figure 7).[38,39] Differential diagnoses are benign hypervascular lesions (*e.g.*, hemangioma, focal nodular hyperplasia, and adenomas) and hypervascular metastasis.

Hypovascular nodules: Only about 10% of HCC are hypovascular[38] and the diagnosis can be challenging. However, in a patient with high risk to develop HCC, hypovascular nodules are suspicious.

Diffuse hepatocellular carcinoma

Diffuse hepatocellular carcinoma is a rare aggressive form of HCC characterized by poorly defined margins and atypical enhancement patterns (mild heterogeneous enhancement, most commonly hypovascular). Frequently, there is involvement of the portal and hepatic veins with thrombosis (Figure 8).[38]

Hepatocellular carcinoma in non-cirrhotic liver

Twenty percent of HCCs may occur in a non-cirrhotic liver. The radiological appearance of such HCCs is larger, well-demarcated, solitary lesions with large areas of necrosis; they are usually diagnosed at a later stage.[40]

Differential diagnosis

Although arterial hyperenhancement is considered the most consistent feature of HCC, it is also present in other non-malignant lesions especially small non-malignant ones, which contributes to the high incidence of false positives.

Vascular disorders

Transient arterial enhancement due to focal obstruction of a distal parenchymal portal vein or nontumorous arterioportal shunts, for example, is often seen in the cirrhotic liver. Usually, these vascular disorders are peripheral, wedge-shaped lesions, isointense to surrounding parenchyma on pre-contrast images and do not present restricted diffusion or displace internal vasculature.[36-38]

Focal confluent hepatic fibrosis

Observed in end-stage liver disease, focal confluent hepatic fibrosis can be mass-like and mistaken for HCC once it presents similar low signal intensity relative to the liver on T1WI and hyperintensity on T2WI. However, unlike HCC, it is usually associated with atrophy and capsular retraction of the affected segment, as well as delayed contrast enhancement. [36-38]

Hemangiomas, focal nodular hyperplasia, and hepatic adenomas

Other benign lesions such as hemangiomas, focal nodular hyperplasia, and hepatic adenomas are rare in the cirrhotic liver, probably because of the process of cirrhosis, and they can be difficult to distinguish from HCC. [36-38]

Intrahepatic cholangiocarcinoma

Intrahepatic cholangiocarcinoma usually shows rim enhancement with progressive and concentric filling of contrast material in the later phases, which would be an atypical pattern of enhancement for HCC (Figure 9). Other features more commonly associated with intrahepatic cholangiocarcinoma than HCC are intrahepatic biliary duct dilation distal to the tumor and associated capsular retraction. Association with tumoral thrombosis is rare and when narrowing or obstruction of the portal vein occurs, the latter are usually due to external compression.[18]

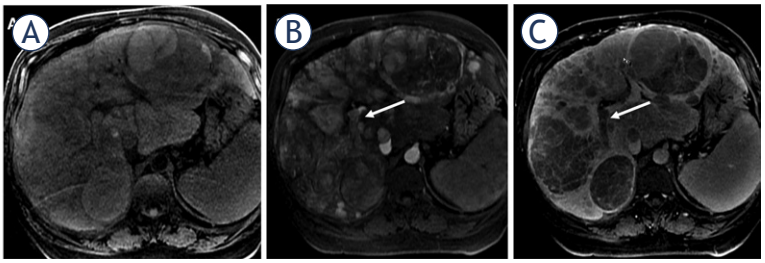

FIGURE 8. 69-year-old man with cirrhosis due to alcohol with diffuse infiltrative HCC **(A)**. Diffuse hepatic mass with areas of hypervascular arterial phase **(B)** and washout appearance **(C),** with tumoral thrombus within the right portal vein (arrows).

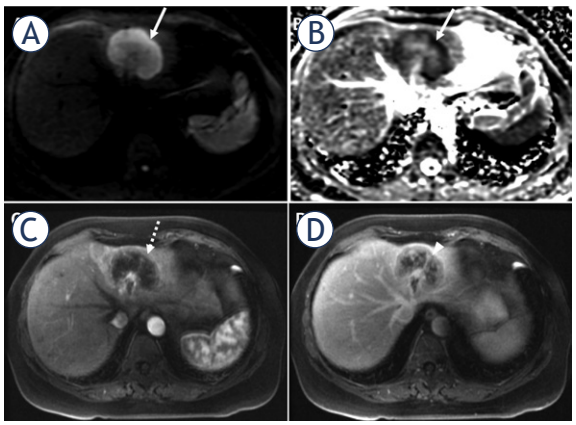

FIGURE 9. 65-year-old woman without liver disease with surgically-proven intrahepatic cholangiocarcinoma confirmed. Nodule in the left hepatic lobe with peripheral restricted diffusion (arrows) **(A, B)**, rim of arterial hyperenhancement (dashed arrow), and peripheral washout appearance (arrowhead).

Hepatocellular-cholangiocarcinoma

Combined hepatocellular-cholangiocarcinoma (cHCC-CC) is a rare variant of primary hepatic cancer that is clinically and pathologically distinct from pure HCC. Imaging features are variable depending on the predominant histologic component, and although they overlap more frequently with those of cholangiocarcinoma, they can also mimic HCC.[18,40,41] cHCC-CC may appear hypointense on T1WI and iso to hyperintense on T2WI with or without central hypointense focus, which represents a central cholangiocarcinoma or fibrotic component.[19,43] On dynamic imaging, early ring enhancement with centripetal progression or heterogeneous early enhancement with partial washout are possible presentations.[41] On MR imaging with a hepatocellular agent, irregular shape, strong peripheral enhancement, and absence of target sign favor cHCC-CC, particularly the HCC predominant type.[42]

TABLE 4. Main classifications used to assess tumor response after locoregional treatment

Criteria	System	Response		Definition
Size	**WHO**	**CR**		Disappearance of all TL
		PR		≥ 50% decrease in CP of TL
		SD		< 50% decrease to ≤25% increase in CP of TL
		PD		> 25% increase from maximum response of TL
	RECIST	**CR**		Disappearance of all TL
		PR		≥ 30% decrease in MD of TL
		SD		< 30% decrease to ≤20% increase in MD of TL
		PD		> 20% increase from maximum response of TL
Necrosis	**mRECIST**	**CR**		Disappearance of any intratumoral enhancement in all TL
		PR		≥ 30% decrease in SMD of enhancing tissue in TL
		SD		< 30% decrease to ≤20% in SMD of enhancing tissue in TL
		PD		> 20% increase in amount of enhancing tissue in TL
	$EASL_{meas}$	**CR**		Disappearance of any intratumoral enhancement in all TL
	and	**PR**		≥ 50% decrease in amount of enhancing tissue in TL
	$EASL_{est}$	**SD**		< 50% decrease in amount of enhancing tissue in TL
		PD		> 25% increase in amount of enhancing tissue in TL and/or new enhancement in previously treated lesions
	LI-RADS	**Nonviable**		No suspicious lesion enhancement
		Equivocal		Atypical enhancement not meeting criteria to viable tumor
		Viable		Nodular, mass-like, or thick irregular tissue in or along the treated lesion with any of the following: arterial phase hyperenhancement or washout appearance or enhanced similar to pretreatment
				100% of tumor necrosis or reduction
	RECICL	**TE4**	**a**	Necrotized area larger than the tumor (enough ablative margin)
			b	Necrotized area similar in size to the tumor (insufficient ablative margin)
		TE3		50–100% of tumor necrosis or reduction
		TE2		Other effect than TE3 and TE1
		TE1		Tumor enlargement of > 25% regardless of necrosis

CR = complete response, CP = cross-product, EASL = European Association for the Study of Liver, LI-RADS = Liver Imaging Reporting and Data System, MD = maximum diameter, PD = progressive disease, PR = partial response, RECIST = Response Evaluation Criteria for Solid Tumors, mRECIST = modified RECIST, RECICL = Response Evaluation Criteria in Cancer of the Liver, SD = stable disease, SMD = sum of maximum diameters, TE = treatment effect, TL = target lesion(s), WHO = World Health Organization

Hypervascular metastases

Hypervascular metastases may also be a diagnostic challenge and typically arise from primary neuroendocrine tumors (pancreatic islet cell tumor, carcinoid tumor, and pheochromocytoma), renal cell carcinoma, thyroid carcinoma, choriocarcinoma, and melanoma.[43] They are generally irregular with indistinct margins and hyperintense on T2WI with a central cystic or necrotic component and with a variable sign on T1WI, depending on the presence of blood, melanin, and other substances that present high signal on this sequence. On dynamic imaging, they show perilesional rim enhancement and irregular washout on delayed images.[44]

MRI after locoregional therapy of HCC

Surgical resection or transplantation is the standard treatment of HCC. However, most patients are not eligible for resection and the waiting list for liver transplantation is long. Locoregional therapies can be performed as curative treatment, mainly in small HCC, or as a bridge before transplantation. The goal of locoregional therapy is to achieve tumor necrosis. Overall, treated tumors appear with no internal enhancement on postcontrast phases and viable tumors may have areas of arterial phase hyperenhancement with or without washout ap-

TABLE 5. MRI and CT estimated sensitivity for the detection of hepatocellular carcinoma (HCC)

	MRI	CT	CEUS
Overall	82%	77%	73%
Tumor size ≥ 2 cm	96%	94%	94%
Tumor size < 2 cm	66%	63%	77%

CEUS = contrast-enhanced ultrasound

pearance (Figure 6).[44,45] Table 4 shows the main systems used to assess tumor response after locoregional treatment.

Diagnostic performance

The imaging diagnosis of HCC using only the features on dynamic MRI is highly specific. The overall MRI sensitivity for detection of HCC is 81%, against 68% using CT.[46] The dynamic contrast enhanced arterial phase is the most sensitive and specific sequence (>95%).[47]

MRI is especially sensitive for the detection of lesions larger than 2 cm. On the other hand, for the detection of small tumors, although MRI still outperforms CT, the sensitivity remains disappointing.[48-53] This can be explained by the high frequency of atypical enhancement patterns these small lesions present.[52] Regarding contrast-enhanced ultrasound (CEUS), it is not recommended as a first-line imaging technique, but improvements have been made in the differential diagnosis of cholangiocarcinoma and hepatocellular carcinoma and some studies have shown it to be more specific than CT and MRI for nodules between 10 and 20 mm.[12] Table 5 summarizes and compares the sensitivity of MRI, CT, and CEUS for the detection of HCC according to tumor size.[51]

As an attempt to improve the performance of MRI among small HCC, the combined use of DWI with conventional dynamic MRI[54] as well as the use of contrast agents other than gadolinium-based contrast media have been proposed.[55] The combination of super-paramagnetic iron oxide particles with gadolinium-based contrast media have been shown to increase the sensitivity for the detection of HCC measuring 1–2 cm to 92%.[56]

After local therapies, MRI has also shown to be specific but not sensitive for the detection of small foci of recurrent or residual tumor.[57,58] In this context, DWI has shown promising results for evaluating response to treatment.

Future directions

Radiomics

Advances in technology have allowed for quantitative features to be extracted from imaging scans, adding value to clinical decision-making. In oncology, quantitative radiomics features may allow for the assessment of tumor characteristics including cellularity, perfusion, and oxygenation that can help in characterizing tumors characterization, assessing treatment response, and predicting treatment response. Considering that MRI involves different sequences with several physical mechanisms, the use of MRI in radiomics is promising.[59]

Radiogenomics

Both quantitative and qualitative data extracted from imaging scans can also be correlated with genetic profiles. It has been demonstrated that imaging phenotypes reflect underlying genomics[59] and can guide the treatment of those patients, which is important in the new era of personalized medicine.

Positron emission tomography (PET)-MRI

Positron Emission Tomography (PET)-MRI combines high contrast and anatomical resolution from MRI with wide metabolic properties from PET. This technique is promising considering several new radiotracers. PET-MRI could be especially beneficial for evaluating tumor characteristics.[60-62]

While conventional imaging modalities (MRI and CT) are preferable for detecting HCC, PET can offer additional information about functional or metabolic characteristics of the tumor. Several radiotracers have been used to achieve this objective, including 18F-fluorodeoxyglucose (18F-FDG) to estimate glucose consumption and choline labelled with either 11C (Cho) or 18F (FCho) to reflect cell-membrane metabolism and tumor proliferation.[63-65]

18F-FDG is the most widely used radiotracer in oncology and has great sensitivity for detecting metastases from most cancers. FDG uptake correlates with the degree of HCC differentiation, with a higher avidity for poorly differentiated HCC.[66] On the other hand, choline shows strong avidity for HCC, especially in well and moderately-differentiated tumors.[68] Some studies showed that a dual-tracer PET using FDG and choline has the best performance to detect HCC[66-68] as these tracers complement each other in the detection of HCC based on its histological differentiation. This combination

may also be a prognostic indicator, with worst outcomes associated with FDG-PET captation.[68]

Perfusion MRI

Perfusion MRI is a function imaging technique that can provide quantitative data regarding tumor microvasculature. Several studies demonstrated that perfusion MRI can assess tumor response after locoregional therapies, such as transcatheter arterial chemoembolization and radiofrequency ablation.[69,70] Perfusion MRI can detect vasculature changes of HCC before and after therapy. It is a promising tool in the diagnosis of HCC, as it can be used to target lesions for therapy, to evaluate the efficacy of the treatments and to evaluate recurrence.[69-71]

Conclusions

In summary, MRI is an essential imaging modality in the diagnostic arsenal of HCC and is especially indicated for the evaluation of small lesions, unclear lesions on CT, and lesions after locoregional therapies. Considering the multiple sequences included on MRI, there is a huge potential to extract several imaging biomarkers that reflect the tumor microenvironment and which, in the future, may add decision-making value in the management of patients with HCC.

Acknowledgments

The authors would like to thank Joanne Chin for her editorial support on this manuscript.

This research was funded in part through the NIH/NCI Cancer Center Support Grant P30 CA008748. The work by Romina Grazia Giancipoli was partially supported by a scholarship awarded by ISSNAF Imaging Science Chapter.

References

1. Ferenci P, Fried M, Labrecque D, Bruix J, Sherman M, Omata M, et al. Hepatocellular carcinoma (HCC): a global perspective. *J Clin Gastroenterol* 2010; **44:** 239-45. doi: 10.1097/MCG.0b013e3181d46ef2
2. Torre LA, Bray F, Siegel RL, Ferlay J, Lortet-Tieulent J, Jemal A. Global cancer statistics 2012. *CA Cancer J Clin* 2015; **65:** 87-108. doi: 10.3322/caac.21262
3. Siegel RL, Miller KD, Jemal A. Cancer statistics, 2018. *CA Cancer J Clin* 2018; **68:** 7-30. doi: 10.3322/caac.21442
4. Tang A, Hallouch O, Chernyak V, Kamaya A, Sirlin CB. Epidemiology of hepatocellular carcinoma: target population for surveillance and diagnosis. *Abdom Radiol (NY)* 2018; **43:** 13-25. doi: 10.1007/s00261-017-1209-1
5. Krinsky GA, Lee VS. MR imaging of cirrhotic nodules. *Abdom Imaging* 2000; **25:** 471-82.
6. Nishida N, Goel A. Genetic and epigenetic signatures in human hepatocellular carcinoma: a systematic review. *Curr Genomics* 2011; **12:** 130-7. doi: 10.2174/138920211795564359
7. Choi JY, Lee JM, Sirlin CB. CT and MR imaging diagnosis and staging of hepatocellular carcinoma: part I. Development, growth, and spread: key pathologic and imaging aspects. *Radiology* 2014; **272:** 635-54. doi: 10.1148/radiol.14132361.
8. Crissien AM, Frenette C. Current management of hepatocellular carcinoma. *Gastroenterol Hepatol (NY)* 2014; **10:** 153-61. PMCID: PMC4014047
9. European Association For The Study Of The Liver, European Organisation For Research And Treatment Of Cancer. EASL-EORTC clinical practice guidelines: management of hepatocellular carcinoma. *J Hepatol* 2012; **56:** 908-43. doi: 10.1016/j.jhep.2011.12.001
10. Elsayes KM, Hooker JC, Agrons MM, Kielar AZ, Tang A, Fowler KJ, et al. 2017 Version of LI-RADS for CT and MR imaging: an update. *Radiographics* 2017; **37:** 1994-2017. doi: 10.1148/rg.2017170098.
11. Arif-Tiwari H, Kalb B, Chundru S, Sharma P, Costello J, Guessner RW, et al. MRI of hepatocellular carcinoma: an update of current practices. *Diagn Interv Radiol* 2014; **20:** 209-21. doi: 10.5152/dir.2014.13370.
12. Heimbach JK, Kulik LM, Finn RS, Sirlin CB, Abecassis MM, Roberts LR, et al. AASLD guidelines for the treatment of hepatocellular carcinoma. *Hepatology* 2018; **67:** 358-80. doi: 10.1002/hep.29086.
13. Wald C, Russo MW, Heimbach JK, Hussain HK, Pomfret EA, Bruix J. New OPTN/UNOS policy for liver transplant allocation: standardization of liver imaging, diagnosis, classification, and reporting of hepatocellular carcinoma. *Radiology* 2013; **266:** 376-82. doi: 10.1148/radiol.12121698
14. Kambadakone AR, Fung A, Gupta RT, et al. LI-RADS technical requirements for CT, MRI, and contrast-enhanced ultrasound. *Abdom Radiol (NY)* 2018; **43:** 56-74. doi: 10.1007/s00261-017-1345-7.
15. Le Moigne F, Durieux M, Bancel B, Boublay N, Boussel L, Ducerf C, et al. Impact of diffusion-weighted MR imaging on the characterization of small hepatocellular carcinoma in the cirrhotic liver. *Magn Reson Imaging* 2012; **30:** 656-65. doi: 10.1016/j.mri.2012.01.002
16. Mannelli L, Nougaret S, Vargas HA, Do RK. Advances in diffusion-weighted imaging. *Radiol Clin North Am* 2015; **53:** 569-81. doi: 10.1016/j.rcl.2015.01.002
17. Mannelli L, Bhargava P, Osman SF, Raz E, Moshiri M, Laffi G, et al. Diffusion-weighted imaging of the liver: a comprehensive review. *Curr Probl Diagn Radiol* 2013; **42:** 77-83. doi: 10.1067/j.cpradiol.2012.07.001
18. Horvat N, Nikolovski I, Long N, Gerst S, Zheng J, Pak LM, et al. Imaging features of hepatocellular carcinoma compared to intrahepatic cholangiocarcinoma and combined tumor on MRI using liver imaging and data system (LI-RADS) version 2014. *Abdom Radiol (NY)* 2018; **43:** 169-78. doi: 10.1007/s00261-017-1261-x
19. Mannelli L, Kim S, Hajdu CH, Babb JS, Taouli B. Serial diffusion-weighted MRI in patients with hepatocellular carcinoma: prediction and assessment of response to transarterial chemoembolization. Preliminary experience. *Eur J Radiol* 2013; **82:** 577-82. doi: 10.1016/j.ejrad.2012.11.026
20. Chegai F, Merolla S, Greco L, Nezzo M, Mannelli L, Orlacchio A. Re: Baseline and early MR apparent diffusion coefficient quantification as a predictor of response of unresectable hepatocellular carcinoma to doxorubicin drug-eluting bead chemoembolization. *J Vasc Interv Radiol* 2016; **27:** 1456-8. doi: 10.1016/j.jvir.2016.05.007
21. Gluskin JS, Chegai F, Monti S, Squillaci E, Mannelli L. Hepatocellular carcinoma and diffusion-weighted MRI: detection and evaluation of treatment response. *J Cancer* 2016; **7:** 1565-70. doi: 10.7150/jca.14582
22. Park MS, Kim S, Patel J, Hajdu CH, Do RK, Mannelli L, et al. Hepatocellular carcinoma: detection with diffusion-weighted versus contrast-enhanced magnetic resonance imaging in pretransplant patients. *Hepatology* 2012; **56:** 140-8. doi: 10.1002/hep.25681
23. Agostini A, Kircher MF, Do R, Borgheresi A, Monti S, Giovagnoni A, et al. Magnetic resonance imaging of the liver (including biliary contrast agents) part 1: technical considerations and contrast materials. *Semin Roentgenol* 2016; **51:** 308-16. doi: 10.1053/j.ro.2016.05.015
24. Ramalho J, Ramalho M. Gadolinium deposition and chronic toxicity. *Magn Reson Imaging Clin N Am* 2017; **25:** 765-78. doi: 10.1016/j.mric.2017.06.007

25. Hernando D, Levin YS, Sirlin CB, Reeder SB. Quantification of liver iron with MRI: state of the art and remaining challenges. *J Magn Reson Imaging* 2014; **40:** 1003-21. doi: 10.1002/jmri.24584

26. Agostini A, Kircher MF, Do RK, Borgheresi A, Monti S, Giovagnoni A. Magnetic resonanance imaging of the liver (including biliary contrast agents) part 2: protocols for liver magnetic resonanance imaging and characterization of common focal liver lesions. *Semin Roentgenol* 2016; **51:** 317-33. doi: 10.1053/j.ro.2016.05.016

27. Liu D, Song B, Huang ZX, Wu B, Tang HH. [The iron content of hepatocellular carcinoma associated nodules: study of histopathology and MR imaging]. [Chinese]. *Sichuan Da Xue Xue Bao Yi Xue Ban* 2016; **47:** 376-81. PMID: 27468484

28. Siripongsakun S, Lee JK, Raman SS, Tong MJ, Sayre J, Lu DS. MRI detection of intratumoral fat in hepatocellular carcinoma: potential biomarker for a more favorable prognosis. *AJR Am J Roentgenol* 2012; **199:** 1018-25. doi: 10.2214/AJR.12.8632

29. Singh S, Venkatesh SK, Loomba R, Wang Z, Sirlin C, Chen J, et al. Magnetic resonance elastography for staging liver fibrosis in non-alcoholic fatty liver disease: a diagnostic accuracy systematic review and individual participant data pooled analysis. *Eur Radiol* 2016; **26:** 1431-40. doi: 10.1007/s00330-015-3949-z

30. Thompson SM, Wang J, Chandan VS, Glaser KJ, Roberts LR, Ehman RL, et al. MR elastography of hepatocellular carcinoma: correlation of tumor stiffness with histopathology features-preliminary findings. *Magn Reson Imaging* 2017; **37:** 41-5. doi: 10.1016/j.mri.2016.11.005

31. Gordic S, Ayache JB, Kennedy P, Besa C, Wagner M, Bane O, et al. Value of tumor stiffness measured with MR elastography for assessment of response of hepatocellular carcinoma to locoregional therapy. *Abdom Radiol (NY)* 2017; **42:** 1685-94. doi: 10.1007/s00261-017-1066-y

32. Hanna RF, Aguirre DA, Kased N, Emery SC, Peterson MR, Sirlin CB. Cirrhosis-associated hepatocellular nodules: correlation of histopathologic and MR imaging features. *Radiographics* 2008; **28:** 747-69. doi: 10.1148/rg.283055108

33. Efremidis SC, Hytiroglou P. The multistep process of hepatocarcinogenesis in cirrhosis with imaging correlation. *Eur Radiol* 2002; **12:** 753-64. doi: 10.1007/s00330-001-1142-z

34. Efremidis SC, Hytiroglou P, Matsui O. Enhancement patterns and signal-intensity characteristics of small hepatocellular carcinoma in cirrhosis: pathologic basis and diagnostic challenges. *Eur Radiol* 2007; **17:** 2969-82. doi: 10.1007/s00330-007-0705-z

35. Jeong YY, Yim NY, Kang HK. Hepatocellular carcinoma in the cirrhotic liver with helical CT and MRI: imaging spectrum and pitfalls of cirrhosis-related nodules. *AJR Am J Roentgenol* 2005; **185:** 1024-32. doi: 10.2214/AJR.04.1096

36. Sadek AG, Mitchell DG, Siegelman ES, Outwater EK, Matteucci T, Hann HW. Early hepatocellular carcinoma that develops within macroregenerative nodules: growth rate depicted at serial MR imaging. *Radiology* 1995; 195753-6. doi: 10.1148/radiology.195.3.7754006

37. Willatt JM, Hussain HK, Adusumilli S, Marrero JA. MR Imaging of hepatocellular carcinoma in the cirrhotic liver: challenges and controversies. *Radiology* 2008; **247:** 311-30. doi: 10.1148/radiol.2472061331

38. Roumanis PS, Bhargava P, Kimia Aubin G, Choi JI, Demirjian AN, Thayer DA, et al. Atypical magnetic resonance imaging findings in hepatocellular carcinoma. *Curr Probl Diagn Radiol* 2015; **44:** 237-45. doi: 10.1067/j.cpradiol.2014.03.002

39. Mannelli L, Hoang MV, Sabath AP, Linnau KF. An unusual oral mass. *Gastroenterology* 2012; **142:** e14-5. doi.org/10.1053/j.gastro.2011.08.047

40. Trevisani F, Frigerio M, Santi V, Grignaschi A, Bernardi M. Hepatocellular carcinoma in non-cirrhotic liver: a reappraisal. *Dig Liver Dis* 2010; **42:** 341-7. doi: 10.1016/j.dld.2009.09.002

41. Potretzke TA, Tan BR, Doyle MB, Brunt EM, Heiken JP, Fowler KJ. Imaging features of biphenotypic primary liver carcinoma (hepatocholangiocarcinoma) and the potential to mimic hepatocellular carcinoma: LI-RADS analysis of CT and MRI features in 61 cases. *AJR Am J Roentgenol 2016*; **207:** 25-31. doi: 10.2214/AJR.15.14997

42. Maximin S, Ganeshan DM, Shanbhogue AK, Dighe MK, Yeh MM, Kolokythas O, et al. Current update on combined hepatocellular-cholangiocarcinoma. *Eur J Radiol Open* 2014; **1:** 40-8. doi: 10.1016/j.ejro.2014.07.001

43. Mannelli L, Monti S, Grieco V, Matesan M. Hepatic lesions in a cirrhotic liver: primary or metastases? *J Nucl Med Technol* 2017; **45:** 50-2. doi: 10.2967/jnmt.116.183228.

44. Khosa F, Khan AN, Eisenberg RL. Hypervascular liver lesions on MRI. *AJR Am J Roentgenol* 2011; **197:** W204-20. doi: 10.2214/AJR.10.5382

45. Ayuso C, Rimola J, Garcia-Criado A. Imaging of HCC. *Abdom Imaging* 2012; **37:** 215-30. doi: 10.1007/s00261-011-9794-x

46. Mannelli L, Kim S, Hajdu CH, Babb JS, Clark TW, Taouli B. Assessment of tumor necrosis of hepatocellular carcinoma after chemoembolization: diffusion-weighted and contrast-enhanced MRI with histopathologic correlation of the explanted liver. *AJR Am J Roentgenol* 2009; **193:** 1044-52. doi: 10.2214/AJR.08.1461

47. Colli A, Fraquelli M, Casazza G, Massironi S, Colucci A, Conte D, et al. Accuracy of ultrasonography, spiral CT, magnetic resonance, and alpha-fetoprotein in diagnosing hepatocellular carcinoma: a systematic review. *Am J Gastroenterol* 2006; **101:** 513-23. doi: 10.1111/j.1572-0241.2006.00467.x

48. Becker-Weidman DJ, Kalb B, Sharma P, Kitajima HD, Lurie CR, Chen Z, et al. Hepatocellular carcinoma lesion characterization: single-institution clinical performance review of multiphase gadolinium-enhanced MR imaging--comparison to prior same-center results after MR systems improvements. *Radiology* 2011; **261:** 824-33. doi: 10.1148/radiol.11110157

49. Krinsky GA, Lee VS, Theise ND, Weinreb JC, Morgan GR, Diflo T, et al. Transplantation for hepatocellular carcinoma and cirrhosis: sensitivity of magnetic resonance imaging. *Liver Transpl* 2002; **8:** 1156-64. doi: 10.1053/jlts.2002.35670

50. Burrel M, Llovet JM, Ayuso C, Iglesias C, Sala M, Miquel R, et al. MRI angiography is superior to helical CT for detection of HCC prior to liver transplantation: an explant correlation. *Hepatology* 2003; **38:** 1034-42. doi: 10.1053/jhep.2003.50409

51. Lee YJ, Lee JM, Lee JS, Lee HY, Park BH, Kim YH, et al. Hepatocellular carcinoma: diagnostic performance of multidetector CT and MR imaging-a systematic review and meta-analysis. *Radiology* 2015; **275:** 97-109. doi: 10.1148/radiol.14140690

52. Forner A, Vilana R, Ayuso C, Bianchi L, Solé M, Ayuso JR, et al. Diagnosis of hepatic nodules 20 mm or smaller in cirrhosis: Prospective validation of the noninvasive diagnostic criteria for hepatocellular carcinoma. *Hepatology* 2008; **47:** 97-104. doi: 10.1002/hep.21966

53. Chou R, Cuevas C, Fu R, Devine B, Wasson N, Ginsburg A, et al. Imaging techniques for the diagnosis of hepatocellular carcinoma: a systematic review and meta-analysis. *Ann Intern Med* 2015; **162:** 697-711. doi: 10.7326/M14-2509

54. Xu PJ, Yan FH, Wang JH, Shan Y, Ji Y, Chen CZ. Contribution of diffusion-weighted magnetic resonance imaging in the characterization of hepatocellular carcinomas and dysplastic nodules in cirrhotic liver. *J Comput Assist Tomogr* 2010; **34:** 506-12. doi: 10.1097/RCT.0b013e3181da3671

55. Kierans AS, Kang SK, Rosenkrantz AB. The diagnostic performance of dynamic contrast-enhanced MR imaging for detection of small hepatocellular carcinoma measuring up to 2 cm: a meta-analysis. *Radiology* 2016; **278:** 82-94. doi: 10.1148/radiol.2015150177

56. Ward J, Guthrie JA, Scott DJ, Atchley J, Wilson D, Davies MH, et al. Hepatocellular carcinoma in the cirrhotic liver: double-contrast MR imaging for diagnosis. *Radiology* 2000; **216:** 154-62. doi: 10.1148/radiology.216.1.r00jl24154

57. Lu DS, Yu NC, Raman SS, Limanond P, Lassman C, Murray K, et al. Radiofrequency ablation of hepatocellular carcinoma: treatment success as defined by histologic examination of the explanted liver. *Radiology* 2005; **234:** 954-60. doi: 10.1148/radiol.2343040153

58. Buscarini L, Buscarini E, Di Stasi M, Vallisa D, Quaretti P, Rocca A. Percutaneous radiofrequency ablation of small hepatocellular carcinoma: long-term results. *Eur Radiol* 2001; **11:** 914-21. doi: 10.1007/s003300000659

59. Kuo MD, Gollub J, Sirlin CB, Ooi C, Chen X. Radiogenomic analysis to identify imaging phenotypes associated with drug response gene expression programs in hepatocellular carcinoma. *J Vasc Interv Radiol* 2007; **18:** 821-31. doi: 10.1016/j.jvir.2007.04.031

60. Jadvar H, Colletti PM. Competitive advantage of PET/MRI. *Eur J Radiol* 2014; **83:** 84-94. doi: 10.1016/j.ejrad.2013.05.028

61. Kong E, Chun KA, Cho IH. Quantitative assessment of simultaneous F-18 FDG PET/MRI in patients with various types of hepatic tumors: correlation between glucose metabolism and apparent diffusion coefficient. *PLoS One* 2017; **12:** e0180184. doi: 10.1371/journal.pone.0180184

62. Sun L, Wu H, Guan YS. Positron emission tomography/computer tomography: challenge to conventional imaging modalities in evaluating primary and metastatic liver malignancies. *World J Gastroenterol* 2007; **13:** 2775-83.

63. Talbot JN, Gutman F, Fartoux L, Grange JD, Ganne N, Kerrou K, et al. PET/CT in patients with hepatocellular carcinoma using [(18)F]fluorocholine: preliminary comparison with [(18)F]FDG PET/CT. *Eur J Nucl Med Mol Imaging* 2006; **33:** 1285-9. doi: 10.1007/s00259-006-0164-9

64. Mertens K, Slaets D, Lambert B, Acou M, De Vos F, Goethals I. PET with (18)F-labelled choline-based tracers for tumour imaging: a review of the literature. *Eur J Nucl Med Mol Imaging* 2010; **37:** 2188-93. doi: 10.1007/s00259-010-1496-z

65. Yang SH, Suh KS, Lee HW, et al. The role of (18)F-FDG-PET imaging for the selection of liver transplantation candidates among hepatocellular carcinoma patients. *Liver Transpl* 2006; **12:** 1655-60. doi: 10.1002/lt.20861

66. Bertagna F, Bertoli M, Bosio G, Biasiotto G, Sadeghi R, Giubbini R, et al. Diagnostic role of radiolabelled choline PET or PET/CT in hepatocellular carcinoma: a systematic review and meta-analysis. *Hepatol Int* 2014; **8:** 493-500. doi: 10.1007/s12072-014-9566-0

67. Ho CL, Chen S, Yeung DW, Cheng TK. Dual-tracer PET/CT imaging in evaluation of metastatic hepatocellular carcinoma. *J Nucl Med* 2007; **48:** 902-9. doi: 10.2967/jnumed.106.036673

68. Castilla-Lièvre MA, Franco D, Gervais P, Kuhnast B, Agostini H, Marthey L, et al. Diagnostic value of combining ^{11}C-choline and ^{18}F-FDG PET/CT in hepatocellular carcinoma. *Eur J Nucl Med Mol Imaging* 2016; **43:** 852-9. doi: 10.1007/s00259-015-3241-0

69. Shao GL, Zheng JP, Guo LW, Chen YT, Zeng H, Yao Z. Evaluation of efficacy of transcatheter arterial chemoembolization combined with computed tomography-guided radiofrequency ablation for hepatocellular carcinoma using magnetic resonance diffusion weighted imaging and computed tomography perfusion imaging: A prospective study. *Medicine (Baltimore)* 2017; **96:** e5518. doi: 10.1097/MD.0000000000005518

70. Chen X, Xiao E, Shu D, Yang C, Liang B, He Z, et al. Evaluating the therapeutic effect of hepatocellular carcinoma treated with transcatheter arterial chemoembolization by magnetic resonance perfusion imaging. *Eur J Gastroenterol Hepatol* 2014; **26:** 109-13. doi: 10.1097/MEG.0b013e328363716e

71. Bayle M, Clerc-Urmès I, Ayav A, Bronowicki JP, Petit I, Orry X, et al. Computed tomographic perfusion with 160-mm coverage: comparative analysis of hepatocellular carcinoma treated by two transarterial chemoembolization courses relative to magnetic resonance imaging findings. *Abdom Radiol (NY)* 2018. doi: 10.1007/s00261-018-1714-x

review

Immune RECIST criteria and symptomatic pseudoprogression in non-small cell lung cancer patients treated with immunotherapy

Martina Vrankar[1], Mojca Unk[2]

[1] Department of Radiotherapy, Institute of Oncology Ljubljana, Ljubljana, Slovenia
[2] Department of Medical Oncology, Institute of Oncology Ljubljana, Ljubljana, Slovenia

Radiol Oncol 2018; 52(4): 365-369.

Received 5 February 2018
Accepted 12 March 2018

Correspondence to: Martina Vrankar, M.D., Ph.D., Institute of Oncology Ljubljana, Zaloška 2, 1000 Ljubljana, Slovenia.
Phone: +386 1 5879 629; Fax: +386 1 5879 400, E-mail: mvrankar@onko-i.si

Disclosure: No potential conflicts of interest were disclosed.

Background. Uncommon response during immunotherapy is a new challenging issue in oncology practice. Recently, new criteria for evaluation of response to immunotherapy *immune response evaluation criteria in solid tumors* (iRECIST) were accepted. According to iRECIST, worsening of performance status (PS) accompanied to pseudoprogression reflects most probably the true progression of the malignant disease.

Methods. A systematic review of the literature was made by using several electronic database with the following search criteria: symptomatic pseudoprogression, atypical response, immunotherapy and lung cancer.

Results. In the literature, we identified five reports of seven patients treated with immunotherapy that met the inclusion criteria. We also report our experience of patient with pseudoprogression and almost complete response after one dose of immunotherapy.

Conclusions. As seen from our review, iRECIST criteria might be insufficient in distinguishing true progression from pseudoprogression in some patients with advanced NSCLC treated with immunotherapy. More precise assessment methods are urgently needed.

Key words: symptomatic pseudoprogression; atypical response; immunotherapy; lung cancer

Introduction

Immunotherapy is a new therapeutic strategy for increasing number of malignancies including non small-cell lung cancer (NSCLC). Check point inhibitors affecting programmed death 1/programmed death ligand 1 (PD-1/PD-L1) signaling pathway have become key drugs against metastatic NSCLC.[1-5] Since the action of check point inhibitors is different from cytotoxic and targeted therapy also the responses to immunotherapy could be atypical.

One of unexpected response named pseudoprogression, which is characterized by radiologic enlargement of the tumor burden, followed by regression or appearance of new lesions, was first recognized in metastatic melanoma patients treated with ipilimumab.[6,7] Pseudoprogression was observed in up to 10% of melanoma patients progressing on immunotherapy and is associated with favorable long-term survival.[8] Radiologic pseudoprogression in patients with metastatic NSCLC treated with anti-PD-1/PD-L1 therapy is reported less common than in melanoma patients in the range of 0–6%.[9-15]

Standard for the evaluation of radiologic response of the tumors to treatment is *response evaluation criteria in solid tumors* (RECIST) system 1.1.[16] Recently, after few immune adjusted criteria in the past, new criteria for evaluation of response to immunotherapy immune RECIST (iRECIST) were proposed and accepted.[7] Most important change in iRECIST is requirement for confirmation of tumor enlargement after a minimum of 4 weeks and no

later than 8 weeks from the last evaluation. Related to this, new terminus for unconfirmed (iUCD) and confirmed progressive disease (iCPD) were accepted. Some other aspects are highlighted in iRECIST regarding pseudoprogression. Worsening of clinical and performance status (PS) should not be accompanied with pseudoprogression since it most probably reflects the true progression of the malignancy.[7]

Here we present the single institution experience of symptomatic pseudoprogression after one application of anti PD-L1 therapy in a patient with metastatic NSCLC followed by dramatic treatment response to immunotherapy and report on the review of symptomatic pseudoprogressions from literature.

Methods

A systematic review of the literature was made by using several electronic database: PubMed (US National Library of Medicine, http://www.ncbi.nlm.nih.gov/pubmed), Scopus (Elsevier, http://www.scopus.com/), Google Scholar (https://scholar.google.it/), Web of Science (Thomson Reuters, http://apps.webofknowledge.com/), De Gruyter (https://www.degruyter.com/) and Cochrane Library (http://www.cochranelibrary.com/), with the following search criteria: symptomatic pseudoprogression, atypical response, immunotherapy and lung cancer.

Results

Altogether, five reports of seven patients treated with immunotherapy were identified that met the inclusion criteria (Table 1).[17-21] In our analysis, three males and five females (including our case) were included with median age of 63 years (range 46–68). PD-L1 expression was reported in three patients, all treated with pembrolizumab. In all patients, good partial or almost complete response was observed between six and twelve weeks of treatment, that lasted at the time of report. All other patients with unknown PD-L1 expression were treated with nivolumab. Only one of them continued treatment for 12 months at the time of the report.

We present our case of 67 year-old female patient that was presented in September 2016 with primary metastatic lung adenocarcinoma of the left upper lobe with negative biopsy for epidermal growth factor receptor (EGFR) mutation, anaplastic lymphoma kinase (ALK) and ROS1 rearrangement. Due to extensive disease with metastases in the lung, axillary and abdominal lymph nodes, bones, left kidney and suprarenal gland with symptoms of pain in left hip, anorexia, fatigue and PS 2 she started treatment with urgent radiotherapy of the mediastinum, bulky mass on the left neck and left hip. After the pain was relieved with palliative radiotherapy, she started chemotherapy (ChT) with pemetrexed and carboplatin. Immediately after completing 4 cycles of ChT a progressive disease in the lung, right supraclavicular region, both suprarenal glands and subcutaneously was revealed, confirmed by FDG PET-CT (Figure 1). Aspiration biopsy of the lymph node in supraclavicular region was performed at that time and 100% of PD-L1 expression was found. While waiting for the result of PD-L1 expression her clinical condition worsened with aggravation of pain, muscle weakness, febrile state with no signs of infection and respiratory insufficiency. Nevertheless we decided to treat her with immunotherapy after her state was stabilized with supportive care. Her PS was scored as 2 at that time. In March 8th 2017 she received first cycle of pembrolizumab. Two weeks later her condition aggravated to PS 4 with more pain, loss of appetite and occasional somnolence. Immunotherapy was stopped and she was referred to palliative care 22 days after 1st cycle of pembrolizumab and thereafter lost from control. Three months later patient surprisingly called her oncologist. She was at home working in the garden with almost no pain, asking for continuation of treatment with pembrolizumad. On medical examination few days later in June 2017 she was in PS 1 and actually continued treatment with immunotherapy. One week after second dose of pembrolizumab on June 2017 FDG PET-CT was performed and almost complete response was found (Figure 2). Patient continued treatment with immunotherapy and until February 2018 she received 13 doses with further clinical and radiological stable disease.

Discussion

To the best of our knowledge, we are the first that report on symptomatic pseudoprogression followed by almost complete response in a patient with metastatic NSCLC three months after one dose of checkpoint inhibitor. Immunotherapy has unique action and promotes immune system to incite inflammation directed to tumor with no direct

TABLE 1. Symptomatic pseudo progression: review of the literature

Author, (Year), reference	Sex/ age (years)	Histology	Initial stage	Line of systemic therapy	PD-L1 expression	Anti-PD-1/PD-L1	Time to PP	Symptoms of PP	Time to response (months)	Subsequent treatment (time)
Sarfay *et al.* (2016)[17]	F/68	squamous NSCLC	locally advanced	2	NR	nivolumab	1 week	Pain, sys.inflam.reac.	4 weeks	NC (6m)
Kolla *et al.* (2016)[18]	M/46	SCLC	NR	11	NR	nivolumab	NR	SVCS, stenting req., Card. tamponade, Pericard.req. Card.tamponade,	8 weeks	NC (12m)
	F/54	adenoca EGFR ex21	metastatic	5	NR	nivolumab	NR	Pericard.req.	8 weeks	IT S, osi
Izumida *et al.* (2017)[19]	M/64	adenoca	metastatic	6	NR	nivolumab	2 months	Gen.det.	3 months	IT S, IT reint. (11m)
Kumagai *et al.* (2017)[20]	F/62	adenoca	locally advanced	7	NR	nivolumab	12 weeks	Hemoptysis, art.embol.req.	20 weeks	Pacli, S-1
Hochmair *et al.* (2017)[21]	M/63	adenoca	locally advanced	2	90%	pembrolizumab	2 months	Resp.insuf. (O2 req) Gen.det.,	6 weeks after PP	NC (13m)
	F/63	adenoca	metastatic	2	Highly	pembrolizumab	4 weeks	Resp.insuf.(O2 req)	3 months	NC (19m)
Vrankar *et al.* (2018)	F/67	adenoca	metastatic	2	100%	pembrolizumab	2 weeks	Gen.det.,	3 months	IT reint. (11m)

adenoca = adenocarcinoma; art.= arterial; card.= cardiac; det.= deterioration; embol.= embolization; ex21 = exon 21; gen.= general; insuf.= insufficiency; IT = immunotherapy; m = months; NC = not changed; NR = not reported, osi = osimertinib; pacli = paclitaxel; pericard.= pericardiocentesis; PP = pseudo progression; req.= required; reint.= reinitiated; resp.= respiratory; S = stopped; S-1 = tegafur/gimeracil/oteracil; SVCS = syndrome vena cava superior; sys.inflam.reac.= systemic inflammatory reaction

cytotoxic impact on the tumor growth.[22] As a result, atypical responses are observed such as delayed responses, pseudoprogression, hyperprogression and abscopal effect.[6] These unusual phenomenas could be explained by T cell recruitment and infiltration into the tumor together with edema and necrosis.[13] Also, the time of immune activation and onset of clinical activity are not predictable yet.

In our case, symptomatic pseudoprogression was accompanied by delayed response after only one dose of check point inhibitor. This phenomena opens questions about appropriate timing, dosage and frequency of immunotherapy. PD-1 and PD-L1 inhibitors nivolumab, pembrolizumab and atezolizumab were recently approved for the treatment of advanced NSCLC and medical products are prescribed every two or three weeks.[23-28] As immunotherapy harness the host immune system in targeting the tumor, it could also trigger systemic inflammatory response, which could be in some patients followed by vigorous deterioration of clinical and performance status.[29] It seems that especially patients with high expression of PD-L1 might have extensive systemic inflammatory response and current prescribed schedule of immunotherapy cause overtreatment. A marker of systemic inflammatory response that was extensively studied is pretreatment neutrophil-to-lymphocyte ratio (NLR).[30-32] In the retrospective cohort study of 175 patients with metastatic NSCLC treated with nivolumab, pretreatment NLR ≥ 5 was associated with statistically inferior overall survival and progression free survival.[33] NLR was not associated with response to nivolumab. In this cohort pseudoprogression was observed in 2.9% of patients.[33]

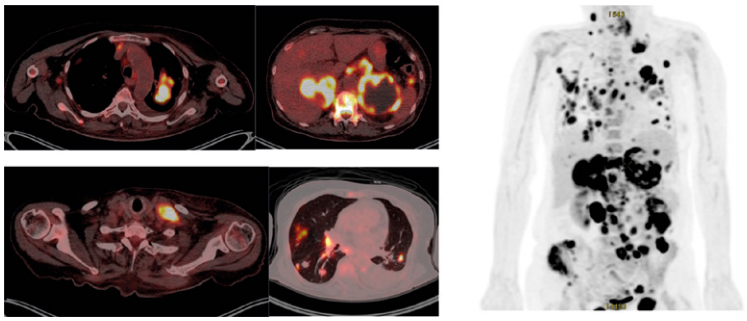

FIGURE 1. PET CT of non-small cell lung cancer patient from Institute of Oncology Ljubljana, at progression of disease after chemotherapy and before immunotherapy on March 2017.

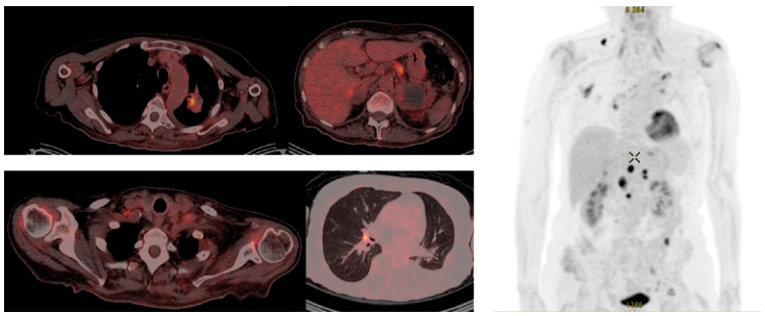

FIGURE 2. PET CT of non-small cell lung cancer patient from Institute of Oncology Ljubljana, three months after immunotherapy on June 2017.

The differences in progression free survival (PFS) and overall survival (OS) related to NLR were also demonstrated in a study of metastatic melanoma patients treated with ipilimumab.[34] Whether NLR is prognostic or predictive factor for OS is not clear and more data are needed for final conclusions.

In the literature we found 7 cases of patient with NSCLC treated with check point inhibitors that had evidence of pseudoprogression accompanied with worsening of clinical symptoms or PS. Five patients had worsening of disease-related symptoms that needed major intervention and had deterioration to PS 4. Treatment with checkpoint inhibitors was continued at the time of pseudoprogression since there was no alternative treatment options available.[17,18,20,21] In spite of iRECIST recommended discontinuation of treatment in case of radiological pseudoprogression combined with deterioration of PS, all seven patients experienced improvement to PS 0–1. All patients had benefit from continuation of treatment and four of them were on treatment over 11 months.

Differentiation of pseudoprogression from true progression is a growing clinical challenge that could prevent from interruption of effective therapy or loosing time with ineffective treatment. Expression of PD-L1 is the most studied predictor biomarker for anti-PD-L1 therapy.[35-37] Trials with pembrolizumab demonstrated improved outcomes in metastatic NSCLC patients with PD-L1 expression ≥ 50%.[23,25] Three patients in our review with symptomatic pseudoprogression that were treated with pembrolizumab had PD-L1 expression over 50%. There are no clear data so far to connect incidence of pseudoprogression and high PD-L1 expression.

In few reports, pseudoprogression was confirmed with biopsy. In one of the cases, biopsy revealed fibrotic tissue with infiltrating T lymphocytes but no viable tumor cells and in second case, necrotic tissue with T cell infiltration was found.[6] Biopsy is the most useful in distinguishing pseudoprogression from true progression. Unfortunately, the invasive procedures, which are usually needed, patients often refuse.

Most important imaging techniques used in daily clinical practice for evaluation of response to immunotherapy in NSCLC with iRECIST are CT, MRI and PET CT.[16] Some other imaging technics and radiotracers are under investigation for better interpretation of atypical responses with immunotherapy. Dual Energy CT (DECT) can better revealed changes in the intratumoral vascularization, while Immuno-PET is a new metabolic imaging strategy that combine labeled monoclonal antibodies specific for T cells antigens.[38,39]

Conclusions

Uncommon response during immunotherapy is a challenging issue in the current oncology practice. As seen from our review, iRECIST criteria might be insufficient in distinguishing true progression from pseudoprogression in some cases, especially in patients with performance status deterioration. More precise assessment methods are urgently needed and some promising are under investigation. Besides iRECIST criteria, considering PD-L1 expression and histological features might be useful approach in clinical decision for immunotherapy continuation.

References

1. Pardoll DM. The blockade of immune checkpoints in cancer immunotherapy. *Nat Rev Cancer* 2012; **12:** 252-64. doi: 10.1038/nrc3239
2. Brahmer J, Reckamp KL, Baas P, Crinò L, Eberhardt WE, Poddubskaya E, et al. Nivolumab versus docetaxel in advanced squamous-cell non-small-cell lung cancer. *N Engl J Med* 2015; **373:** 123-35. doi: 10.1056/NEJMoa1504627
3. Borghaei H, Paz-Ares L, Horn L, Spigel DR, Steins M, Ready NE, et al. Nivolumab versus docetaxel in advanced nonsquamous non-small-cell lung cancer. *N Engl J Med* 2015; **373:** 1627-39. doi: 10.1056/NEJMoa1507643
4. Garon EB, Rizvi NA, Hui R, Leighl N, Balmanoukian AS, Eder JP, et al. Pembrolizumab for the treatment of non-small-cell lung cancer. *N Engl J Med* 2015; **372:** 2018-28. doi: 10.1056/NEJMoa1501824
5. Reck M, Rodríguez-Abreu D, Robinson AG, Hui R, Csőszi T, Fülöp A, et al. Pembrolizumab versus chemotherapy for PD-L1-positive non-small-cell lung cancer. *N Engl J Med* 2016; **375:** 1823-33. doi: 10.1056/NEJMoa1606774
6. Wolchok JD, Hoos A, O'Day S, Weber JS, Hamid O, Lebbé C, et al. Guidelines for the evaluation of immune therapy activity in solid tumors: immune-related response criteria. *Clin Cancer Res* 2009; **15:** 7412-20. doi: 10.1158/1078-0432.CCR-09-1624.
7. Seymour L, Bogaerts J, Perrone A, Ford R, Schwartz LH, Mandrekar S, et al. iRECIST: guidelines for response criteria for use in trials testing immunotherapeutics. *Lancet Oncol* 2017; **18:** e143-52. doi: 10.1016/S1470-2045(17)30074-8
8. Hodi FS, Hwu WJ, Kefford R. Evaluation of immune-related response criteria and RECIST v1.1 in patients with advanced melanoma treated with pembrolizumab. *J Clin Oncol* 2016; **34:** 1510-7. doi: 10.1200/JCO.2015.64.0391
9. Kurra V, Sullivan RJ, Gainor JF, Hodi FS, Gandhi L, Sadow CA, et al. Pseudoprogression in cancer immunotherapy: rates, time course and patient outcomes. [abstract]. *J Clin Oncol* 2016; **34(15 Suppl):** No. 6580. doi: 10.1200/JCO.2016.34.15_suppl.6580
10. Hammer M, Bagley S, Aggarwal C, Bauml J, Nachiappan AC, Simone CB 2nd, et al. Thoracic imaging of non-small cell lung cancer treated with anti-programmed death receptor-1 therapy. *Curr Prob Diagn Radiol* 2018 [Epub ahead of print]. doi: 10.1067/j.cpradiol.2018.01.005
11. Borghaei H, Paz-Ares L, Horn L, Spigel DR, Steins M, Ready NE, et al. Nivolumab versus docetaxel in advanced nonsquamous non-small-cell lung cancer. *N Engl J Med* 2015; **373:** 1627-39. doi: 10.1056/NEJMoa1507643
12. Gettinger SN, Horn L, Gandhi L, Spigel DR, Antonia SJ, Rizvi NA, et al. Overall survival and long-term safety of nivolumab (anti-programmed death 1 antibody, BMS-936558, ONO-4538) in patients with previously treated advanced non-small-cell lung cancer. *J Clin Oncol* 2015; **33**: 2004-12. doi: 10.1200/JCO.2014.58.3708

13. Chiou VL, Burotto M. Pseudoprogression and immune-related response in solid tumors. *J Clin Oncol* 2015; **33:** 3541-3. doi: 10.1200/JCO.2015.61.6870

14. Nishino M, Ramaiya NH, Chambers ES, Adeni AE, Hatabu H, Jänne PA, et al. Immune-related response assessment during PD-1 inhibitor therapy in advanced non-small-cell lung cancer patients. *J Immunother Cancer* 2016; **4:** 84. doi: 10.1186/s40425-016-0193-2

15. Kim HK, Heo MH, Lee HS, Sun JM, Lee SH, Ahn JS, et al. Comparison of RECIST to immune-related response criteria in patients with non-small cell lung cancer treated with immune-checkpoint inhibitors. *Cancer Chemother Pharmacol* 2017; **80:** 591-8. doi: 10.1007/s00280-017-3396-4

16. Eisenhauer EA, Therasse P, Bogaerts J, Schwartz LH, Sargent D, Ford R, et al. New response evaluation criteria in solid tumours: revised RECIST guideline (version 1.1). *Eur J Cancer* 2009; **45:** 228-47. doi: 10.1016/j.ejca.2008.10.026

17. Sarfaty M, Moore A, Dudnik E, Peled N. Not only for melanoma. Subcutaneous pseudoprogression in lung squamous-cell carcinoma treated with nivolumab: a case report. *Medicine (Baltimore)* 2017; **96:** e5951. doi: 10.1097/MD.0000000000005951

18. Kolla BC, Patel MR. Recurrent pleural effusions and cardiac tamponade as possible manifestations of pseudoprogression associated with nivolumab therapy - a report of two cases. *J Immunother Cancer* 2016 **4:** 80. doi: 10.1186/s40425-016-0185-2

19. Izumida T, Kawagishi Y, Tsuji H. Pseudoprogression in lung adenocarcinoma during treatment with nivolumab. *BMJ Case Reports* 2017; doi:10.1136/bcr-2017-219919. [cited 2018 Feb 2]. Available at http://casereports.bmj.com/content/2017/bcr-2017-219919.full

20. Kumagai T, Kimura M, Inoue T, Tamiya M, Nishino K, Imamura F. Delayed pseudoprogression of lung adenocarcinoma accompanied with interstitial lung disease during chemotherapy after nivolumab treatment. *Thorac Cancer* 2017; **8:** 275-7. doi: 10.1111/1759-7714.12431

21. Hochmair MJ, Schwab S, Burghuber OC, Krenbek D, Prosch H. Symptomatic pseudo-progression followed by significant treatment response in two lung cancer patients treated with immunotherapy. *Lung Cancer* 2017; **113:** 4-6. doi: 10.1016/j.lungcan.2017.08.020

22. Schreiber RD, Old LJ, Smyth MJ. Cancer immunoediting: integrating immunity's roles in cancer suppression and promotion. *Science* 2011; **331:** 1565-70. doi: 10.1126/science.1203486

23. Garon EB, Naiyer AR, Hui R, Leighl N, Balmanoukian AS, Eder JP, et al. Pembrolizumab for the treatment of non-small-cell lung cancer. *N Engl J Med* 2015; **372:** 2018-28. doi: 10.1056/NEJMoa1501824

24. Brahmer J, Reckamp KL, Baas P, Crinò L, Eberhardt WEE, Poddubskaya E, et al. Nivolumab versus docetaxel in advanced squamous-cell non-small-cell lung cancer. *N Engl J Med* 2015; **373:** 123-35. doi: 10.1056/NEJMoa1504627

25. Reck M, Rodríguez-Abreu D, Robinson AG, Hui R, Csőszi T, Fülöp A, et al. Pembrolizumab versus chemotherapy for PD-L1-positive non-small-cell lung cancer. *N Engl J Med* 2016; **375:** 1823-33. doi: 10.1056/NEJMoa1606774

26. Rittmeyer A, Barlesi F, Waterkamp D, Park K, Ciardiello F, von Pawel J, et al. Atezolizumab versus docetaxel in patients with previously treated non-small-cell lung cancer (OAK): a phase 3, open-label, multicentre randomised controlled trial. *Lancet* 2017; **389:** 255-65. doi: 10.1016/S0140-6736(16)32517-X

27. Fehrenbacher L, Spira A, Ballinger M, Kowanetz M, Vansteenkiste J, Mazieres J, et al. Atezolizumab versus docetaxel for patients with previously treated non-small-cell lung cancer (POPLAR): a multicentre, open-label, phase 2 randomised controlled trial. *Lancet* 2016; **387:** 1837-46. doi: 10.1016/S0140-6736(16)00587-0

28. Peters S, Gettinger S, Johnson ML, Jänne PA, Garassino MC, Christoph D, et al. Phase II trial of atezolizumab as first-line or subsequent therapy for patients with programmed death-ligand 1-selected advanced non-small-cell lung cancer (BIRCH). *J Clin Oncol* 2017; **35:** 2781-9. doi: 10.1200/JCO.2016.71.9476

29. Hanahan D, Weinberg RA. Hallmarks of cancer: the next generation. *Cell* 2011; **144:** 646-74. doi: 10.1016/j.cell.2011.02.013

30. Guthrie GJ, Charles KA, Roxburgh CS, Horgan PG, McMillan DC, Clarke SJ. The systemic inflammation-based neutrophil-lymphocyte ratio: experience in patients with cancer. *Crit Re Oncol Hematol* 2013; **88:** 218-30. doi: 10.1016/j.critrevonc.2013.03.010

31. Kang MH, Go SI, Song HN, Lee A, Kim SH, Kang JH, et al. The prognostic impact of the neutrophil-to-lymphocyte ratio in patients with small-cell lung cancer. *Br J Cancer* 2014; **111:** 452-60. doi: 10.1038/bjc.2014.317

32. Templeton AJ, McNamara MG, Šeruga B, Vera-Badillo FE, Aneja P, Ocaña A, et al. Prognostic role of neutrophil-to-lymphocyte ratio in solid tumors: a systematic review and meta-analysis. *J Natl Cancer Inst* 2014; **106:** dju124. doi: 10.1093/jnci/dju124

33. Bagley SJ, Kothari S, Aggarwal C, Bauml JM, Alley EW, Evans TL, et al. Pretreatment neutrophil-to-lymphocyte ratio as a marker of outcomes in nivolumab-treated patients with advanced non-small-cell lung cancer. *Lung Cancer* 2017; **106:** 1-7. doi: 10.1016/j.lungcan.2017.01.013

34. Ferrucci PF, Gandini S, Battaglia A, Alfieri S, Di Giacomo AM, Giannarelli D, et al. Baseline neutrophil-to-lymphocyte ratio is associated with outcome of ipilimumab-treated metastatic melanoma patients. *Br J Cancer* 2015; **112:** 1904-10. doi: 10.1038/bjc.2015.180

35. Vrankar M, Zwitter M, Kern I, Stanic K. PD-L1 expression can be regarded as prognostic factor for survival of non-small cell lung cancer patients after chemoradiotherapy. *Neoplasma* 2018; **59:** 101-6. doi: 10.4149/neo_2018_170206N77

36. Wang A, Wang HY, Liu Y, Zhao MC, Zhang HJ, Lu ZY, et al. The prognostic value of PD-L1 expression for non-small cell lung cancer patients: a meta-analysis. *Eur J Surg Oncol* 2015; **41:** 450-6. doi:10.1016/j.ejso.2015.01.020

37. Zhou Z, Zhan P, Song Y. PD-L1 over-expression and survival in patients with non-small cell lung cancer : a meta-analysis. *Transl Lung Cancer Res* 2015; **4:** 203-8. doi: 10.3978/j.issn.2218-6751.2015.03.02

38. Saba L, Poreu M, Schmid B, Flohr T. Dual energy CT: basic principles. In: Cecco CN, Laghi A, Schoepf UJ, Meinel FG, editors. *Dual energy CT in oncology*. Cham, Germany: Springer. p. 1-20.

39. Bensch F, Veen E, Jorritsma A. First-in-human PET imaging with the PD-L1 antibody 89Zr-atezolizumab. Paper presented at: AACR Annual Meeting, Washington Convention Center, April 2, 2017. CT017.

research article

Thyroid cancer detection rate and associated risk factors in patients with thyroid nodules classified as Bethesda category III

Magdalena Mileva[1], Bojana Stoilovska[1], Anamarija Jovanovska[1], Ana Ugrinska[1], Gordana Petrushevska[2], Slavica Kostadinova-Kunovska[2], Daniela Miladinova[1], Venjamin Majstorov[1]

[1] Institute of Pathophysiology and Nuclear Medicine, Faculty of Medicine, Ss. Cyril and Methodius University, Skopje, Republic of Macedonia

[2] Institute of Pathology, Faculty of Medicine, Ss. Cyril and Methodius University, Skopje, Republic of Macedonia

Radiol Oncol 2018; 52(4): 370-376.

Received 19 June 2018
Accepted 23 August 2018

Correspondence: Magdalena Mileva, M.D., Institute of Pathophysiology and Nuclear Medicine, Faculty of Medicine, Ss. Cyril and Methodius University, St. Mother Teresa 17, 1000 Skopje, Republic of Macedonia. Phone: +389 7027 3091; E-mail: m.mileva@medf.ukim.edu.mk

Disclosure: No potential conflicts of interest were disclosed.

Background. Ultrasound guided fine-needle aspiration (FNA) is a standard procedure for thyroid nodules management and selecting patients for surgical treatment. Atypia of undetermined significance (AUS) or follicular lesion of undetermined significance (FLUS), as stated by The Bethesda System for Reporting Thyroid Cytopathology, is a diagnostic category with an implied malignancy risk of 5–15%. The aim of our study was to review cytology and histopathology reports, as well as clinical and ultrasound data, for thyroid nodules reported as AUS/FLUS, in order to evaluate the malignancy rate and to assess factors associated with malignant outcome.

Patients and methods. A total of 112 AUS/FLUS thyroid nodules in 105 patients were evaluated, of which 85 (75.9%) were referred to surgery, 21 (18.8%) were followed-up by repeat FNA and 6 nodules (5.3%) were clinically observed. Each was categorized in two final diagnostic groups - benign or malignant, which were further compared to clinical data of patients and ultrasonographic features of the nodules.

Results. Final diagnosis of malignancy was reached in 35 cases (31.2%) and 77 (68.8%) had benign lesions. The most frequent type of cancer was papillary thyroid carcinoma (PTC) - 58.1% PTC and 25.8% had follicular variant of PTC. Patients' younger age, smaller nodule size, hypoechoic nodule and presence of calcifications were shown to be statistically significant risk factors for malignancy.

Conclusions. The rate of malignancy for the AUS/FLUS diagnostic category in our study was higher than estimated by the Bethesda System. Clinical and ultrasound factors should be considered when decision for patient treatment is being made.

Key words: thyroid nodule; cytology; fine-needle aspiration; ultrasonography; thyroid carcinoma

Introduction

Thyroid nodules are very common finding in the general population. Their detection increases with the use of high frequency ultrasound (US) with a varying prevalence of up to 68%[1], higher in females compared to males and increasing with age.[2] A proper management of thyroid nodules is needed because, even though most cases are of benign etiology, they still carry a malignancy risk, roughly around 5–15% of all detected nodules.[3–5] According to the American Cancer Society, among both men and women, the largest annual increase of cancer incidence rates in the USA from 2006 to 2010 was for thyroid cancer.[6] US guided fine-needle aspiration (FNA) has become the initial test for evaluation of thyroid nodules, a standard tool for detecting thyroid cancer and it provides a better selection

of patients for surgical treatment. In order to have a uniform terminology for reporting the results of FNA and a better communication and understanding among cytopathologists and clinicians, in 2007 The Bethesda System for Reporting Thyroid Cytopathology (TBSRTC) was developed. The implementation of TBSRTC has improved the quality of FNA reporting and has reduced the overall rate of unnecessary thyroid surgeries.[7] However, Bethesda category III (atypia of undetermined significance [AUS] or follicular lesion of undetermined significance [FLUS]) carries controversy as a result of inconsistent usage among pathologists and institutions, its heterogeneity and difficulty to determine the true risk of malignancy for an AUS/FLUS nodule because not all cases in this diagnostic category are referred to surgical treatment.[8] The aim of this study was to evaluate the malignancy risk of thyroid nodules reported as Bethesda category III (AUS/FLUS) on initial FNA and to assess the clinical and US factors associated with malignancy outcome.

Patients and methods

We retrospectively reviewed 4738 cases of thyroid US guided FNAs that were performed at the outpatient's thyroid unit of the Institute of Pathophysiology and Nuclear Medicine, Faculty of Medicine, Ss Cyril and Methodius University, Skopje, from January 2012 to December 2016. In this period, 281 out of the 4738 (5.93%) thyroid nodules were diagnosed as Bethesda Category III. Among them 175 cases were excluded: 167 because of no available data for follow-up and eight because of multinodular goiter (no data about the specific nodule that was category III on FNA, and therefore no significant relation with the histology outcome). The remaining 112 nodules in 105 patients were included in this study. Clinical outcome for the aspirated thyroid nodule was categorized in two final diagnostic groups – benign and malignant. Benign final diagnostic group included: nodules with confirmed benign diagnosis on histopathology report after surgical treatment, nodules diagnosed as Bethesda category II on repeat FNA (rFNA) and nodules which were clinically monitored for at least 6 months with no increase on US (same in size or decreased). Malignant final diagnostic outcome was defined as confirmed malignancy on histopathology report after immediate surgery or Bethesda category V or VI on rFNA (and later confirmed on histopathology). Decision for surgical treatment was mostly based on clinical features (such as age, nodule size), US characteristics of the nodule in question and patient preference.

Clinical features, US findings and pathology records were reviewed for each case. The final diagnostic groups were compared for age, gender, nodule size, US features (nodule composition, echogenicity, vascularization and calcifications) and results from a thyroid ^{99m} Tc-pertechnetate scan. According to the scan, the thyroid nodules were classified into one of three groups: hypofunctioning (cold nodule with reduced radioisotope uptake), isofunctioning nodule (with radioisotope uptake comparable to the surrounding non-nodular tissue) and hyperfunctioning (hot nodule with increased ^{99m} Tc-pertechnetate tracer uptake).

Ultrasonography for detecting thyroid nodules was performed with a high-resolution broadband linear array transducer (LN 12-3, Philips HD6 machine). Cameco syringe pistol with 20ml syringe and 21G needle were used for the US guided FNA of the nodules. Each US examination and subsequent FNA was performed by the same nuclear medicine specialist. The cytology smears were prepared when needle contents were expelled onto a glass slide and smeared using a second slide. Two types of slides were done for each lesion: one fixed in 95% ethanol and Papanicolaou stained, and other air dried and May Grunwald-Giemsa stained. Cytology findings were reported by a cytopathologist with more than 10 years experience in the field at the Institute of pathology, Faculty of Medicine, Ss Cyril and Methodius University, Skopje.

Statistical analysis was performed using IBM SPSS Statistics v20 software. Categorical variables for US features and malignancy rates were compared using $\chi 2$ tests and Fisher's exact tests when appropriate. Continuous variables were compared using t-test. Logistic regression analysis was performed to assess the odds ratios for the risk of malignancy according to clinical and US features and multivariate logistic regression with a backward stepwise selection method was performed to select independent predictors of malignancy. In all cases p-value < 0.05 was considered statistically significant.

Results

A total of 112 Bethesda category III nodules from 105 patients were included in this study. The clinical data and US features of all nodules are shown in Table 1. Among the 112 nodules, 35 (31.2%) had

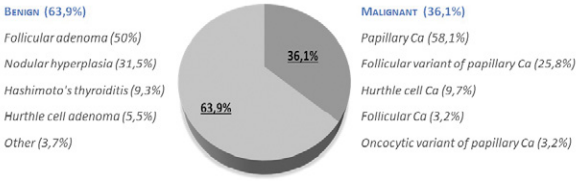

FIGURE 1. Histologic outcomes of Bethesda Category III nodules from patients who underwent direct surgical treatment. Malignancies were found in 36.1% of AUS/FLUS nodules who were managed with surgery without a repeat cytology. Papillary Thyroid Carcinoma and its Follicular variant were the most common types of cancer, accounting for a total of 83.9% of all malignancies. Among the benign lesions, Follicular adenomas presented in 50% of these cases, and Nodular hyperplasia was second in line with a frequency of 31.5%.

final diagnosis of malignancy and 77 (68.8%) had benign lesions. Of the total number, 85 nodules (75.9%) from 81 patient received direct surgical treatment, 21 (18.8%) were followed-up by rFNA and 6 (5.3%) were clinically observed. The malignancy rate for patients who received immediate surgical treatment was 36.1%. Papillary thyroid carcinoma (PTC) accounted for most of the malignant outcomes (58.1% PTC and 25.8% follicular variant of PTC) and among the benign histopathology outcomes, 50% of the cases were follicular adenoma (Figure 1). Of the 21 nodules undergoing rFNA, 16 (76.2%) were categorized as benign lesions (Bethesda II, none of whom underwent surgical treatment), 1 (4.8%) was suspicious for follicular neoplasm (Bethesda IV, later confirmed as Follicular Adenoma on histopathology report), and in 4 (19.0%) the second FNA was suspicious for malignancy (Bethesda V, later histopathologically confirmed malignancy in all 4 cases, all of whom were PTC). The remaining 6 nodules were monitored within an average of 7.6 months, in which time they showed no changes or regression in the US evaluation.

A comparison of clinical data and the final diagnostic outcome – benign or malignant group, is summarized in Table 2. Patients with malignant outcome were significantly younger that those with benign outcome ($p < 0.01$, OR 0.953) and malignant nodules were significantly smaller in size than the benign nodules ($p < 0.05$, OR 0.952). The mean age and nodule size for patients referred to surgery was 51.96 ± 12.33 years and 24 ± 9.33mm, and 56 ± 13.72 years and 21.6±9.69mm for patients managed with rFNA or observation, although these differences were not statistically significant. Thyroid scan was performed in total of 60 cases (53.6%) and univariate analysis showed no significant difference between the benign and malignant groups by thyroid scan characteristics (Table 2).

As shown in Table 3, when US features of benign and malignant Bethesda III nodules were compared, most of the malignant nodules had solid composition on US (82.9%); however, this difference was not statistically significant. On the other

TABLE 1. Clinical data of patients and US features of Bethesda category III nodules

Variables		
Patients, n	105	
Age (y), range	52,9 ± 12,7*	(24–77)
Gender		
Male	18	17.10%
Female	87	82.90%
Thyroid nodules, n (total)	**112**	
Benign	**77**	**68.8%**
Malignant	**35**	**31.2%**
Nodule size (mm), range	23,4 ± 9,4*	(8–60)
US features		
Composition		
Solid	83	74.1%
Mixed	25	22.3%
Cystic	4	3.6%
Echogenicity		
Anechoic	3	2.7%
Hypoechoic	56	50.0%
Isoechoic	47	42.0%
Hyperechoic	6	5.4%
Calcifications		
No calcifications	88	78.6%
Microcalcifications	17	15.2%
Macrocalcifications	7	6.3%
Vascularisation		
No vascularisation	20	1.,9%
Low	18	16.1%
Peripheral	16	14.3%
Central	58	51.8%
Thyroid scan		
No scan	52	46.4%
Hypofunctioning (Cold)	19	17.0%
Isofunctioning	34	30.3%
Hyperfunctioning (Hot)	7	6.3%

* Mean ± standard deviation

TABLE 2. Comparison of clinical data of benign and malignant thyroid nodules in 105 patients with Bethesda III cytology report

Variables	Final outcome		p-value
	Benign (n = 71)	Malignant (n = 34)	
Age (y),	54.9 ± 11.7*	48 ± 14.2*	< 0.01 (0.005)
range	(25–77)	(24–71)	OR 0.953 (95% CI 0.922–0.986)
Gender			ns (0,506)
Male	14 (19.7%)	4 (11.7%)	
Female	57 (80.3%)	30 (88.3%)	
Nodule size (mm),	24.6 ± 9.1*	20.7 ± 9.8*	< 0.05 (0.048)
range	(10–60)	(8–47)	OR 0.952 (95% CI 0.907-1.00)
Thyroid scan	**number of nodules:**		ns (0.117)
Hypofunctioning (Cold)	10 (23.8%)	9 (50.0%)	
Isofunctioning	25 (59.5%)	9 (50.0%)	
Hyperfunctioning (Hot)	7 (16.7%)	0 (0.0%)	

* mean ± standard deviation; n = number of patients; OR = odds ratio; ns = non significant

TABLE 3. Comparison of US features of benign and malignant thyroid nodules with Bethesda III cytology report

Variables	Final outcome		p-value
	Benign n = 77 (68.8%)	Malignant n = 35 (31.2%)	
Composition			ns (0.372)
Solid	54 (70.1%)	29 (82.9%)	
Mixed	20 (26.0%)	5 (14.3%)	
Cystic	3 (3.9%)	1 (2.9%)	
Echogenicity			
Anechoic	3 (3.9%)	0 (0.0%)	ns (0.999)
Hypoechoic	31 (40.3%)	25 (71.4%)	< 0.01 (0.003)
			OR 3.710 (95% CI 1.565–8.795)
Isoechoic	38 (49.4%)	9 (25.7%)	< 0.05 (0.021)
			OR 0.355 (95% CI 0.147–0.856)
Hyperechoic	5 (6.5%)	1 (2.9%)	ns (0.216)
Calcifications			
No calcifications	68 (88.3%)	20 (57.1%)	< 0.01 (0.000)
			OR 0.176 (95% CI 0.067–0.463)
Microcalcifications	8 (10.4%)	9 (25.7%)	< 0.05 (0.042)
			OR 2.986 (95% CI 1.041-8.564)
Macrocalcifications	1 (1.3%)	6 (17.1%)	< 0.05 (0.012)
			OR 15.724 (95% CI 1.814–136.318)
Vascularisation			
No vascularisation	10 (13.0%)	10 (28.6%)	ns (0.051)
Peripheral	15 (19.5%)	1 (2.9%)	< 0.05 (0.046)
			OR 0.122 (95% CI 015–0.961)
Central	41 (53.2%)	17 (48.6%)	ns (0.646)
Low	11 (14.3%)	7 (20%)	ns (0.447)

n = number of nodules; ns = non significant; OR = odds ratio

hand, hypoechogenicity ($p < 0.01$), presence of microcalcifications ($p < 0.05$) and macrocalcifications ($p < 0.05$) were significant risk factors of malignancy on univariate analysis, with odds ratios of 3.710, 2.986 and 15.724, respectively. Isoechogenicity ($p < 0.05$), absence of calcifications ($p < 0.01$) and peripheral vascularization ($p < 0.05$) of the nodules were US features significantly associated with benign outcome.

On multivariate logistic regression model, age ($p < 0.0001$, OR 0.964, 95% CI 0.950–0.979), hypoechogenicity ($p = 0.005$, OR 3.914, 95%CI 1,516–10.106), microcalcifications ($p < 0.05$, OR 3.601, 95% CI 1.102–11.772) and macrocalcifications ($p = 0.01$, OR 21.001, 95% CI 2.058–214.296) remained as significant independent predictors of malignancy.

Discussion

The Bethesda System for Reporting Thyroid Cytopathology proposes limited usage of diagnostic category III (AUS/FLUS) of approximately 7 % or less of all thyroid FNAs.[8] In our study, in a period of 4 years, only 5.93% of all thyroid FNAs were reported as AUS/FLUS which is within the recommended 7%. On the other hand, according to TBSRTC, the risk of malignancy for this diagnostic category is estimated to be only 5–15%[8], but in our retrospective study the malignancy rate was considerably higher; final diagnosis of malignancy had 31.2% of all cases included and 36.1% of the cases who underwent immediate surgical resection. PTC and its follicular variant accounted for 83.9 % of all malignant tumors. Recent studies have also reported malignancy rates well above the predicted 5–15%. Gweon *et al*. reported a relatively high overall risk of malignancy for initial Bethesda III thyroid nodules of 55.5% and even higher for nodules with direct surgery (78.3%).[9] Ho *et al.* presented a range of the true prevalence of malignancy, lying between a lower-bound estimate of 26.6% which included all AUS/FLUS nodules (assuming all observed nodules were benign, decision subject to verification bias) and an upper-bound estimate of 37.8% risk of malignancy which was calculated based only on the AUS/FLUS nodules selected to undergo surgery after initial or repeated Bethesda III cytology.[10] In other studies, the risk of malignancy was found to be 35.3–59.5%[11–13], again higher compared to the proposed one in the Bethesda System. On the other hand, in their cohort study, Nagarkatti *et al.* reported an overall malignancy rate of 15.7%, even though almost 75% of the included 203 patients had surgery and they also found that PTC was the most common, with total of 70% of all cases.[14] In another study with a total of 96 malignant diagnoses even 90% of them were papillary carcinomas.[15]

In most of the cases, different clinical and especially ultrasonographic features impact the decision for AUS/FLUS nodule management, considering that some of those features have association with higher malignancy risk. Several studies have shown various results about the influence of age as a risk factor of thyroid malignancy. Ryu *et al.* reported that older age (≥40 years) is associated with an increased risk of malignancy[11], whereas others found that age is not a significant predictor of malignancy in AUS/FLUS nodules.[9,13] Conversely, Godazandeh *et al.* reported that in younger patients the prevalence of thyroid carcinoma is higher[16], and in another study surgery without rFNA is recommended for younger patients.[14] Latter findings are in concordance with our results that younger age is a significant independent factor for malignancy in this Bethesda diagnostic category. Nevertheless, this could be because of a selection bias based on younger patients being referred to surgery more often in our study, though this finding was not statistically significant. Nodule size is reported to have no predictive value of malignancy and it should not be used as a reliable factor for clinical decision making[16,17], although Kamran *et al.* suggest a threshold of approximately 2 cm in nodule diameter with strong evidence that size > 2 cm is associated with an increased risk of well-differentiated thyroid cancer.[18] We found that nodules in malignant group are significantly smaller than those in the benign group, but on the multivariate analysis this factor was not confirmed to be an independent predictor for malignancy. We found that nodules in malignant group are significantly smaller than those in the benign group, but on the multivariate analysis this factor was not confirmed to be an independent predictor for malignancy.

According to the 2015 American Thyroid Association Management Guidelines for Adult Patients with Thyroid Nodules and Differentiated Thyroid Cancer, hyperfunctioning nodules do not require FNA, since they rarely harbor malignancy.[19] Although it is generally accepted that the risk of cancer in a hyperfunctioning thyroid nodule is low, in 14 case series which Mirfakhraee *et al.* recently reviewed, the risk was estimated to be 3%.[20] In our study, the total number of evaluated nodules which underwent thyroid scintigraphy

was not sufficient to estimate the malignancy risk in AUS/FLUS hyperfunctioning thyroid nodules; nevertheless, there was no malignant hyperfunctioning nodule in our group.

Marked hypoechogenicity, microcalcifications, irregular margins, taller than wide shape, and central vascularization are considered US features most likely related to malignancy.[21,22] In a meta-analysis including nine studies and a total of 1851 nodules with indeterminate cytology aspirates, only the presence of microcalcifications was significantly associated with malignancy and central vascularization presented with the best specificity (96%).[3] This finding is consistent with our results regarding microcalcifications as predictor of malignancy, with OR of 3.601 on multivariate analysis. We found that macrocalcifications are as well associated with malignancy in Bethesda III nodules ($p = 0.012$). Both (micro- and macrocalcifications) are considered as suspicious US features by the Korean Society of Thyroid Radiology.[23] Similarly, Jeong *et al.* reported that presence of micro and macrocalcicfications had significantly higher odds compared with no calcifications (OR: 5.17 and 12.22, respectively). However, they did not find statistically significant odds for marked hypoechogencity ($p = 0.17$).[12] In a previous study, with 395 analyzed Bethesda III nodules, when the US features of repeat Bethesda III nodules were evaluated, there was again no significant association between marked hypoehogenicity of the nodule and malignant outcome.[13] The reason for this discrepancy from our results, considering the relatively high statistical significance for hypoechoic nodules that we found ($p = 0.003$), might be in the absence of further subclassification into mild, moderate and marked level of hypoechogenicity in our study. We did not find any significance between central vascularization of the nodules and malignant outcome, a result in concordance with a meta-analysis performed on 5 studies including 540 nodules, which indicated that there was no significant difference in internal vascularity (95% CI: -72.067, 2.824) between malignant and benign thyroid nodules.[24] We did not evaluate margins and taller than wide shape, since these parameters were not always available in the US reports included in this study.

Because this was an observational retrospective study it had several limitations. First, 62.3% of all AUS/FLUS nodules (175/281) were excluded from the analysis because of lack of follow-up data. Second, the decision for clinical management in some extend was influenced from patient preference so that potential clinical or US risk factors were not considered. And finally, observed nodules without histopathological confirmation could have been subject of a verification bias, since they can also carry a malignant potential. Given that most of the published studies are also retrospective, this could contribute to the vast variations in the malignancy rates detected for AUS/FLUS nodules. Therefore, more prospective studies using Bethesda System are required in order to provide further insight and define more accurate risk stratification and patient management recommendations. Recent studies have also emphasized the importance of molecular testing, particularly BRAF ^{V600E} mutation detection and its role as an adjunct to clinical and US features for better decision making.[25,26] In a study which included 52 nodules with indeterminate cytology, molecular testing had positive predictive value of 100% for these lesions.[27] In another recently published meta-analysis with a total of 88 studies included, the mutation rate of BRAF ^{V600E} was 13.77% in AUS/FLUS category with a low sensitivity (40.1%) but significantly high specificity of 99.5% while evaluating the diagnostic value of BRAF ^{V600E} testing.[28] Therefore, molecular analysis can additionally help clinicians in guiding patient management, if routinely available.

Conclusions

In conclusion, the risk of malignancy in AUS/FLUS nodules in our study was higher than estimated by TBSRTC. Recommendation for further management should not be based solely on pathology reports from FNA or rFNA. All clinical and US risk factors (such as patient age, hypoechogenic nodules and presence of calcifications) should be taken into consideration in reaching final decision for patient treatment.

References

1. Guth S, Theune U, Aberle J, Galach A, Bamberger CM. Very high prevalence of thyroid nodules detected by high frequency (13 MHz) ultrasound examination. *Eur J Clin Invest* 2009; **39:** 699-706. doi: 10.1111/j.1365-2362.2009.02162.x

2. Jiang H, Tian Y, Yan W, Kong Y, Wang H, Wang A, et al. The prevalence of thyroid nodules and an analysis of related lifestyle factors in Beijing communities. *Int J Environ Res Public Health* 2016; **13:** 1-11. doi: 10.3390/ijerph13040442

3. Remonti LR, Kramer CK, Leitao CB, Pinto LCF, Gross JL. Thyroid ultrasound features and risk of carcinoma: a systematic review and meta-analysis of observational studies. *Thyroid* 2015; **25:** 538-50. doi: 10.1089/thy.2014.0353

4. Frates MC, Benson CB, Doubilet PM, Kunreuther E, Contreras M, Cibas ES, et al. Prevalence and distribution of carcinoma in patients with solitary and multiple thyroid nodules on sonography. *J Clin Endocrinol Metab* 2006; **91:** 3411-17. doi: 10.1210/jc.2006-0690

5. Welker MJ, Orlov D. Thyroid nodules. *Am Fam Physician* 2003; **67:** 559-66; 573.

6. Siegel R, Ma J, Zou Z, Jemal A. Cancer statistics, 2014. *CA Cancer J Clin* 2014; **64:** 9-29. doi: 10.3322/caac.21208

7. Crowe A, Linder A, Hameed O, Salih C, Roberson J, Gidley J, et al. The impact of implementation of the Bethesda System for Reporting Thyroid Cytopathology on the quality of reporting, 'risk' of malignancy, surgical rate, and rate of frozen sections requested for thyroid lesions. *Cancer Cytopathol* 2011; **119:** 315-21. doi: 10.1002/cncy.20174

8. Cibas ES, Ali SZ. The 2017 Bethesda System for Reporting Thyroid Cytopathology. *J Am Soc Cytopathol* 2017; **6:** 217-22. doi: 10.1016/j.jasc.2017.09.002

9. Gweon HM, Son EJ, Youk JH, Kim JA. Thyroid nodules with Bethesda system III cytology: can ultrasonography guide the next step? *Ann Surg Oncol* 2013; **20:** 3083-8. doi: 10.1245/s10434-013-2990-x

10. Ho AS, Sarti EE, Jain KS, Wang H, Nixon IJ, Shaha AR, et al. Malignancy rate in thyroid nodules classified as Bethesda category III (AUS/FLUS). *Thyroid* 2014; **24:** 832-9. doi: 10.1089/thy.2013.0317

11. Ryu YJ, Jung YS, Yoon HC, Hwang MJ, Shin SH, Cho JS, et al. Atypia of undetermined significance on thyroid fine needle aspiration: surgical outcome and risk factors for malignancy. *Ann Surg Treat Res* 2014; **86:** 109. doi: 10.4174/astr.2014.86.3.109

12. Jeong SH, Sook HH, Lee EH. Outcome of Bethesda III thyroid nodules and its correlation with ultrasonographic features and BRAF. Poster presented at European Congress of Radiology; 2013 March 7-11; Vienna, Austria. No. C-0842. doi: 10.1594/ecr2013/C-0842

13. Yoo MR, Gweon HM, Park AY, Cho KE, Kim J, Youk JH, et al. Repeat diagnoses of Bethesda category III thyroid nodules: what to do next? *PLoS One* 2015; **10:** 1-10. doi: 10.1371/journal.pone.0130138

14. Nagarkatti SS, Faquin WC, Lubitz CC, Garcia DM, Barbesino G, Ross DS, et al. The management of thyroid nodules with atypical cytology on fine needle aspiration biopsy. *Ann Surg Oncol* 2013; **20:** 1-13. doi: 10.1245/s10434-012-2601-2

15. Vanderlaan PA, Marqusee E, Krane JF. Usefulness of diagnostic qualifiers for thyroid fine-needle aspirations with atypia of undetermined significance. *Am J Clin Pathol* 2011; **136:** 572-7. doi: 10.1309/AJCPO0BQ2YSKPXXP

16. Godazandeh G, Kashi Z, Zargamataj S, Fazli M, Ebadi R, Kerdabadi EH, et al. Evaluation the relationship between thyroid nodule size with malignancy and accuracy of fine needle aspiration biopsy (FNAB). *Acta Inform Medica* 2016; **24:** 347-51. doi: 10.5455/aim.2016.24.347-351

17. McHenry CR, Huh ES, Machekano RN. Is nodule size an independent predictor of thyroid malignancy? *Surgery* 2018; **144:** 1062-9. doi: 10.1016/j.surg.2008.07.021

18. Kamran SC, Marqusee E, Kim M, Frates M, Ritner J, Peters H, et al. Thyroid nodule size and prediction of cancer. *J Clin Endocrinol Metab* 2013; **98:** 564-70. doi: 10.1210/jc.2012-2968

19. Haugen BR, Alexander EK, Bible KC, Doherty GM, Mandel SJ, Nikiforov YE, et al. 2015 American thyroid association management guidelines for adult patients with thyroid nodules and differentiated thyroid cancer: The American thyroid association guidelines task force on thyroid nodules and differentiated thyroid cancer. *Thyroid* 2016; **26:** 1-133. doi: 10.1089/thy.2015.0020

20. Mirfakhraee S, Mathews D, Peng L, Woodruff S, Zigman JM. A solitary hyperfunctioning thyroid nodule harboring thyroid carcinoma: review of the literature. *Thyroid Res* 2013; **6:** 7. doi: 10.1186/1756-6614-6-7

21. Kwak JY. Indications for fine needle aspiration in thyroid nodules. *Endocrinol Metab* 2013; **28:** 81-5. doi: 10.3803/EnM.2013.28.2.81

22. Lingam RK, Qarib MH, Tolley NS. Evaluating thyroid nodules: Predicting and selecting malignant nodules for fine-needle aspiration (FNA) cytology. *Insights Imaging* 2013; **4:** 617-24. doi: 10.1007/s13244-013-0256-6

23. Moon WJ, Baek JH, Jung SL, Kim DW, Kim EK, Kwak JY, et al. Ultrasonography and the ultrasound-based management of thyroid nodules: consensus statement and recommendations. *Korean J Radiol* 2011; **12:** 1-14. doi: 10.3348/kjr.2011.12.1.1

24. Khadra H, Bakeer M, Hauch A, Hu T, Kandil E. Is vascular flow a predictor of malignant thyroid nodules? A meta-analysis. *Gland Surg* 2016; **5:** 576-82. doi: 10.21037/gs.2016.12.14

25. Maia F, Zantut-Wittmann D. Thyroid nodule management: clinical, ultrasound and cytopathological parameters for predicting malignancy. *Clinics* 2012; **67:** 945-54. doi: 10.6061/clinics/2012(08)15

26. Ohori N, Nikiforova M, Schoedel K, Lebeau S, Hodak S, Seethala RR, et al. Contribution of molecular testing to thyroid fine-needle aspiration cytology of 'follicular lesion of undetermined significance/atypia of undetermined significance'. *Cancer Cytopathol* 2010; **118:** 17-23. doi: 10.1002/cncy.20063

27. Nikiforov YE, Steward DL, Robinson-Smith TM, Haugen BR, Klopper JP, Zhu Z, et al. Molecular testing for mutations in improving the fine-needle aspiration diagnosis of thyroid nodules. *J Clin Endocrinol Metab* 2009; **94:** 2092-8. doi: 10.1210/jc.2009-0247

28. Su X, Jiang X, Xu X, Wang W, Teng X, Shao A, et al. Diagnostic value of BRAF (V600E)-mutation analysis in fine-needle aspiration of thyroid nodules: a meta-analysis. *Onco Targets Ther* 2016; **9:** 2495-509. doi: 10.2147/OTT.S101800

research article

Optic nerve ultrasound for fluid status assessment in patients with severe preeclampsia

Gabrijela Brzan Simenc[1], Jana Ambrozic[2], Katja Prokselj[2], Natasa Tul[1], Marta Cvijic[2], Tomislav Mirkovic[3], Helmut Karl Lackner[4], Miha Lucovnik[1]

[1] Department of Perinatology, Division of Obstetrics and Gynecology, University Medical Center Ljubljana, Slovenia
[2] Department of Cardiology, University Medical Center Ljubljana, Slovenia
[3] Department of Anesthesiology and Intensive Therapy, University Medical Center Ljubljana, Slovenia
[4] Otto Loewi Research Center, Section of Physiology, Medical University of Graz, Austria

Radiol Oncol 2018; 52(4): 377-382.

Received 9 August 2018
Accepted 2 November 2018

Correspondence to: Miha Lucovnik, M.D., Ph.D., Division of Obstetrics and Gynecology, University Medical Centre Ljubljana, Šlajmerjeva 4, SI-1000 Ljubljana, Slovenia. Phone: +386 31 318 681; Fax: +386 1 439 75 90; E-mail: miha.lucovnik@kclj.si

Disclosure: No potential conflicts of interest were disclosed.

Background. There are no data on usefulness of optic nerve sheath diameter (ONSD) as a marker of patient's fluid status in preeclampsia. The objective was to examine potential correlation between ONSD and lung ultrasound estimates of extravascular lung water in severe preeclampsia.

Patients and methods. Thirty patients with severe preeclampsia were included. Optic and lung ultrasound were performed within 24 hours from delivery. ONSD was measured 3 mm behind the globe. Lung ultrasound Echo Comet Score (ECS) was obtained summing B-lines ("comet tails") in parasternal intercostal spaces bilaterally. Pearson's correlation analysis was used to assess the relationship between ONSD and ECS ($p < 0.05$ significant).

Results. Median ONSD was 5.7 mm (range 3.8–7.5 mm). Median ECS value was 19 (range 0-24). Statistically significant correlation was found between ONSD and ECS ($r^2 = 0.464$; $p < 0.001$).

Conclusions. Significant correlation between ONSD and ECS suggests optic ultrasound could be used for assessing fluid status and guiding peripartum fluid therapy in patients with severe preeclampsia.

Key words: preeclampsia; fluid status; ocular ultrasound; optic nerve sheath diameter; lung ultrasound; comet tail (B-lines) sign

Introduction

Preeclampsia, a multisystem disorder characterized by new-onset hypertension and either proteinuria or end-organ dysfunction after 20 weeks of gestation, affects 2 to 5% of pregnancies.[1-4] The ability to assess fluid status is fundamental for optimal management of preeclamptic patients. Insufficient intravascular volume results in decreased oxygen delivery to tissues and exacerbates organ dysfunction.[5,6] On the other hand, fluid excesses can lead to tissue edema due to extravascular fluid accumulation, which is especially pronounced in preeclampsia because of altered endothelial function causing increased capillary permeability.[5,7-9] The Confidential Enquiry into Maternal Deaths in the United Kingdom reported six deaths between 1994 and 1996 due to adult respiratory distress syndrome that appeared to be related to poor fluid management in women with preeclampsia.[10] On the basis of this report, recommendations on limiting intravenous fluids to not more than to 80 ml/hour or 1 ml/kg/hour have been made.[11] Higher rates may, however, be necessary in some preeclamptic patients to adequately correct tissue hypoperfusion.[12,13] A quick, non-invasive, bedside

test to assess fluid status of patients with preeclampsia would, therefore, be very helpful to clinicians working in obstetric units.

Ultrasound measurement of optic nerve sheath diameter (ONSD) has been described as a simple and reliable means of determining increased intracranial pressure due to cerebral edema in non-pregnant critically ill patients.[14,15] Signs of cerebral edema have been reported on magnetic resonance imaging in 71% to 100% of patients with preeclampsia and ONSD has recently been described to be increased in these patients.[16-20] It is not clear, however, whether increased ONSD can be used as a marker of systemic tissue edema and fluid overload in this disease. The concern is that once dilated, ONSD could stay in pathologic values for several days. Therefore, more data on correlation between ONSD and other markers of fluid status are needed before ONSD measurements can be recommended as a guide to peripartum fluid management in preeclampsia.

Studies by our group and others have demonstrated that severe preeclampsia is associated with an increase in extravascular lung water (EVLW), which can be identified by lung ultrasound before appearance of clinical signs of pulmonary edema.[13,21] The aim of the present study was to examine potential correlation between ONSD values and lung ultrasound estimates of EVLW in patients with severe preeclampsia.

Patients and methods

This prospective, observational study was performed at a single tertiary perinatal center from April 2015 to April 2017. Research was conducted following the Helsinki Declaration. All women included in the study provided written informed consent for study participation. The National Medical Ethics Committee approved the study (Project number 83/09/14, approved on 09/16/2014).

Study participants

Consecutively admitted patients with singleton pregnancies complicated by severe preeclampsia were included in the study at hospital admission. Severe preeclampsia was defined by severe features of preeclampsia using the American College of Obstetricians and Gynecologist Task Force on Hypertension in Pregnancy recommendations: new-onset cerebral or visual disturbances; pulmonary oedema; thrombocytopenia (platelet count < 100,000 /microliter); elevated liver enzymes (transaminases) to twice the normal upper limit, severe persistent pain in the right upper or middle upper abdomen that does not respond to medication and is not explained by another condition or both; renal insufficiency (serum creatinine > 97 μmol/L), or a doubling of serum creatinine in the absence of other renal disease; systolic blood pressure ≥ 160 mm Hg or a diastolic blood pressure ≥ 110 mm Hg measured on more than one occasion at least 4 hours apart while the patient is on bed rest (unless antihypertensive therapy was initiated before this time).[22] As per our institution's standard protocol all patients were managed in a high dependency setting antepartum and at least 24 hours post-delivery. Blood pressure was monitored continuously. Fluid intake and urine output were assessed hourly, and blood tests were repeated at least every 12 hours to monitor kidney function, electrolytes, full blood count, transaminases, and bilirubin. Magnesium sulphate was used for eclampsia prophylaxis as a 4 g intravenous loading dose, followed by 1 g/hour infusion. Antihypertensive treatment with intravenous hydralazine or labetalol was used to maintain systolic blood pressure at < 160 mmHg and diastolic blood pressure at < 110 mmHg. Intravenous and oral fluid intake was minimized, and neither fluids nor diuretics were routinely administered to treat oliguria.

Optic nerve sheath diameter (ONSD) and extravascular lung water (EVLW) measurements

Ultrasound examination was performed using Vivid S6 scanner (GE Vingmed Ultrasound) within 24 hours from delivery. A 8L-RS linear probe was used for ONSD measurements and a 3Sc-RC cardiac probe for EVLW measurements.

ONSD measurements were performed in supine patients according to previously published protocol.[14,15,19,23,24] Ultrasound gel was applied over the closed upper eyelid. Ultrasound probe was placed on the temporal area of the eyelid. The probe was then angled in order to display the entry of the optic nerve into the globe. ONSD was measured 3 mm behind the globe in the transverse plane perpendicular to the optic nerve. For each optic nerve three measurements were made. The reported ONSD corresponds to the mean of the six values obtained for each patient (three measurements for each eye). Three mm behind the ocular globe, the optic nerve sheath is surrounded only by orbital fat and can distend in cases of raised intracranial pres-

sure due to cerebral oedema. ONSD of > 5.8 mm has been shown to detect increased intracranial pressure with a sensitivity of 90% and a specificity of 84%.[25] Figure 1 presents an optic ultrasound image of one of the patients with severe preeclampsia included in the study. An increased ONSD can be clearly seen (Figure 1).

Lung ultrasound was performed according to a systematic protocol in supine patients.[26,27] Increased amount of EVLW can be diagnosed by multiple B-lines or "comet tails" (Figure 2).[28] B-lines are discrete laser-like vertical hyperechoic reverberation artefacts that arise from the pleural line and extend to the bottom of the screen without fading, and move synchronously with lung sliding.[28] They represent a reverberation artefact through oedematous interlobular septa or alveoli.[26,28] The sum of B-lines found in four areas in the parasternal line on the right (from the second to the fifth intercostal space), and in three areas in the parasternal line on the left (from the second to the fourth intercostal space) yielded the Echo Comet Score (ECS) denoting the amount of EVLW.

Inter-observer and intra-observer reproducibility for ONSD and EVLW measurements was validated at offline analyses in 10 randomly selected subjects (five preeclamptic patients and five controls) by two independent operators. The second operator was blinded to the patient's status (preeclampsia with severe features or control group).

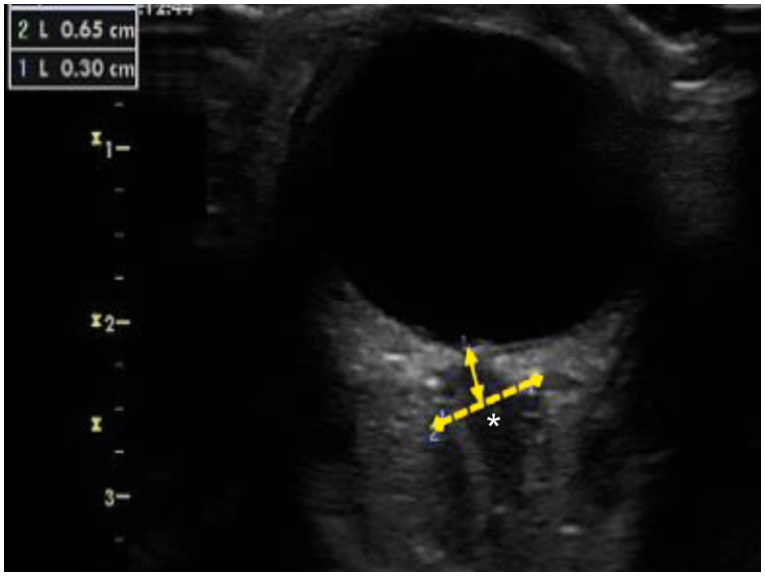

FIGURE 1. Increased optic nerve sheath diameter in one of the patients with severe preeclampsia included in the study (*).

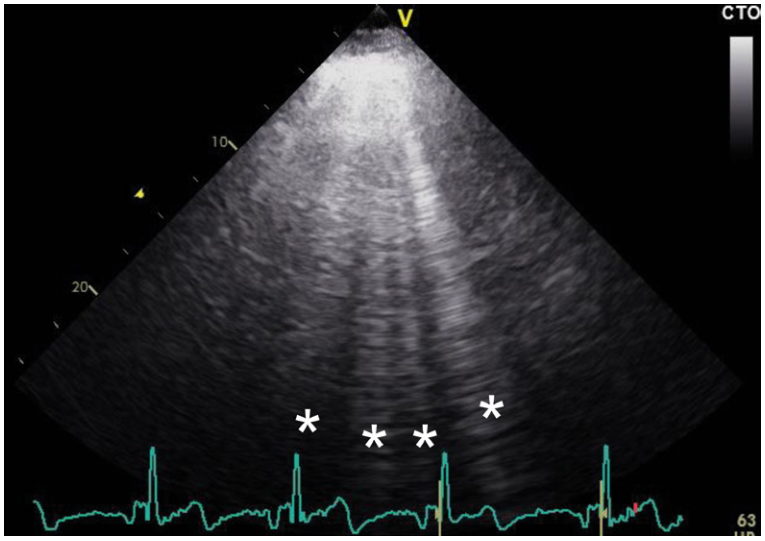

FIGURE 2. B-lines or "comet tails" (*) arising from the pleural line and spreading up to the edge of the screen representing excess of extravascular lung water in one of the patients with severe preeclampsia included in the study.

Statistical analysis

Intra-class correlation coefficient (ICC) was used to test inter-observer and intra-observer reproducibility of the analysed parameters. Pearson's correlation analysis was used to assess the relationship between ONSD and ECS measurements. A two-tailed p value < 0.05 was considered statistically significant. The software used for statistical analysis was IBM SPSS Statistics for Windows Version 21.0 (Armonk, NY: IBM Corp.).

Results

Thirty severe preeclamptic patients were included in the study. Maternal race was Caucasian in all but one case of an Asian woman. None of the women included admitted to tobacco smoking, alcohol or drug abuse during pregnancy. None of the participants had chronic hypertension, pre-existent or gestational diabetes mellitus. None had prior ocular surgery or ocular trauma. Median maternal age was 31 years (range 21–44 years); median maternal pre-pregnancy body mass index was 23 kg/m^2 (range 19–32 kg/m^2), and median gestational age at study inclusion was 32 5/7 weeks (range 22 3/7–39 4/7 weeks). Twenty-three (77%) patients were nulliparous. Severe features of preeclampsia meeting the inclusion criteria were: hypertension in all 30 cases, headache in 14 (47%) cases, visual disturbances in four (13%) cases, elevated liver enzymes in 10 (33%) cases, thrombocytopenia in three (10%)

TABLE 1. Median and range of B-lines in four parasternal intercostal areas on the right (from the second to the fifth intercostal space) and three parasternal intercostal areas on the left (from the second to the fourth intercostal space)

Parasternal area	Median number of B-lines	Range
2nd intercostal space right	0	0–3
3rd intercostal space right	2	0–6
4th intercostal space right	4	1–4
5th intercostal space right	3	1–7
2nd intercostal space left	3	0–6
3rd intercostal space left	2	0–8
4th intercostal space left	3	0–6

cases, and right upper abdomen pain in five (17%) cases.

All 30 patients were treated with magnesium sulphate as per our institution's protocol. Magnesium sulphate was being administered as a continuous intravenous infusion of 1 g/ hour (in a 50 ml/hour infusion) during all ultrasound examinations. In 24 (80%) patients, magnesium sulphate infusion was the only intravenous fluid intake. In six (20%) patients, additional 30 ml/hour infusion of crystalloids was being administered (always limiting intravenous fluid administration to 80 ml/hour). Intravenous hydralazine was necessary for blood pressure control in six (20%) patients.

Median ONSD value was 5.7 mm (inter-quartile range 5.2–6.0 mm; range 3.8–7.5 mm). Thirteen (43%) patients had ONSD > 5.8 mm. Median ECS value was 19 (range 0–24). Table 1 presents median and range values of B-lines in all areas analyzed.

Intra- and inter-observer agreement was excellent for ONSD measurements (ICC 0.973 [0.890–0.993] and ICC 0.960 [0.839–0.990], respectively). Similarly, intra- and inter-observer agreement was also excellent for EVLW measurements (ICC 0.968 [0.915–0.987] and ICC 0.898 [0.846–0.993], respectively).

Statistically significant correlation was found between ONSD and ECS values ($r^2 = 0.464$; $p < 0.001$) (Figure 3).

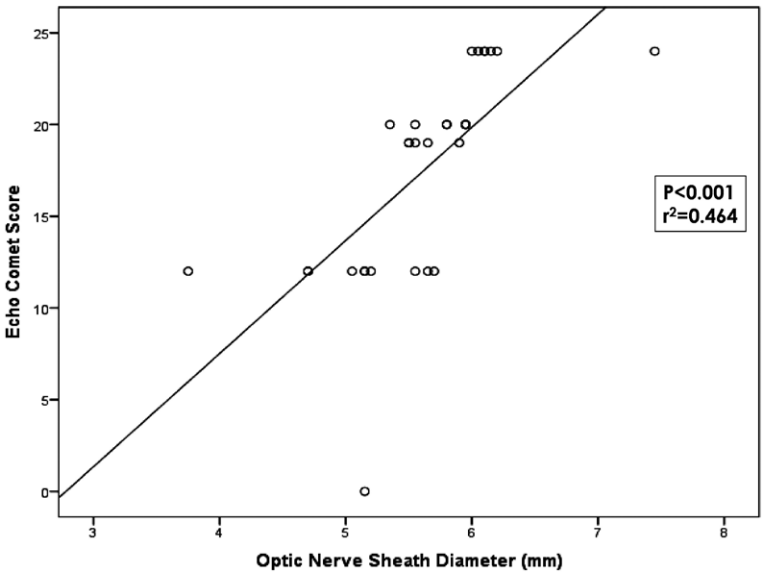

FIGURE 3. Correlation between optic nerve sheath diameter and lung ultrasound Echo Comet Score

Discussion

The main finding of our study is that ONSD correlates significantly with the amount of EVLW in severe preeclampsia. A dilated optic nerve, therefore, indicates systemic edema and fluid overload in patients with this condition.

The majority of studies on ONSD have been performed in traumatic brain injury patients.[14,23,29,30] These studies demonstrated that ONSD correlates well with invasive measurements of intracranial pressure.[14,15] Optic ultrasound has also been found to be a useful diagnostic tool for detecting intracranial hypertension in patients with meningitis, stroke, hepatic encephalopathy, epilepsy, and mountain sickness.[31-35] Dubost *et al.* and our group have recently reported increased ONSD values in preeclamptic patients compared to healthy pregnant women.[19,20] None of optic ultrasound studies in preeclampsia has, however, compared ONSD neither with direct intracranial pressure measurements nor with radiologic imaging methods. Therefore, all assumptions on intracranial hypertension in severe preeclampsia have to be viewed as such, since they are based on ultrasound findings alone. Moreover, ONSD was not associated with neurological symptoms in neither of these two studies.[19,20] Regardless of whether increased ONSD in preeclampsia denotes actual increased intracranial pressure, it could be a potential marker of generalized edema. No study to date examined the correlation between ONSD and measures of extravascular fluid in tissues other than the central nervous system. Extravascular fluid in pulmonary interstitium and alveoli is especially concerning in severe preeclampsia, as pulmonary edema continues to be an important cause of maternal morbidity and even mortality.[7,10] There are no published data on normal numbers of B-lines in anterior intercostal

spaces in healthy pregnant women. Two studies to date compared lung ultrasound measurements in severe preeclampsia *vs.* healthy pregnant controls. Both used the 28-rib interspaces technique dividing the chest wall in 12 areas on the left and 16 areas on the right anterior and lateral hemithorax. The sum of B-lines in preeclamptic patients was significantly higher than in healthy pregnancies (31 *vs.* 3, p = 0.02 in the study by Zieleskiewicz *et al.*, and 22 *vs.* 6, p = 0.002 in the study by Ambrozic *et al.*).[13,21] Numbers of B-lines in healthy pregnancy were, therefore, significantly lower than the median of 19 found in the present study even when posterior lung areas were examined. Our results show that optic ultrasound can help identifying preeclampsia patients with fluid overload in whom additional fluid administration should be avoided and who may even benefit from diuretic therapy.

Despite several advantages of lung ultrasound for identifying excess EVLW, such as its safety in pregnancy by avoidance of ionizing radiation, this technique still requires several measurements and could be time consuming. Optic ultrasound is also a safe and repeatable diagnostic tool, which is even quicker and simpler to perform than lung ultrasound. According to our results it also seems to be effective in diagnosing excess EVLW in patients with severe preeclampsia.

The study has several limitations. One of the main drawbacks is the small study population. The small number of patients included is the result of our decision to focus only on patients with severe preeclampsia. We chose to include only preeclamptic patients with severe features as these are truly critically ill pregnant patients which could mostly benefit from accurate assessment of fluid status. Future research is needed to refute or confirm our findings and to determine whether our results could be generalizable to all patients with preeclampsia, *i.e.* also to those with milder forms of disease. Future studies are also needed to assess reproducibility of ONSD measurements in everyday clinical practice. Previous publications have reported excellent inter- and intra-observer reproducibility of optic ultrasound as well as steep learning curve of the technique but only within research settings.[20,29] Another important limitation of the study is its observational nature which does not allow drawing conclusions on prognostic value of ONSD measurements in patients with severe preeclampsia.

In conclusion, ocular ultrasound seems to be a non-invasive and easy-to-learn method for evaluating overall fluid status in patients with severe preeclampsia. It could be especially useful in identifying those preeclamptic patients in which additional fluid intake should be avoided as it could result in pulmonary edema or other complications associated with fluid overload. Further studies are needed to examine the effectiveness of this diagnostic method for reducing maternal complications related to poor fluid management in severe preeclampsia.

References

1. Ananth CV, Keyes KM, Wapner RJ. Pre-eclampsia rates in the United States, 1980-2010: age-period-cohort analysis. *BMJ* 2013; **347:** f6564. doi: 10.1136/bmj.f6564
2. Hernández-Díaz S, Toh S, Cnattingius S. Risk of pre-eclampsia in first and subsequent pregnancies: prospective cohort study. *BMJ* 2009; **338:** b2255. doi: 10.1136/bmj.b2255
3. Duley L. The global impact of preeclampsia and eclampsia. *Semin Perinatol* 2009; **33:** 130-7. doi: 10.1053/j.semperi.2009.02.010
4. Hutcheon JA, Lisonkova S, Joseph KS. Epidemiology of pre-eclampsia and the other hypertensive disorders of pregnancy. *Best Pract Res Clin Obstet Gynaecol* 2011; **25:** 391-3. doi: 10.1016/j.bpobgyn.2011.01.006
5. Douglas JJ, Walley KR. Fluid choices impact outcome in septic shock. *Curr Opin Crit Care* 2014; **20:** 378-84. doi: 10.1097/MCC.0000000000000116
6. Hayes MA, Timmins AC, Yau EH, Palazzo M, Hinds CJ, Watson D. Elevation of systemic oxygen delivery in the treatment of critically ill patients. *N Engl J Med* 1994; **330:** 1717-22. doi: 10.1056/NEJM199406163302404
7. Dennis AT, Solnordal CB. Acute pulmonary oedema in pregnant women. *Anaesthesia* 2012; **67:** 646-59. doi: 10.1111/j.1365-2044.2012.07055.x
8. Boyd JH, Forbes J, Nakada TA, Walley KR, Russell JA. Fluid resuscitation in septic shock: a positive fluid balance and elevated central venous pressure are associated with increased mortality. *Crit Care Med* 2011; **39:** 259-65. doi: 10.1097/CCM.0b013e3181feeb15
9. Chaiworapongsa T, Chaemsaithong P, Yeo L, Romero R. Pre-eclampsia. Current understanding of its pathophysiology. *Nat Rev Nephrol* 2014; **10:** 466-80. doi: 10.1038/nrneph
10. Lewis G. *The confidential enquiry into maternal and child health (CEMACH). Saving mothers' lives: reviewing maternal deaths to make motherhood safer 2003-2005. The seventh report on confidential enquiries into maternal deaths in the United Kingdom.* London: CEMACH; 2007.
11. Royal College of Obstetricians and Gynaecologists. *Hypertension in pregnancy. The management of hypertensive disorders during pregnancy. NICE clinical guideline 107*. London: FiSH Books; 2011.
12. Brun C, Zieleskiewicz L, Textoris J, Muller L, Bellefleur JP, Antonini F, et al. Prediction of fluid responsiveness in severe preeclamptic patients with oliguria. *Intensive Care Med* 2013; **39:** 593-600. doi: 10.1007/s00134-012-2770-2
13. Ambrozic J, Brzan Simenc G, Prokselj K, Tul N, Cvijic M, Lucovnik M. Lung and cardiac ultrasound for hemodynamic monitoring of patients with severe pre-eclampsia. *Ultrasound Obstet Gynecol* 2017; **49:** 104-9. doi: 10.1002/uog.17331
14. Geeraerts T, Merceron S, Benhamou D, Vigue´ B, Duranteau J. Non-invasive assessment of intracranial pressure using ocular sonography in neurocritical care patients. *Intensive Care Med* 2008; **34:** 2062-7. doi: 10.1007/s00134-008-1149-x
15. Dubourg J, Javouhey E, Geeraerts T, Messerer M, Kassai B. Ultrasonography of optic nerve sheath diameter for detection of raised intracranial pressure: a systematic review and meta-analysis. *Intensive Care Med* 2011; **37:** 1059-68. doi: 10.1007/s00134-011-2224-2
16. Loureiro R, Leite CC, Kahhale S, Freire S, Sousa B, Cardoso EF, et al. Diffusion imaging may predict reversible brain lesions in eclampsia and severe preeclampsia: Initial experience. *Am J Obstet Gynecol* 2003; **189:** 1350-5. doi: 10.1067/S0002-9378(03)00651-3

17. Schwartz RB, Feske SK, Polak JF, DeGirolami U, Iaia A, Beckner KM, et al. Preeclampsia-eclampsia: clinical and neuroradiographic correlates and insights into the pathogenesis of hypertensive encephalopathy. *Radiology* 2000; **217:** 371-6. doi: 10.1148/radiology.217.2.r00nv44371

18. Zeeman GG, Fleckenstein JL, Twickler DM, Cunningham FG. Cerebral infarction in eclampsia. *Am J Obstet Gynecol* 2004; **190:** 714-20. doi:10.1016/j.ajog.2003.09.015

19. Dubost C, Le Gouez A, Jouffroy V, Roger-Cristoph S, Benhamou D, Mercier FJ, et al. Optic nerve sheath diameter used as ultrasonographic assessment of the incidence of raised intracranial pressure in preeclampsia: a pilot study. *Anesthesiology* 2012; **116:** 1066-71. doi: 10.1097/ALN.0b013e318246ea1a

20. Brzan Simenc G, Ambrozic J, Prokselj K, Tul N, Cvijic M, Mirkovic T, et al. Ocular ultrasonography for diagnosing increased intracranial pressure in patients with severe preeclampsia. *Int J Obstet Anesth* 2018; [Epub ahead of print]. doi: 10.1016/j.ijoa.2018.06.005

21. Zieleskiewicz L, Contargyris C, Brun C, Touret M, Vellin A, Antonini F, et al. Lung ultrasound predicts interstitial syndrome and hemodynamic profile in parturients with severe preeclampsia. *Anesthesiology* 2014; **120:** 906-14. doi: 10.1097/ALN.0000000000000102

22. American College of Obstetricians and Gynecologists. Task Force on Hypertension in Pregnancy. *Hypertension in Pregnancy*. Washinton: ACOG; 2013.

23. Geeraerts T, Launey Y, Martin L, Pottecher J, Vigue´ B, Duranteau J, et al. Ultrasonography of the optic nerve sheath may be useful for detecting raised intracranial pressure after severe brain injury. *Intensive Care Med* 2007; **33:** 1704-11. doi: 10.1007/s00134-007-0797-6

24. Hansen HC, Helmke K. Validation of the optic nerve sheath response to changing cerebrospinal fluid pressure: Ultrasound findings during intrathecal infusion tests. *J Neurosurg* 1997; **87:** 34-40. doi: 10.3171/jns.1997.87.1.0034

25. Bäuerle J, Nedelmann M. Sonographic assessment of the optic nerve sheath in idiopathic intracranial hypertension. *J Neurol* 2011; **258:** 2014-9. doi: 10.1007/s00415-011-6059-0

26. Volpicelli G, Elbarbary M, Blaivas M, Lichtenstein DA, Mathis G, Kirkpatrick AW, et al. International Liaison Committee on Lung Ultrasound (ILC-LUS) for International Consensus Conference on Lung Ultrasound (ICC-LUS): International evidence-based recommendations for point-of-care lung ultrasound. *Intensive Care Med* 2012; **38:** 577-91. doi: 10.1007/s00134-012-2513-4

27. Bouhemad B, Mongodi S, Via G, Rouquette I. Ultrasound for "lung monitoring" of ventilated patients. *Anesthesiology* 2015; **122:** 437-47. doi: 10.1097/ALN.0000000000000558

28. Lichtenstein D, Mézière G, Biderman P, Gepner A, Barré O. The comet-tail artifact. An ultrasound sign of alveolar-interstitial syndrome. *Am J Respir Crit Care Med* 1997; **156:** 1640-46. doi: 10.1093/eurheartj/ehw164

29. Tayal VS, Neulander M, Norton HJ, Foster T, Saunders T, Blaivas M. Emergency department sonographic measurement of optic nerve sheath diameter to detect findings of increased intracranial pressure in adult head injury patients. *Ann Emerg Med* 2007; **49:** 508-14. doi: 10.1016/j.annemergmed.2006.06.040

30. Legrand A, Jeanjean P, Delanghe F, Peltier J, Lecat B, Dupont H. Estimation of optic nerve sheath diameter on an initial brain computed tomography scan can contribute prognostic information in traumatic brain injury patients. *Crit Care* 2013; **17:** R61. doi: 10.1186/cc12589

31. Nabeta HW, Bahr NC, Rhein J, Fossland N, Kiragga AN, Meya DB, et al. Accuracy of noninvasive intraocular pressure or optic nerve sheath diameter measurements for predicting elevated intracranial pressure in cryptococcal meningitis. *Open Forum Infect Dis* 2014; **1:** 093. doi: 10.1093/ofid/ofu093

32. Shirodkar CG, Rao SM, Mutkule DP, Harde YR, Venkategowda PM, Mahesh MU. Optic nerve sheath diameter as a marker for evaluation and prognostication of intracranial pressure in Indian patients: An observational study. *Indian J Crit Care Med* 2014; **18:** 728-34. doi: 10.4103/0972-5229.144015

33. Kim YK, Seo H, Yu J, Hwang GS. Noninvasive estimation of raised intracranial pressure using ocular ultrasonography in liver transplant recipients with acute liver failure -A report of two cases-. *Korean J Anesthesiol* 2013; **64:** 451-5. doi: 10.4097/kjae.2013.64.5.451

34. Manno E, Motevallian M, Mfochive A, Navarra M. Ultrasonography of the optic nerve sheath suggested elevated intracranial pressure in epilepsy: case report. *Internet J Anesthesiol* 2013; **26:** 262-5. doi: 10.4103/ija.IJA_473_16

35. Fagenholz PJ, Gutman JA, Murray AF, Noble VE, Camargo CA Jr, Harris NS. Optic nerve sheath diameter correlates with the presence and severity of acute mountain sickness: evidence for increased intracranial pressure. *J Appl Physiol (1985)* 2009; **106:** 1207-11. doi: 10.1152/japplphysiol.01188.2007

research article

Ultrasonographic changes in the liver tumors as indicators of adequate tumor coverage with electric field for effective electrochemotherapy

Nina Boc[1], Ibrahim Edhemovic[1], Bor Kos[2], Maja M. Music[1], Erik Brecelj[1], Blaz Trotovsek[3], Masa Bosnjak[1], Mihajlo Djokic[3], Damijan Miklavcic[2], Maja Cemazar[1,4], Gregor Sersa[1,5]

[1] Institute of Oncology Ljubljana, Ljubljana, Slovenia
[2] Faculty of Electrical Engineering, University of Ljubljana, Ljubljana, Slovenia
[3] University Medical Center, Ljubljana, Ljubljana, Slovenia
[4] Faculty of Health Sciences, University of Primorska, Izola, Slovenia
[5] Faculty of Health Sciences, University of Ljubljana, Ljubljana, Slovenia

Radiol Oncol 2018; 52(4): 383-391.

Received 3 September 2018
Accepted 4 October 2018

Correspondence to: Prof. Gregor Serša, Ph.D., Institute of Oncology Ljubljana, Zaloska 2, SI-1000 Ljubljana, Slovenia. E-mail: gsersa@onko-i.si

Disclosure: Damijan Miklavčič holds patents on electrochemotherapy that have been licensed to IGEA S.p.a (Carpi, Italy) and is also a consultant to various companies with an interest in electroporation based technologies and treatments. The other authors have no competing interests.

Background. The aim of the study was to characterize ultrasonographic (US) findings during and after electrochemotherapy of liver tumors to determine the actual ablation zone and to verify the coverage of the treated tumor with a sufficiently strong electric field for effective electrochemotherapy.

Patients and methods. US findings from two representative patients that describe immediate and delayed tumor changes after electrochemotherapy of colorectal liver metastases are presented.

Results. The US findings were interrelated with magnetic resonance imaging (MRI). Electrochemotherapy-treated tumors were exposed to electric pulses based on computational treatment planning. The US findings indicate immediate appearance of hyperechogenic microbubbles along the electrode tracks. Within minutes, the tumors became evenly hyperechogenic, and simultaneously, an oedematous rim was formed presenting as a hypoechogenic formation which persisted for several hours after treatment. The US findings overlapped with computed electric field distribution in the treated tissue, indicating adequate coverage of tumors with sufficiently strong electric field, which may predict an effective treatment outcome.

Conclusions. US provides a tool for assessment of appropriate electrode insertion for intraoperative electrochemotherapy of liver tumors and assessment of the appropriate coverage of a tumor with a sufficiently strong electric field and can serve as predictor of the response of tumors.

Key words: electrochemotherapy; ultrasound; treatment plan; colorectal liver metastases

Introduction

Ablative techniques provide an effective tool for treatment of liver tumors. Radiofrequency ablation is the most frequently used, whereas electroporation-based treatments, *i.e.*, electrochemotherapy (ECT) and irreversible electroporation (IRE), are being explored as possible alternatives.[1–6] The major advantage of electroporation-based treatments over other ablation techniques is their non-thermal

mechanism of action; therefore, they have the advantage of being effective near major blood vessels, since their effectiveness is not reduced by the heat sink effect.[1]

ECT combines chemotherapeutic drugs, bleomycin or cisplatin, to provide therapeutic effectiveness with electroporation of tumors as a drug delivery system, whereas in IRE, cell death is induced by electroporation only.[3,7–9] ECT has recently demonstrated its effectiveness in a first clinical study on liver tumors, *i.e.*, colorectal liver metastases during open surgery.[2,10,11] Effectiveness was demonstrated to be good: 80% of the treated tumors responded completely during the 4-months observation period. The safety of its use was also demonstrated in tumors located near the major liver blood vessels, which were not resectable and not amenable to radiofrequency ablation. The phase I study is now continuing with a phase II study in which ECT was also demonstrated to be effective in tumors that are larger than 3 cm in diameter.[11] Recently similar results were obtained in phase I studi after ECT of hepatocellular carcinoma tumors.[12]

A wide spectrum of imaging techniques is available for the evaluation of the outcome of IRE of liver tumors.[13] Among these techniques are US, computed tomography (CT), magnetic resonance imaging (MRI) and positron emission tomography (PET). All of these techniques contribute to the planning, treatment implementation, visualization of the target volume, and guidance for the electrode placement. MRI has already been utilized for the immediate observation of ablated tissue zones and monitoring of the IRE ablation procedure.[14–16]

ECT is currently performed intraoperatively, and the US is used for tumor identification and electrode placement; however, the US findings immediately after the ECT have not been previously described. In this study, immediate, intermediate and delayed changes in tumors with US were evaluated for assessment and as an indicator of the appropriate coverage of tumors with a sufficiently strong electric field and predictor of the response of tumors .[17,18]

Patients and methods

Patients

Patients were treated by ECT for colorectal liver metastases. The study was approved by the Slovenian National Ethics Committee (#45/09/08), and registered at ClinicalTrials.gov (NCT02352259; First Posted Date: February 2, 2015) and conducted according to the Helsinki declaration. The patients signed an informed consent form. Two representative patients of the trial who were treated at the Institute of Oncology in Ljubljana were selected from this study for presentation.

Patient #1 was a 56-year-old female with a 25 mm recurrent colorectal liver metastasis located in the left liver lobe under the right hemidiaphragm which was diagnosed in early 2016. The patient had previously undergone a right hepatectomy and metastasectomy from Sg. II and IV, which was performed in 2009, and sigmoid colon resection in 2006 (T4N1 sigmoid colon adenocarcinoma). Before the first liver operation in 2006, the patient was treated with chemotherapy, which included oxaliplatin, capecitabine and cetuximab.

Patient #2 was a 59-year-old male diagnosed in 2016 with synchronous, locally advanced rectal cancer and solitary 16 mm liver metastasis in Sg. VII that was adjacent to the right hepatic vein. He received neoadjuvant treatment, which included chemotherapy (FOLFOX, panitumumab) and a short course of radiation (5 x 5 Gy). Previously, he was treated for laryngeal and lung cancer.

Imaging

Standard pretreatment evaluation of patients with colorectal liver metastases included a liver MRI with a hepatospecific contrast agent and a CT of the thorax and abdomen, including the pelvis at least 1 month before ECT. MRI was performed using a 1.5 T GE Medical Systems Optima MR450w (GE, Chicago, IL) and Siemens Magnetom Avanto syngo MR B17 (Siemens, Erlangen, Germany). CT imaging was performed using contrast-enhanced CT (CECT) on a Siemens SOMATOM Definition AS 64 (Siemens, Erlangen, Germany). The patients were reviewed at a multidisciplinary team. The follow-up assessment included a liver MRI with hepatospecific contrast agent CECT within at least 1-2 months after treatment, after 6 months, and until progression of the disease. In the case of Patient #1 also follow up using the US was possible, due to the specific location of the lesion. Evaluation of the target lesion and tumor response were measured according to modified RECIST criteria.[2]

ECT was performed under real-time US guidance using a 7.5-MHz linear-array transducer probe on a portable GE ultrasound machine. The follow-up US was performed using an abdominal probe on a Toshiba Aplio 300 ultrasound apparatus (Toshiba, Otawara, Japan).

Treatment planning

Treatment planning was performed based on pre-operative images (patient 1: CECT; patient 2: contrast-enhanced T1-weighted MRI). The liver and liver vessels were segmented using semi-automated segmentation algorithms that were developed previously and integrated into the web-based tool, Visifield (www.visifield.com, University of Ljubljana).[19,20] Electrodes were modelled as conductive cylinders based on commercially available individual needle electrodes (IGEA, Carpi, Italy).[9] The direction of electrode access was determined by the performing surgeon.

Given the direction of electrodes, a treatment plan was prepared for both patients by optimizing the voltages between four electrodes positioned in a rectangular pattern in the healthy liver parenchyma. The optimization was performed by solving the Laplace equation for the electric potential in tissue using the finite element method.[21] Since the pulses are delivered to the electrodes in pairs, the computation was performed for each pair of electrodes separately (in total, 6 pairs for 4 electrodes), and the maximum electric field from each pair combined was used to determine the cumulative coverage of a tumor. By sequentially activating the electrodes in this way, a larger tumor volume can be covered with sufficiently strong electric fields.[7] The goal of the optimization was to ensure a 100% coverage of the clinical target volume with electric field above 400 V/cm and to limit the maximum current delivered to the tissue to be below 50 A (hardware limit of the IGEA Cliniporator Vitae pulse generator).[22]

Electrochemotherapy

ECT was performed using the same treatment protocol as defined by the SOP for ECT of cutaneous tumors regarding the drug dosage and electrical parameters (*i.e.* pulse duration and number of pulses) of electroporation.[23] The procedure was adapted for the treatment of liver tumors during open surgery as previously described.[2,24,25]

For patient #1, a transthoracic approach through the diaphragm was chosen due to expected adhesions from previous liver resection and because of the subdiaphragmatic location of the metastasis. Initially, we planned to use long individual needle electrodes and a variable geometry approach (Supplementary data: Table S1, Figure S1); however, during the operation, the plan was changed due to limited space in the thorax. Therefore, a hexagonal electrode array with 3-cm long needles with fixed geometry was used.[9] The electrodes were inserted 8 times to cover the entire tumor.

Patient #2 was operated after neoadjuvant treatment (see above). We planned ECT for him because his liver metastasis was located on the right hepatic vein, which would have required a right hepatectomy simultaneously with a low anterior rectal resection. This was considered to be too extensive of a procedure; therefore, ECT and simultaneous low anterior rectal resection were performed.

The treatment plan was prepared based on the pre-operative MRI or CECT images (Supplementary data: Table S1, Figure S1). The calculation of the optimal electrode placement for specific access was performed. The treatment plan included placing four electrodes located in the safety margin around the tumor and one electrode located centrally in the tumor. The electric pulse amplitudes, which would result in a 100% coverage of a tumor with electric fields above 400 V/cm, were calculated (Supplementary data: Table S1).

Reconstruction of the imaging plane

To attempt to correlate the results of the numerical modelling with observed changes in ultrasound images, the US imaging plane was reconstructed by synthetically generating a 2-D image from the segmented volumetric pre-treatment images with the same dimensions as the US images. The spatial origin and angles of the pseudo-US image were manually adjusted to register the intraoperative US with the anatomical landmarks (tumor location, liver shape and major blood vessels position).[26,27] To verify this reconstruction, the segmented US images were compared with the reconstructed imaging plane using the Dice-Sørensen coefficient.[28] The mean value of this coefficient was 0.66, while the standard deviation was 0.10.

Results

ECT was used for the treatment of the liver tumors. US imaging was used for the identification of the electrode placement according to the treatment plan (Supplementary data: Table 1, Figure S1). Two representative cases are presented, and US specific changes are described for identification of adequate tumor coverage with sufficiently strong electric field to ensure electroporation and thus effective ECT.

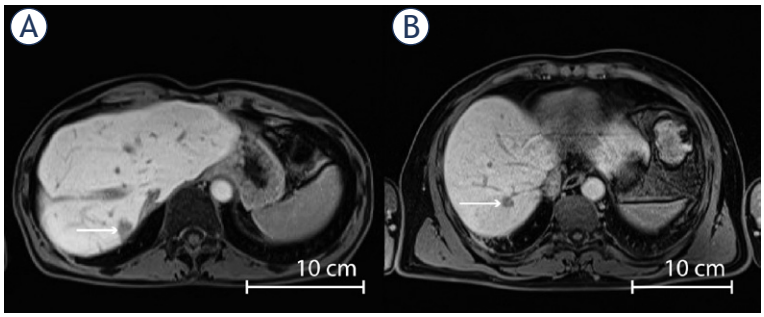

FIGURE 1. Colorectal liver metastases in difficult-to-treat locations. Locations of metastases to be treated with electrochemotherapy are indicated by white arrows **(A)** subdiafragmally in the liver remnant after right hepatectomy; **(B)** segment VII near the right hepatic vein.

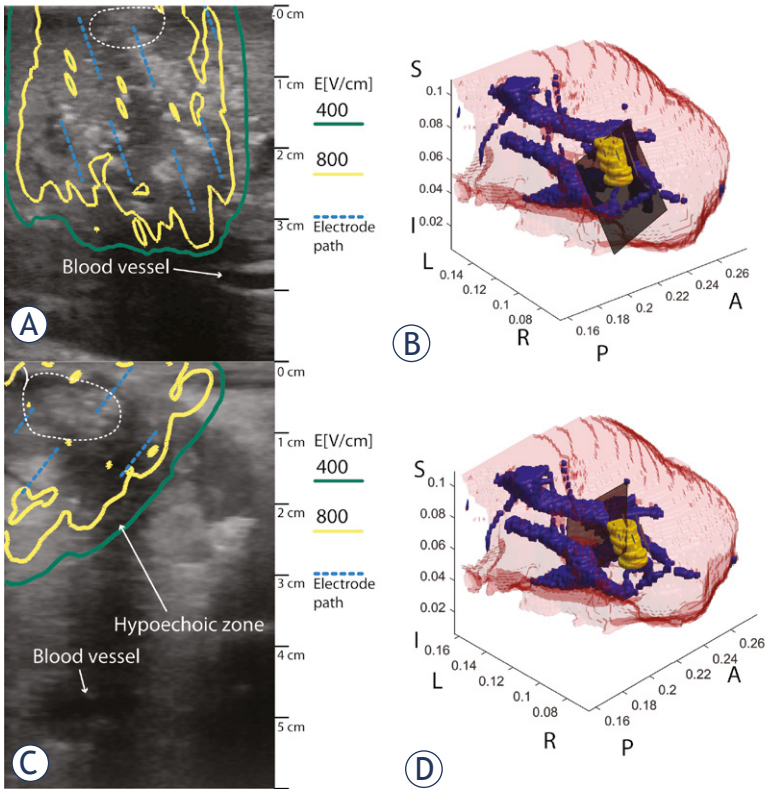

FIGURE 2. Effects of electrochemotherapy as is visible in the ultrasound imaging. **(A)** Immediate effect of microbubbles formation in the electrode track (5 min). Location of the metastasis is indicated by the dashed white curve. Overlaid is a contour plot showing iso-contours of the electric field of 400 and 800 V/cm, yellow and green solid curves, respectively. Electrode locations for one array location are indicated by blue dashed lines **(B)** Illustration of the ultrasound imaging plane in the reconstructed 3-D geometry of the liver. The tumor is shown in yellow, blood vessels are shown in blue, and the liver surface is shown in transparent red. The imaging plane is shown in black. One location of the electrode array is also shown. **(C)** Microbubbles are resorbed, the hypoechoic area represents the electroporated area, and the hyperechoic tumor is well demarcated within the ablation zone (5-15 min). Location of the metastasis is indicated by dashed white curve. Overlaid are the electric field iso-contours after delivery of all pulses as in **(A)**. **(D)** Illustration of the imaging plane and location. Colors as in **(C)**. Anatomic directions in **(C)** and **(F)** are indicated as follows: A – anterior, P – posterior, L – left, R – right, S – superior, I – inferior.

Tumour identification and treatment

The first case (patient #1) had liver metastasis of a colorectal tumor that was 20 mm in diameter, located subdiafragmally in the liver remnant after a right hepatectomy (Figure 1 A). Due to its location, we decided to perform ECT with trans-thoracic access using hexagonal electrodes. Therefore, the treatment plan was not executed as originally foreseen.

The second case (patient #2) had liver metastasis of a colorectal tumor in segment VII that was near the right hepatic vein and 19 mm in diameter (Figure 1 B). Due to its location, we decided to perform ECT using long needle electrodes. The placement of the electrodes was US-guided and confirmed to be close to the treatment plan.

Ultrasonographic findings following ECT

The ablation zone was monitored by the US immediately after delivery of electric pulses during the ECT session. In patient #1, it was also possible to monitor the outcome using US few days and also several months after ECT and compare it to MRI due to the tumor's location and trans-thoracic approach. Based on US observations of immediate effects, the tumor coverage with a sufficiently high electric field can be predicted, whereas the intermediate effects can confirm adequate coverage of the tumor with an effective electric field. The late effects indicated the progressive resorption of the treated zone within a few months after efficient ECT.

Immediate effects

Immediate effects of ECT were observed after delivery of the first electric pulses and up to 1.5 h thereafter. The observed US changes were followed in the ablation zone to identify whether they appear in the entire treated tumor for possible indication of effective electroporation of the tumor. The observed changes can be further divided into two phases that were observed in both patient #1 and patient #2.

The 1st phase took up to 5 minutes after the delivery of electric pulses. The hyperechoic microbubbles were observed along the electrode tracks and were visible immediately *i.e.* within a few seconds after the pulses were triggered and later within the entire ablation zone (Figure 2 A).

During the 2nd phase, after 5-15 min, microbubbles were distributed throughout the treated tumor, and the tumor became hyperechoic and surrounded

by a hypoechoic zone. The hypoechoic zone (5-15 mm wide) represents the electroporated area within the normal liver tissue represents the treatment safety margin. Because the tumor within this hypoechoic area is differentiated as hyperechoic, this approach can predict adequate coverage of the treated tumor with an adequate electric field, when the hyperechogenicity is evenly distributed throughout an ECT-treated tumor (Figure 2 C). To confirm this finding, the ablation zone was correlated with the placement of the electrodes. The hypoechoic area coincided with the predicted area that needed to be treated for complete coverage of a tumor for its effective ablation (Figure 2 A, C).

Similar findings were also observed in the second case (patient #2), where long individual needle electrodes were used for the variable electrode configuration. The electrode track was already observed few seconds after electroporation (Figure 3 A) followed by hypoechoic changes and microbubble formation in the 2nd phase after 5-15 minutes (Figure 3 C). This patient underwent another surgical procedure within the same operation after ECT. This enabled the investigation of the ablation zone 1.5 h after ECT (Figure 3 E). The hypoechoic ablation zone was visible with a clearly demarcated and evenly hyperechoic tumor. Based on the observation in patient #1, we assumed that the tumor was adequately electroporated with a sufficient safety margin. Again, the hypoechoic area coincided with the predicted area that needed to be treated for complete coverage of the tumor for its effective eradication (Figure 3 A, C, E).

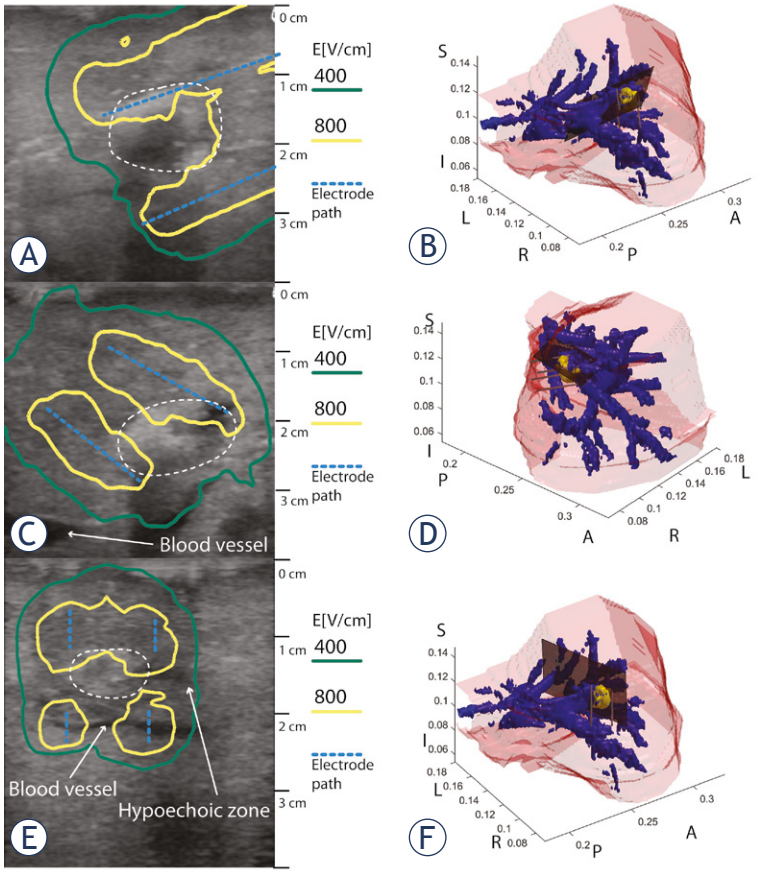

FIGURE 3. Effects of electrochemotherapy (ECT) as visible in the US imaging. **(A)** Immediate effect of microbubble formation in the electrode track immediately after electroporation (5 min). Location of the metastasis is indicated by the dashed white curve. Overlaid is a contour plot showing iso-contours of the electric field of 400 and 800 V/cm, yellow and green solid curves, respectively. Electrode locations are indicated by dashed blue lines **(B)** Illustration of the US imaging plane in the reconstructed 3-D geometry of the liver. The tumor is shown in yellow, blood vessels in blue, and the liver surface in transparent red. The imaging plane is shown in black. **(C)** First hyperechoic changes and microbubbles after treatment (5-15 minutes). Location of the metastasis is indicated by dashed curve. Overlaid are the electric field iso-contours. Colors as in **(A)**. **(D)** Illustration of the imaging plane and location. Colors as in **(B)**. **(E)** Hyperechoic tumor in the hypoechoic ablation zone 1.5 h after ECT. Location of the metastasis is indicated by dashed white curve. Electric field and electrodes are shown as above. **(F)** Illustration of the imaging plane and location. Colors as in **(B)**. Anatomic directions in **(B)**, **(D)**, and **(F)** are indicated as follows: A – anterior, P – posterior, L – left, R – right, S – superior, I – inferior.

Intermediate effects as observed by US after a few days

Four days after ECT US of the metastasis in patient #1 she presented with an 18-mm hyperechoic formation surrounded by a 5-mm hypoechoic area, which is most likely the oedematous area of the liver parenchyma, or the safety margin (Figure 4). The metastasis had a similar appearance as immediately after the ECT. In this case, transabdominal US imaging of the ECT-treated metastasis was possible due to the specific location and the transthoracic approach, which did not result in the air in the abdominal cavity.

Late effects

The response to the treatment was evaluated 5 months after the treatment by US and compared to the MRI in patient #1. This evaluation was possible due to the specific location of the metastasis, which also enabled the verification of its appearance by US. Five months after ECT, US and MRI showed the metastasis in patient #1 as a fibrotic residuum without the hypoechoic rim. The size of the metastasis was not significantly reduced (Figure 5 A, B). The appearance was as a complete response, which was also present 7 months after ECT; however, at that time, the size was significantly reduced to 11 mm from the original 20 mm in the greatest diameter, indicating the slow resorption of the treated metastasis. Similar MRI findings were shown in patient #2, 3 months after ECT in which the treated

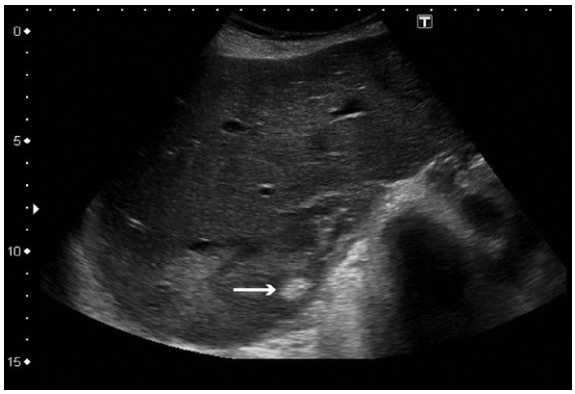

FIGURE 4. Transabdominal US of liver metastasis 4 days after electrochemotherapy. The metastasis was well demarcated and hyperechoic (indicated by the white arrow) in the hypoechoic ablation zone.

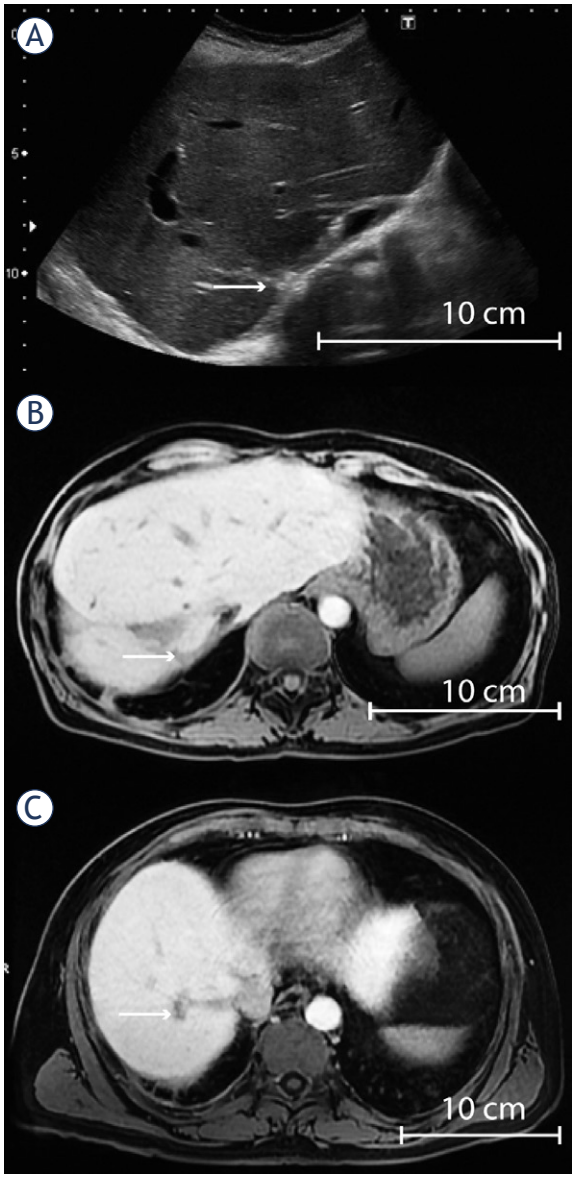

metastasis was reduced from 19 to 13 mm in diameter (Figure 5 C).

Discussion

Monitoring changes in the tissue during and after ablative techniques, including ECT, is important to evaluate the progress of the procedure and its result. It is important not to overestimate or underestimate the ablative zone because both have their drawbacks. Therefore, treatment monitoring and understanding the imaging findings to predict the tumor response to ECT are important.

We observed that hyperechoic foci are indicators of the electroporated tissue (tumor), and when the area coincides with the whole tumor mass, it indicates adequate tumor coverage with sufficiently strong electric field. The hyperechogenic microbubbles that form around the electrodes are a consequence of electrochemical reactions on the electrodes.[29–32] These are gaseous bubbles that then disperse throughout the tumors. Monitoring the hyperechogenicity of the tumors is thus important for monitoring the treatment of liver tumors during intraoperative ECT, where US helps not only with proper electrode placement but also has an important role in assessment and as an indicator of the tumor coverage with a sufficiently strong electric field. This is important for the electroporation of the whole tumor to facilitate bleomycin entry into the tumor cells, which can then exert its potent cytotoxic effect on cells.[33] Around the tumour and in the normal tissue, a hypoechogenic rim is formed, indicating tissue edema. This observation is due to the blockade of the tumor perfusion due to the electric pulse application and water leakage out of the tissue.[34] The formation of the safety halo around a tumour further supports the presumption that a tumour was adequately covered by the effective electric field during the ECT (Figure 6).

Treatment planning for ECT and IRE is gaining in its importance[1], specifically with a new web-based tool that will enable the spread of this approach.[20] Treatment planning based on numerical methods for computing the electric field is the best

FIGURE 5. Late effects of electrochemotherapy (ECT). **(A)** US image 5 months after ECT in patient #1. **(B)** MRI 5 months after ECT in patient #1. Metastasis of reduced size presented as a fibrotic residuum without the edematous rim. **(C)** MRI 3 months after ECT in patient #2. The metastasis of reduced size presented as a fibrotic residuum without the edematous rim. All lesions are indicated by white arrows.

tool for verifying the feasibility of electroporation-based treatments and determining the optimal electrode placement for successful coverage of the entire tumor during treatment in advance of the treatment. The placement of the electrodes is critical, since placement errors can lead to insufficient coverage of the target tissue.[18] Coupling with stereotactic navigation or optical navigation has been shown to be feasible, and CT guidance is often used for percutaneous IRE treatments.[35–37] However, in situations when the placing of the electrodes cannot follow the treatment plan, *e.g.*, due to tumour growth between imaging and the time of the treatment, poor contrast of the tumour in pre-treatment imaging or unforeseen difficulties in placing the electrodes according to the treatment plan, a tool to verify the coverage of the tumour with sufficient electric fields is important. MRI imaging has been proposed for monitoring the electric field during pulse delivery; however, the clinical application still requires further developments, such as MRI-compatible pulse generators and electrodes.[15,16] US thus lends itself as a tool for monitoring the immediate tissue response: the appearance of hyperechoic and hypoechoic changes are possibly indicative of tissue electroporation, and when the area coincides with the treated tumor and the treatment plan, as shown in this study, then the complete response of the treated tumor can be anticipated.

Interestingly, the US findings are comparable with the MRI findings – a hyperechoic tumor with a hypoechoic rim, which was shown to be the safety margin. Most likely, the hypoechoic rim represents the edematous normal tissue, which gradually resorbs after electroporation/pulse delivery , as shown also in this study. This could also be related to the differential effect of ECT on the normal versus tumor tissue vasculature, which has been demonstrated in a mouse model using window chamber microscopy.[38,39]

US has already been used for the observation of tissue changes after IRE in the study on pigs. In the acute period, a hypoechoic area with well-demarcated margins appeared. Therefore, the ablation zone can be predicted by measuring the external hyperechoic rim that forms 90–120 minutes after IRE. The rim is possibly attributable to evolving hemorrhagic infiltration via widened sinusoids.[40] Our study demonstrates similar findings after reversible electroporation, though in the ECT treated cancer patients.

The response of a tumour after ECT is slow due to its mode of action, *i.e.*, due to slow killing of the dividing cells that occurs due to the internalization of the bleomycin by electroporation.[41,42] The treated tumor gradually changes into fibrotic tissue during a period of 4 months, as shown in the MRI images. Later, the tumor progressively shrinks with slow resorption of the necrotic tumor tissue and fibrosis.[42]

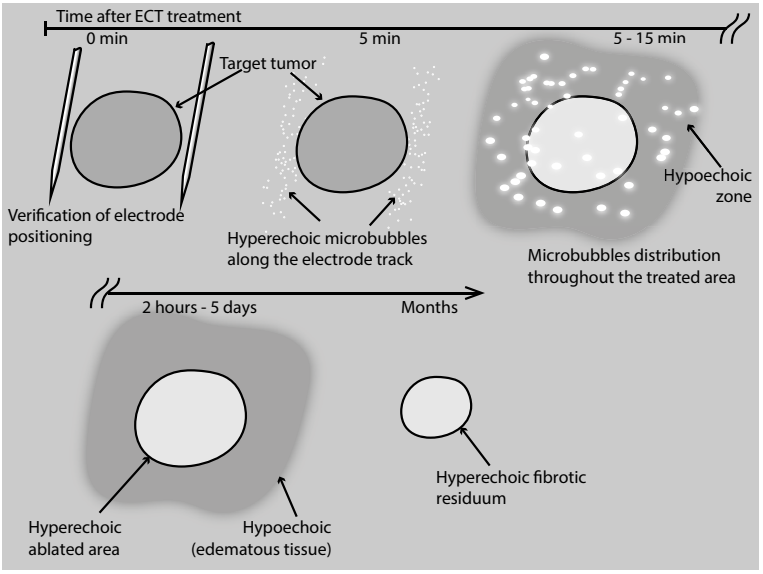

FIGURE 6. Schematic representation of the timeline of ultrasonographic changes after the delivery of electrochemotherapy treatment.

In conclusion, we have described US post-ECT changes that can serve as an indicator of tumor coverage with a sufficiently strong electric field and a predictor of the response of the tumors. The US findings during the treatment are comparable with the MRI findings during the follow-up period.

Acknowledgments

The authors would like to thank Tjaša Maslo, Andrej Vogrin, and Marija Brelih for assisting with segmentation of the ultrasound images. The authors acknowledge the financial support from the state budget for the Slovenian Research Agency (ARRS) under various grants (P3-0003, P2-0249, and Z3-7126). The research was conducted in the scope of LEA EBAM (French-Slovenian European Associated Laboratory: Pulsed Electric Fields Applications in Biology and Medicine).

Data availability

The data pertaining to this manuscript are available at the figshare repository under DOI: 10.6084/m9.figshare.5422858.

Author contribution statement

NB, IE, MM, BT and GS conceived and designed the experiments, BK, NB, IE, EB, BT, MB and MD performed the experiments; BK, NB, MM analyzed the data; GS, BK, NB, MC and DM wrote the manuscript; BK prepared the figures. All authors read and approved the final version of the manuscript.

References

1. Miklavcic D, Davalos RV. Electrochemotherapy (ECT) and irreversible electroporation (IRE) -advanced techniques for treating deep-seated tumors based on electroporation. *Biomed Eng Online* 2015; **14:** I1. doi: 10.1186/1475-925X-14-S3-I1
2. Edhemovic I, Brecelj E, Gasljevic G, Marolt Music M, Gorjup V, Mali B, et al. Intraoperative electrochemotherapy of colorectal liver metastases. *J Surg Oncol* 2014; **110:** 320-7. doi: 10.1002/jso.23625
3. Rubinsky B. Irreversible electroporation in medicine. *Technol Cancer Res Treat* 2007; **6:** 255-60. doi: 10.1007/978-3-642-05420-4
4. Chapiro J, Geschwind J-F. Science to practice: systemic implications of ablative tumor therapies - reality uncovered and myths exposed? *Radiology* 2016; **280:** 329-31. doi: 10.1148/radiol.2016160505
5. Coletti L, Battaglia V, De Simone P, Turturici L, Bartolozzi C, Filipponi F. Safety and feasibility of electrochemotherapy in patients with unresectable colorectal liver metastases: a pilot study. *Int J Surg* 2017; **44:** 26-32. doi: 10.1016/j.ijsu.2017.06.033
6. Campana LG, Clover AJP, Valpione S, Quaglino P, Gehl J, Kunte C, et al. Recommendations for improving the quality of reporting clinical electrochemotherapy studies based on qualitative systematic review. *Radiol Oncol* 2016; **50:** 1-13. doi: 10.1515/raon-2016-0006
7. Yarmush ML, Golberg A, Serša G, Kotnik T, Miklavčič D. Electroporation-based technologies for medicine: principles, applications, and challenges. *Annu Rev Biomed Eng* 2014; **16:** 295-320. doi: 10.1146/annurev-bioeng-071813-104622
8. Chunlan J, Davalos RV, Bischof JC. A review of basic to clinical studies of irreversible electroporation therapy. *Biomed Eng IEEE Trans* 2015; **62:** 4-20. doi: 10.1109/TBME.2014.2367543
9. Miklavčič D, Mali B, Kos B, Heller R, Serša G. Electrochemotherapy: from the drawing board into medical practice. *Biomed Eng Online* 2014; **13:** 29. doi: 10.1186/1475-925X-13-29
10. Edhemovic I. Electrochemotherapy: a new technological approach in treatment of metastases in the liver. *Technol Cancer Res Treat* 2011; **10:** 475-85. doi: 10.7785/tcrt.2012.500224
11. Edhemovic I, Brecelj E. Electrochemotherapy of liver tumors: colorectal liver metastasis. In: Vernier PT, Rubinsky B, Juergen F. Miklavcic D, Rols MP, Raso J, et al, editors. *Handbook of electroporation*. Springer International Publishing; 2016. p. 1-12. doi: 10.1007/978-3-319-26779-1_98-1
12. Djokic M, Cemazar M, Popovic P, Kos B, Dezman R, Bosnjak M, et al. Electrochemotherapy as treatment option for hepatocellular carcinoma, a prospective pilot study. *EJSO* 2018; **44:** 651-7. doi: 10.1016/j.ejso.2018.01.090
13. Neal II RE, Cheung W, Kavnoudias H, Thomson KR. Spectrum of imaging and characteristics for liver tumors treated with irreversible electroporation. *J Biomed Sci Eng* 2012; **05:** 813-8. doi: 10.4236/jbise.2012.512A102
14. Zhang Y, Guo Y, Ragin AB, Lewandowski RJ, Yang G-Y, Nijm GM, et al. MR Imaging to assess immediate response to irreversible electroporation for targeted ablation of liver tissues: Preclinical feasibility studies in a rodent model. *Radiology* 2010; **256:** 424-32. doi: 10.1148/radiol.10091955
15. Kranjc M, Kranjc S, Bajd F, Serša G, Serša I, Miklavčič D. Predicting irreversible electroporation-induced tissue damage by means of magnetic resonance electrical impedance tomography. *Sci Rep* 2017; **7:** 10323. doi: 10.1038/s41598-017-10846-5
16. Kranjc M, Markelc B, Bajd F, Čemažar M, Serša I, Blagus T, et al. In situ monitoring of electric field distribution in mouse tumor during electroporation. *Radiology* 2015; **274:** 115-23. doi: 10.1148/radiol.14140311
17. Miklavcic D, Corovic S, Pucihar G, Pavselj N. Importance of tumour coverage by sufficiently high local electric field for effective electrochemotherapy. *EJC Supplements* 2006; **4**: 45-51. doi: 10.1016/j.ejcsup.2006.08.006
18. Miklavcic D, Snoj M, Zupanic A, Kos B, Cemazar M, Kropivnik M, et al. Towards treatment planning and treatment of deep-seated solid tumors by electrochemotherapy. *Biomed Eng Online* 2010; **9**: 10. doi: 10.1186/1475-925X-9-10
19. Marčan M, Kos B , Miklavčič D. Effect of blood vessel segmentation on the outcome of electroporation-based treatments of liver tumors. *PLoS One* 2015; **10:** e0125591. doi: 10.1371/journal.pone.0125591
20. Marčan M, Pavliha D, Kos B, Forjanič T, Miklavčič D. Web-based tool for visualization of electric field distribution in deep-seated body structures and planning of electroporation-based treatments. *Biomed Eng Online* 2015; **14 Suppl 3:** S4. doi: 10.1186/1475-925X-14-S3-S4
21. Zupanic A, Kos B, Miklavcic D. Treatment planning of electroporation-based medical interventions: electrochemotherapy, gene electrotransfer and irreversible electroporation. *Phys Med Biol* 2012; **57:** 5425-40. doi: 10.1088/0031-9155/57/17/5425
22. Cliniporator BC. Medical electroporation of tumors. In: Vernier PT, Rubinsky B, Juergen F. Miklavcic D, Rols MP, Raso J, et al, editors. *Handbook of electroporation*. Springer International Publishing; 2017. p. 1-36. doi: 10.1007/978-3-319-26779-1_214-1
23. Gehl J, Sersa G, Matthiessen LW, Muir T, Soden D, Occhini A, et al. Updated standard operating procedures for electrochemotherapy of cutaneous tumours and skin metastases. *Acta Oncol* 2018; **57**: 874-82. doi: 10.1080/0284186X.2018.1454602
24. Edhemovic I, Gadzijev EM, Brecelj E, Miklavcic D, Kos B, Zupanic A, et al. Electrochemotherapy: a new technological approach in treatment of metastases in the liver. *Technol Cancer Res Treat* 2011; **10:** 475-85. doi: 10.1109/TNB.2011.2128340
25. Mali B, Gorjup V, Edhemovic I, Brecelj E, Cemazar M, Sersa G, et al. Electrochemotherapy of colorectal liver metastases - an observational study of its effects on the electrocardiogram. *Biomed Eng Online* 2015; **14 Suppl 3:** S5. doi: 10.1186/1475-925X-14-S3-S5
26. De Buck S, Maes F, Ector J, Bogaert J, Dymarkowski S, Heidbüchel H, et al. An augmented reality system for patient-specific guidance of cardiac catheter ablation procedures. *IEEE Trans Med Imaging* 2005; **24:** 1512-4. doi: 10.1109/TMI.2005.857661
27. King AP, Rhode KS, Ma Y, Yao C, Jansen C, Razavi R, et al. Registering preprocedure volumetric images with intraprocedure 3-D ultrasound using an ultrasound imaging model. *IEEE Trans Med Imaging* 2010; **29:** 924-37. doi: 10.1109/TMI.2010.2040189
28. Zijdenbos AP, Dawant BM, Margolin RA, Palmer AC. Morphometric analysis of white matter lesions in MR images: method and validation. *IEEE Trans Med Imaging* 1994; **13:** 716-24. doi: 10.1109/42.363096
29. Saulis G, Lapė R, Pranevičiūtė R , Mickevičius D. Changes of the solution pH due to exposure by high-voltage electric pulses. *Bioelectrochemistry* 2005; **67:** 101-8. doi: 10.1016/j.bioelechem.2005.03.001
30. Maglietti F, Michinski S, Olaiz N, Castro M, Suárez C , Marshall G. The role of Ph fronts in tissue electroporation based treatments. *PLoS One* 2013; **8:** e80167. doi: 10.1371/journal.pone.0080167
31. Stehling MK, Guenther E, Mikus P, Klein N, Rubinsky L , Rubinsky B. Synergistic combination of electrolysis and electroporation for tissue ablation. *PLoS One* 2016; **11:** e0148317. doi: 10.1371/journal.pone.0148317
32. Rubinsky L, Guenther E, Mikus P, Stehling M , Rubinsky B. Electrolytic effects during tissue ablation by electroporation. *Technol Cancer Res Treat* 2016; **15**: NP95-NP103. doi: 10.1177/1533034615601549
33. Orlowski S , Mir LM. Cell electropermeabilization: a new tool for biochemical and pharmacological studies. *Biochim Biophys Acta* 1993; **1154:** 51-63.
34. Jarm T, Cemazar M, Miklavcic D , Sersa G. Antivascular effects of electrochemotherapy: implications in treatment of bleeding metastases. *Expert Rev Anticancer Ther* 2010; **10:** 729-46. doi: 10.1586/era.10.43

35. Groselj A, Kos B, Cemazar M, Urbancic J, Kragelj G, Bosnjak M, et al. Coupling treatment planning with navigation system: a new technological approach in treatment of head and neck tumors by electrochemotherapy. *Biomed Eng Online* 2015; **14 Suppl 3:** S2. doi: 10.1186/1475-925X-14-S3-S2

36. Narayanan G, Hosein PJ, Beulaygue IC, Froud T, Scheffer HJ, Venkat SR, et al. Percutaneous image-guided irreversible electroporation for the treatment of unresectable, locally advanced pancreatic adenocarcinoma. *J Vasc Interv Radiol* 2017; **28:** 342-48. doi: 10.1016/j.jvir.2016.10.023

37. Beyer LP, Pregler B, Michalik K, Niessen C, Dollinger M, Müller M, et al. Evaluation of a robotic system for irreversible electroporation (IRE) of malignant liver tumors: initial results. *Int J Comput Assist Radiol Surg* 2017; **12:** 803-9. doi: 10.1007/s11548-016-1485-1

38. Markelc B, Sersa G , Cemazar M. Differential mechanisms associated with vascular disrupting action of electrochemotherapy: Intravital microscopy on the level of single normal and tumor blood vessels. *PLoS One* 2013; **8:** e59557. doi: 10.1371/journal.pone.0059557

39. Granata V, Fusco R, Setola SV, Piccirillo M, Leongito M, Palaia R, et al. Early radiological assessment of locally advanced pancreatic cancer treated with electrochemotherapy. *World J Gastroenterol* 2017; **23**: 4767-78 doi: 10.3748/wjg.v23.i26.4767

40. Appelbaum L, Ben-David E, Sosna J, Nissenbaum Y , Goldberg SN. US Findings after irreversible electroporation ablation: Radiologic-pathologic correlation. *Radiology* 2012; **262:** 117-25. doi: 10.1148/radiol.11110475

41. Orlowski S, Belehradek J, Paoletti C , Mir LM. Transient electropermeabilization of cells in culture. Increase of the cytotoxicity of anticancer drugs. *Biochem Pharmacol* 1988; **37**: 4727-33. doi: 10.1016/0006-2952(88)90344-9

42. Gasljevic G, Edhemovic I, Cemazar M, Brecelj E, Gadzijev EM, Music MM, et al. Histopathological findings in colorectal liver metastases after electrochemotherapy. *PLoS One* 2017; **12:** e0180709. doi: 10.1371/journal.pone.0180709

research article

Nuclear magnetic resonance metabolic fingerprint of bevacizumab in mutant IDH1 glioma cells

Tanja Mesti[1,6], Nadia Bouchemal[2], Claire Banissi[1], Mohamed N. Triba[2], Carole Marbeuf-Gueye[2], Maja Cemazar[3], Laurence Le Moyec[4], Antoine F. Carpentier [1, 5], Philippe Savarin[3], Janja Ocvirk[6]

[1] Laboratoire de Recherches Biochirurgicales, Université Paris Descartes, Hôpital Européen Georges Pompidou, Paris, France
[2] CSPBAT, UMR 7244, CNRS, Université Paris 13, Sorbonne Paris Cité, Bobigny, France
[3] Department of Experimental Oncology, Institute of Oncology Ljubljana, Ljubljana, Slovenia
[4] Unité de Biologie Intégrative des Adaptations à l'Exercice, Université d'Evry, Evry, France
[5] Assistance Publique-Hôpitaux de Paris, Hôpital Avicenne, Service de Neurologie, Bobigny, France
[6] Division of Medical Oncology, Institute of Oncology Ljubljana, Ljubljana, Slovenia

Radiol Oncol 2018; 52(4): 392-398.

Received 30 November 2017
Accepted 21 October 2018

Correspondence to: Assoc. Prof. Janja Ocvirk, M.D., Ph.D., Institute of Oncology Ljubljana, Zaloška 2, Ljubljana. Phone: +386 1 5879 220; Fax: +386 1 5879 305; E-mail: jocvirk@onko-i.si

Disclosure: No potential conflicts of interest were disclosed.

Background. Malignant gliomas are rapidly growing tumours that extensively invade the brain and have bad prognosis. Our study was performed to assess the metabolic effects of bevacizumab on the glioma cells carrying the IDH1 mutation, a mutation, associated with better prognosis and treatment outcome. Bevacizumab is known to inhibit tumour growth by neutralizing the biological activity of vascular endothelial growth factor (VEGF). However, the direct effects of bevacizumab on tumour cells metabolism remain poorly known.

Materials and methods. The immunoassay and MTT assay were used to assess the concentration of secreted VEGF and cell viability after bevacizumab exposure. Metabolomic studies on cells were performed using high resolution magic angle spinning spectroscopy (HRMAS).

Results. mIDH1-U87 cells secreted VEGF (13 ng/mL). Regardless, bevacizumab had no cytotoxic effect, even after a 72h exposure and with doses as high as 1 mg/mL. Yet, HRMAS analysis showed a significant effect of bevacizumab (0.1 mg/mL) on the metabolic phenotype of mIDH1-U87 cells with elevation of 2-hydroxyglutarate and changes in glutamine group metabolites (alanine, glutamate, glycine) and lipids (polyunsaturated fatty acids [PUFA], glycerophosphocholine, and phosphocholine).

Conclusions. In mIDH1-U87 cells, changes in glutamine group metabolites and lipids were identified as metabolic markers of bevacizumab treatment. These data support the possibility of a functional tricarboxylic acid cycle that runs in reductive manner, as a probable mechanism of action of bevacizumab in IDH1 mutated gliomas and propose a new target pathway for effective treatment of malignant gliomas.

Key words: idh1 mutation, malignant glioma, bevacizumab, metabolic fingerprint

Introduction

Malignant gliomas are rapidly growing tumours that extensively invade the brain and critically depend upon angiogenesis. Malignant gliomas are known to secrete vascular endothelial growth factor (VEGF) to stimulate angiogenesis.[1] The IDH1 (NADP+-dependent isocitrate dehydrogenase) mutation occurs in the vast majority of WHO grade II or III gliomas and secondary glioblastomas. The p.Arg132His mutation (substitution from arginine to histidine) of isocitrate dehydrogenase 1

(IDH1-R132H) is not only a frequent alteration (> 70%) but is also a major prognostic marker in malignant gliomas. Patients with an IDH1 mutation have better treatment outcomes and better survival.[2] A number of studies have analysed the role of IDH mutations in cancer.[3,4] The main biochemical alteration associated with these mutations is the gain of a new enzymatic activity in which mutant IDH reduces α-ketoglutarate (α-KG, also called 2-oxoglutarate) to 2-hydroxyglutarate (2-HG). This is in contrast to wild-type IDH1, which catalyzes the NADP+-dependent oxidative decarboxylation of isocitrate into α-KG. As a result, mutant IDH1 leads to elevated levels of 2-HG in tumour cells.[5] The tumorigenic effects of elevated 2-HG may be related to widespread changes in histone and DNA methylation.[6]

The use of metabolic profiling in conjunction with data mining tools allows the study of differences between normal and cancer cells and provides insights into the metabolic processes within cells and tumour tissues. NMR high resonance magic angle spinning (HRMAS) analysis is a very specific method with high potential for assessing subtle changes in the metabolic profiles of cells.[7-11] Using HRMAS, we have already shown that the VEGF inhibitor bevacizumab, which is used in recurrent glioblastoma, does not significantly impact the metabolism of wild-type U87 cells. This was in contrast to the VEGFR2-selective inhibitor SU1498 which elicits a dramatic increase in lipids, polyunsaturated fatty acids (PUFAs) in particular, due to an apoptotic response that is accompanied by accumulation of lipid droplets prior to DNA fragmentation, as we documented.[12]

To date, there has been no published study in the literature examining the direct metabolic effect of bevacizumab on mIDH1 cells. Therefore, we performed HRMAS analysis of the metabolic effect of bevacizumab (0.1 mg/mL) on a glioma U87 cell line that carries the IDH1-R132H mutation (mIDH1-U87) and we present our data. First, we assessed the drug's effects on cell proliferation, cell morphology, and VEGF secretion. Afterwards, we investigated the metabolic impact of bevacizumab on tumour cells by HRMAS. We report that bevacizumab has a significant effect on the metabolic phenotype of mIDH1-U87 cells, causing elevation of 2-hydroxyglutarate and changes in levels of the glutamine group of metabolites (alanine, glutamate, glycine) and in lipid signal (PUFA, glycerophosphocholine [GPC], and phosphocholine [PC]). Studying these metabolites by magnetic resonance spectroscopy (MRS) in patient samples could provide an early surrogate marker of bevacizumab response in tumour cells and, thus, might have a significant impact on clinical practice. These data support the possibility of a functional tricarboxylic acid cycle that runs in reductive manner, as a probable mechanism of action of bevacizumab in IDH1 mutated gliomas. With this we give not only new data of bevacizumab mechanism of action, but also we propose a new target pathway for effective treatment of malignant gliomas.

Materials and methods

Cell phenotype, VEGF secretion and sensitivity to drugs

The mIDH1-U87 (U87 cell line stably transfected with IDH1-R132H with a lentiviral vector, and was kindly provided by Marc Sanson [Hôpital de la Salpêtrière, Paris, France]) was maintained in Eagle's minimal essential medium (EMEM) with 10% foetal calf serum, 2 mM L-glutamine, 100 U/mL penicillin, and 100 µg/mL streptomycin (Lonza, Verviers, Belgium). bevacizumab (Roche, Paris, France) was diluted with culture medium to working concentrations before use. As a control, a stock solution containing the corresponding excipient was prepared with 60 mg/mL of trehalose dehydrate, 5.8 mg/mL sodium dihydrogen phosphate monohydrate, and 1.5 mg di-sodium hydrogen phosphate dihydrate (all from Sigma Aldrich, Saint-Quentin Fallavier, France). VEGF secretion was assessed with the Quantikine ELISA kit for human VEGF (R&D Systems, Abingdon, UK), following the manufacturer's instructions. The cells proliferation was assessed as follows: The mIDH1-U87 cells were seeded into and allowed to attach overnight. Cells (seeded in 24-well plates; 30,000 cells/well) were treated for 72 h with bevacizumab (from 0.1 mg/mL to 1 mg/mL) in triplicate wells. Duplicate experiments were performed. Cell viability was then assessed with the MTT assay following the procedure of Mosmann.[13] The percentage of surviving cells is expressed as the ratio of optical density of treated cells versus untreated cells.

^{1}H-NMR spectroscopy

Subconfluent mIDH1-U87 cells (4 x 10^6 cells/60 mm diameter cell culture dishes) were incubated for 24 h and then treated with bevacizumab (0.1 mg/mL) or trehalose (0.24 mg/mL) for 24 h. The cells (6 x 10^6 cells/dish) were then harvested in 0.5 mL cold (4°C) phosphate-buffered saline (PBS) in deu-

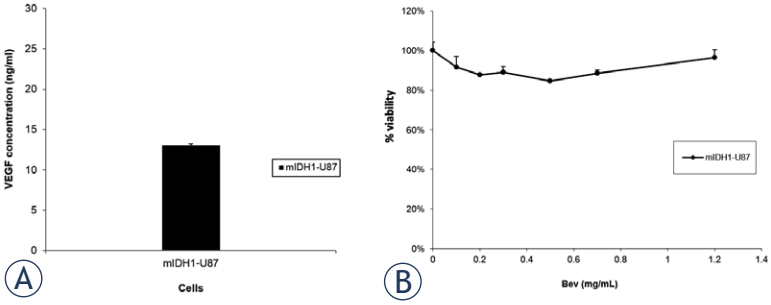

FIGURE 1. mIDH1-U87 vascular endothelial growth factor (VEGF) secretion and cell viability. **(A)** VEGF secretion ofmIDH1-U87 cells was assessed with immunoassay **(B)** Cell viability (%) of mIDH1-U87 cell lines after 72 h bevacizumab treatment at different cell line viability. Concentrations (0.1 mg/mL to 1 mg/mL) was assessed with the MTT assay. Bevacizumab has no significant effect ($p > 0.05$) on mIDH1-U87 cell line viability.

terated water (Eurisotop, Gif-Sur-Yvette, France) using a cell scraper and were washed twice. After centrifugation (3 min at 4°C, 300 g), 50 µl inserts were filled with 6 million cells (using one insert per dish). Inserts were snap-frozen until NMR experiments. Ten inserts from different culture flasks were done for each condition (hereafter referred to as technical replicates) according to standard procedures.[8] Cultures grown independently (in separate flasks and at different dates) were performed for each condition (hereafter referred to as biological replicates). The metabolomic profiles of cells were investigated in vitro with HRMAS. Spectra were acquired at 500 MHz on a Bruker AVANCE III NMR spectrometer (Bruker, Wissembourg, France), with an HRMAS probe. All experiments were performed at 294 K. Rotation rate was 4 kHz. Water signal was suppressed by a presaturation sequence using low power irradiation at the frequency of water. To remove broad signals produced by proteins and compounds exhibiting slow reorientation, a CPMG pulse sequence was used. The scan number was 128, the repetition rate of the spectra was 5 s. For resonance assignment purposes, TOCSY and JRES were also acquired. Spectra were first processed using NMRPipe[14] with an exponential function corresponding to 0.3 Hz line broadening prior to Fourier transforms. Spectra were phased, and a baseline correction was applied between -0.5 and 10.5 ppm. The spectra were divided into 11,000 regions of 0.001 ppm width called buckets. Solvent signal was excluded. Each bucket was integrated and scaled using probabilistic quotient normalization

Statistical analyses and metabolite identification in HRMAS spectra

Data for physiological processes are shown as mean values of at least two different experiments and expressed as means ± S.D. The data were first tested for normality of distribution and the differences between the experimental groups were evaluated by Student's t-test for one-way analysis of variance. A p value of less than 0.05 ($p < 0.05$) was considered to be statistically significant. SigmaPlot statistical software was used.

Principal component analysis (PCA) was conducted to detect any outliers based on NMR signal variability, defined as observations situated outside the 95% confidence region of the model. Orthogonal projection to latent structure (OPLS) analysis was performed when no significant differences were observed with the PCA analysis. A leave-one-out internal cross-validation procedure was used to calculate the predictability of the model. The ability of the model to describe data and to correctly predict new data is expressed by the values of the parameters R2 and Q2. R2=1 indicates a perfect description of the data while Q2 = 1 indicates a perfect prediction of new data. Results are visualized by the scores and loadings plots. The scores plot shows the separation between groups. Scores are represented as a projection of the different samples on the predictive (Tpred) and the orthogonal (Torth) component. The loadings plot shows the distribution of the corresponding variables responsible for the separation observed in the scores plot. PCA and OPLS were conducted using SIMCA-P12 (Umetrics) and in-house Matlab (Mathworks) code based on the Trygg and Wold method.[15] For metabolites considered as discriminant by the multivariate analysis, concentrations of metabolites were calculated by integration of their NMR signal.

Results

VEGF secretion was found (13 ng/mL) in the culture medium after 24 h incubation of mIDH1-U87cells (Figure 1A). Bevacizumab, even in concentrations up to 1 mg/mL, and regardless of the exposure time, had no effect on mIDH1-U87 cell line viability (Figure 1B).

In order to study the metabolic impact of bevacizumab on the mIDH1-U87 glioblastoma cell line, we characterized the bevacizumab fingerprint on mIDH1-U87 cells using the same approach as de-

scribed for assessment of the metabolic fingerprint of bevacizumab on U87 cells, using trehalose-treated mIDH1-U87 cells as a control. The model was first calculated using a test set composed of 2 different culture sets (biological replicates) of trehalose-treated cells (each composed of 10 culture flasks), and 2 different cultures of bevacizumab-treated cells (each composed of 10 culture flasks). The corresponding score plot is presented in Figure 2. An OPLS model was calculated to characterize the metabolomic effect of bevacizumab on mIDH1-U87 cells (Figure 2A). The predictive ability of the model Q^2 was 0.93). To test the predictive ability of the model, a validation set was used. A projection of new samples (new trehalose-treated culture sets versus new bevacizumab-treated culture cells) was done using the model calculated with the test set. The score plot for the validation set is shown in Figure 2B. The AUROC obtained for the validation set was 0.82, which corresponds to good sensitivity and specificity of the prediction. The corresponding loadings coefficients plot is shown in Figure 2C. Using 2D experiments, Chenomx and HMDB database, the main metabolites, modified by bevacizumab treatment, were identified as (Figure 2D and Table 1), choline metabolite, GPC, in the area 3.65-3.71 ppm, with an increase of 35%, taurine (3.3–3.42 ppm) with an increase of 30%, alanine (1.475 ppm), glutamate (2.11/2.34/2.55/3.02 ppm) with an increase of 25%, creatine in the area 2.95 ppm and 3.02 ppm with an increase of 15% and 25%, respectively, and 2-HG (1.84/2.24/3 ppm) with an increase of 20%. Also, there were significant metabolite changes in the 3.2 ppm area identified as phosphocholine with an increase of 7%, in the same area where the GPC/choline ratio was also increased by 9%. Glycine was detected as increased in the 3.6 ppm area, but as NMR peaks were superimposed, the quantification of this metabolite was not possible.

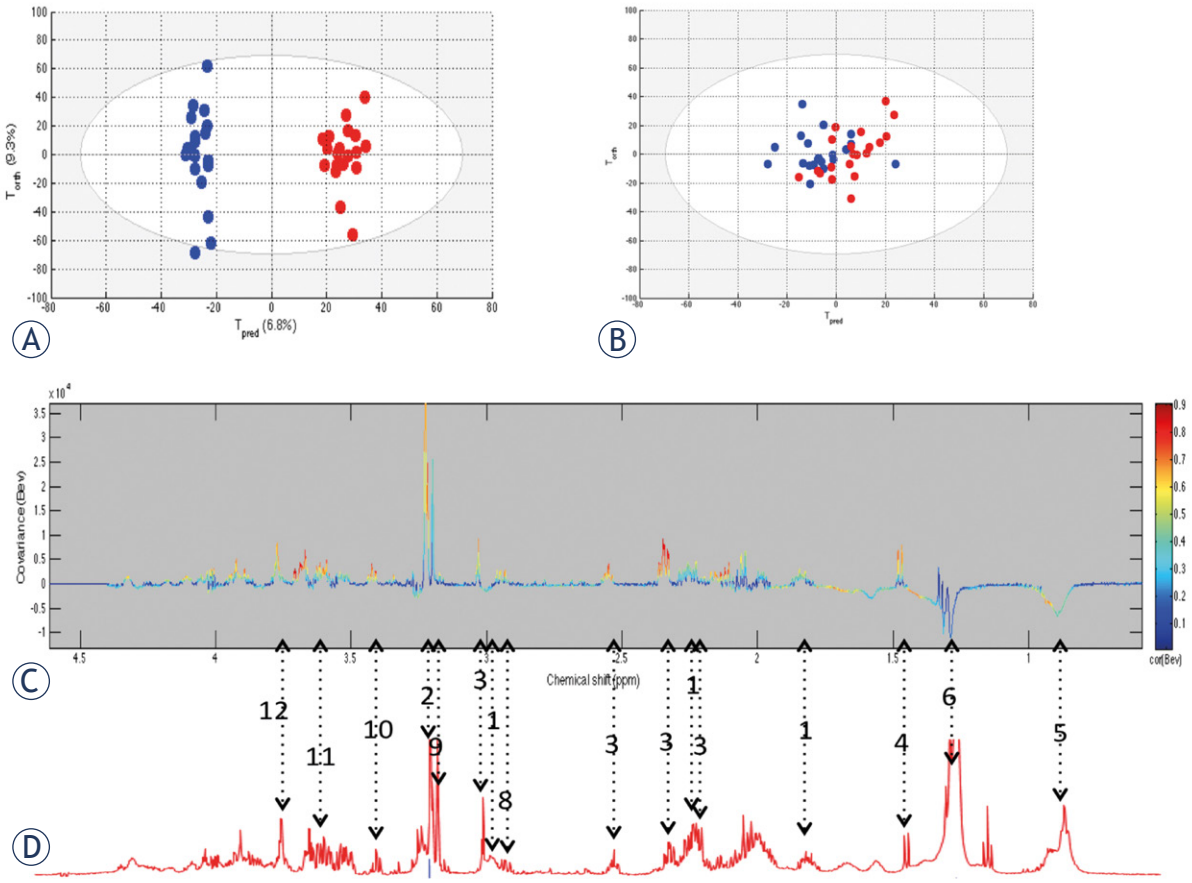

FIGURE 2. (A) Orthogonal projection to latent structure (OPLS)-DA score plot to discriminate metabolic effects of trehalose (blue) and bevacizumab (red) on mIDH1-U87 cells. **(B)** Projection of the spectra corresponding to the validation set. **(C)** OPLS loadings plot for mIDH1-U87 metabolic changes (significant changes marked with colours other than dark blue) after bevacizumab treatment. ^{1}H CPMG spectrum of cells incubated with bevacizumab **(D, RED)**.

TABLE 1. Principal discriminant metabolites. An up arrow (↑) ↑↓ corresponds to an increase of the concentration induced by bevacizumab

Peak number	Chemical shift (ppm)	Attributions	Concentration variations Induced by Bev	
1	184/2.24/3	2OH-glutarate	↑	20%
2	3.22	GPC/chol	↑	9%
3	2.11/2.34/2.55/3 02	glutamate	↑	25%
4	1.475	alanine	↑	25%
5	0.88	(CH2)n-CH3	↓	32%
6	1.28	(CH 2)n-CH2-(CH2)m	↓	20%
7	2.95	creatine	↑	15%
8	3.02	creatine	↑	25%
9	3.2	Pcholine	↑	7%
10	3.3-3.42	Taurine	↑	30%
11	3.6	glycine	↑	ND
12	3.65-3.71	GPC	↑	35%

Bev = bevacizumab; GPC = glycerophosphocholine; ND = not determined; Pcholine = phosphocholine

Discussion

Using sensitive method as HRMAS analysis for the first time, we report, that Bevacizumab has a significant effect on metabolic phenotype of mIDH-U87 cells. It is presented with elevation of 2 hydroxyglutarate and changes in the group of glutamine metabolites (alanine, glutamate, glycine) and lipid signal (PUFA, glycerophosphocholine and phosphocholine). The HRMAS experiments were performed after 24 h exposure to bevacizumab, at a time point when no toxicity was observed by the MTT reduction assay, emphasizing the sensitivity of the HRMAS for detection of early drug-induced alterations of cancer cells.

Using HRMAS, we already showed that VEGF inhibitor, Bevacizumab does not significantly impact the metabolism of wild-type U87 cells, contrary to VEGFR2 selective inhibitor SU1498, with dramatic increase in lipids, and in particular in polyunsaturated fatty acids (PUFAs), due to an apoptotic response with accumulation of lipid droplets prior to DNA fragmentation, as we documented.[12]

The main biochemical alteration associated with the IDH-1 mutation is the gain of a new enzymatic activity which decreases α-ketoglutarate (α-KG) concentrations and increases 2-hydroxyglutarate (2-HG) concentrations. This is in contrast to wild-type IDH1, which catalyses the NADP+-dependent oxidative decarboxylation of isocitrate into α-KG. As a result, mutant IDH1 leads to elevated levels of 2-HG in tumour cells.[5] The exact mechanism through which mutant IDH1 and 2-HG induce oncogenesis continues to be investigated, but recent studies confirm the hypothesis that 2-HG can competitively inhibit α-KG–dependent enzymes, which normally act to transfer amine groups from free amino acids to α-KG, as a first step in amino acid breakdown for oxidation in the tricarboxylic acid (TCA) cycle.[6] TCA down-regulation has been associated with a selective advantage for cancer cells. Nutrients are converted to building blocks, such as amino acids and lipids, which are used for proliferation rather than being oxidized in the TCA cycle.[16]

According to our research data and using 2D experiments and the HMDB (Human Metabolome DataBase), the main metabolites modified by bevacizumab treatment were identified as GPC with a concentration increase of 35% in the area 3.65-3.71 ppm, taurine (3.3–3.42 ppm) with an increase of 30%, and there were significant metabolite changes in the 3.2 ppm area identified as PC with an increase of 7%, and in the GPC/choline ratio with an increase of 9%. GPC and PC have well-documented roles in membrane phospholipid breakdown[17]. Ex vivo MRS studies of brain tumours have identified several biomarkers of tumour growth and apoptosis, among which are increased levels of choline-containing compounds, possibly due to cell membrane disruption and altered phospholipid metabolism.[18] PC and GPC accumulation reflect early stages of growth arrest or apoptosis.[19] The analysis of cisplatin-mediated apoptosis on ovarian cancer cells, showed enhanced apoptosis that was measured by increased PC and GPC concentrations.[20] Elevated fatty acids and choline metabolism may be a sign of inhibited cell growth or apoptosis. In a study on human breast cancer cells, the increase in lipids (detected at 5.35, 1.3, and 0.9 ppm by NMR) during cytotoxic drug treatment was associated with mitochondrial damage, lipid droplet development, and formation of autophagic vacuoles.[21] In malignant cells and tumours, appearance of a lipid peak at 1.3 ppm from CH2CH2CH2 has commonly been associated with ongoing cell death processes.[22-24] In glioma cells, it has been demonstrated that PUFAs accumulate in BT4C glioma during gene therapy-induced programmed cell death (PCD), with pattern recognition identifying significant lipid changes 8-fold higher than normal in the area of 5.3 ppm and 2.8 ppm, corresponding to CH=CH and $CH=CHCH_2CH=CH$, and 2 fold higher than normal in the area of 0.9 ppm and 1.3 ppm, corresponding to CH_2-CH_3 and CH_2-CH_2-CH_2, as

the most significant for monitoring the dynamics of PCD.[25] On the other hand, an HRMAS study on glioma biopsies has shown that the taurine signal may be a robust apoptotic biomarker that is independent of tumour necrotic status. Namely, this study showed that taurine significantly correlated with apoptosis in both non-necrotic (R = 0.727, p = 0.003) and necrotic (R = 0.626, p = 0.0005) biopsies, but the PUFA changes in the 2.8 ppm area, observed in other studies as a marker of apoptosis, correlated only in non-necrotic biopsies (R = 0.705, $p < 0.005$).[26] This is in agreement with our data, as we identified significant changes in the lipid area (0.88 ppm and 1.28 ppm), with (CH_2)n-CH_3 and (CH_2)n-CH_2-(CH_2)m signals, defined as PUFAs, being impacted with decreases of 32% and 20%, respectively, and an increase of 30% of taurine (3.3 - 3.42 ppm). This data also suggests that taurine may be a better biomarker of apoptosis in glial tumours than the change in PUFAs, which obviously differs according to the type of the tumour and correlates better with non-necrotic cancer types. Clearly it also correlates with the treatment used, as we had published the HRMAS analysis data of apoptotic impact of elevated PUFA by SU1498 treatment on U87 cells.[12] The action of creatine has been shown to be linked with energy metabolism (formation of creatine phosphate) and inhibition of excitotoxicity. Decreased creatine has already been reported as a marker for highly proliferative cells and is found in gliomas.[27] This is in contrast to its antioxidant and antiproliferative effects when elevated[28], as also demonstrated in our work where bevacizumab treatment on mIDH1-U87 cells produced elevated creatine in the area 2.95 ppm and 3.02 ppm with increases of 15% and 25%, respectively.

Furthermore, although we didn't detect lactate changes, other metabolites important for the TCA cycle and glutaminolysis were significantly impacted as shown by an increase of 20% for glutamate (2.11/2.34/2.55/3.02 ppm), alanine (1.475 ppm), and 2-HG (1.84/2.24/3 ppm), and a significant increase in glycine in the 3.6 ppm area. As the NMR peaks were superimposed, the quantification of glycine was not possible. It has been already reported that mIDH1-U87 cells have lower concentrations of glutamate, lactate, and PC, and higher concentrations of GPC and 2-HG.[29] Reitman *et al*., found similar changes in their analysis of IDH1-R132H mutated glioma cells, reporting a significant drop in glutamate, glutathione, aspartate, and PC, and an increase in 2-HG and GPC.[30] These data show that the TCA cycle is still functional with glutamine as a key nutrient providing substantial alternative input of nutrients[31], and also proapoptotic activity, as glutamate, alanine, and glycine have already been reported as biomarker candidates for cell apoptosis.[32] Metabolic rewiring is an established hallmark of cancer and, beyond the Warburg phenomenon with the use of glucose in hypoxic conditions and production of lactate, other changes can be observed, such as a functional TCA cycle that uses glutamine as a key nutrient to provide a substantial alternative input of nutrients into the TCA cycle (anaplerosis).[31] A study on melanoma cells showed that in normoxia, but especially in hypoxia, glutamine provided a strong anaplerotic input to the TCA cycle via reductive flux from α-KG to citrate.[33] IDH1-R132H expression results in elevated flux from glutamine to 2-HG through glutamate and α-KG.[34] Thus, glutamate may become depleted, as it is converted first to α-KG and then to 2-HG. Except for the elevation of numerous free amino acids, IDH1-R132H cells show depletion of TCA cycle intermediates and elevation of lipid precursors such as GPC with a decrease of phosphatidylcholine.

The TCA cycle typically runs in the oxidative direction, but in our case, as other studies have shown, that in mammalian cells including glioblastoma cells, a reverse (reductive) flux between citrate and α-ketoglutarate can also exist when glutamine is used as carbon source.[35-37] In that manner, glutamine contributes to production of alanine, which is usually the product of glycolysis and fatty acid synthesis. In the process, free ammonia is generated that can induce autophagy.[35-37]

Conclusions

Our study was performed to assess the metabolic effects of Bevacizumab on the glioma cells carrying the IDH1 mutation, and for the first time we present data of the direct effects of bevacizumab on tumour cells metabolism. We observed dramatic changes in the metabolic phenotype of mIDH1-U87 cells after only 24h exposure to Bevacizumab using HRMAS Proton Magnetic Resonance Spectroscopy Analysis. We detected elevation of 2-HG levels and changes in the area of glutaminolysis metabolites and lipids (PUFA, GPC, and PC) as early markers of the metabolic effect of bevacizumab on mIDH1-U87 cells. These data support the possibility of a functional TCA cycle that runs in reductive direction inducing autophagy, as a probable mechanism of action of bevacizumab in IDH1-mutated glioma. Studying these metabolites by Magnetic Resonance

Spectroscopy (MRS) in patient samples could provide an early surrogate marker of bevacizumab response in tumour cells and, thus, might have a significant impact on clinical practice.

With this we give not only new data of Bevacizumab mechanism of action, but also we propose a new target pathway for effective treatment of malignant gliomas.

References

1. Kaur B, Khwaja FW, Severson EA, Matheny SL, Brat DJ, Van Meir EG. Hypoxia and the hypoxia-inducible-factor pathway in glioma growth and angiogenesis. *Neuro Oncol* 2005; **7:** 134-53. doi: 10.1215/S1152851704001115
2. Mesti T, Ocvirk J. Malignant gliomas: old and new systemic treatment approaches. *Radiol Oncol* 2016; **50:** 129-38. doi: 10.1515/raon-2015-0003
3. Yang H, Ye D, Guan KL, Xiong Y. IDH1 and IDH2 mutations in tumorigenesis: mechanistic insights and clinical perspectives. *Clin Cancer Res* 2012; **18:** 5562-71. doi: 10.1158/1078-0432.CCR-12-1773
4. Losman JA, Kaelin WG, Jr. What a difference a hydroxyl makes: mutant IDH, (R)-2-hydroxyglutarate, and cancer. *Genes Dev* 2013; **27:** 836-52. doi: 10.1101/gad.217406.113
5. Dang L, White DW, Gross S, Bennett BD, Bittinger MA, Driggers EM, et al. Cancer-associated IDH1 mutations produce 2-hydroxyglutarate. *Nature* 2009; **462:** 739-44. doi: 10.1038/nature08617
6. Figueroa ME, Abdel-Wahab O, Lu C, Ward PS, Patel J, Shih A, et al. Leukemic IDH1 and IDH2 mutations result in a hypermethylation phenotype, disrupt TET2 function, and impair hematopoietic differentiation. *Cancer Cell* 2010; **18:** 553-67. doi: 10.1016/j.ccr.2010.11.015
7. Duarte IF, Marques J, Ladeirinha AF, Rocha C, Lamego I, Calheiros R, et al. Analytical approaches toward successful human cell metabolome studies by NMR spectroscopy. *Anal Chem* 2009; **81:** 5023-32. doi: 10.1021/ac900545q
8. Cuperlovic-Culf M, Barnett DA, Culf AS, Chute I. Cell culture metabolomics: applications and future directions. *Drug Discov Today* 2010; **15:** 610-21. doi: 10.1016/j.drudis.2010.06.012
9. Dietmair S, Timmins NE, Gray PP, Nielsen LK, Kromer JO. Towards quantitative metabolomics of mammalian cells: development of a metabolite extraction protocol. *Anal Biochem* 2010; **404:** 155-64. doi: 10.1016/j.ab.2010.04.031
10. Kronthaler J, Gstraunthaler G, Heel C. Optimizing high-throughput metabolomic biomarker screening: a study of quenching solutions to freeze intracellular metabolism in CHO cells. *Omics* 2012; **16:** 90-7. doi: 10.1089/omi.2011.0048
11. Triba MN, Starzec A, Bouchemal N, Guenin E, Perret GY, Le Moyec L. Metabolomic profiling with NMR discriminates between biphosphonate and doxorubicin effects on B16 melanoma cells. *NMR Biomed* 2010; **23:** 1009-16. doi: 10.1002/nbm.1516
12. Mesti T, Savarin P, Triba MN, Le Moyec L, Ocvirk J, Banissi C, et al. Metabolic impact of anti-angiogenic agents on U87 glioma cells. *PLoS One* 2014; **9:** e99198 doi: 10.1371/journal.pone.0099198
13. Mosmann T. Rapid colorimetric assay for cellular growth and survival: application to proliferation and cytotoxicity assays. *J Immunol Methods* 1983; **65:** 55-63. doi.org/10.1016/0022-1759(83)90303-4
14. Delaglio F, Grzesiek S, Vuister GW, Zhu G, Pfeifer J, Bax A. NMRPipe: a multidimensional spectral processing system based on UNIX pipes. *J Biomol NMR* 1995; **6:** 277-93.
15. Trygg J, Wold S. Orthogonal projections to latent structures (O-PLS). *Journal of Chemometrics* 2002; **16:** 119-28. doi: 10.1002/cem.695
16. Vander Heiden MG, Cantley LC, Thompson CB. Understanding the Warburg effect: The metabolic requirements of cell proliferation. *Science* 2009; **324:** 1029-33. doi: 10.1126/science.1160809
17. Billah MM, Anthes JC. The regulation and cellular functions of phosphatidylcholine hydrolysis. *Biochem J* 1990; **269:** 281-91. PMCID: PMC1131573
18. Horska A, Barker PB. Imaging of brain tumors: MR spectroscopy and metabolic imaging. *Neuroimaging Clin N Am* 2010; **20:** 293-310. doi: 10.1016/j.nic.2010.04.003
19. Cheng LL, Anthony DC, Comite AR, Black PM, Tzika AA, Gonzalez RG. Quantification of microheterogeneity in glioblastoma multiforme with ex vivo high-resolution magic-angle spinning (HRMAS) proton magnetic resonance spectroscopy. *Neuro Oncol* 2010; **2:** 87-95. doi: 10.1093/neuonc/2.2.87.
20. Maurmann L, Belkacemi L, Adams NR, Majmudar PM, Moghaddas S, Bose RN. A novel cisplatin mediated apoptosis pathway is associated with acid sphingomyelinase and FAS proapoptotic protein activation in ovarian cancer. *Apoptosis* 2015; **20:** 960-74. doi: 10.1007/s10495-015-1124-2
21. Delikatny EJ, Cooper WA, Brammah S, Sathasivam N, Rideout DC. Nuclear magnetic resonance-visible lipids induced by cationic lipophilic chemotherapeutic agents are accompanied by increased lipid droplet formation and damaged mitochondria. *Cancer Res* 2002; **62:** 1394-400.
22. Blankenberg FG, Storrs RW, Naumovski L, Goralski T, Spielman D. Detection of apoptotic cell death by proton nuclear magnetic resonance spectroscopy. *Blood* 1996; **87:** 1951-6.
23. Blankenberg FG, Katsikis PD, Storrs RW, Beaulieu C, Spielman D, Chen JY, et al. Quantitative analysis of apoptotic cell death using proton nuclear magnetic resonance spectroscopy. *Blood* 1997; **89:** 3778-86.
24. Al-Saffar NM, Titley JC, Robertson D, Clarke PA, Jackson LE, Leach MO, et al. Apoptosis is associated with triacylglycerol accumulation in Jurkat T-cells. *Br J Cancer* 2002; **86:** 963-70. doi: 10.1038/sj.bjc.6600188.
25. Griffin JL, Lehtimäki KK, Valonen PK, Gröhn OH, Kettunen MI, Ylä-Herttuala S, et al. Assignment of 1H nuclear magnetic resonance visible polyunsaturated fatty acids in BT4C gliomas undergoing ganciclovir-thymidine kinase gene therapy-induced programmed cell death. *Cancer Res* 2003; **63:** 3195-201.
26. Opstad KS, Bell BA, Griffiths JR, Howe FA. Taurine: a potential marker of apoptosis in gliomas. *Briti J Cancer* 2009; **100:** 789-94. doi: 10.1038/sj.bjc.6604933
27. Tien RD, Lai PH, Smith JS, Lazeyras F. Single-voxel proton brain spectroscopy exam (PROBE/SV) in patients with primary brain tumors. *AJR Am J Roentgenol* 1996; **167:** 201-9. doi: 10.2214/ajr.167.1.8659372
28. Kolpakova ME, Veselkina OS, Vlasov TD. Creatine in cell metabolism and its protective action in cerebral ischemia. *Neurosci Behav Physiol* 2015; **45:** 476-82. doi: 10.1007/s11055-015-0098-4
29. Izquierdo-Garcia JL, Viswanath P, Eriksson P, Chaumeil MM, Pieper RO, Phillips JJ, et al. Metabolic reprogramming in mutant IDH1 glioma cells. *PLoS One* 2015; **10:** e0118781. doi: 10.1371/journal.pone.0118781
30. Reitman ZJ, Jin G, Karoly ED, Spasojevic I, Yang J, Kinzler KW, et al. Profiling the effects of isocitrate dehydrogenase 1 and 2 mutations on the cellular metabolome. *Proc Natl Acad Sci USA* 2011; **108:** 3270-5. doi: 10.1073/pnas.1019393108
31. Dang CV. Rethinking the Warburg effect with Myc micromanaging glutamine metabolism. *Cancer Res* 2010; **70:** 859-62. doi: 10.1158/0008-5472.CAN-09-3556
32. Halama A, Moller G, Adamski J. Metabolic signatures in apoptotic human cancer cell lines. *Omics* 2011; **15:** 325-35 doi: 10.1089/omi.2010.0121
33. Scott DA, Richardson AD, Filipp FV, Knutzen CA, Chiang GG, Ronai ZA, et al. Comparative metabolic flux profiling of melanoma cell lines: beyond the Warburg effect. *J Biol Chem* 2011; **286:** 42626-34. doi: 10.1074/jbc.M111.282046
34. Dang L, White DW, Gross S, Bennett BD, Bittinger MA, Driggers EM, et al. Cancer-associated IDH1 mutations produce 2-hydroxyglutarate. *Nature* 2009; **462:** 739-44. doi: 10.1038/nature08617
35. DeBerardinis RJ, Mancuso A, Daikhin E, Nissim I, Yudkoff M, Wehrli S, et al. Beyond aerobic glycolysis: transformed cells can engage in glutamine metabolism that exceeds the requirement for protein and nucleotide synthesis. *Proc Natl Acad Sci USA* 2007; **104:** 19345-50. doi: 10.1073/pnas.0709747104
36. Metallo CM, Walther JL, Stephanopoulos G. Evaluation of 13C isotopic tracers for metabolic flux analysis in mammalian cells. *J Biotechnol* 2009; **144:** 167-74. doi: 10.1016/j.jbiotec.2009.07.010
37. Ward PS, Patel J, Wise DR, Abdel-Wahab O, Bennett BD, Coller HA, et al. The common feature of leukemia-associated IDH1 and IDH2 mutations is a neomorphic enzyme activity converting alpha-ketoglutarate to 2-hydroxyglutarate. *Cancer Cell* 2010; **17:** 225-34. doi: 10.1016/j.ccr.2010.01.020

research article

Randomised trial of HPV self-sampling among non-attenders in the Slovenian cervical screening programme ZORA: comparing three different screening approaches

Urska Ivanus[1,2], Tine Jerman[1], Alenka Repse Fokter[3], Iztok Takac[4], Veronika Kloboves Prevodnik[5], Mateja Marcec[4], Ursula Salobir Gajsek[6], Maja Pakiz[4], Jakob Koren[6], Simona Hutter Celik[7], Kristina Gornik Kramberger[7], Ulrika Klopcic[5], Rajko Kavalar[7], Simona Sramek Zatler[3], Biljana Grcar Kuzmanov[8], Mojca Florjancic[1], Natasa Nolde[5], Srdjan Novakovic[9], Mario Poljak[10], Maja Primic Zakelj[1]

[1] National Cervical Cancer Screening Programme and Registry ZORA, Epidemiology and Cancer Registry, Institute of Oncology Ljubljana, Ljubljana, Slovenia
[2] Faculty of Medicine, University of Ljubljana, Ljubljana, Slovenia
[3] Department of Pathology and Cytology, Celje General Hospital, Celje
[4] University Department of Gynaecology and Perinatology, University Medical Centre Maribor, Maribor, Slovenia
[5] Department of Cytopathology, Institute of Oncology Ljubljana, Ljubljana, Slovenia
[6] Department of Gynaecology and Obstetrics, General Hospital Celje, Celje, Slovenia
[7] Department of Pathology, University Medical Centre Maribor, Maribor, Slovenia
[8] Department of Pathology, Institute of Oncology Ljubljana, Ljubljana, Slovenia
[9] Department of Molecular Diagnostics, Institute of Oncology Ljubljana, Ljubljana, Slovenia
[10] Institute of Microbiology and Immunology, Faculty of Medicine, University of Ljubljana, Ljubljana, Slovenia

Radiol Oncol 2018; 52(4): 399-412.

Received 20 May 2018
Accepted 13 July 2018

Correspondence to: Urška Ivanuš M.D., Ph.D., National Cervical Cancer Screening Programme and Registry ZORA, Epidemiology and Cancer Registry, Institute of Oncology Ljubljana, Zaloška 2, SI-1000 Ljubljana, Slovenia. Phone: +386 41 901 478; E-mail: uivanus@onko-i.si

Disclosure: No potential conflicts of interest were disclosed.

Background. To overcome obstacles within the Slovenian organised cervical cancer screening programme, a randomised pilot study of human papillomavirus (HPV) self-sampling among non-attenders was performed, aiming to assess three different screening approaches.

Participants and methods. Non-attenders aged 30–64 years from two Slovenian regions were randomised to two HPV self-sampling groups–the opt-in (I1, n = 14.400) and the opt-out (I2, n = 9.556), with a control group (P, n = 2.600). Self-collected samples were analysed using the Hybrid Capture 2 assay. HPV-positive women were invited to a colposcopy. The overall and type-specific intention-to-screen response rates and histological outcomes with a positive predictive value (PPV) according to the women's age, the screening approach, the level of protection resulting from previous screening history, and the region of residence were assessed.

Results. Of the 26.556 women enrolled, 8.972 (33.8%) responded with self-sample for HPV testing and/or traditional cytology within one year of enrolment. Response rates were 37.7%, 34.0% and 18.4% ($p < 0.050$) for opt-out, opt-in and control groups. Cervical intraepithelial neoplasia (CIN)2+ was diagnosed in 3.9/1.000, 3.4/1.000, and 3.1/1.000 women ($p > 0.050$), respectively. PPV of the HPV self-sampling was 12.0% and 9.6% for CIN2+ and CIN3+. The highest PPV was obtained in non-attenders in screening programme for more than 10-years and concordant results of HPV testing with 40.8% for CIN2+ and 38.8% for CIN3+.

Conclusions. The results of our study show that a high response to HPV self-sampling can be achieved also in an opt-in approach, if women are encouraged to choose between self-sampling at home and screening with gynaecologist. In addition, clinically important risk difference for a high-grade cervical lesion exists in the case of a positive result of HPV testing on self-collected samples, depending on the length of the interval since last screening. Stratified management of these women should be strongly considered. Women who were not screened with cytology for at least 10 years should be referred to immediate colposcopy for histology verification instead to delayed re-testing.

Key words: cervical cancer; screening programme; non-attenders; cytology; HPV; self-sampling

Introduction

Cervical cancer screening programmes have successfully reduced the incidence of and mortality from cervical cancer in several countries.[1-3] In well-organised population-based programmes with good screening test coverage, around half or more of new cases are detected in non-attenders, who usually represent the minority of the eligible population.[4] Furthermore, these cancers are more often diagnosed in advanced stages, requiring more invasive treatment and subsequently leading to lower quality of life and survival.[5-7] Similar findings were identified in Slovenia after the implementation of the national, population-based, organised cervical cancer screening national programme (NP) ZORA.[8]

The NP ZORA was implemented in 2003 with conventional cytology in three-year screening intervals for women aged 20–64 years. The three-year coverage of the target population with a screening test is just above 70%, and its five-year coverage is just above 80%.[8] Higher coverage is observed in younger women and reaches 80% in the 20–24 age group. It drops below 70% in women above 50 and is just below 55% in the oldest age group of women aged from 60 to 64. Coverage also varies between administrative units.[8] Slovenia is among the European countries with the highest historical cervical cancer incidence rates but is also among the countries with the most pronounced decline in cervical cancer incidence rates over time.[9] The steepest decline was observed after the implementation of the NP ZORA, with the annual change being -5.8% in 2003–2015.[3] Non-attenders in the NP ZORA account for 50–60% of new cervical cancer cases, among which more than 80% are diagnosed at FIGO stage II or higher, compared to regular attenders where only 20% of cancers are diagnosed at stage II or higher.[10]

Non-attendance is the main limiting factor for achieving the full health benefit of screening programmes at the population level in a well-organised, high-quality screening setting. Recent systematic reviews and meta-analyses have shown that offering human papillomavirus (HPV) self-sampling at home to non-attenders can significantly increase attendance and the detection of high-grade cervical lesions, compared to currently widely used reminder letters for clinician-based screening.[11] Consequently, the recently renewed European guidelines for quality assurance in cervical cancer screening[12] recommend that countries with organised screening assess whether HPV self-sampling is feasible and cost-effective for non-attenders in the local setting. If it is, countries are encouraged to upgrade their existing screening programmes, but only if they can provide careful monitoring and evaluation of the desired performance and outcomes after implementation. Since HPV self-sampling has similar sensitivity as cytology but lower sensitivity than HPV testing of practitioner-obtained cervical samples[13], HPV self-sampling is recommended only for non-attenders in the organised programmes and not for all women.[12]

There are two main approaches to self-sampling, and there is lack of evidence which of them has a higher overall effect among non-attenders and is more cost-effective. With the opt-out approach, self-sampling devices (testers) are sent by regular mail to non-attenders, while with the opt-in approach, women are invited to order a tester or a tester can be picked up at a local pharmacy.[11] Since response rates in early randomised opt-in studies were comparable to control groups and much lower than in opt-out studies[14-16], the opt-in approach was not favoured in further studies.[11] When implementing a new intervention at the population level, however, it is necessary to keep costs as low as possible. Due to high wastage of distributed testers, the opt-out approach might be less feasible in terms of cost-effectiveness, while the opt-in approach mitigates this problem. To the best of our knowledge, only two studies have been published until now that suggest that the opt-in approach could generate a high response. A recent Swedish study showed a significantly higher response in opt-in self-sampling compared to both a reminder letter and a reminder telephone call, but the study did not include an opt-out group.[16] Only one, very recent, randomised study, conducted in Denmark, showed a higher response in an opt-in self-sampling group compared to a control group, but even there the response was lower than in the opt-out group.[17]

The available evidence supports the implementation of HPV self-sampling in countries with well-organised screening, such as Slovenia. The aim of the present study, performed among non-attenders in the NP ZORA, was to compare three approaches (opt-out, opt-in and a reminder letter for screening at the clinic) in a randomised setting within an ongoing, population-based screening programme with relatively high coverage. Two main research questions were probed: (1) is it possible to reach an adequate response rate in the opt-in compared opt-out approach if women are given the option to order a tester for HPV self-sampling or visit a

gynaecologist for cytology and are encouraged to select their preferred option? and (2) should the same follow-up diagnostic procedure be used for all women following a positive result of HPV test performed on self-collected samples taken at home or should a stratified approach be considered?

Participants and methods

Study protocol

The study was designed as a pilot for HPV self-sampling among non-attenders in the NP ZORA. It was an open label, multi-arm study with a randomised design. Study protocol is summarised below; full protocol is described in details in Supplementary material (SupMat 1).

Women were eligible for the study if they were aged 30–64, had no cytology result registered in the National Cervical Cancer Screening Registry (the ZORA registry) in the last four years, had their permanent residence in the Celje or Maribor regions, and had no recorded hysterectomy in the ZORA registry. Total of 26.556 eligible women were randomly selected from the ZORA registry and randomly allocated to the opt-in (I1, n = 14.400), opt-out (I2, n = 9.956) or control (P, n = 2.600) groups (Figure 1). The eligible women were randomly selected and allocated once per month, using a random number generator in R.[18] The randomisation was stratified by five-year age groups, screening history and region of residence. Ten random selections and allocations were done in 2015, as described in the supplementary material (SupMat 1). Invitation letters with attached questioner for double-checking the eligibility criteria were sent within a month of the enrolment to all selected women, between 6 January and 1 December 2015. Women were excluded from further correspondence in three distinct stages; after the initial letter was sent but before a tester was sent, after a tester was sent or after the result of the HPV test performed on a self-collected sample was sent (Figure 1).

During the study, all the women had free access to regular cytological screening with their personal gynaecologist (PG), who are the providers of cervical screening in Slovenia. Women in the intervention groups were invited to take a cervicovaginal sample with a self-sampling device (tester) at their home, following the manufacturer's instructions, and send it to the laboratory by ordinary mail as soon as possible.

Three different testers were used in the opt-out study group: Qvintip (Aprovix AB, Uppsala, Sweden), HerSwab (Eve Medical, Toronto, Canada) and Delphi Screener (Delphi Bioscience, Scherpenzeel, the Netherlands). In the opt-in study group, only Qvintip was used. All self-collected samples were tested for the presence of 13 high-risk HPV types using the clinically validated test Hybrid Capture 2 High-Risk HPV DNA assay (HC2, Qiagen, Hilden, Germany), following the manufacturer's instructions. The cut-off value of RLU/CO = 1.00 pg/ml was used to distinguish between positive and negative HPV results. Self-collected samples were evaluated for cellularity control by visual pellet assessment after centrifugation. Self-collected samples with negative HC2 result and no visual pellet were processed further. The DNA concentration was measured and, if it was below a cut-off point of 5 ng/ul, the sample was regarded as technically inadequate. Cytological and histological evaluations were performed by certified pathologists participating in the NP ZORA.

The result of the HPV test and further recommendations were sent to all responders. If the result was HPV negative, it was recommended to the woman that she attend a regular cytological screening examination after three years. All women with a HPV positive result were offered an appointment for a colposcopy at a regional hospital (University Clinical Centre Maribor or Celje General Hospital). Women with technically inadequate self-collected samples received invitation to visit their PG. In the case of an abnormal colposcopy result, a biopsy was taken; no blind biopsies were taken. Women were managed according to the national guidelines.[19]

The study was coordinated by the Institute of Oncology Ljubljana. It was conducted in compliance with the Helsinki Declaration and was approved by the National Medical Ethics Committee at the Slovenian Ministry of Health (consents Nos. 155/03/13 and 136/04/14). It was financed by the Slovenian Research Agency and the Slovenian Ministry of Health (trial No. L3-5512).

Primary and secondary outcomes

The primary outcomes were: (1) intention-to-screen response rates among all enrolled women and (2) high-grade histology outcomes among all enrolled women and all responders according to the age of the woman, opt-in and the opt-out approach, region of residence and the level of protection resulting from previous screening history. The intention-to-screen response rate was computed as a proportion of enrolled women (all women who were

FIGURE 1. Flow diagram of 26.556 non-attenders in the organised Slovenian cervical cancer screening programme ZORA, randomly selected from a screening registry for pilot implementation of HPV self-sampling and randomly allocated to the opt-in (I1), opt-out (I2) and control (P) study group.

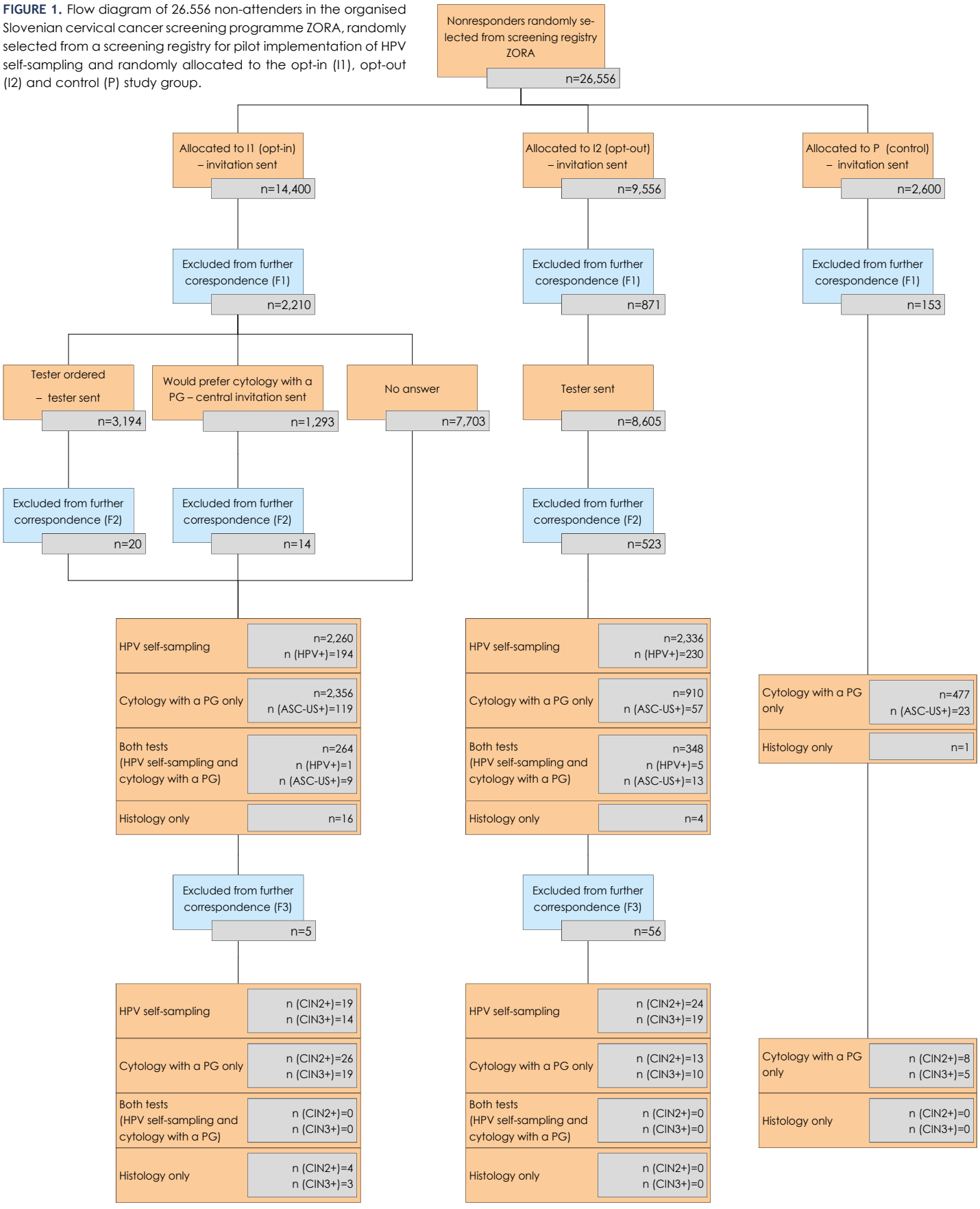

randomly selected from the ZORA registry) with a response within one year after the enrolment. The response was defined as having an HPV test performed on self-collected sample and/or cytology with PG within one year after the enrolment. The response types were classified as 'HPV self-sampling only' (type A response), 'cytology screening with a PG only' (type B response), or 'both tests' (both HPV test on self-collected sample and cytology screening with a PG, type C response). Very few women visited PG for a cytological screening after the enrolment, but only a histological sample was taken from the cervix, mostly because the changes of the cervix were already visible. These women were considered type B responders. The high-grade histological outcome was defined as the diagnosis of a cervical intraepithelial neoplasia (CIN)2+ or CIN3+ lesion within one year after enrolment in the study. High-grade histology outcomes were computed as a proportion of women with the CIN2+ or CIN3+ outcome among all the enrolled women and among the responders. PPV of the HPV test was computed as a proportion of women with a high-grade histological outcome among all the women who attended colposcopy after a positive HPV test. Cytological and histological outcomes within one year after the enrolment were identified for all the enrolled women by linking the study database with the ZORA registry. If a woman had more than one histological outcome, the lesion with the highest grade was used in calculations.

Secondary outcomes were: (1) tester ordering in the opt-in study group, (2) the results of the HPV test on self-collected sample, (3) the compliance at further examinations for women with a positive HPV test, and a (4) positive concordance of the result of the HPV testing on self-collected samples and on samples taken by a practitioner. The tester ordering was computed as a proportion of the women enrolled in the opt-in study group who opted in for a tester among all the women enrolled in opt-in study group. The results of screening tests are presented as the proportions of positive and the proportions of technically inadequate self-collected samples. The compliance was computed as the proportion of all the women who attended the examination either at a regional clinic or with their PG from all the women with a positive HPV test performed on self-collected sample. The results of the HPV testing on self-collected samples and on practitioner-obtained samples were concordant if both were positive at the cut-off value RLU/CO = 1.00 pg/ml.

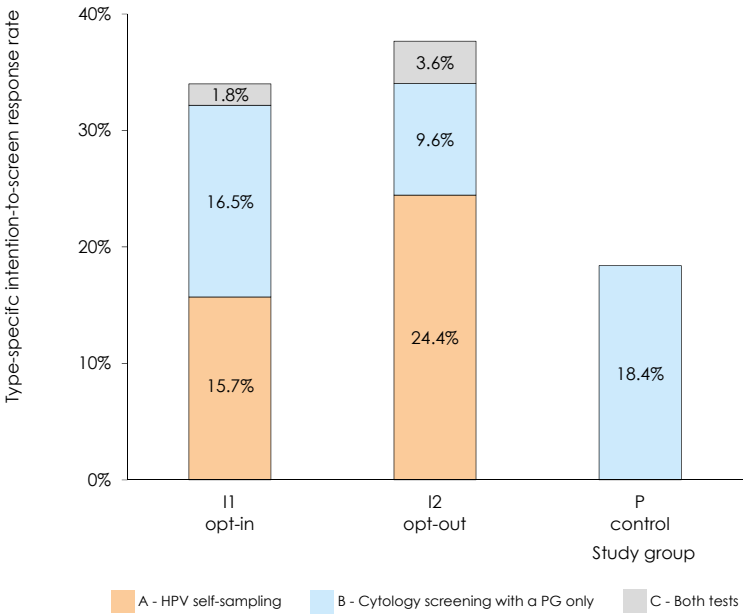

FIGURE 2. Intention-to-screen response rate in study groups opt-in (I1), opt-out (I2) and comparison (P) by three types of response: HPV self-sampling (type A response), cytology screening with a PG only (type B response) or both (HPV self-sampling and cytology screening with a PG only, type C response).

Statistical analyses

Response rates were analysed only on the intention-to-screen basis. The effect size was estimated as a relative risk ratio within the 95% confidence interval (CI). Predefined subgroup analyses of possible significant predictors for the response and histological outcomes were performed with the aim to identify common characteristics of responders and approaches with the highest response rate and high-grade lesions detection (Table 2 and Table 3). The univariate logistic regression was used to assess if the outcome was significantly associated with the possible predictor. The multivariate logistic regression analysis was performed for all primary and secondary outcomes to adjust the outcome for predefined predictors. The predefined predictors included in these analyses were the woman's age, the region of residence, the level of protection, and the study group. The data on predictors were obtained from the ZORA registry at the time of the random selection. The level of protection due to previous screening history was categorised as 'medium protection' if the last cytology was done 4–9 years prior to the enrolment and as 'no/low protection' if the last cytology was done 10 years or more prior to the enrolment or if the woman didn't have any cytology result in the ZORA registry. Age was used as a continuous variable in all univariate and

multivariate analyses. In the subgroup analysis, women's age was described in terms of the mean and the 95% confidence intervals. Other possible predictors were described as proportions; chi-square test was used to determine if the observed difference in the distribution of proportions within subgroups was statistically significant. Additional analyses were performed to explore type-specific response rates (Figure 2), high-grade disease outcomes among responders, and high-grade disease outcomes in subgroups of women with the highest PPV for high-grade disease. All analyses were conducted with SPPS 22.0 (SPSS; Chicago, IL, USA) and the open source programme language R, using 2-tailed tests and the significance level $\alpha = 0.050$.[18] We have used the random number generator in the programme language R for the study group selection, programme language R was also used for the calculations of relative risk ratios and their 95% confidence intervals.

Results

Characteristics of women

In total, 26.556 non-attenders in the Slovenian organised cervical cancer screening programme ZORA were randomly selected and randomly allocated to three study groups: the opt-in group (I1, n = 14.400), the opt-out group (I2, n = 9.556), and the control group (P, n = 2.600) (Figure 1).

Table 1 shows the characteristics of the enrolled women. The mean age was 49.8 years (95% CI: 49.7–50.0) and was similar across all study groups. 41.6% of women were permanently residing in the Celje region and 58.4% in the Maribor region. More than half of the enrolled women (53.1%) had no/low level of protection. The distribution of women according to the level of protection differed significantly between the study groups, most likely due to the refreshment of the target population with new women with medium protection who became eligible for the study between samplings and because different study groups were included at different samplings (SupMat 1).

Altogether 3.852 (14.5%) women were excluded from further correspondence at different stages during the study after the initial invitation letter with a questionnaire was sent (Figure 1). Major reasons were a previous unregistered hysterectomy reported by woman via questionnaire attached to the study invitation letters (4.0%, 1.075/26.556), undelivered invitation letter due to unknown address or unaccepted mail (3.6%, 947/26.556), recent cytology not yet registered in the ZORA registry (2.2%, 591/26.556), living abroad (2.0%, 537/26.556), rejection of participation in the study (1.9%, 500/26.556), or other reasons, such as virginity, severe disability, current pregnancy, or other (0.8%, 202/26.556).

TABLE 1. Characteristics of women enrolled in the study

All randomly selected and allocated women	Total		STUDY GROUPS			
	Number	%	I1 opt-in	I2 opt-out	P control	P-value
Number	26,556	100.0	14,400	9,556	2,600	
Age						
Mean age (95% CI)	49.8 (49.7-50.0)		49.8 (49.7-50.0)	49.8 (49.6-50.0)	50.0 (49.6-50.3)	
Level of protection						
medium	12,464	46.9	6,796	4,540	1,128	*0.001**
no/low	14,092	53.1	7,604	5,016	1,472	
Region						
Celje	11,055	41.6	5,996	3,984	1,075	*0.951*
Maribor	15,501	58.4	8,404	5,572	1,525	

**Statistically significant result at a = 0.05.*

Response

Out of 26.556 enrolled women, 8.972 (33.8%) self-collected a sample for the HPV test or attended screening with their PG up to one year after the initial invitation letter was sent. In the univariate analysis, the overall response rate was significantly associated with the study groups, age of women and the level of protection, but not to the region of residence. After the adjustment in the multivariate analysis, the overall response was significantly associated with all the predictors.

Table 2 shows intention-to-screen response rates in study groups. The response rates were significantly different among all study groups. Response was 2.0-times higher (95% CI: 1.9–2.2) in the opt-out study group than in the control study group (37.7% *vs.* 18.4%), 1.8-times higher (95% CI: 1.7–2.0) in the opt-in study group than in the control study group (34.0% *vs.* 18.4%) and 1.11-times higher (95% CI: 1.07–1.15) in the opt-out study group than in the opt-in study group (37.7% *vs.* 34.0%). Women with medium protection had a 2.8-times higher (95% CI: 2.7–2.9) response rate than women with no/low protection (51.1% *vs.* 18.5%). The responders from the Maribor region were also statistically significantly older than responders from the Celje region.

Response rates also remained significantly different among study groups in a stratified analysis of the subgroup of women with medium and with no/low protection due to the past screening history (Table 3). In the subgroup of women with no/

TABLE 2. The main results by their predictors. Intention-to-screen response rates, the mean age of responders and histological outcomes are presented as absolute numbers, proportions (per 100 or 1.000) and 95% confidence intervals (CI) by the study group, the region of residence and the level of protection

			Number of women	Intention to screen response rate per 100 (%) with 95% CI	Mean age (95% CI) of responders	Intetion to screen histology outcome			
						HSIL/CIN2+		HSIL/CIN3+	
						no.	per 1000 (‰) with 95% CI	no.	per 1000 (‰) with 95% CI
ALL WOMEN	All women		26,556	33.8% (33.2%–34.4%)	49.0 (48.7-49.2)	94	3.5‰ (2.9‰–4.4‰)	71	2.7‰ (2.1‰–3.4‰)
	Responders		8,972						
STUDY GROUPS	I1 opt-in	all	14,400	34.0% (33.2%–34.8%)	49.0 (48.7-49.3)	49	3.4‰ (2.5‰–4.5‰)	36	2.5‰ (1.8‰–3.5‰)
		responders	4,896						
	I2 opt-out	all	9,556	37.7% (36.7%–38.6%)	49.0 (48.6-49.3)	37	3.9‰ (2.8‰–5.4‰)	30	3.1‰ (2.2‰–4.5‰)
		responders	3,598						
	P control	all	2,600	18.4% (16.9%–19.9%)	48.0 (47.2-48.9)	8	3.1‰ (1.4‰–6.3‰)	5	1.9‰ (0.7‰–4.8‰)
		responders	478						
	p-value			< 0.000*		0.766		0.557	
REGION	Celje	all	11,055	33.2% (32.3%–34.0%)	48.3 (47.9-48.6)	38	3.4‰ (2.5‰–4.8‰)	28	2.5‰ (1.7‰–3.7‰)
		responders	3,666						
	Maribor	all	15,501	34.2% (33.5%–35.0%)	49.4 (49.2-49.7)	56	3.6‰ (2.8‰–4.7‰)	43	2.8‰ (2.0‰–3.8‰)
		responders	5,306						
	p-value			0.070		0.813		0.708	
LEVEL OF PROTECTION	Medium	all	12,464	51.1% (50.2%–52.0%)	48.4 (48.2-48.7)	48	3.9‰ (2.9‰–5.1‰)	33	2.6‰ (1.9‰–3.8‰)
		responders	6,367						
	No/low	all	14,092	18.5% (17.8%–19.1%)	51.1 (50.9-51.3)	46	3.3‰ (2.4‰–4.4‰)	38	2.7‰ (1.9‰–3.7‰)
		responders	2,605						
	p-value			<0.000*		0.422		0.838	

**Statistically significant result at a = 0.05.*

low protection, the response was also significantly higher in the Maribor (19.5%) than the Celje region (17.0%).

Type-specific response

Out of 26.556 enrolled women, 4.596 (17.3%) women performed only HPV self-sampling, (type A response), 3.764 (14.2%) attended screening with their PG only (type B response) and 612 (2.3%) women performed both HPV self-sampling and attended the screening with the selected PG (type C response). In total, 5.208 HPV tests performed on self-collected samples (4.596 + 612) and 4.355 cytological results (3.743 + 612) were registered during the study. Among 3.764 women with the type B response, 3.743 had the cytology result recorded and 21 had only the histology result recorded (without cytology). Most women with the type C response first had the HPV testing on self-collected sample and later decided to additionally attend the cytological screening with their PG (92.6%, 567/612).

Figure 2 shows the intention-to-screen response rate by the type of response in all the three study groups. Distribution of type A and type B response rates in opt-in and opt-out group differed in such

way, that type A response was statistically significantly higher in opt-out compared to opt-in group (24.4% *vs.* 15.7%, 95% CI do not overlap) and contrary, the type B response was statistically significantly higher in opt-in compared to opt-out group (16.5% *vs.* 9.6%, 95% CI do not overlap) and at the same time comparable to the response in the control group (18.4%, overlapping 95% CI with the opt-in but not with the opt-out study group) (Table 2 at SupMat2). Only a small proportion of women – 1.8% in the opt-in study group and 3.6% in the opt-out study group – had the type C response. The supplementary material provides further data regarding the statistically significant differences in the type A, B and C response rates among the study groups (SupMat 2).

Tester order in the opt-in group

Out of 14.400 women in the opt-in study group, 22.2% (3.194/14.400; 95% CI: 21.5%–22.9%) ordered the tester. The ordering was significantly associated with the region and the level of protection. It was 1.1-times higher (95% CI: 1.1–1.2) in the Maribor than the Celje region (23.4% *vs.* 20.4%), and 1.6-times higher (95% CI: 1.5–1.7) in women with medium compared to no/low protection (27.4% *vs.* 17.5%). Out of 3.194 women who ordered the tester, 2.524 (79.0%; 95% CI: 77.6%–80.4%) returned the self-collected sample. The response after the test order was significantly associated with the age and the level of protection. It was higher in elderly women and women with medium protection (81.6%, 1.520/1.863) than in younger women and women with low/no protection (75.4%, 1.004/1.331).

Results of HPV testing on self-collected samples

The overall HPV positivity rate in the total study population was 8.3% (95% CI: 7.5%–9.0%); the HPV was detected in 430 out of 5.208 self-collected samples (Figure 1). HPV positivity was 7.7% (195/2.524; 95% CI: 6.7%–8.9%) in the opt-in study group and 8.8% (235/2.684; 95% CI: 7.7%–9.9%) in the opt-out study group, the difference was not statistically significant. HPV positivity was also not significantly associated with the region and the level of protection. To the contrary, younger women had significantly higher positivity rates than older women in both intervention study groups.

The rate of technically inadequate self-collected samples was 1.4% (75/5.208; 95% CI: 1.1%–1.8%). Women with technically inadequate self-collected samples (mean age 56.0; 95% CI: 54.2–57.8) were significantly older than all the women who self-collected a sample for the HPV test (mean age 50.3 years; 95% CI: 50.1–50.6). The HPV test rate of technically inadequate self-collected samples was not associated with the study group, region, or the level of protection.

Compliance with a follow-up examination after a positive HPV test

Out of 430 women with a positive result of HPV testing on self-collected samples, 388 (90.2%) complied with a further follow-up examination; 333 (77.4%) attended the prescheduled examination at a colposcopy clinic, and 55 (12.8%) visited a PG. 42 (9.8%) of women with a positive result of HPV testing on self-collected didn't respond to the invitation for a further follow-up examination. The compliance was significantly higher in women from the Maribor region (92.9%, 234/252) and women with the medium protection (94.3%, 263/279) than in women from the Celje region (86.5%, 154/178) and women with no/low protection (82.8%, 125/151). The multivariate analysis confirmed that compliance was not associated with the age of the women or the study group.

Out of 333 women who attended a further examination, 146 (43.8%) had a positive result of the

TABLE 3. Response rate stratified by the level of protection due to previous screening. Intention-to-screen response rates are presented as absolute numbers, proportions (per 100) and 95% confidence intervals (CI) by the study group and the region of residence

			Level of protection			
			Medium		No/low	
			Number of women	Response rate per 100 (%) with 95% CI	Number of women	Response rate per 100 (%) with 95% CI
STUDY GROUPS	I1 opt-in	all	6,796	51.5% (50.3%–52.7%)	7,604	18.3% (17.5%–19.2%)
		responders	3,501		1,395	
	I2 opt-out	all	4,540	54.8% (53.3%–56.2%)	5,016	22.2% (21.0%–23.3%)
		responders	2,486		1,112	
	P control	all	1,128	33.7% (30.9%–36.5%)	1,472	6.7% (5.5%–8.1%)
		responders	380		98	
	p-value		< 0.000*		< 0.000*	
REGION	Celje	all	5,361	50.4% (49.0%–51.7%)	5,694	17.0% (16.0%–18.0%)
		responders	2,700		966	
	Maribor	all	7,103	51.6% (50.5%–52.8%)	8,398	19.5% (18.7%–20.4%)
		responders	3,667		1,639	
	p-value		0.163		<0.000*	

**Statistically significant result at a = 0.05.*

TABLE 4. Positive predictive value (PPV) of HPV test for CIN2+ and CIN3+ in women who had undergone colposcopy after a positive HPV test on self-collected sample and in women with concordant results of both HPV tests. Results are stratified by the level of protection due to previous screening

	Number of women with				PPV	
	all	colposcopy	CIN2+	CIN3+	CIN2+	CIN3+
Positive result of HPV test on self-collected sample						
all women	430	333	40	32	12.0%	9.6%
women with medium protection	279	223	18	12	8.1%	5.4%
women with no/low protection	151	110	22	20	20.0%	18.2%
Concordant* results of HPV tests						
all women	na**	146	34	29	23.3%	19.9%
women with medium protection	na	97	14	10	14.4%	10.3%
women with no/low protection	na	49	20	19	40.8%	38.8%

**Results of HPV tests were concordant, if HPV test on self-collected sample as well as sample taken by a practitioner were positive.*
***Results not available (na), since only women with colposcopy had a sample taken by a practitioner.*

second HPV test carried out on a cervical sample obtained by the practitioner. The follow-up examination took place on mean of 57 days (median 48, range 13–317 days) after the self-collected sample was received in the laboratory by mail. Women with concordant positive results of the HPV testing on self-collected samples and on a practitioner-obtained cervical samples were younger (mean age 44.6 years; 95% CI: 42.9–46.3) than women with discordant results (mean age 49.3 years; 95% CI: 47.8–50.9). In the multivariate analysis, the concordance was not significantly associated with the study group, region, or the level of protection.

Histological outcomes

In one year after the enrolment, 94 women were diagnosed with CIN2+ and among those 71 with CIN3+. Among the 94 CIN2+, there were 11 cervical carcinomas (3 adenocarcinomas, 8 squamous carcinomas), 59 CIN3, 23 CIN2 and a single case of vaginal intraepithelial neoplasia (VaIN) grade 3. Ten out of eleven cervical carcinomas were diagnosed in women with no/low protection, and one in women with medium protection. Ten out of eleven carcinomas were diagnosed in women enrolled in intervention groups, and one in women enrolled in the control group. Eight of eleven carcinomas were diagnosed in women with the type B response; four of those only had a histological result without cytology. Five carcinomas were diagnosed in FIGO stage I (two in IA1 and three in IA2), four in stage IIB and two in stage IIIB. No CIN2+ was observed in the 612 women who underwent both tests (type C response).

The probability of the CIN2+ or CIN3+ outcome (per 1.000 women, ‰) among 26.556 enrolled women was 3.5‰ and 2.7‰, respectively (Table 2). The probability for the detection of CIN2+ or CIN3+ after the enrolment was significantly higher in younger women, in both the univariate and multivariate analysis, and it was decreasing with age. The study group, region and level of protection were not significantly associated with the CIN2+ or CIN3+ outcome.

An additional analysis was done to evaluate the detection of CIN2+ and CIN3+ among the responders. The CIN2+ or CIN3+ detection rate in responders was 10.5‰ (94/8.972) and 7.9‰, respectively (71/8.972) and was significantly associated with age and the level of protection, but not to the study group or region. The detection of CIN2+ or CIN3+ was significantly higher in younger than older responders. The responders with no/low protection had a significantly higher probability for high-grade lesions; 17.7‰ (46/2.605) had CIN2+ and 14.6‰ (38/2605) had CIN3+; compared to the responders with medium protection, where 7.5‰ (48/6.367) had CIN2+ and 5.2‰ (33/6.367) CIN3+. The estimated prevalence rate for the invasive cervical cancer was 383.9/100.000 in study responders with no/low protection (10/2.605), compared to 15.7/100.000 in the study responders with medium protection (1/6.367).

Positive predictive value of HPV testing on self-collected samples

Out of 333 women with a positive result of the HPV test performed on a self-collected sample who had colposcopy at a follow-up examination, 40 (12.0%) were diagnosed as CIN2+ and 32 (9.6%) as CIN3+ (Table 4). The PPV for CIN2+ and CIN3+ were significantly associated with the level of protection in both univariate and multivariate analyses. The women with no/low protection had 2.5-times higher (20.0% *vs.* 8.1%; 95% CI: 1.4–4.4) PPV for CIN2+ and 3.4-times higher (18.2% v 5.4%; 95% CI: 1.7–6.7) PPV

for CIN3+ than women with medium protection. Age was a significant predictor only in the multivariate analysis for CIN2+. The study group and region were not significantly associated with PPV.

PPV was even higher in women with concordant positive HPV test results. Out of 146 women with concordant positive HPV test results, 34 (23.3%) were diagnosed with CIN2+ and 29 (19.9%) with CIN3+ (Table 4). Women with no/low protection and concordant positive HPV test results had the highest risk for a high-grade lesion; it was 40.8% (20/49) for CIN2+ and 38.8% (19/49) for CIN3+. The risk was significantly higher in this group than in women with medium protection and concordant positive HPV test results, where the corresponding risks were 14.4% (14/97) and 10.3%, respectively (10/97). In the multivariate analysis, this difference also remained significant after adjustment. In women with concordant positive HPV test result, age, study group, and region were not significantly associated with the high-grade histology outcome.

Discussion

The Slovenian HPV self-sampling study was carried out as a randomised study within an ongoing organised cervical cancer screening programme, with the aim to explore the possible predictors for the intention-to-screen response rates and high-grade histology outcome, including PPV among non-attenders in the programme. Some predictors were related to the intervention (screening approach) and some were related to women's characteristics (age, region of residence, and level of protection from previous screening). In the multivariate analysis, the response rate was significantly associated with all the predictors. It was significantly higher in the opt-out approach compared to the opt-in approach and in the opt-in approach compared to a regular reminder. A significantly better response rate was detected in younger women, women with medium protection and women from the Maribor region. We also observed a difference in the type-specific response between the study groups. The response to attend routine cytology-based screening was higher in the opt-in approach group, while the HPV self-sampling response was higher in the opt-out approach group. In the multivariate analysis, the histology outcome among all the enrolled women was associated only with age, with younger women having a significantly higher probability to be diagnosed with a high-grade lesion. However, the detection of high-grade lesions among responders was significantly associated with age and the level of protection. The responders with no/low protection had significantly higher detection rates of both CIN2+ and CIN3+ and significantly higher PPV for both CIN2+ and CIN3+, compared to women with medium protection, probably reflecting a higher background risk as well as lack of the screening effect in the women who did not participate in screening for a longer time.

Response

The response rates in all study groups were higher than the pooled response rates in intervention groups of the most recent meta-analysis on the subject.[11] In our study, the response rates were 37.7% (95% CI: 36.7–38.6), 34.0% (95% CI: 33.2–34.8), and 18.4% (95% CI: 16.9–19.9) in the opt-out, opt-in and control groups, respectively, compared to the meta-analysis, where the response rates were 23.6 % (95% CI: 20.2–27.3), 14.0 % (95% CI: 8.0–21.4), 10.3% (95% CI: 6.2–15.2%) in the opt-out, opt-in, opt-out control and opt-in control approach, respectively.[11] Additionally, some previously published randomised studies reported similar response rates in the opt-out and control groups, *e.g.* 34.2% and 17.6%, respectively, in the Netherlands[19], and 39.0% in the opt-out group in a Swedish study.[20] The opt-in responses recorded in our study were also in line with a recently published randomised Danish study (30.9%) and a less powered Swedish study (24.5%), which are, to the best of our knowledge, the only published randomised studies that showed a significantly higher response in the opt-in group than in the control group; however, the second study was without the opt-out group.[16,17] Additionally, high overall response rates in opt-in groups were reached in some previous non-randomised studies, *e.g.* 39.1% in the Swedish[22] and 34.2% in the Danish study.[23]

A high response rate obtained in the opt-in group (close to one obtained in the opt-out group, but still significantly lower) is probably the most important finding of our study. Thus, the opt-in/control group response ratio was significantly higher in our study (1.8; 95% CI: 1.7–2.0) than the one recorded in the most recent meta-analysis (0.97; 95% CI: 0.65–1.46).[11] High overall response in the opt-in group is a consequence of high response to cytology, since in the opt-in group, more women attended the screening with a PG than performed the HPV self sampling. A relatively high response rate to cytology was also observed in some other opt-in[15,16,23] and opt-out studies[24]; however, the HPV

self-sampling response rate in those studies was always higher than the response rate to cytology. To our knowledge, there is only one recent study that obtained the higher response rate to cytology.[17] In contrast, the opt-out/control group response ratio in our study was comparable to the pooled results of previous studies (our study: 2.0; 95% CI: 1.9–2.2 vs meta-analyses: 2.4; 95% CI: 1.7–3.3).[11]

A high response in the opt-in group documented in our study could be explained by several factors. First, we provided women with a choice and encouraged them to either order a tester for HPV testing or make an appointment with a PG. They could have made an appointment by themselves, but in the case that they returned the questionnaire stating that they would prefer screening with a PG, we sent them a regular invitation letter and due to local health insurance rules, PGs must screen women with such an invitation not later than three months after the request for a screening appointment. Second, since women in the opt-in group had to devote more effort to undergo screening (they had to order a tester), we sent them two reminders to order the tester. Therefore, women in the opt-in study group could have received up to five invitation letters (the initial invitation letter, two reminders for ordering the tester, the letter with the tester package, and a reminder to return the sample), compared to women in the opt-out group, who according to the study protocol could have not received any reminders to order the tester. We used each contact as an opportunity to inform women why it was important to perform the screening and provided them with the option to communicate with us via a survey, telephone or email. Third, cytology and the HPV testing responders had different timelines for a response.[25] One-year follow-up time in our study provided women with enough time to arrange their appointment and attend the screening with a PG. In comparison to our study, follow-up times in some of the other randomised studies were shorter (starting from 3 months)[11], thus the full cytological response might not have yet been achieved. Fourth, mandatory recording of cytological results in the central screening registry enabled us to trace the clear majority of cytological results and to assess this type of response reliably.

Histological outcomes

CIN2+ was diagnosed in 3.6‰ (86/23.956 – 95% CI: 2.9‰–4.5‰) of all the women enrolled in the intervention groups and in 10.1‰ (86/8.494 – 95% CI: 8.2‰–12.6‰) of all responders in the intervention groups. These results are in line with the recent meta-analysis where the corresponding probabilities were 2.9‰ (95% CI: 1.6–4.6‰) and 9.3‰ (95% CI: 6.8–12.1‰).[11] We didn't record any significant difference in CIN2+ outcomes between the study groups; however, the probability for the CIN2+ diagnosis after the enrolment was higher in the opt-out group (3.9‰) and the opt-in group (3.4‰) than in the control group (3.1‰). This is in line with previous studies that suggested that CIN2+ outcomes among all the enrolled women were related to the response rate and were, due to a higher response, higher in opt-out self-sampling groups than opt-in and control groups.[11] Our study might be underpowered for the detection of high-grade lesions, since it was scaled to detect difference in the response rates. However, it should be noted that we observed an insignificantly higher detection rate of CIN2+ among the women who performed cytology with PG in both intervention groups (12.6‰ in opt-in and 14.2‰ in opt-out), compared to women with the HPV testing (8.4‰ and 10.3‰) (data not shown). If the difference is real, that could be explained either as a high sensitivity of cytological screening by PGs and/or that women with a higher risk for CIN2+ (potentially some of them already symptomatic) preferred screening by PGs over HPV testing on self-collected samples. It should be noted that 7/10 women with cervical carcinoma who were enrolled in the intervention arm preferred cytological screening with PG; in four of them, the FIGO stage at diagnosis was IIB+. Only 3/10 women with cervical carcinoma preferred self-sampling (FIGO stages IA1, IA2 and IIB). It should also be emphasised that no single case of CIN2+ was detected among 612 women who preferred screening with both HPV self-sampling and PG, which might be explained as a low risk of disease among the women with negative HPV test among the women who overuse health interventions compared to women who don't.[26]

Results of HPV testing on self-collected samples

HPV positivity rate among women who performed HPV self-sampling was 8.3% (95% CI: 7.5%–9.0%), which is significantly lower than in a recent meta-analysis (10.5%, 95% CI: 9.1%–12.9%).[11] It is well known that HPV positivity rate is country- and age-specific. Lower HPV positivity rate recorded in our study could be related to a relatively high mean age of the HPV self-sampling responders, which was 50.3 years. In comparison to the results

of a Slovenian study performed among 4.431 women aged 20–64 who regularly attended the national cervical cancer screening programme, we recorded a higher HPV positivity rate in all age groups except in the oldest women, aged 60–64 years.[27] This can be explained either as a higher risk of HPV infection and cervical disease among non-attenders in the screening programme or as the detection of vaginal HPV infections in self-sampling samples that do not necessarily correlate with cervical HPV infections detected in practitioner-obtained cervical samples. A higher HPV positivity rate due to the detection of vaginal infections with low-risk HPV types might limit the cost-effectiveness of self-sampling due to a higher referral; however, it should be emphasised that one woman with a positive HPV test was diagnosed with VaIN3.

Compliance with a follow-up examination after a positive HPV test

The compliance with a follow-up examination in our study was 90.2%, which is at the upper edge of the 95% confidence interval of the recent meta-analysis, where the compliance was 82.2% (95% CI; 65.8–94.4).[11] The achieved high compliance was most probably the result of prescheduled appointments, personal contacts via telephone with women who did not attend, and two prescheduled reminders. In our study the compliance was significantly related to the region of residence and the level of protection, so a different local context and the difference in the previous screening history might have contributed to the heterogeneity of results in various studies.

The concordance of positive results of HPV testing performed on self-collected samples and on practitioner-obtained cervical samples was 43.8% compared to 52.0% in a recent Norwegian study (considering only HC2 results)[28], 58.7% and 68.8% in Dutch studies[29,30] and 73.3% in Swedish study.[22] The concordance is also associated with the time difference between the two samplings, which mean value was 57 days in our study; during this time, some transitional HPV infections might have cleared. Concordance could be lower also due to the detection of vaginal HPV infections in self-collected samples.

Positive predictive value of HPV testing on self-collected samples

PPV of a test or testing strategy is important for justifying further diagnostic and therapeutic procedures and can be used in risk-based management approach. If the risk is low for the underlying disease after a positive HPV test (PPV for CIN2+ <2% and CIN3+ <3%), the woman can be referred to regular screening.[13,31] If the risk of the underlying disease is high (PPV for CIN2+ >20% and CIN3+ >10%), the woman should be referred to colposcopy. Women with an intermediate risk should be triaged or followed up. In our study, the PPV of the HPV testing on self-collected samples was 12.0% for CIN2+ and 9.6% for CIN3+, which represents an intermediate risk with PPV for CIN3+, close to the cut-off for high risk. The women with a positive result of the second HPV test, performed on the practitioner-obtained cervical sample taken after mean of 57 days after a positive initial HPV testing had a much higher risk for the underlying disease, which justified immediate colposcopy (PPV was 23.3% for CIN2+ and 19.9% for CIN3+). However, there was a subgroup of women, with no/low protection due to a previous screening history, where the PPV of the HPV testing on self-collected samples was high enough (20.0% for CIN2+ and 18.2% for CIN3+) to justify immediate colposcopy. This could imply that more than one management strategy would be appropriate for the women with an initially positive HPV testing on self-collected samples.

Strengths and limitation of the study

The key strengths of our study were a large sample size and the fact that the study was performed in the setting of an organised routine cervical cancer screening programme, which allows assessment of the efficacy as well as effectiveness of a possible upgrade to the Slovenian national screening programme with HPV self-sampling for non-attenders with efficient triage strategy. To the best of our knowledge, this is one of the first randomised studies among non-attenders of an organised screening programme with three study groups: the opt-in, the opt-out and the classic reminders approach, which achieved a relatively high response in the opt-in scenario compared to the opt-out scenario. The randomised study design with predetermined possible predictors for response and the risk of disease will allow us to identify the benefits and risks of both approaches: the opt-in and the opt-out, the best strategy to upgrade the programme, and the related costs. Because colposcopy was done per the protocol in women with a positive HPV results, PPV was computed for different subgroups of women. This will allow informed evidence-based decisions regarding the risk-stratified diagnos-

tic and treatment follow-up of women who had a positive result of HPV testing on self-collected samples.

The main limitations of our study were that women with a positive result of the HPV testing had more intensive per protocol diagnostic follow-up (including colposcopy) than women with abnormal cytology, who were managed according to the national guidelines. This may account for the verification bias for histological outcomes when comparing the results of the HPV testing on self-collected samples to cytology with PG or to previous studies which did not include an extensive colposcopy. However, the proportion of women with histology result in one year after their enrolment was similar and even higher in type B responders (4.0% of responders) compared to 3.4% in type A responders, and the detection rates of CIN2+ and CIN3+ lesions between type A and type B responders did not differ significantly (data not shown). The main reason for more intensive per protocol diagnostic follow-up for women with positive result of the HPV test was to reliably assess the risk for the underlying high-grade disease among those women. Furthermore, an additional cervical sample taken during a follow-up examination will enable the comparison of different triage strategies for women with a positive HPV result. We initially included some women who appeared to be eligible at the time of their enrolment, but were later found to be non-eligible due to hysterectomy and recent cytology with a PG, but not yet registered in the ZORA registry. We, however, anticipated such situation, which will also certainly be present during future real-life HPV self-sampling of non-attenders. Because of this and the randomised nature of our study, we did not compute corrected response rates, and histological results and all analyses were made on the intention-to-screen basis (with all the enrolled women in the denominator).

Conclusions

In conclusion, an upgrade of the Slovenian cervical cancer screening programme ZORA with opt-out or opt-in HPV self-sampling could lead to a higher coverage of the target population. Also, stratified management of women with a positive result of the HPV testing on self-collected samples, according to their characteristics and background risk for the high-grade disease, should be strongly considered. Our study showed that high response rate could also be reached in opt-in settings if women were given a choice to attend the screening with the PG or order tester for HPV self-sampling and if access to screening is free and available without significant additional effort. Our results suggest that in real-life screening settings, the opt-in approach might be almost as effective in the overall high-grade disease detection among all the eligible women as the opt-out approach while being superior regarding cost-effectiveness. However, an in-depth analysis should be done to identify the most cost-effective HPV self-sampling approach in the local setting. Although the difference in PPVs of the HPV testing for high-grade disease among specific subgroups of women in our study supports the concept of risk-based management of women[31], further in-depth analysis is needed to clarify the role of potential PPV predictors after a positive result of HPV testing on self-collected samples.

Acknowledgment

The authors would like to thank Mojca Kuster from the NP ZORA coordination centre at the Institute of Oncology Ljubljana for her kind and professional communication with the enrolled women and staff at both colposcopy clinics and for the very much appreciated help with the study logistic. Special thanks goes to the staff of the colposcopy units at all three institutions: Tatjana Kodrič, Andrej Cokan, Sarah Dobnik, Jure Knez, Marica Miklavc, Marcela Živko, Aleksandra Muhič, Sonja Bebar, Sebastjan Merlo and Marta Janežič. We would also like to thank the staff from cytology and molecular laboratories at University Clinical Centre Maribor, General Hospital Celje and Institute of Oncology Ljubljana for their valuable work an contribution to the study: Nina Irgel, Lidija Salobir, Nevenka Štiglic Toš, Ana Katarina Seher, Branko Antolovič, Maja Fras, Barbara Jelen, Patricija Pernat, Saša Praznic, Živa Pohar Marinšek, Sandra Jezeršek, Simona Uhan Kastelic, Janja Zalar, Mojca Lešnjak, Simon Buček, Uršula Prosenc Zmrzljak, Marina Bučić, Slavica Vuzem and Barbara Verk. Special thanks also to a team of epidemiologists from Epidemiology and Cancer Registry unit at the Institute of Oncology Ljubljana for the initial support with setting up the project database and discussions regarding the study protocol. Last but not least, we also thank all the women who participated in the study.

Study was approved for public funding by the Slovenian Research Agency (ARRS) (project number L3-5512). It was financed by ARRS and Ministry of

Health of Republic of Slovenia. Materials used in the study were obtained free of charges or with discount from manufacturers. ARRS, Ministry of Health and manufacturers didn`t have any role in the design of the study, study execution, analyses, interpretation of the data, or decision to submit results.

References

1. International Agency for Research on Cancer (2005). Cervix Cancer Screening. IARC handbooks of cancer prevention, Vol. 10. Lyon: IARCPress. [cited 2018 Apr 15]. Available from: http://www.iarc.fr/en/publications/pdfs-online/prev/handbook10/index.php
2. Vaccarella S, Lortet-Tieulent J, Plummer M, Franceschi S, Bray F. Worldwide trends in cervical cancer incidence: impact of screening against changes in disease risk factors. *Eur J Cancer* 2013; **49:** 3262-73. doi: 10.1016/j.ejca.2013.04.024
3. Zadnik V, Primic Zakelj M, Lokar K, Jarm K, Ivanus U, Zagar T. Cancer burden in Slovenia with the time trends analysis. *Radiol Oncol* 2017; **51:** 47-55. doi: 10.1515/raon-2017-0008
4. Spence AR, Goggin P, Franco EL. Process of care failures in invasive cervical cancer: systematic review and meta-analysis. *Prev Med* 2007; **45:** 93-106. doi: 10.1016/j.ypmed.2007.06.007
5. Sigurdsson K, Hrafnkelsson J, Geirsson G, Gudmundsson J, Salvarsdóttir A. Screening as a prognostic factor in cervical cancer: analysis of survival and prognostic factors based on Icelandic population data, 1964-1988. *Gynecol Oncol* 1991; **43:** 64-70.
6. Takac I, Ursic-Vrscaj M, Repse-Fokter A, Kodric T, Rakar S, Mozina A, et al. Clinicopathological characteristics of cervical cancer between 2003 and 2005, after the introduction of a national cancer screening program in Slovenia. *Eur J Obstet Gynecol Reprod Biol* 2008; **140:** 82-9. doi: 10.1016/j.ejogrb.2008.02.019
7. Landy R, Pesola F, Castañón A, Sasieni P. Impact of cervical screening on cervical cancer mortality: estimation using stage-specific results from a nested case-control study. *Br J Cancer* 2016; **115:** 1140-46. doi: 10.1038/bjc.2016.290
8. [National Cervical Cancer Screening Programme ZORA.] [Slovenian]. DP ZORA: Kazalniki. [online] https://zora.onko-i.si/ [Accessed 2018 Mar 29]. Available at: https://zora.onko-i.si/publikacije/kazalniki/
9. Elfstrom KM, Arnheim-Dahlstrom L, von Karsa L, Dillner J. Cervical cancer screening in Europe: quality assurance and organisation of programmes. *Eur J Cancer* 2015; **51:** 950-68. doi: 10.1016/j.ejca.2015.03.008
10. Ivanuš U, Primic Žakelj M. [HPV self-sampling among non-responders to cervical cancer screening programmes: systematic review]. [Slovenian]. *Onkologija* 2012; **2:** 78-86. Available also online (in Slovenian language only): https://www.onko-i.si/fileadmin/onko/datoteke/dokumenti/Onkologija_Letnik_XVI_st_2/7_Onkologija_2_2012_samoodvzem.pdf
11. Verdoodt F, Jentschke M, Hillemanns P, Racey CS, Snijders PJ, Arbyn M. Reaching women who do not participate in the regular cervical cancer screening programme by offering self-sampling kits: a systematic review and meta-analysis of randomised trials. *Eur J Cancer* 2015; **51:** 2375-85. doi: 10.1016/j.ejca.2015.07.006
12. Von Karsa L, Arbyn A, De Vuyst H, Dillner J, Dillner L, Franceschi S, et al. (2015). Executive summary. In: European guidelines for quality assurance in cervical cancer screening. Second edition, Supplements. Anttila A, Arbyn A, De Vuyst H, Dillner J, Dillner L, Franceschi S, et al, editors. Luxembourg: Office for Official Publications of the European Union. p. XIII–XXIV. [cited 2018 Apr 10]. Available from: https://publications.europa.eu/en/publication-detail/-/publication/a41a4c40-0626-4556-af5b-2619dd1d5ddc/language-en
13. Arbyn M, Verdoodt F, Snijders PJ, Verhoef VM, Suonio E, Dillner L, et al. Accuracy of human papillomavirus testing on self-collected versus clinician-collected samples: a meta-analysis. *Lancet Oncol* 2014; **15:** 172-83. doi: 10.1016/S1470-2045(13)70570-9
14. Giorgi Rossi P, Marsili LM, Camilloni L, Iossa A, Lattanzi A, Sani C, et al; Self-Sampling Study Working Group. The effect of self-sampled HPV testing on participation to cervical cancer screening in Italy: a randomised controlled trial (ISRCTN96071600). *Br J Cancer* 2011; **104:** 248-54. doi: 10.1038/sj.bjc.6606040
15. Giorgi Rossi P, Fortunato C, Barbarino P, Boveri S, Caroli S, Del Mistro A, et al. HPV Self-sampling Italian Working Group. Self-sampling to increase participation in cervical cancer screening: an RCT comparing home mailing, distribution in pharmacies, and recall letter. *Br J Cancer* 2015; **112:** 667-75. doi: 10.1038/bjc.2015.11
16. Broberg G, Gyrd-Hansen D, Miao Jonasson J, Ryd ML, Holtenman M, Milsom I, et al. Increasing participation in cervical cancer screening: offering a HPV self-test to long-term non-attendees as part of RACOMIP, a Swedish randomized controlled trial. *Int J Cancer* 2014; **134:** 2223-30. doi: https://doi.org/10.1002/ijc.28545
17. Tranberg M, Bech BH, Blaakær J, Jensen JS, Svanholm H, Andersen B. Preventing cervical cancer using HPV self-sampling: direct mailing of test-kits increases screening participation more than timely opt-in procedures - a randomized controlled trial. *BMC Cancer* 2018; **18:** 273. doi: 10.1186/s12885-018-4165-4
18. R Core Team. R: A language and environment for statistical computing. Vienna: R Foundation for Statistical Computing. 2012. ISBN 3-900051-07-0, URL. Available from: http://www.R-project.org/
19. Ursic-Vrscaj M, Rakar S, Možina A, Kobal B, Takač I, Deisinger I, et al. [Guidelines for management of women with cervical precancerous lesions]. [Slovenian] In: Ursic-Vrscaj M, editor. Ljubljana: Institute of Oncology Ljubljana; 2011. [cited 2018 Mar 15]. Available at (in Slovene language only): https://zora.onko-i.si/fileadmin/user_upload/dokumenti/strokovna_priporocila/2011_Smernice_web.pdf
20. Bais AG, van Kemenade FJ, Berkhof J, Verheijen RH, Snijders PJ, Voorhorst F, et al. Human papillomavirus testing on self-sampled cervicovaginal brushes: an effective alternative to protect nonresponders in cervical screening programs. *Int J Cancer* 2007; **120:** 1505-10. doi: 10.1002/ijc.22484
21. Wikström I, Lindell M, Sanner K, Wilander E. Self-sampling and HPV testing or ordinary Pap-smear in women not regularly attending screening: a randomised study. *Br J Cancer* 2011; **105:** 337-9. doi: 10.1038/bjc.2011.236
22. Sanner K, Wikström I, Strand A, Lindell M, Wilander E. Self-sampling of the vaginal fluid at home combined with high-risk HPV testing. *Br J Cancer* 2009; **101:** 871-4. doi: 10.1038/sj.bjc.6605194
23. Lam JU, Rebolj M, Møller Ejegod D, Pedersen H, Rygaard C, Lynge E, et al. Human papillomavirus self-sampling for screening nonattenders: opt-in pilot implementation with electronic communication platforms. *Int J Cancer* 2017; **140:** 2212-19. doi: 10.1002/ijc.30647
24. Cadman L, Wilkes S, Mansour D, Austin J, Ashdown-Barr L, Edwards R, et al. A randomized controlled trial in non-responders from Newcastle upon Tyne invited to return a self-sample for Human Papillomavirus testing versus repeat invitation for cervical screening. *J Med Screen* 2015; **22:** 28-37. doi: 10.1177/0969141314558785
25. Kitchener H, Gittins M, Cruickshank M, Moseley C, Fletcher S, Albrow R, et al. A cluster randomized trial of strategies to increase uptake amongst young women invited for their first cervical screen: The STRATEGIC trial. *J Med Screen* 2017. doi: 10.1177/0969141317696518 [Epub ahead of print]
26. Dugué PA, Lynge E, Rebolj M. Mortality of non-participants in cervical screening: Register-based cohort study. *Int J Cancer* 2014; **134:** 2674-82. doi: 10.1002/ijc.28586
27. Učakar V, Poljak M, Klavs I. Pre-vaccination prevalence and distribution of high-risk human papillomavirus (HPV) types in Slovenian women: a cervical cancer screening based study. *Vaccine* 2012; **30:** 116-20. doi: 10.1016/j.vaccine.2011.10.066
28. Enerly E, Bonde J, Schee K, Pedersen H, Lönnberg S, Nygård M. Self-Sampling for human papillomavirus testing among non-attenders increases attendance to the Norwegian Cervical Cancer Screening Programme. *PLoS One* 2016; **11:** e0151978. doi: 10.1371/journal.pone.0151978
29. Gök M, van Kemenade FJ, Heideman DA, Berkhof J, Rozendaal L, Spruyt JW, et al. Experience with high-risk human papillomavirus testing on vaginal brush-based self-samples of non-attendees of the cervical screening program. *Int J Cancer* 2012; **130:** 1128-35. doi: 10.1002/ijc.26128
30. Gök M, Heideman DA, van Kemenade FJ, Berkhof J, Rozendaal L, Spruyt JW, et al. HPV testing on self collected cervicovaginal lavage specimens as screening method for women who do not attend cervical screening: cohort study. *BMJ* 2010; **340:** c1040. doi: 10.1136/bmj.c1040. Erratum in: *BMJ* 2016; **353:** i2823.
31. Castle PE, Sideri M, Jeronimo J, Solomon D, Schiffman M. Risk assessment to guide the prevention of cervical cancer. *Am J Obstet Gynecol* 2007; **197:** 356.e1-6. doi: 10.1016/j.ajog.2007.07.049

research article

Interval cancers after negative immunochemical test compared to screen and non-responders' detected cancers in Slovenian colorectal cancer screening programme

Dominika Novak Mlakar[1,2], Tatjana Kofol Bric[1], Ana Lucija Škrjanec[1], Mateja Krajc[3]

[1] National Institute of Public Health, Cancer Screening, Ljubljana, Slovenia
[2] University of Ljubljana, Faculty of Medicine, Ljubljana, Slovenia
[3] Institute of Oncology Ljubljana, Cancer Genetic Clinic, Ljubljana, Slovenia

Radiol Oncol 2018; 52(4): 413-421.

Received 17 April 2018
Accepted 20 May 2018

Correspondence to: Assist. Prof. Mateja Krajc, M.D., Ph.D., Institute of Oncology Ljubljana, Zaloška cesta 2, SI-1000 Ljubljana, Slovenia. Phone: + 386 1 5879 635; Fax: + 386 1 5879 400; E-mail: mkrajc@onko-i.si

Disclosure: No potential conflicts of interest were disclosed.

Background. We assessed the incidence and characteristics of interval cancers after faecal immunochemical occult blood test and calculated the test sensitivity in Slovenian colorectal cancer screening programme.

Patients and methods. The analysis included the population aged between 50 to 69 years, which was invited for screening between April 2011 and December 2012. The persons were followed-up until the next foreseen invitation, in average for 2 years. The data on interval cancers and cancers in non-responders were obtained from cancer registry. Gender, age, years of schooling, the cancer site and stage were compared among three observed groups. We used the proportional incidence method to calculate the screening test sensitivity.

Results. Among 502,488 persons invited for screening, 493 cancers were detected after positive screening test, 79 interval cancers after negative faecal immunochemical test and 395 in non-responders. The proportion of interval cancers was 13.8%. Among the three observed groups cancers were more frequent in men ($p = 0.009$) and in persons aged 60+ years ($p < 0.001$). Comparing screen detected and cancers in non-responders with interval cancers more interval cancers were detected in persons with 10 years of schooling or more ($p = 0.029$ and $p = 0.001$), in stage III ($p = 0.027$) and IV ($p < 0.001$), and in right hemicolon ($p < 0.001$). Interval cancers were more frequently in stage I than non-responders cancers ($p = 0.004$). Test sensitivity of faecal immunochemical test was 88.45%.

Conclusions. Interval cancers in Slovenian screening programme were detected in expected proportions as in similar programmes. Test sensitivity was among the highest when compared to similar programmes and was accomplished using test kit for two stool samples.

Key words: colorectal cancer screening; faecal immunochemical test; interval cancer; screen detected cancer; cancer in non-responders; test sensitivity

Introduction

Colorectal cancer is a major public health problem in developed world. In 2012, it was the third most common cancer in the world with 1.4 million new cases and was responsible for 8.5% of all cancer-related deaths.[1] In Slovenia, the average incidence of colorectal cancer in the period 2009-2013 was 1,569 cases per year. Incidence rate was higher in men (92.4/100,000) than in women (60.8/100,000). It was the third most common cancer and was responsible for 13.6% of all cancer-related deaths.[2]

In 2003, Council of the European Union proposed to member states to introduce a population based organised screening programme for three cancer sites (colorectum, cervix and breast) and

thus reduce the burden caused by the disease.[3] The implementation of organized population colorectal cancer screening proved to reduce the mortality successfully. Using a guaiac screening test, the colorectal cancer mortality in apparently healthy population with moderate risk was reduced by 15.0 to 33.0%.[4-6]

European Guidelines for Quality Assurance in Colorectal Cancer Screening and Diagnosis recommend faecal occult blood test as a screening test.[7] It does not have a diagnostic characteristic in detecting colorectal neoplasms, since any intestinal bleeding can result in positive test.[7,8] Therefore, colonoscopy is recommended as a diagnostic method for detecting premalignant and early stage cancers after positive screening tests.[7,8]

Next to positive effects, screening also has some negative effects for the screenees if the test result is false positive or false negative.[3] A good screening test should have a small number of false positive results and, even more important, a small number of false negative results in those who already have cancer.[4] Experience show that in colorectal cancer screening programmes the so-called interval cancers are detected after negative screening tests.[7,9]

As published definitions of interval cancer differ, it is difficult to compare results of different studies. A group of experts has been working on the recommended definitions of interval cancer after a negative screening test and after colonoscopy or any other comparable diagnostic test.[7] International working group has developed a nomenclature for the definition and description of interval cancers in colorectal cancer screening programme.[10]

Interval cancer rarely appears in previously healthy intestinal mucosa in the period between two screening tests. Most probably screening test misses some neoplasms.[10,11] The proportion of interval cancers is an important performance indicator of the screening programme and it reflects the test sensitivity (false negative) as well as the incidence of newly detected cancers which were not present during the screening.[7,11] According to the European guidelines, the data on the incidence of interval cancers should be collected and reported, which enables the monitoring of programme effectiveness.[7]

More frequent incidence of colorectal cancer in men, in older people and in persons with lower socio-economic status is reflected in screen detected cancers, whereas there is no uniform conclusion regarding the characteristics of interval cancer incidence. These findings can contribute to the adaptation of screening programmes to groups at higher risk for interval cancer.[1,2,11-13]

In 2008, a colorectal cancer screening pilot project confirmed the feasibility of planned procedures as well as the effectiveness of cancer detection in early stages with the organized population screening in Slovenia.[14] In April 2009, a national colorectal cancer screening programme named Programme Svit, started in Slovenia.[15] Each programme screening round lasts for two years. In first three screening rounds, the target group included men and women aged 50 to 69 years. Since 2015, the upper age limit of target population is set to 74 years.[15]

In our study, we analysed the data on interval cancers after negative result of faecal immunochemical test in Slovenian colorectal cancer screening programme. The data on interval cancers are important for the assessment of screening test sensitivity. The aim of the analysis was to assess the incidence and characteristics of interval cancers in colorectal cancer screening programme as well as the characteristics of the affected population, and to compare them to screen detected cancers and cancers in non-responders. Data on interval cancers after follow-up colonoscopy without detected cancer were not available yet in Slovenian colorectal cancer screening programme and were not the topic of this article.

Patients and methods

Population and research design

The study population represent the total target population of the colorectal cancer screening programme in Slovenia at the time being. People were invited in the second programme screening round, which lasted from April 2011 until December 2012. We divided the cohort into three groups, namely non-responders which did not respond to the invitation or returned the test kit, test positive population, and test negative population. We followed-up all groups for two years and extracted records of their new colorectal cancers from Cancer Registry of Republic of Slovenia. For the study purpose, we obtained the data on cancers detected during the follow-up period until the end of incidence year 2014 from cancer registry in 2017. This ensured the time, in which the cancer registry was able to identify cancers detected within and out of the screening programme and to obtain all the necessary data. Demographic data of the followed-up population (name, family name, date of birth, address of residence) were obtained from Central Population Registry. To calculate the follow-up time in person-years we obtained the data on deceased persons in

all three groups from Causes of Deaths Database of the National Institute of Public Health.

The data on the educational attainment of cancer cases patient were obtained from the Republic of Slovenia Statistical Office database. Educational attainment was converted into two groups, whereby less and up to including 9 years of schooling represents primary school, 10 or more years of schooling represents vocational or secondary school, higher educational level and all subsequent levels.

The data on faecal immunochemical tests, colonoscopies results and the characteristics of screen detected cancers were obtained from national central colorectal cancer screening registry. The data on interval and non-responders' cancer cases were obtained from the cancer registry.

The invitation and screening test

The population, aged 50 to 69 years, which was invited into the second programme screening round, received the invitation to participate in the screening programme. Persons, who have decided to participate and have returned the signed consent, received test kits for two stool samples unless they had self-reported permanent and temporary exclusion criteria. Exclusion criteria for the participation in screening programme are described in Slovene guidelines for colorectal cancer screening quality assurance.[16]

Permanent exclusion criteria group included persons with (i) chronic inflammatory bowel disease; (ii) adenoma; and (iii) colorectal cancer diagnosed prior to entering the screening programme.

Persons, who have undergone a colonoscopy procedure in the past three years and the above mentioned pathology was not detected, were included in the group with temporary exclusion criteria and were again invited for screening in the next programme screening round.

At first, a qualitative immunochemical test for faecal occult blood (MagStream HT, Fujirebio, Japan) was used as a screening test. After the new public tender for screening test supply the quantitative immunochemical test (OC – Sensor, Eiken Chemical Co, Tokyo, Japan) has been used since 2011. The latter test enables the measurement of haemoglobin quantity in the stool sample, which was not possible with the qualitative test indicating only positive or negative result. We used two stool samples in each test kit from the start of the screening programme. Positive result in quantitative test meant that haemoglobin value in one of two stool samples was higher than 20 μg Hb/g of stool or higher than 100 ng Hb/mL of buffer. Among the study population, which has performed a screening test, 23.9% of persons had a qualitative test and 76.1% performed a quantitative test.

Screening test results

Persons with negative screening test received the test results with an explanation that specimen samples did not exceed the haemoglobin cut-off value and that they do not need additional tests, but have to be aware of new symptoms.

Persons with positive test results were referred to the colonoscopy. Colonoscopies were performed in average in 42 days after the stool samples analysis. In some cases, the colonoscopy date was postponed due to patient's health condition or his/her wish to undergo the colonoscopy in a particular colonoscopy centre, where waiting period was longer.

Colorectal cancer cases classification according to detection mode

In order to identify the cancer cases among the study population we linked individual data with cancer registry data based on the uniform identification number. For all three cancer detection mode groups (screen detected, interval cancers after negative faecal screening tests, non-responders' cancers), we used the cancer registry to obtain the data on cancer TNM stage, cancer site, histological type and diagnosis date.

Cancer cases, who had negative faecal screening test and a colorectal cancer diagnosis in cancer registry, were classified as patients with interval cancer. Cancer diagnosis date was between the date of stool sample testing and the date of the next foreseen screening or before new invitation to the next screening round.

Cancer cases, who had positive screening test, with a lesion detected and histologically confirmed as cancer were classified as screen detected cancer. In screen detected cancer group two subgroups of patients were followed. In the first subgroup, colonoscopy was performed within the screening programme. In the second subgroup, cancer was detected with colonoscopy outside the screening programme after positive immunochemical test in the screening programme and cancer diagnosis date registered in cancer registry was inside six months from positive test in the screening.

Cancer cases, who did not respond to the invitation or did not supply the stool samples, were classified as non-responder cancer patients. They had

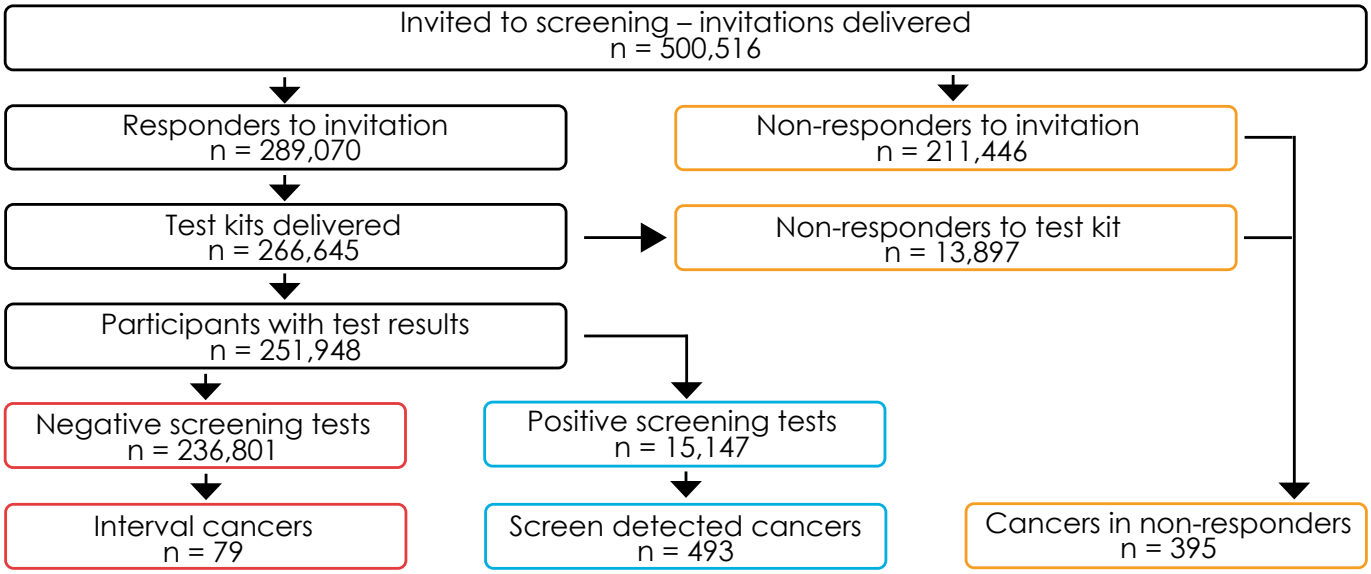

FIGURE 1. Colorectal cancer screening flowchart, including screen detected, interval and non-responders' cancers.

colorectal cancer diagnosis in cancer registry. The diagnosis date was between the date of the sent invitation or test kit and the date of invitation to the next screening round.

Cases, which were detected between caecum and splenic flexure (according to ICD-10, codes C180-C185, except C181), were classified as proximal colorectal cancers. Cases, detected in and between descendent colon and rectum (ICD-10 codes C186-C20), were classified as cancers in the left (distal) part of the colorectum.

The analysis included cancer cases with histological diagnosis according to International classification of diseases for oncology with codes 8010/3 to 8580/3.[17] The following neoplasms were also detected in colorectum; but were not included in the analysis: neoplasms without microscopic confirmation, lymphomas, 8124/3-Cloacogenic carcinoma, 8240/3-Carcinoid tumour, NOS, 8249/3-Atypical carcinoid tumour and 8936/3-Gastrointestinal stromal sarcoma.

Ethical aspects of the research

Republic of Slovenia National Medical Ethics Committee passed a signed consent for the research at the sessions on 16th April 2013 (Nr. 129/04/13) and 14th May 2013 (Nr. 166/05/13).

Statistical analysis

We used Pearson Chi-Square Test to calculate statistically significant differences among groups of patients with screen detected cancers, interval cancers and non-responder cancers as well as the characteristics of detected cancers.

The proportion of interval cancers after negative screening test was calculated by the division of the number of interval cancers with the sum of interval and screen detected cancers. To assess the screening test sensitivity, we used the proportional incidence method.[18-20] Screening test sensitivity was calculated using the following equation: $\{1 - ((\alpha * I_{screen}) / (I_{under} - (1- \alpha) * I_{non\text{-}screen}))\} * 100$. Cancer incidence was expressed at 100,000 person-years.[18-20] The a in the formula represents the proportion of screened persons, I_{screen} represents the incidence of interval cancers detected after the negative screening test, I_{under} represents the incidence of colorectal cancers in the population aged 50 to 69 years prior to the introduction of the screening programme, and $I_{non\text{-}screen}$ represents the incidence of non-responder colorectal cancers. The statistical significance level was set to $p < 0.05$. For data analysis, we used SPSS statistical programme package, version 21.0 for Windows.

Results

From April 2011 to December 2012, we mailed 502,488 invitations for participation in the screening to target population individuals aged 50 to 69 years, out of which 49.7% were men and 50.3% were women. 12.7% of them were newly invited to the screening programme and 87.3% were invited

TABLE 1. Selected characteristics of colorectal cancer patients and their disease

		Screen detected cancer (SDC)		Interval cancer (IC)		Non-responders cancer (NRC)		p value (SDC vs IC)	p value (IC vs NRC)	p value (SDC vs NRC)
		Number	%	Number	%	Number	%			
Cancer total		493		79		395				
Age	50-54	89	18.1	12	15.2	73	18.5	0.101	0.323	0.119
	55-59	93	18.9	10	12.7	63	15.9			
	60-64	182	36.9	26	32.9	145	36.7			
	65 ≤	129	26.2	31	39.2	114	28.9			
Gender	Male	308	62.5	50	63.3	271	68.6	0.889	0.356	0.057
	Female	185	37.5	29	36.7	124	31.4			
Years of schooling	≤ 9 years	146	29.6	14	17.7	160	40.5	0.029	< 0.001	0.001
	≥ 10 years	342	69.4	64	81.0	230	58.2			
	Unknown	5	1.0	1	1.3	5	1.3			
Cancer site	Distal colon	380	77.1	39	49.4	301	76.2	< 0.001	< 0.001	0.759
	Proximal colon	113	22.9	40	50.6	94	23.8			
TNM stage	I	251	50.9	16	20.3	32	8.1	< 0.001	0.023	< 0.001
	II	99	20.1	17	21.5	87	22.0			
	III	104	21.1	25	31.6	124	31.4			
	IV	39	7.9	19	24.1	132	33.4			
	Unknown	0		2	2.5	20	5.1			

for the second time. 500,516 (99.6%) invitations were delivered. As many as 289,070 (57.8%) persons have responded to the invitations (Figure 1). Due to the exclusion criteria, 22,425 (7.7%) persons were not sent a test kit. Test kits for two stool samples were mailed to 266,645 (92.2%) persons who were eligible for screening. As many as 252,653 persons returned the stool samples. Among people with delivered invitation, without the ones with exclusions criteria, 52.8% were screened. Among the persons with adequate stool samples, 236,801 (94.0%) had negative screening test. Among the persons with positive screening test (15,147 or 6.0%), 92.2% of them had undergone a colonoscopy in one of the colonoscopy centres appointed by the screening organization.

Table 1 shows the characteristics of study population and detected cancers in case of interval, screen detected and non-responders' cancers. Among 502,488 persons invited for screening, 493 cancers were detected after positive screening test followed by colonoscopy, 79 interval cancers after negative faecal immunochemical test and 395 in non-responders.

Out of 493 screen detected cancer patients, 467 had colonoscopy in one of the appointed centres and 26 outside the screening program. The analysis showed that 88 (17.8%) screen detected cancer cases were diagnosed because of the positive result of the second stool sample, whereas the first stool sample test result was negative. Among non-responders with diagnosed cancer, 374 persons did not respond to the invitation into the screening programme, while 21 persons responded to the invitation but did not return the test kit.

Among the persons with interval cancer, 57 were provided with a quantitative faecal immunochemical test, which enables the measurement of haemoglobin value in the stool sample. In 43 (75.4%) study persons with interval cancer after the negative quantitative test, the haemoglobin value was between 0.0 and 50 ng Hb/mL of buffer, among them there was no trace of haemoglobin (0.0 ng Hb/mL buffer) in none of the stool samples in 14 persons.

Among the persons with positive test result, the cancer was significantly more often detected in men ($p = 0.009$) and in persons aged 60+ years ($p < 0.001$). The results were similar in interval cancers after the negative screening test and in non-responders' cancers, where there were also significantly more cancer cases in men ($p = 0.001$ and $p < 0.001$) and in persons aged 60+ years ($p < 0.001$ and $p < 0.001$).

FIT test sensitivity = 88.45% =

$$= \left\{1 - \frac{a \times I_{screen}}{I_{under} - (1-a) \times I_{non\text{-}screen}}\right\} \times 100 =$$

$$= \left\{1 - \frac{0.528 \times 16.77}{118.96 - (1-0.528) \times 89.68}\right\} \times 100$$

FIGURE 2. Test sensitivity adjusted for selection bias according to the proportional incidence method formula.

In the comparison between interval cancers and screen detected cancers, there were no differences in cancer incidence according to gender and age groups. Among the interval cancer patients, there were significantly more persons, who had 10 years or more of schooling. In screen detected cancer patients, there were more persons with less than 10 years of schooling ($p = 0.029$). Screen detected cancers were significantly more frequent in the left part of the colon, while interval cancers were more frequent in the right part of the colon ($p < 0.001$). In screen detected cases more cancers were in stage I ($p < 0.001$), whereas in interval cancers more were in stage III ($p = 0.027$) and stage IV ($p < 0.001$).

In the comparison between interval cancers and non-responders' cancers, there was no difference in cancer incidence according to gender and age groups. Among the interval cancer patients, more persons had 10 years of schooling or more, while among the non-responder cancer patients there were more persons with less than 10 years of schooling ($p = 0.001$). Non-responders' cancers were more frequent in the left part of the colon, while interval cancers were more frequent in the right part of the colon ($p < 0.001$). In interval cancers compared to non-responders' cancers more were detected in stage I ($p = 0.004$).

In the comparison between screen detected cancers and non-responders' cancers, there was no difference according to gender or age groups. Among the non-responder cancer patients, there were more persons with less than 10 years of schooling, compared to screen detected cancer patients, where there were more persons with 10 years of schooling or more ($p = 0.001$). Cancers in both groups were more frequent in the left part of the colon, but there was no significant difference in comparison with the right part of the colon. In screen detected cancers more were in stage I ($p < 0.001$), whereas more non-responder cancers were in stage II ($p = 0.016$) and IV ($p < 0.001$).

The proportion of interval cancers among cancers detected in second screening round was 13.8%, which means 79 interval cancers after the negative screening test according to the sum of screen detected and interval cancers (493 + 79). The test sensitivity of faecal immunochemical test used for colorectal cancer screening was 88.45% (Figure 2).

Discussion

The analysis represents the first evaluation of the Slovenian colorectal cancer screening programme focused on assessing the incidence and the characteristics of interval cancers after the negative faecal immunochemical screening test, the characteristics of patients with interval cancer, and the comparison of interval cancers with screen detected cancers and cancers in non-responders.

The proportion of interval cancers detected after negative faecal immunochemical screening test was 13.8%. It has somewhat differed in published studies possibly due to different types of immunochemical tests used, different cut-off values set for test positivity, and the number of required stool samples. In Slovenia, two stool samples are required. In research by Zorzi *et al*., the proportion of interval cancers after the negative screening test was 12%[13], in research by Zappa *et al*., the proportion was 11%[21], in Netherlands 23%[22] and in Basque Country (Spain), the proportion was 6.8%[23]. Slovenian data can be compared with data, published in research by Zorzi *et al*.[13] and with data from Basque Country in Spain[23], because the same type of immunochemical tests and the same cut-off value for positive test were used. Despite the fact that in Slovenia two stool samples are used in the screening programme, the proportion of interval cancers is similar to Zorzi *et al.* research.[13]

On six screen detected cancers, one case of interval cancer after negative faecal immunochemical test was detected in Slovenian screening programme, which is less than elsewhere.[22]

It has been reported that the screened population is at lower risk of colorectal cancer than the general population.[20,24] This was associated with a healthier lifestyle, greater attention to symptoms and signs of possible diseases and higher participation rate in the screening programme.[20,24] In test sensitivity calculation it would be therefore inappropriate to use the general underlying incidence rates to estimate the expected cancers in the screened population (selection bias).[18-20] That is why we used proportional incidence method to calculate test sensitivity. It includes proportion of screened persons, incidence of interval cancers detected after the negative screening test, incidence

of colorectal cancers in the population prior to the introduction of the screening programme and incidence of non-responders' colorectal cancers.

The test sensitivity of the faecal immunochemical screening test was 88.45%. Test sensitivity in other screening programmes rated between 77.0% and 87.0%.[13,21,22,25] Proportional incidence method with the consideration of selection bias was used in Slovenia and in research by Zorzi *et al*.[13] In the latter, test sensitivity was 79.3%; taking into account that only one stool sample was used in a screening episode, while in Slovenia, two stool samples were tested. The age of target population was the same in both programmes. Despite the similar scope of the target population, Zorzi *et al*.[13] reported more detected interval cancers. The use of two stool samples in our research might contributed to higher test sensitivity. Most likely, the proportion of cancers which could be detected as interval cancers, were already detected in the screening process, because of the positive second sample test result, which added 88 screen detected cancers, and this equals to 17.8% of all screen detected cancers.

The present data analysis on detected cancers has, similarly as researches in Italy, Spain, Scotland and Netherlands, confirmed that screen detected cancers are statistically more often detected in lower, more favourable stages (TNM stage I) compared to interval cancers or non-responders' detected cancers. In the latter, more cancers were detected in stages III and IV.[13,22,23,25,26] Promising finding that interval cancers are more frequently detected in stage I than non responders' cancers deserves further research.

As we expected, results of our study showed that there are significant differences between cancer sites in the colorectum according to detection mode. Significantly more screen detected and non-responders' cancers were detected in the left part of the colon, while more interval cancers were detected in the right part of the colon. This is in accordance with findings in researches by Portillo *et al*.[23], Steele *et al*.[26], Morris *et al*.[27], and Gill *et al*..[28] In Italy[13], there were no differences in the sites of interval cancers. In Netherlands' research, more cancers (interval, screen detected and non-responders') were detected in the left part of the colon[22], and in Spanish research, interval cancers, compared to screen detected cancers, were more frequently detected in the rectum[25]. Differences in cancer site within the colorectum were observed across different studies.[11,13,26,27] Possible explanation for this is that the screening test is being less effective at detecting right sided cancers in comparison with left sided lesions.[11,13,27] Haemoglobin from right sided colon lesions has longer time available to degrade when passing the colorectum and more false negative results may appear for right sided cancers.[11,27]

All three groups of cancer cases in our study (screen detected, interval and non-responders'), Table 1, did not differ significantly according to gender or age group; in general, cancers were more frequent among older people (aged 60+) and males. Similar results were found in Netherlands and in Spain.[22,23,25] However, in two studies, where they used guaiac test (in Scotland and in Finland), proportion of interval cancers was higher in women compared to men.[11,29]

In order to estimate the influence of person's socio-economic status on cancer incidence, the income or person's education or the deprivation category of the neighbourhood in which this person lives is used. Socio-economic status was not an important factor for interval, non-responder or screen detected cancer in some studies.[22,23,28] In research by Steele *et al*.[26], significantly more interval and screen detected cancers were found in people living in less deprived surroundings compared to non-responders' detected cancers. This confirms the fact that persons with good socio-economic status are more responsively joining the screening programme. In our research, we used the educational attainment expressed in years of schooling as the socio-economic status indicator and it proved as significant for different mode of cancer detection. Persons with 10 or more years of schooling had significantly more interval and screen detected cancers. Impact of education on screen detected cancer group can be interpreted in the same way as impact of neighbourhood deprivation index of the study in Scotland. Among Slovenian non-responders cancer patients there is significantly more persons with less than 10 years of schooling.

In one fourth of interval cancer patients with negative quantitative screening test, the presence of haemoglobin was not detected at the time of two stool samples analysis (the value of haemoglobin was 0.0 ng Hb/mL). This confirms the fact that some cancers would be missed regardless of cut-off value for positive test result. Similar as in research by Barnett KN *et al*.[30], we find that it is important to empower and inform people that in spite of the negative screening test, cancer can appear; therefore, they need to carefully monitor the symptoms, which indicate that diseases processes can be developing in the colon and rectum, which demand immediate visit to the general practitioner.[30] Out of 57

persons with interval cancer who used quantitative screening test, as many as 43 (75.4%) had haemoglobin value under 50 ng Hb/mL of buffer. Digby *et al*.[31] report similar findings. In their study, 23 (74.2%) out of 31 persons with interval cancer had haemoglobin value under 50 ng Hb/mL of buffer. The data of Slovenian and Scottish researches show that most persons with interval cancer had much lower haemoglobin value in stool samples, which were analysed prior to cancer diagnosis, as was set as cut-off value for positive screen test result. The cut-off value for positive screening test result in Slovenian research was the value of haemoglobin higher than 100 ng Hb/mL of buffer in at least one of two stool samples, while in Digby *et al*.[31], the cut-off value was set at 400 ng Hb/mL of buffer.

As an advantage of our research, we should mention that in Slovenia we have population based national cancer registry with good quality data, from where we obtained the data on interval cancers and non-responders' cancers, as well as the cancer incidence prior to the introduction of screening. This enabled the calculation of test sensitivity following the proportional incidence method while considering the selection bias. Personal identification number enabled individual linkage of screening with cancer incidence data.

The limitation of screening registry at the time of the study is that it does not have legally guaranteed access to data on exclusion criteria in target population and it, therefore, has to rely on patients' self-reported data on colorectal diseases, which can sometimes be unreliable. It is possible that symptomatic persons who were already in diagnostic procedure, attended for screening. If colonoscopies after the positive immunochemical test in the screening were performed outside the screening programme, it depended on patients themselves if they forwarded the colonoscopy results to the screening registry. 7.8% of people with positive faecal immunochemical test did not undergo a colonoscopy inside the screening programme, but some of them have undergone a colonoscopy outside the screening programme. We could not estimate for how many of them we were not able to obtain the colonoscopy results with premalignant or non-malignant findings. From cancer registry only cancer cases are available.

Conclusions

The proportion of interval cancers after immunochemical faecal occult blood test in Slovenian colorectal cancer screening programme is similar to other programmes in Europe. Test sensitivity for immunochemical faecal test is among the highest when compared to similar programmes, which can be attributed to the analysis of two stool samples. Even the lowering of cut-off value for positive test result to the lowest noticeable value would not eliminate the interval cancers, because they are sometimes found in persons where there were no trace of faecal blood.

Important differences in stages and sites of detected cancers among interval, screen detected and non-responders' cancers are found. There are differences in socio-economic status of persons, in which cancer was detected as interval or screen detected, as well as in those, which were diagnosed with cancer without responding to the screening. In latter, there are characteristically more persons with lower education. Due to the more frequent diagnoses of cancer in higher stages among non-responders, there is a need for better awareness raising among the target population on the fact that participation in the screening programme enables early detection of cancer or its prevention.

References

1. Ferlay J, Soerjomataram I, Dikshit R, Eser S, Mathers C,Rebelo M. Cancer incidence and mortality worldwide: sources, methods and major patterns in GLOBOCAN 2012. *Int J Cancer* 2015; **136:** E359-86. doi: 10.1002/ijc.29210
2. Zadnik V, Primic Zakelj M, Lokar K, Jarm K, Ivanus U, Zagar T. Cancer burden in Slovenia with the time trends analysis. *Radiol Oncol* 2017; **51:** 47-55. doi: 10.1515/raon-2017-0008
3. Proposal for a Council Recommendation on Cancer Screening. Commission of the European Communities. 2003/0093(CNS). [cited 2018 Mar 15]. Available from: http://ec.europa.eu/health/ph_determinants/genetics/documents/com_2003_0230_en.pdf
4. Mandel JS, Bond JH, Church TR, Snover DC, Bradley GM, Schuman LM, et al. Reducing mortality from colorectal cancer by screening for fecal occult blood. Minnesota Colon Cancer Control Study. *N Engl J Med* 1993; **328:** 1365-71. doi: 10.1056/NEJM199305133281901
5. Kronborg O, Fenger C, Olsen J, Jorgensen OD, Sondergaard O. Randomised study of screening for colorectal cancer with faecal-occult-blood test. *Lancet* 1996; **348:** 1467-71. doi: 10.1016/S0140-6736(96)03430-7
6. Hardcastle JD, Chamberlain JO, Robinson MH, Moss SM, Amar SS, Balfour TW, et al. Randomised controlled trial of faecal-occult-blood screening for colorectal cancer. *Lancet* 1996; **348:** 1472-7. doi: 10.1016/S0140-6736(96)03386-7
7. Segnan N, Patnick J, von Karsa L, editors. European Guidelines for Quality Assurance in Colorectal Cancer Screening and Diagnosis. First edition. European Commission. Luxembourg: Publications Office of the European Union; 2010 [cited 2018 Mar 15]. Available from: http://www.stopdarmkanker.be/BOEKJE/boekEU.pdf
8. Duffy MJ, van Rossum LG, van Turenhout ST, Malminiemi O, Sturgeon C, Lamerz R, et al. Use of faecal markers in screening for colorectal neoplasia: a European group on tumor markers position paper. *Int J Cancer* 2011; **128:** 3-11. doi: 10.1002/ijc.25654
9. Raffle A, Gray M. Screening: Evidence and Practice. Oxford: University Press; 2007.

10. Sanduleanu S, le Clercq CM, Dekker E, Meijer GA, Rabeneck L, Rutter MD, et al. Definition and taxonomy of interval colorectal cancers: a proposal for standardising nomenclature. *Gut* 2015; **64:** 1257-67. doi: 10.1136/gutjnl-2014-307992

11. Steele RJ, McClements P, Watling C, Libby G, Weller D, Brewster DH, et al. Interval cancers in a FOBT-based colorectal cancer population screening programme: implications for stage, gender and tumour site. *Gut* 2012; **6:** 576-81. doi: 10.1136/gutjnl-2011-300535

12. Grazzini G, Visioli CB, Zorzi M, Ciatto S, Banovich F, Bonanomi AG, et al. Immunochemical faecal occult blood test: number of samples and positivity cutoff. What is the best strategy for colorectal cancer screening? *Br J Cancer* 2009; **100:** 259-65. doi: 10.1038/sj.bjc.6604864

13. Zorzi M, Fedato C, Grazzini G, Stocco FC, Banovich F, Bortoli A, et al. High sensitivity of five colorectal screening programmes with faecal immunochemical test in the Veneto Region, Italy. *Gut* 2011; **60:** 944-9. doi: 10.1136/gut.2010.223982

14. Tepeš B, Stefanovič M, Bračko M, Frković Grazio S, Maučec Zakotnik J, Novak Mlakar D, et al. [Slovenian colorectal cancer screening programme SVIT - results of pilot phase.] [Slovenian]. *Zdrav Vestn* 2010; **79:** 403-11.

15. Tepeš B, Bracko M, Novak Mlakar D, Stefanovic M, Stabuc B, Frkovic Grazio S, et al. Results of the FIT-based National Colorectal Cancer Screening Program in Slovenia. *J Clin Gastroenterol* 2017; **51:** e52-9. doi: 10.1097/MCG.0000000000000662

16. Tepeš B, Kasesnik K, Novak Mlakar D, editos. [Slovenian guidelines of colorectal cancer screening programme SVIT: Slovenian guidelines ensure the quality of colorectal cancer screening.] [Slovenian]. First edition. Ljubljana: Nacionalni inštitut za javno zdravje; 2016.

17. International Classification of Diseases for Oncology, 3rd Edition. Geneva, Switzerland: World Health Organization; 2000.

18. Hakama M, Auvinen A, Day NE, Miller AB. Sensitivity in cancer screening. *J Med Screen* 2007; **14:** 174-7. doi: 10.1258/096914107782912077

19. Malila N, Oivanen T, Malminiemi O, Hakama M. Test, episode, and programme sensitivities of screening for colorectal cancer as a public health policy in Finland: experimental design. *BMJ* 2008; **337:** a2261. doi: 10.1136/bmj.a2261

20. GISCoR Working Group, Zorzi M (Coordinator). Detection of the interval cancers and estimate of the sensitivity of colorectal cancer screening programmes. Working report. *Epidemiol Prev* 2013; **37 (2-3 Suppl 1)** [cited 2018 Mar 15]. Available from: http://www.epiprev.it/materiali/2013/EP2-3/S1_GISCOR/GISCOR_2013_Eng_def.pdf

21. Zappa M, Castiglione G, Paci E, Grazzini G, Rubeca T, Turco P, et al. Measuring interval cancers in population-based screening using different assays of fecal occult blood testing: the District of Florence experience. *Int J Cancer* 2001; **92**: 151-4. doi: 10.1002/1097-0215(200102)9999:9999<::AID-IJC1149>3.0.CO;2-6

22. van der Vlugt M, Grobbee EJ, Bossuyt PMM, Bos A, Bongers E, Spijker W, et al. Interval Colorectal Cancer Incidence Among Subjects Undergoing Multiple Rounds of Fecal Immunochemical Testing. *Gastroenterology* 2017; **153:** 439-47. doi: 10.1053/j.gastro.2017.05.004

23. Portillo I, Arana-Arri E, Idigoras I, Bilbao I, Martínez-Indart L, World LB, et al. Colorectal and interval cancers of the Colorectal Cancer Screening Program in the Basque Country (Spain). *J Gastroenterol* 2017; **23:** 2731-42. doi: 10.3748/wjg.v23.i15.2731

24. Senore C, Armaroli P, Silvani M, Andreoni B, Bisanti L, Marai L, et al. Comparing different strategies for colorectal cancer screening in Italy: predictors of patients' participation. *Am J Gastroenterol* 2010; **105:** 188-98. doi: 10.1038/ajg.2009.583

25. Garcia M, Domènech X, Vidal C, Torné E, Milà N, Binefa G, et al. Interval Cancers in a Population-Based Screening Program for Colorectal Cancer in Catalonia, Spain. *Gastroenterol Res Pract* 2015; **2015:** 672410. Published online 2015 Feb 24. doi: 10.1155/2015/672410

26. Steele RJ, Stanners G, Lang J, Brewster DH, Carey FA, Fraser CG. Interval cancers in a national colorectal cancer screening programme. *United European Gastroenterol J* 2016; **4:** 587-94. doi: 10.1177/2050640615624294

27. Morris EJA, Whitehouse LE, Farrell T, Nickerson C, Thomas JD, Quirke P, et al. A retrospective observational study examining the characteristics and outcomes of tumours diagnosed within and without of the English NHS Bowel Cancer Screening Programme. *Br J Cancer* 2012; **107:** 757-64. doi: 10.1038/bjc.2012.331

28. Gill MD, Bramble MG, Rees CJ, Lee TJ, Bradburn DM, Mills SJ. Comparison of screen-detected and interval colorectal cancers in the Bowel Cancer Screening Programme. *Br J Cancer* 2012; **107:** 417-21. doi: 10.1038/bjc.2012.305

29. Paimela H, Malila N, Palva T, Hakulinen T, Vertio H, Järvinen H. Early detection of colorectal cancer with faecal occult blood test screening. *Br J Surg* 2010; **97:** 1567-71. doi: 10.1002/bjs.7150

30. Barnett KN, Weller D, Smith S, Steele RJ, Vedsted P, Orbell S, et al. The contribution of a negative colorectal screening test result to symptom appraisal and help-seeking behaviour among patients subsequently diagnosed with an interval colorectal cancer. *Health Expect* 2018. doi: 10.1111/hex.12672

31. Digby J, Fraser CG, Carey FA, Lang J, Stanners G, Steele RJ. Interval cancers using a quantitative faecal immunochemical test (FIT) for haemoglobin when colonoscopy capacity is limited. *J Med Screen* 2016; **23:** 130-4. doi: 10.1177/0969141315609634

research article

Dynamic expression of 11 miRNAs in 83 consecutive primary and corresponding recurrent glioblastoma: correlation to treatment, time to recurrence, overall survival and MGMT methylation status

Bostjan Matos*[1], Emanuela Bostjancic*[2], Alenka Matjasic[2], Mara Popovic[3], Damjan Glavac[2]

[1] Department of Neurosurgery, University Clinical Center, Ljubljana, Slovenia
[2] Department of Molecular Genetics, Institute of Pathology, Faculty of Medicine, University of Ljubljana, Ljubljana, Slovenia
[3] Institute of Pathology, Faculty of Medicine, University of Ljubljana, Ljubljana, Slovenia

Radiol Oncol 2018; 52(4): 422-432.

Received 6 August 2018
Accepted 3 September 2018

Correspondence to: Damjan Glavač, Ph.D., Department of Molecular Genetics, Institute of Pathology, Korytkova 2, Faculty of Medicine, SI-1000 Ljubljana, Slovenia. Phone: +386 1 543 7180, Fax: +386 1 543 7181; E-mail: damjan.glavac@mf.uni-lj.si

Disclosure: No potential conflicts of interest were disclosed.

*Authors contributed equally to this work.

Background. Glioblastoma (GBM) is the most common and the most malignant glioma subtype. Among numerous genetic alterations, miRNAs contribute to pathogenesis of GBM and it is suggested that also to GBM recurrence and resistance to therapy. Based on publications, we have selected 11 miRNAs and analyzed their expression in GBM. We hypothesized that selected miRNAs are differentially expressed and involved in primary as well as in recurrent GBM, that show significant expressional differences when different treatment options are in question, and that are related to certain patients and tumor characteristics.

Patients and methods. Paraffin embedded tissues, obtained from primary and corresponding recurrent tumor from 83 patients with primary GBM were used. Eleven miRNAs (*miR-7, miR-9, miR-15b, miR-21, miR-26b, miR-124a, miR-199a, let-7a, let-7b, let-7d,* and *let-7f*) were selected for qPCR expression analysis. For patients who received temozolamide (TMZ) as chemotherapeutic drug, O6-methylguanine-DNA methyltransferase (MGMT) methylation status was defined using the methyl-specific PCR.

Results. There was a significant change in expression of *miR-7, miR-9, miR-21, miR-26b, mirR-124a, miR-199a* and *let-7f* in recurrent tumor compared to the primary. In recurrent tumor, *miR-15b, let-7d* and *let-7f* significantly changed comparing both treatment options. We also observed difference in progression free survival between patients that received radiotherapy and patients that received radiotherapy and chemotherapy, and longer survival for patients who received chemotherapy after second surgery compared to not treated patients. *miR-26b* showed correlation to progression free survival and *let-7f* to overall survival. We did not find any expression difference between the tumors with and without methylated MGMT.

Conclusions. Our data suggest that analyzed miRNAs may not only contribute to pathogenesis of primary GBM, but also to tumor progression and its recurrence. Moreover, expression of certain miRNAs appears to be therapy-dependent and as such they might serve as additional biomarker for recurrence prediction and potentially predict a therapy-resistance.

Key words: glioblastoma; recurrent; radiotherapy; chemotherapy; miRNA; expression

Introduction

Gliomas are the most common primary brain tumors and are classified on the basis of histopathological characteristics. Glioblastoma (GBM) is the most common and malignant glioma subtype characterized by rapid growth and poor prognosis.[1] Like cancer in general, GBM develop as a

consequence of genetic alterations that accumulate with tumor progression. However, pathogenesis of GBM recurrence is still poorly understood. Certain molecular pathways and novel biomarkers have been established as diagnostic, prognostic and predictive markers, such as is epidermal growth factor receptor (EGFR) amplification, O6-methylguanine-DNA methyltransferase (MGMT) methylation and others.[1-3] Among novel biomarkers are non-coding RNAs, of which the most studied are microRNAs (miRNAs). The miRNAs are small RNAs that act as endogenous regulators of gene expressions and function in different physiological processes, contributing to pathogenesis of different types of cancer, including gliomas. miRNA expression might be a potential biomarker for GBM used as diagnostic support or for prognostic and therapeutic application.[4-6] However, differential expression of certain miRNAs might be also involved in pathophysiological mechanisms of GBM recurrence, but there are limited data regarding miRNA expression as GBM progresses (at its recurrence).[7,8] Comprehensive knowledge and understanding of the molecular pathways underlying disease progression, tumor recurrence and response to therapy might be of great importance in future development of more efficient therapies in GBM.

Local infiltration and progressive growth of GBM tumor cells into the adjacent brain tissue invalidate any possibility for a radical surgical tumor resection.[9] Consequently, recurrence is observed in almost all tumors.[7] Additionally, the difficulty in treatment of this lethal disease is in tumor acquisition of several mechanisms of radio and chemo-resistance. In addition to methylation of MGMT[10], a change in miRNA's expression is also a cause for drug resistance in GBM.[11] Several miRNAs have been related to radio- and chemo-sensitivity as well as radio- and chemo-resistance of glioma cells, and recognized as crucial regulators during glioma pathogenesis and progression.[12] However, a certain degree of this aberrant regulation may also be the consequence of treatment.

In aim to characterize at least some miRNAs that might be involved in GBM formation/progression and recurrence, and may also contribute to therapy resistance, we selected 83 consecutive patients with operable recurrent GBM, where samples from first and from second surgery were available. We selected ten miRNAs, which expression was up-regulated (*miR-9, miR-15b, miR-21, miR-26b, let-7a, let-7b, let-7d* and *let-7f*) or down-regulated (*miR-7* and *miR-124a*) in previous studies of GBM, and were differentially expressed from other glioma subtypes.[13] We additionally included *miR-199a*, which is involved in tumorigenesis of various types of cancer, including GBM.[14] The majority of these miRNAs have already been shown to be involved in different tumorigenic processes in GBM or glioma cell lines (Table 1).[4,15] We hypothesized that: (i) selected miRNAs are deregulated in primary as well as in recurrent GBM; (ii) some miRNAs are also differently expressed between primary and recurrent tumor; (iii) expression of selected miRNAs in recurrent GBM is therapy dependent; (iv) progression free survival and overall survival is different between distinct therapies; (v) expression of some miRNAs is related to progression free survival and overall survival; and

TABLE 1. List of the analysed miRNAs with known functions in glioma pathogenesis

MicroRNAs	Invasion	Proliferation	Tu growth	Migration	Cell cycle	Survival/ cell death	Other functions
miR-7	+	+	+	nd	+	+	Differentiation, Vasculogenic mimicry
miR-9	nd	+	nd	+	nd	nd	Self-renewal, Vasculogenic mimicry
miR-15b	+	+	+	nd	+	+	Angiogenesis
miR-21	+	+	+	+	+	+	/
miR-26b	+	+	+	+	nd	+	Vasculogenic mimicry
miR-124	+	+	+	+	+	+	Differentiation, Angiogenesis
miR-199a	nd	+	nd	nd	nd	nd	/
let-7a	nd	+	+	+	nd	nd	/
let-7b	+	nd	nd	+	nd	nd	/
let-7d	nd	nd	nd	nd	nd	nd	/
let-7f	+	+	nd	+	nd	nd	/

+ = involved in tumorigenic process in glioma; nd = not determined yet as involved in tumorigenic process; Tu = tumor; reviewed from Karsy *et al.*[4], Lages *et al.*[13], Silber *et al.*[5], Visani *et al.*[40], Zhang *et al.*[6]

TABLE 2. Demographic and clinicopathological characteristics of patients included in the study

Histopathological diagnosis		GBM, WHO grade IV
Number of cases		83
Mean age (Year)		50 ± 12.8 (min 8, max 71)
Gender	Male	50 (60%)
	Female	33 (40%)
Karnofsky performance status ≥ 80		83
Adjuvant treatment	radiotherapy after first surgery	83/83 (100%)
	chemotherapy after first surgery	54/83 (65%)
	radiotherapy after second surgery	15/83 (18%)
	chemotherapy after second surgery	47/83 (56%)
MGMT methylated (tested in a subset of patients treated with TMZ)	Primary GBM	38/47 (81%)
	Recurrent GBM	46/47 (98%)
Time to recurrence (months)		0.84–67.30
Survival after second surgery (months)		0.03–25.75
Overall survival (months)		0.84–70.48

MGMT = methyl guanine methyl transferase; TMZ = temozolamide

(vi) methylation status of MGMT is in correlation to certain miRNAs.

Patients and methods

Patients and tissue samples

Our retrospective study included eighty-three patients with recurrent GBM. The data were obtained from the patients charts from hospital registry of the Institute of Oncology and from the Cancer Registry of Slovenia. Each patient underwent the first surgery and the second one after the first recurrence of GBM between January 1997 and November 2011 at the University Clinical Centre Ljubljana, Slovenia. The selected patients were consecutive; of the 1117 that underwent the first surgery for GBM, 83 underwent also the second surgeryat tumor recurrence since these patients were capable of re-operation according to clinical standards (Karnofsky performance status over 80). Patients received radiotherapy (RT) after the surgery, and RT with concomitant and adjuvant chemotherapy (ChT) after 2005.

Tissue samples were fixed in 10% buffered formalin and embedded in paraffin (FFPE) for routine diagnostics. The grading criteria based on WHO classification was used.[14] Paired tissue samples were retrieved from the archive of the Institute of Pathology, Faculty of Medicine, University of Ljubljana. Samples were classified in two groups, *i.e.* primary GBM (sample tissue collected at first surgery) and corresponding recurrent GBM (sample tissue collected at second surgery). As control sample RNA FirstChoice Human Brain Reference Total RNA (Cat. no. 6050, Ambion; Invitrogen, USA) was used.

The patients' data, including age, gender and therapy are summarized in Table 2.

RNA isolation from FFPE tissue samples

Tissue samples were cut at 10 μm from FFPE tissue blocks and for the isolation procedure six to eight 10 μm sections were used. Total RNA isolation was performed using miRNeasy FFPE Kit (Qiagen, Germany) according to the manufacturer's protocol. The RNA was eluted in 30 μl of nuclease-free water. The yield was measured spectrophotometrically using the NanoDrop-1000 (Thermo Scientific, USA) and the quality was evaluated on the Bioanalyzer 2100 (Agilent Technologies, USA).

Quantitative real-time PCR (qPCR)

All the reagents were from Qiagen, except where otherwise indicated. Quantitative PCR (qPCR) was carried out using the Rotor Gene-Q Real-Time PCR System and all the qPCR reactions were performed in duplicates or triplicates. Prior to qPCR analysis, two pools of RNA samples were created from FFPE tissue samples (primary, recurrence) and, along with reference RNA, tested for qPCR efficiency. Reverse transcription using miScript reverse transcription kit was performed in a 10 μl reaction master mix with 50 ng of total RNA according to manufacturer instruction. The resulting cDNA was diluted 100-fold and qPCR reaction was carried out in 10 μl PCR master mix, according to manufacturer instruction. As the reference genes, *RNU6B* and *SNORD25* were used based on efficiency results. Tested miRNAs were: *miR-7*, *miR-9*, *miR-15b*, *miR-21*, *miR-26b*, *miR-124a*, *miR-199a*, *let-7a*, *let-7b*, *let-7d*, and *let-7f*.

DNA isolation

In a subset of patients that were treated with temozolamide (TMZ) (n = 47), MGMT methylation status was determined**.** Tissue samples from the first surgery and the surgery at first recurrence were cut at 10 μm from FFPE tissue blocks and for the isolation procedure, six to eight 10 μm sections were

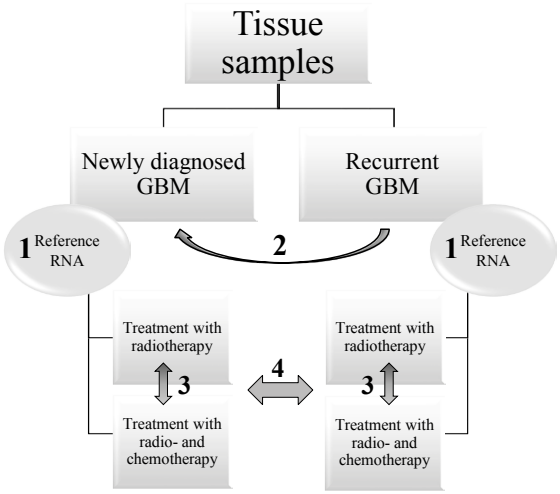

FIGURE 1. Schematic representation of the workflow and statistical comparisons.

GBM = glioblastoma; Reference RNA = Human Brain Reference RNA; 1 = Willcoxon Signed Rank Test between primary glioblastoma and corresponding recurrent glioblastoma using ΔCt; 2 = normalization to Human Brain reference RNA resulting in ΔΔCt; 3 and 4 = Mann-Whitney test between independent groups of samples using ΔΔCt (normalization of glioblastoma samples to Human Brain Reference RNA)

used. Total DNA isolation was performed using QIAamp DNA FFPE Tissue Kit (Qiagen) according to the manufacturer's protocol. The DNA was eluted in 60 µl of nuclease-free water. The yield was measured fluorescently using the Quant-It (Life Technologies) according to manufacturer instruction and Rotor Gene Q (Qiagen).

MGMT methylation status analysis

For determining the MGMT methylation status, methyl-specific polymerase chain reaction (MSP) was used in a two-step approach with primers previously described.[16] Briefly, prior to MSP, 500 ng of DNA was used for bisulfite conversion using innuCONVERT Bisulfite Basic Kit according to manufacturer instruction (Analytik Jena) and stored at -20°C for subsequent MSP. For MSP, 15 ng of bisulfite converted DNA was used with 0.2 µM of each primer for methylated form and 0.3 µM of each primer for unmethylated form, 2 mM of dNTP and 0.25 U of Hot Master Polymerase (5 Prime), all in 10 µl reaction. Amplification was performed according to manufacturer instruction using 59°C for primer annealing. In each run, fully methylated (EpiTect Control DNA, methylated, Qiagen) as well as fully unmethylated controls (EpiTect Control DNA, unmethlyated, Qiagen) were used as assay controls. Results were analyzed using 2% agarose gel. The investigator who analyzed the GBM samples was blinded to all clinical information.

Statistical analysis

To present a relative gene expression the $2^{-\Delta\Delta Ct}$ method was used.[17] For paired samples (primary, recurrent), the calculated ΔCt was tested for statistical significance using Wilcoxon Signed Rank test. For independent group of samples, ΔΔCt was calculated relatively to Human brain Reference RNA and used for Mann-Whitney test (treatment, MGMT status, *etc.*). Kaplan-Meier curve was used to analyze difference in progression free survival (time to recurrence) and overall survival (different treatment options, miRNA expression). Correlations between scale variables (miRNA expression, survival) were calculated using Pearson's and Spearman's correlation coefficient. For all statistical tests, the SPSS analytical software (ver.24 SPSS Inc. IL) was used (cut-off point at $p < 0.05$). The workflow of comparisons is summarized in Figure 1.

Compliance with ethical standards

Study has been approved by Slovene National Medical Ethics Committee (Number 113/05/13).

Results

Expression of miRNAs is changed in primary and recurrent GBM

Comparing expression of analyzed miRNAs to Human Brain Reference RNA (ΔΔCt), we found altered expression for all 11 analyzed miRNAs both in primary as well as in recurrent GBM. Whereas *miR-9* and *miR-21* were mainly up-regulated and *miR-15b* was mainly down-regulated in primary and recurrent GBM, all other miRNAs showed more heterogeneous expression when compared to the Human Brain Reference RNA. Results are summarized in Figure 2.

miRNAs in recurrent GBM are differentially expressed compared to primary GBM

Using calculated ΔCt and Wilcoxon Signed Rank test, we have observed significant alteration in expression for 7 miRNAs between primary and recurrent GBM. Five miRNAs, *miR-9* ($p = 0.016$), *miR-21* ($p < 0.001$), *miR-26b* ($p < 0.001$), *miR-124* (p

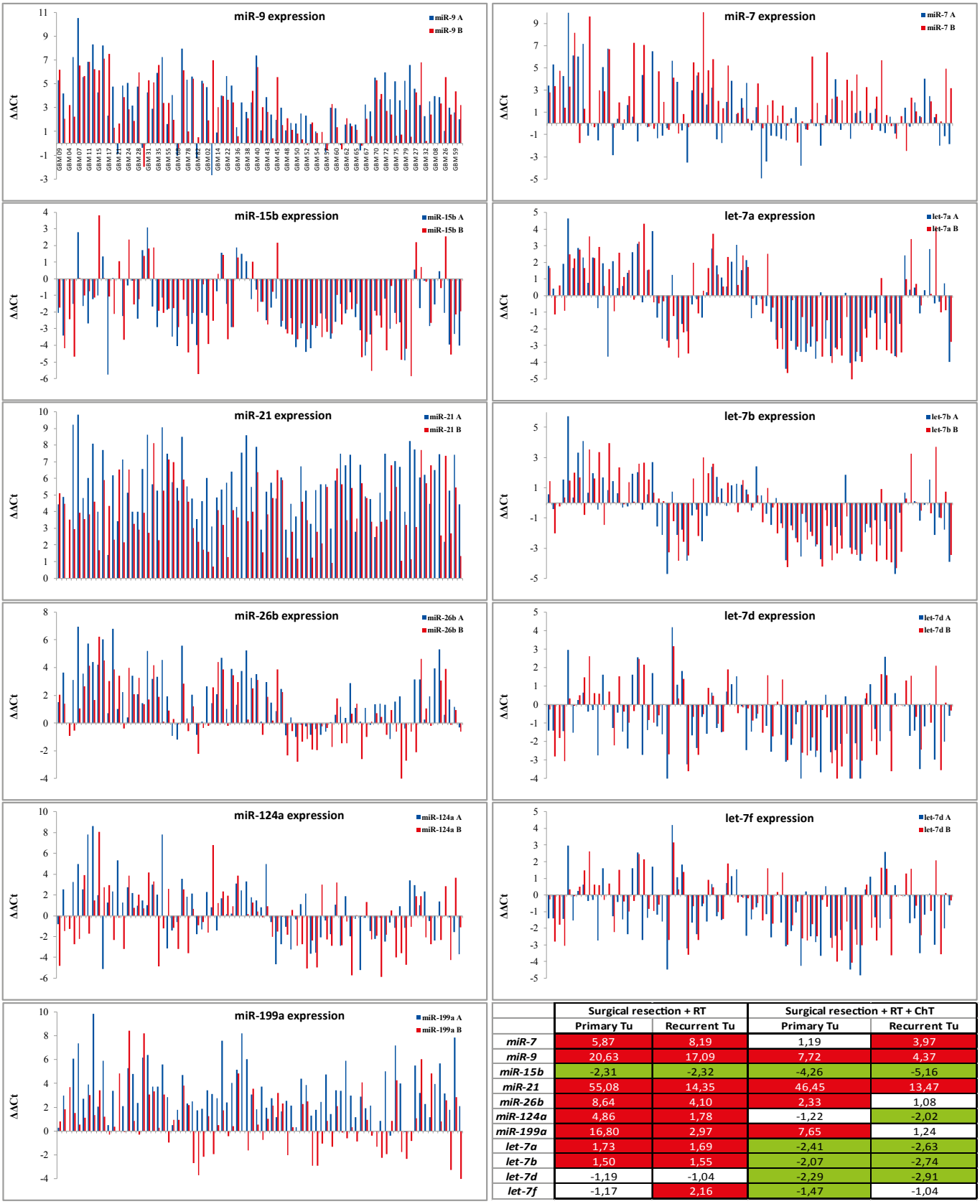

	Surgical resection + RT		Surgical resection + RT + ChT	
	Primary Tu	Recurrent Tu	Primary Tu	Recurrent Tu
miR-7	5,87	8,19	1,19	3,97
miR-9	20,63	17,09	7,72	4,37
miR-15b	-2,31	-2,32	-4,26	-5,16
miR-21	55,08	14,35	46,45	13,47
miR-26b	8,64	4,10	2,33	1,08
miR-124a	4,86	1,78	-1,22	-2,02
miR-199a	16,80	2,97	7,65	1,24
let-7a	1,73	1,69	-2,41	-2,63
let-7b	1,50	1,55	-2,07	-2,74
let-7d	-1,19	-1,04	-2,29	-2,91
let-7f	-1,17	2,16	-1,47	-1,04

FIGURE 2. Expression of miRNAs in primary and recurrent GBM (compared to the Human Brain Reference RNA, ΔΔCt) with Table presenting Average Fold Changes.

ChT = chemotherapy; RT = radiotherapy; A = primary GBM; B = recurrent GBM

= 0.029) and *miR-199a* ($p < 0.001$), were down-regulated, and *miR-7* ($p = 0.001$) and *let-7f* ($p < 0.001$) were up-regulated in recurrent tumors compared to first time surgery. However, all of these miRNAs were differentially expressed also in a subgroup treated with RT and ChT, whereas only four of these showed statistically significant differential expression in a subgroup treated with RT alone. Results are summarized in Figure 3 and Figure 2 (Average Fold Change Table).

Distinctive expression of miRNAs after different treatment options in recurrent GBM

Using Mann-Whitney test for comparing subgroup of patients treated with RT alone to patients treated with RT and ChT (analyzed miRNAs normalized to Human Brain Reference RNA, ΔΔCt), we observed that expression of certain miRNAs was different before treatment (at first surgery) as well as after treatment (at second surgery). Therefore, only those miRNAs that showed significantly differential expression only after treatment (at second surgery) were considered truly as a consequence of treatment. Both *miR-15b* and *miR-7d* were down-regulated compared to Human Brain Reference RNA after treatment, and there was significant change in expression between patients that received RT alone and those that received RT and ChT ($p = 0.013$ for *miR-15b* and $p = 0.008$ for *let-7d*). In patients treated with RT alone, *let-7f* was up-regulated compared to Human Brain Reference RNA at second surgery, whereas it was unchanged in patients that were treated with RT and ChT. There was significant change in expression of *let-7f* between both groups ($p = 0.007$). Results are summarized in Figure 4.

Correlation between progression free survival, survival after second surgery, overall survival, treatment and miRNA expression

There was weak, but statistically significant change in progression free survival between patients who received RT alone and those who received both, RT and ChT after first surgery (7 months and 11 months, respectively; $p = 0.045$). Results are summarized in Figure 5A.

We have also calculated the survival time from second surgery. The number of patients who received RT alone or RT and ChT was too small for reliable analysis of survival time. However, there

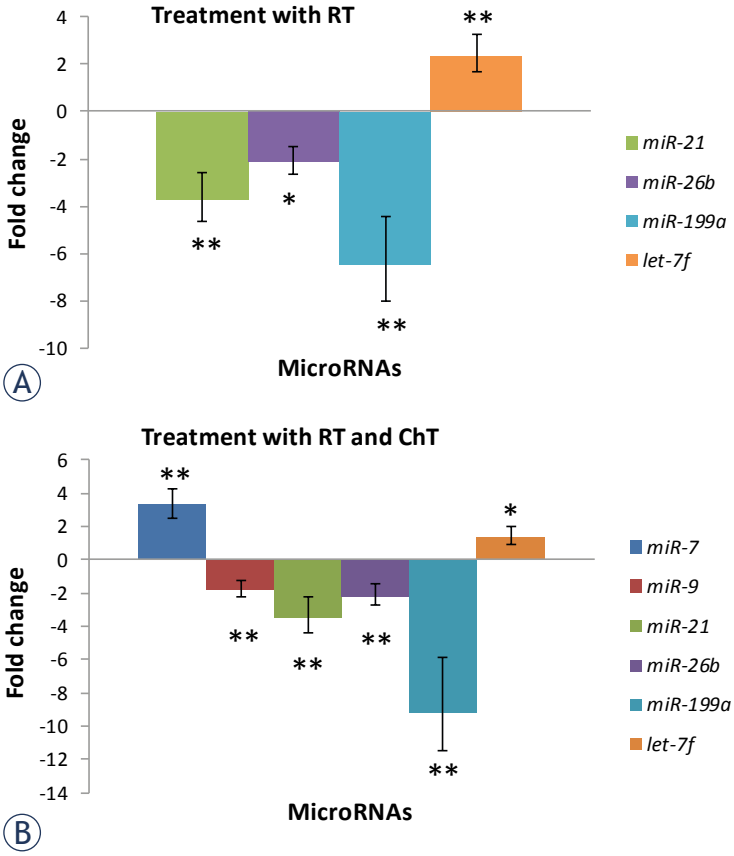

FIGURE 3. Expression of miRNAs in recurrent glioblastoma (GBM) after treatment compared to expression in primary GBM. Results are represented separately for patients treated with RT and those treated with RT and ChT.

ChT = chemotherapy; RT = radiotherapy; * = significant differences in expression of miRNAs, $p < 0.05$; ** = $p < 0.01$

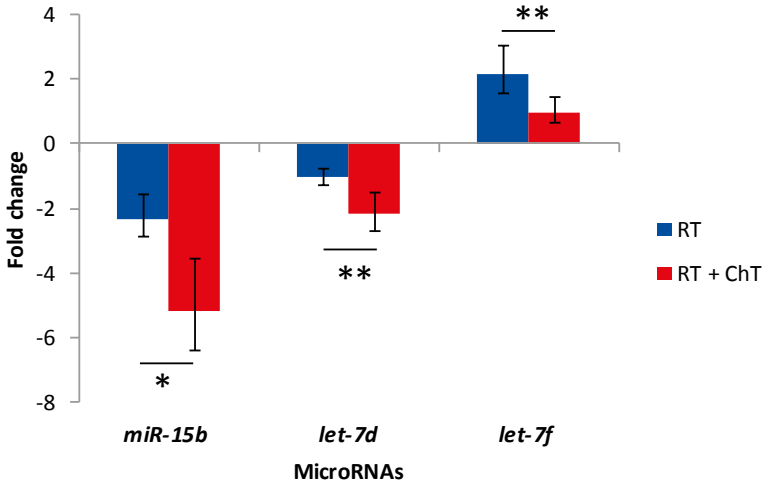

FIGURE 4. Distinctive expression of miRNAs after different treatment options in recurrent glioblastoma

ChT = chemotherapy; RT = radiotherapy; * = $p < 0.05$; ** = $p < 0.01$

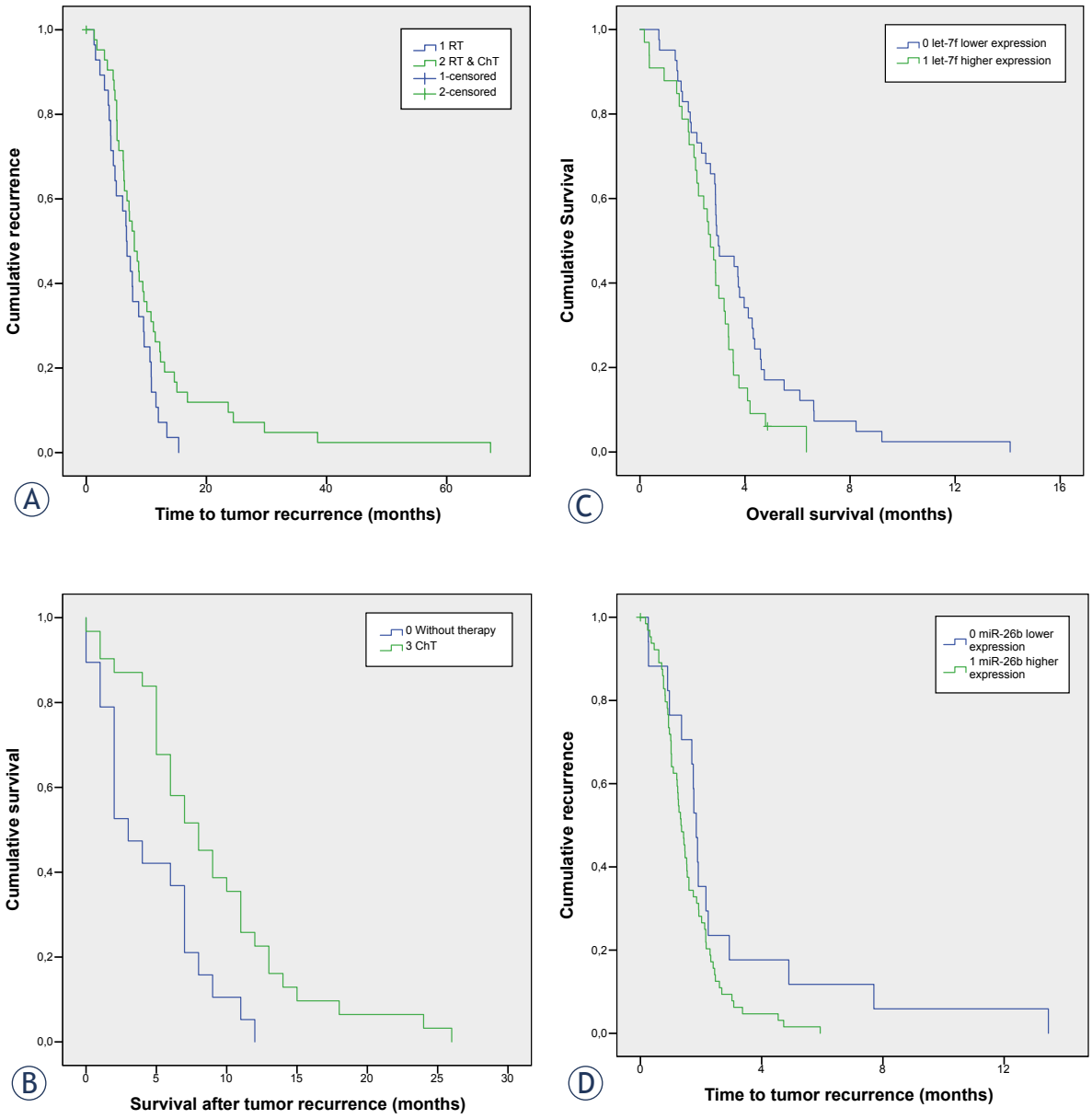

FIGURE 5. Survival curve analyses; **(A)** Progression free survival between patients that received RT alone or both, RT and ChT; **(B)** Survival time after second surgery for patients who received no therapy versus patients who received ChT; **(C)** Progression free survival between patients with up- and downregulated *miR-26b*; **(D)** Progression free survival between patients with up- and downregulated *let-7f*.

ChT = chemotherapy; RT = radiotherapy

was statistically significant longer overall survival for patients who received ChT compared to those that were not treated after second surgery (8 months and 5 months, respectively; p = 0.004). Results are summarized in Figure 5B.

We further calculate Spearman's and Pearson's correlation coefficient between miRNA expression (analyzed miRNAs normalized to Human Brain Reference RNA, ΔΔCt) in primary GBM and progression free survival and overall survival, and found weak inverse correlation for *let-7b* and progression free survival (r = -0.220, p = 0.049) and weak inverse correlation between *let-7f* and overall survival (r = -0.226, *p* = 0.050). We further analysed difference in Kaplan-Meier curve for patients with up- and down-regulated miRNAs and found, that there is a difference in progression free between patients with up- and down-regulated *miR-26b* (p =

0.05, Figure 5C), and difference in overall survival for up- and down regulated *let-7f* (p = 0.021).

miRNAs and MGMT methylation status

Among patients treated with ChT, there were 47 treated with TMZ. Among them, there were 9 patients with unmethylated and 34 with methylated MGMT. All, except one, became methylated in recurrent tumor. Comparing miRNA expression normalized to Human Brain Reference RNA between MGMT methylated and MGMT unmethylated tumors revealed no correlation of investigated miRNA expression to MGMT methylation status.

Discussion

In our 83 consecutive patients operated for primary GBM and re-operated at the first recurrence of GBM, we have analyzed the expression of 11 selected miRNAs (*miR-7, miR-9, miR-15b, miR-21, miR-26b, miR-124a miR-199a, let-7a, let-7b, let-7d,* and *let-7f)*. However, to the best of our knowledge, this is the first report of these miRNAs expression in recurrent GBM.

Expression of analyzed miRNAs in primary and recurrent GBM

We observed differential expression of the majority of analyzed miRNAs in both samples. In primary as well as in recurrent GBM we have observed overall *miR-7* over-expression, although was expression heterogeneous among tumors. In spite of numerous studies on *miR-7* expression, its expression in recurrent GBM has not been analyzed yet. Increased expression of *miR-7* was found to suppress GBM cell proliferation, induce apoptosis, inhibit cell migration *in vitro*, and reduce tumorigenicity *in vivo*.[4] However, in contrast to our study, other research group showed *miR-7* down-regulation in patients with GBM.[18] Possible explanation for different outcomes might be in different normalization strategies used for qPCR (*i.e.* different reference genes used). *miR-9* over-expression, observed in our primary and recurrent GBM samples, might contribute to tumor progression since it has been identified that up-regulation of *miR-9* predicts an unfavorable prognosis and correlates with tumor progression.[19] Similarly to other cancer research[20], we observed increased expression of oncogenic *miR-21* in primary and recurrent GBM, although its' up-regulation in recurrent tumors is significantly lower compared to primary tumors. *miR-26b* was also found to be mainly over-expressed, although there are samples with its down-regulation, but in contrast to our results, it has been shown that *miR-26b* was decreased in glioma cell lines and inversely correlated with the grade of glioma in humans.[21] The discrepancy could be due to different normalization strategies. We normalized expression of miRNAs in GBM samples to Human Brain Reference RNA, in others the normal brain tissue was used for normalization.[21] Expression of *miR-124a* in our research showed up-regulation in certain samples of primary tumors. Published data showed decreased *miR-124a* expression in majority of GBM samples due to hyper-methylation of promoter region of *miR-124a*.[22] Speculatively, different methylation status of *miR-124a* might be observed in our samples. We also observed mainly higher expression level of *miR-199a* in primary GBM samples and near to normal level in recurrent GBM. *miR-199a* up-regulation in gliomas has been related to hypo-methylation of one of two copies of *miR-199a* within genome consequently leading to its up-regulation.[14] *miR-199a* is believed to have diverse biological functions in different tissues. It behaves as a tumor-suppressor in certain cancer types[14]; however, its exact role in GBM is yet to be defined. miRNA of *let-7* family (*let-7a/b/d/f*) showed the most heterogeneous expression across both, primary and recurrent tumor samples.[15,23]

Expression of miRNA in recurrent and primary GBM and its correlation to the choice of therapy

Our data also showed statistically significant alteration of expression of seven miRNAs (*miR-7, miR-9, miR-21, miR-26b, miR-124a, miR-199a* and *let-7f*) between primary and recurrent tumors. After receiving RT and ChT, we observed higher levels of *miR-7* in recurrent compared to the primary GBM, whereas in patients treated solely using RT there was no significant difference in expression. Based on glioma cell line models, up-regulation of *miR-7* increases radio-sensitivity.[24] Several target genes that might be involved in sensitivity of glioma cells to therapy has been shown for *miR-7*, including EGFR, IRS1 and IRS2 regulating differentiation, invasion and proliferation[4], as well as IGF-1R/Akt signalling pathway, regulating cellular growth and glucose metabolism in gliomas.[25,26] We did observe a decreased expression of *miR-9* in recurrent compared to primary GBM, however, *miR-9* is still over-expressed in recurrent GBM. *miR-9* has a

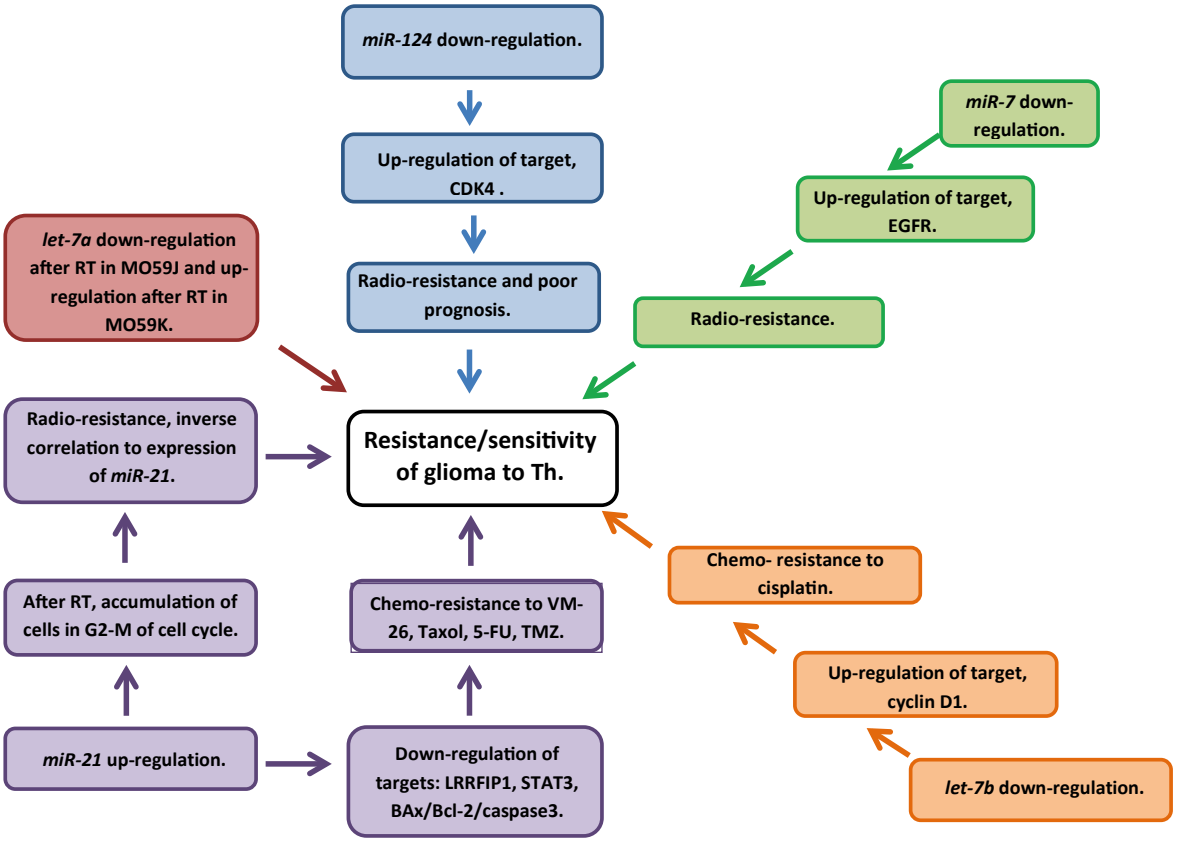

FIGURE 6. Summary of known functions in radio- and chemoresistance and sensitivity of miRNAs analyzed in our study.

role in chemotherapeutic resistance by regulating the p38 mitogen activated protein kinase signaling network, involved in regulation of cell stress and cell differentiation; it influences proliferation and self-renewal of glioma cells by targeting SOX2; and through miRNA regulation of PTCH1, receptor in Sonic Hedgehog signaling.[26] *miR-21* has been shown to be up-regulated in more radio-resistant cell lines [12] mediating the resistance of GBM cells against RT[27] and TMZ.[20] *miR-21* is substantially implicated in pathogenesis of GBM by targeting PTEN, RECK, PDCDC4, TIMP3, BCL2, SPRY2, MTAP, SOX5, JMY, TGFRBR2, TGFBR3, TP73L, APAFI, BMPR2, TOPORS, DAXX, TP53BP2, and PPIF. All this target genes are involved either in pathways of apoptosis, invasion, proliferation and tumor growth either in chemo-resistance.[4] Therefore, all these results suggest that lower expression of *miR-21* after treatment might implicate less resistant glioma cells to therapy; however, as well as *miR-9*, it is still up-regulated in recurrent GBM, possibly contributing to tumor progression.

Decrease expression of *miR-26b* in our recurrent samples compared to primary GBM, could be a consequence of tumor progression. Accordingly, it was found that ectopic expression of *miR-26b* inhibits its proliferation, migration and invasion of human glioma cells by repressing the endogenous level of EphA2 protein.[21] We further observed decrease in *miR-124a* expression in recurrent tumors compared to primary, which might be a consequence of tumor progression. It has been shown that *miR-124a* radio-sensitizes human glioma cells by targeting CDK4.[28] Several other targets have been also demonstrated for *miR-124a*, as are CDK6, SCP1, PTBP1, ITGB1, LAMCI, IQGAPI, RB and STAT3, regulating cell cycle, differentiation, invasion and proliferation of glioma cells and T cell-mediated immune clearance of glioma.[4,29] All these processes may be involved in sensitivity and survival of glioma cells.

In recurrent GBM, but not in primary GBM, we found significant change in expression between samples of patients who were treated with RT and ChT and those that were treated with RT alone for only *miR-15b, let-7d* and *let-7f*. *Let-7f* was over-expressed in recurrent compared to the primary GBM; however, it was up-regulated only in patients treated with RT after first surgery. It has been shown that members of *let-7* miRNA family (including *let-7f*) were mostly up-regulated in more

radio-resistant cell lines[12] suggesting radio-resistant function in glioma cells, since its expression after receiving RT and ChT was back to normal. There was observed normal expression of *let-7d* in GBM patients after receiving RT, however, after treating patients with RT and ChT, its expression was decreased and similar to that in primary GBM. There are limited data about the role of *let-7d* in the cell response to radiation and chemotherapeutic drugs in glioma, since depends on dose, time after irradiation and source of oxidative stress.[30] There are indication that *let-7d* down-regulation in GBM might be involved in modulation of chemo-resistance to TMZ.[11] One of the target genes of *let-7d* is oncogene HMGA2[31] and studies suggest that overexpression of HMGA2 may participate in regulating tumor cell invasion in high grade gliomas.[32] However, whether HMGA2 is up-regulated in GBM due to *let-7d* down-regulation, is yet to be defined. Another miRNA, *miR-15b*, was found in our study to be significantly under-expressed in patients treated with RT and ChT compared to those treated with RT alone. Similarly, to *let-7d*, decrease of *miR-15b* did not change in recurrent GBM compared to primary GBM. *miR-15b* was demonstrated to suppress proliferation and induce apoptosis in glioma cells by targeting CCNE1.[33] *miR-15b* expression decreases with the ascending histopathological grade and its low expression is associated with poor overall survival of patients with high grade gliomas.[34] Already known functions about radio- and chemoresistance/sensitivity and analyzed miRNAs are summarized in Figure 6.

Time to recurrence, survival and overall survival in correlation to therapy and miRNA expression

Finally, in our patients we have observed longer disease free survival in patients treated with RT and ChT after first surgery compared to those treated with RT alone. The standard care treatment of GBM altered importantly after year 2005 when RT alone was replaced by RT associated with chemotherapeutic TMZ in great majority of our patients. Similarly to our results, it has been shown that for patients treated with surgery and RT alone median survival was shorter (12–12.1 months) compared to patients treated additionally with TMZ (14.2–14.6 months).[35]

Investigating miRNAs expression and survival in patients with GBM revealed that, both, *miR-26b* and *let-7f* represent better prognosis when down-regulated. Lower expression of *miR-26b* is in correlation to progression free survival, whereas lower expression of *let-7f* is in correlation to overall survival. To the best of our knowledge, this is the first report describing expression of these two miRNAs to the function of survival in the GBM.

MGMT and miRNAs

Although we did not found any differential expression of investigated miRNAs between methylated and unmethylated MGMT, we did observed change in MGMT methylation status from primary to recurrent GBM. Eight of nine unmethylated samples in primary GBM were methylated in recurrent GBM. This change in methylation status of MGMT is not surprising, since there are several publications describing similar percentage of change; however all changes were from more to less favorable state for tumor progression.[36-39]

Conclusions

In conclusion, our results suggest that in recurrent GBM patients, miRNAs might play important role not only in pathogenesis of GBM, but also in tumor progression and its recurrence, as well as in response to therapy, in overall survival and progression free survival.

Acknowledgements

This work is a part of the PhD thesis of candidate Boštjan Matos, MD. This work was supported by the Slovenian Research Agency (ARRS) (Program P3-0054).

References

1. Ludwig K, Kornblum HI. Molecular markers in glioma. *J Neurooncol* 2017; **134:** 505-12. doi: 10.1007/s11060-017-2379-y
2. Louis DN, Ohgaki H, Wiestler OD, Cavenee WK, Burger PC, Jouvet A, et al. The 2007 WHO classification of tumours of the central nervous system. *Acta Neuropathol* 2007; **114:** 97-109. doi: 10.1007/s00401-007-0243-4
3. Siegal T. Clinical impact of molecular biomarkers in gliomas. *J Clin Neurosci* 2015; **22:** 437-44. doi: 10.1016/j.jocn.2014.10.004
4. Karsy M, Arslan E, Moy F. Current progress on understanding microRNAs in glioblastoma multiforme. *Genes Cancer* 2012; **3:** 3-15. doi: 10.1177/1947601912448068
5. Silber J, James CD, Hodgson JG. microRNAs in gliomas: small regulators of a big problem. *Neuromolecular Med* 2009; **11:** 208-22. doi: 10.1007/s12017-009-8087-9
6. Zhang Y, Dutta A, Abounader R. The role of microRNAs in glioma initiation and progression. *Front Biosci (Landmark Ed)* 2012; **17:** 700-12. PMID: 22201769

7. Ilhan-Mutlu A, Wöhrer A, Berghoff AS, Widhalm G, Marosi C, Wagner L, et al. Comparison of microRNA expression levels between initial and recurrent glioblastoma specimens. *J Neurooncol* 2013; **112:** 347-54. doi: 10.1007/s11060-013-1078-6

8. Yan D, Hao C, Xiao-Feng L, Yu-Chen L, Yu-Bin F, Lei Z. Molecular mechanism of Notch signaling with special emphasis on microRNAs: implications for glioma. *J Cell Physiol* 2018. doi: 10.1002/jcp.26775

9. Bucci MK, Maity A, Janss AJ, Belasco JB, Fisher MJ, Tochner ZA, et al. Near complete surgical resection predicts a favorable outcome in pediatric patients with nonbrainstem, malignant gliomas: results from a single center in the magnetic resonance imaging era. *Cancer* 2004; **101:** 817-24. doi: 10.1002/cncr.20422

10. Cabrini G, Fabbri E, Lo Nigro C, Dechecchi MC, Gambari R. Regulation of expression of O6-methylguanine-DNA methyltransferase and the treatment of glioblastoma (Review). *Int J Oncol* 2015; **47:** 417-28. doi: 10.3892/ijo.2015.3026

11. Tezcan G, Tunca B, Bekar A, Preusser M, Berghoff AS, Egeli U, et al. microRNA expression pattern modulates temozolomide response in GBM tumors with cancer stem cells. *Cell Mol Neurobiol* 2014; **34:** 679-92. doi: 10.1007/s10571-014-0050-0

12. Chaudhry MA, Sachdeva H, Omaruddin RA. Radiation-induced micro-RNA modulation in glioblastoma cells differing in DNA-repair pathways. *DNA Cell Biol* 2010; **29:** 553-61. doi: 10.1089/dna.2009.0978

13. Lages E, Guttin A, El Atifi M, Ramus C, Ipas H, Dupré I, et al. MicroRNA and target protein patterns reveal physiopathological features of glioma subtypes. *PLoS One* 2011; **6:** e20600. doi: 10.1371/journal.pone.0020600

14. Gu S, Cheung HH, Lee TL, Lu G, Poon WS, Chan WY. Molecular mechanisms of regulation and action of microRNA-199a in testicular germ cell tumor and glioblastomas. *PLoS One* 2013; **8:** e83980. doi: 10.1371/journal.pone.0083980

15. Guo Y, Yan K, Fang J, Qu Q, Zhou M, Chen F. Let-7b expression determines response to chemotherapy through the regulation of cyclin D1 in glioblastoma. *J Exp Clin Cancer Res* 2013; **32:** 41. doi: 10.1186/1756-9966-32-41

16. Cankovic M, Mikkelsen T, Rosenblum ML, Zarbo RJ. A simplified laboratory validated assay for MGMT promoter hypermethylation analysis of glioma specimens from formalin-fixed paraffin-embedded tissue. *Lab Invest* 2007; **87:** 392-7. doi: 10.1038/labinvest.3700520

17. Latham GJ. Normalization of microRNA quantitative RT-PCR data in reduced scale experimental designs. *Methods Mol Biol* 2010; **667:** 19-31. doi: 10.1007/978-1-60761-811-9_2

18. Wang XR, Luo H, Li HL, Cao L, Wang XF, Yan W, et al. Overexpressed let-7a inhibits glioma cell malignancy by directly targeting K-ras, independently of PTEN. *Neuro Oncol* 2013; **15:** 1491-501. doi: 10.1093/neuonc/not107

19. Wu Z, Wang L, Li G, Liu H, Fan F, Li Z, et al. Increased expression of microRNA-9 predicts an unfavorable prognosis in human glioma. *Mol Cell Biochem* 2013; **384:** 263-8. doi: 10.1007/s11010-013-1805-5

20. Krichevsky AM, Gabriely G. miR-21: a small multi-faceted RNA. *J Cell Mol Med* 2009; **13:** 39-53. doi: 10.1111/j.1582-4934.2008.00556.x

21. Wu N, Zhao X, Liu M, Liu H, Yao W, Zhang Y, et al. Role of microRNA-26b in glioma development and its mediated regulation on EphA2. *PLoS One* 2011; **6:** e16264. doi: 10.1371/journal.pone.0016264

22. Tivnan A, Zhao J, Johns TG, Day BW, Stringer BW, Boyd AW, et al. The tumor suppressor microRNA, miR-124a, is regulated by epigenetic silencing and by the transcriptional factor, REST in glioblastoma. *Tumour Biol* 2014; **35:** 1459-65. doi: 10.1007/s13277-013-1200-6

23. Yan S, Han X, Xue H, Zhang P, Guo X, Li T, et al. Let-7f inhibits glioma cell proliferation, migration, and invasion by targeting periostin. *J Cell Biochem* 2015; **116:** 1680-92. doi: 10.1002/jcb.25128

24. Lee KM, Choi EJ, Kim IA. microRNA-7 increases radiosensitivity of human cancer cells with activated EGFR-associated signaling. *Radiother Oncol* 2011; **101:** 171-6. doi: 10.1016/j.radonc.2011.05.050

25. Wang B, Sun F, Dong N, Sun Z, Diao Y, Zheng C, et al. MicroRNA-7 directly targets insulin-like growth factor 1 receptor to inhibit cellular growth and glucose metabolism in gliomas. *Diagn Pathol* 2014; **9:** 211. doi: 10.1186/s13000-014-0211-y

26. Ben-Hamo R, Efroni S. Gene expression and network-based analysis reveals a novel role for hsa-miR-9 and drug control over the p38 network in glioblastoma multiforme progression. *Genome Med* 2011; **3:** 77. doi: 10.1186/gm293

27. Chao TF, Xiong HH, Liu W, Chen Y, Zhang JX. MiR-21 mediates the radiation resistance of glioblastoma cells by regulating PDCD4 and hMSH2. *J Huazhong Univ Sci Technolog Med Sci* 2013; **33:** 525-9. doi: 10.1007/s11596-013-1153-4

28. Deng X, Ma L, Wu M, Zhang G, Jin C, Guo Y, et al. miR-124 radiosensitizes human glioma cells by targeting CDK4. *J Neurooncol* 2013; **114:** 263-74. doi: 10.1007/s11060-013-1179-2

29. Wei J, Wang F, Kong LY, Xu S, Doucette T, Ferguson SD, et al. miR-124 inhibits STAT3 signaling to enhance T cell-mediated immune clearance of glioma. *Cancer Res* 2013; **73:** 3913-26. doi: 10.1158/0008-5472.CAN-12-4318

30. Mizoguchi M, Guan Y, Yoshimoto K, Hata N, Amano T, Nakamizo A, et al. Clinical implications of microRNAs in human glioblastoma. *Front Oncol* 2013; **3:** 19. doi: 10.3389/fonc.2013.00019

31. Kolenda T, Przybyła W, Teresiak A, Mackiewicz A, Lamperska KM. The mystery of let-7d - a small RNA with great power. *Contemp Oncol (Pozn)* 2014; **18:** 293-301. doi: 10.5114/wo.2014.44467

32. Kolenda T, Przybyła W, Teresiak A, Mackiewicz A, Lamperska KM. Overexpression of RKIP inhibits cell invasion in glioma cell lines through upregulation of miR-98. *Biomed Res Int* 2013; **2013:** 695179. doi: 10.1155/2013/695179

33. Xia H, Qi Y, Ng SS, Chen X, Chen S, Fang M, et al. MicroRNA-15b regulates cell cycle progression by targeting cyclins in glioma cells. *Biochem Biophys Res Commun* 2009; **380:** 205-10. doi: 10.1016/j.bbrc.2008.12.169

34. Sun G, Yan S, Shi L, Wan Z, Jiang N, Li M, et al. Decreased expression of miR-15b in human gliomasi is associated with poor prognosis. *Cancer Biother Radiopharm* 2015; **30:** 169-73. doi: 10.1089/cbr.2014.1757

35. Stupp R, Mason WP, van den Bent MJ, Weller M, Fisher B, Taphoorn MJ et al. Radiotherapy plus concomitant and adjuvant temozolomide for glioblastoma. *N Engl J Med* 2005; **352:** 987-96.

36. Agarwal S, Suri V, Sharma MC, Sarkar C. Therapy and progression--induced O6-methylguanine-DNA methyltransferase and mismatch repair alterations in recurrent glioblastoma multiforme. *Indian J Cancer* 2015; **52:** 568-73. doi: 10.4103/0019-509x.178403

37. Smrdel U, Popovic M, Zwitter M, Bostjancic E, Zupan A, Kovac V, et al. Long-term survival in glioblastoma: methyl guanine methyl transferase (MGMT) promoter methylation as independent favourable prognostic factor. *Radiol Oncol* 2016; **50:** 394-401. doi: 10.1515/raon-2015-0041

38. Pala A, Schmitz AL, Knoll A, Schneider M, Hlavac M, König R, et al. Is MGMT promoter methylation to be considered in the decision making for recurrent surgery in glioblastoma patients? *Clin Neurol Neurosurg* 2018; **167:** 6-10. doi: 10.1016/j.clineuro.2018.02.003

39. Wick W, Osswald M, Wick A, Winkler F. Treatment of glioblastoma in adults. *Ther Adv Neurol Disord* 2018; **11:** 1756286418790452. doi: 10.1177/1756286418790452

40. Visani M, de Biase D, Marucci G, Cerasoli S, Nigrisoli E, Bacchi Reggiani ML, et al. Expression of 19 microRNAs in glioblastoma and comparison with other brain neoplasia of grades I-III. *Mol Oncol* 2014; **8:** 417-30. doi: 10.1016/j.molonc.2013.12.010

research article

Localization patterns of cathepsins K and X and their predictive value in glioblastoma

Barbara Breznik[1,2], Clara Limback[3,4], Andrej Porcnik[5], Andrej Blejec[6], Miha Koprivnikar Krajnc[1], Roman Bosnjak[5], Janko Kos[7,8], Cornelis J.F. Van Noorden[1,9], Tamara T. Lah[1,2]

[1] Department of Genetic Toxicology and Cancer Biology, National Institute of Biology, Ljubljana, Slovenia
[2] Internationaml Postgraduate School Jozef Stefan, Ljubljana, Slovenia
[3] Department of Histopathology, Charing Cross Hospital, Fulham Palace Road, London, UK
[4] Faculty of Medicine, Imperial College London, South Kensington Campus, London, UK
[5] Department of Neurosurgery, University Clinical Centre Ljubljana, Ljubljana, Slovenia
[6] Department of Organisms and Ecosystems Research, National Institute of Biology, Ljubljana, Slovenia
[7] Department of Pharmaceutical Biology, Faculty of Pharmacy, University of Ljubljana, Ljubljana, Slovenia
[8] Department of Biotechnology, Jozef Stefan Institute, Ljubljana, Slovenia
[9] Amsterdam UMC, Cancer Center Amsterdam, Department of Medical Biology at the Academic Medical Center, Amsterdam, The Netherlands

Radiol Oncol 2018; 52(4): 433-442.

Received 23 May 2018
Accepted 11 September 2018

Correspondence to: Barbara Breznik, Ph.D., Department of Genetic Toxicology and Cancer Biology, National Institute of Biology, Večna pot 111, SI-1000 Ljubljana, Slovenia. Phone: +386 59 232 870; Fax: +386 59 232 715; E-mail: barbara.breznik@nib.si

Disclosure: No potential conflicts of interest were disclosed.

Background. Glioblastoma is a highly aggressive central nervous system neoplasm characterized by extensive infiltration of malignant cells into brain parenchyma, thus preventing complete tumor eradication. Cysteine cathepsins B, S, L and K are involved in cancer progression and are overexpressed in glioblastoma. We report here for the first time that cathepsin X mRNA and protein are also abundantly present in malignant glioma.

Materials and methods. Gene expression of cathepsins K and X was analyzed using publically-available transcriptomic datasets and correlated with glioma grade and glioblastoma subtype. Kaplan-Maier survival analysis was performed to evaluate the predictive value of cathepsin K and X mRNA expression. Cathepsin protein expression was localized and semi-quantified in tumor tissues by immunohistochemistry.

Results. Highest gene expression of cathepsins K and X was found in glioblastoma, in particular in the mesenchymal subtype. Overall, high mRNA expression of cathepsin X, but not that of cathepsin K, correlated with poor patients' survival. Cathepsin K and X proteins were abundantly and heterogeneously expressed in glioblastoma tissue. Immunolabeling of cathepsins K and X was observed in areas of CD133-positive glioblastoma stem cells, localized around arterioles in their niches that also expressed SDF-1a and CD68. mRNA levels of both cathepsins K and X correlated with mRNA levels of markers of glioblastoma stem cells and their niches.

Conclusions. The presence of both cathepsins in glioblastoma stem cell niche regions indicates their possible role in regulation of glioblastoma stem cell homing in their niches. The clinical relevance of this data needs to be elaborated in further prospective studies.

Key words: cathepsins; glioblastoma; immunohistochemistry; patient survival; cancer stem cell niches

Introduction

Glioblastoma (GBM, WHO grade IV) is the most aggressive and also most common primary brain tumor.[1] Despite present treatment strategies, such as surgical removal, radiotherapy and chemotherapy, only 5% of GBM patients survive 5 years and mean patient survival after diagnosis is approximately 1.4 years.[2] These poor survival rates are mainly due to infiltrating type of growth of GBM cells into surrounding brain parenchyma, and extensive tumor heterogeneity.[3,4]

The invasive spread of GBM cells is tightly associated with production and secretion of proteolytic enzymes[5], including lysosomal cysteine cathepsins, belonging to the C1A family of papain-like proteases.[6,7] The cysteine cathepsin family comprises of 11 proteases, sharing the same proteolytic mechanism, based on similar structural elements. However, these proteases have distinct conformations and catalytic activity (Figure S1) and are different with respect to their tissue and cellular distribution patterns and their physiological roles. Cathepsins play distinct roles in cancer progression, including invasion, the development of therapeutic resistance[8] and apoptosis.[9,10] Besides the hydrolysis of selective proteins, cysteine cathepsins participate in proteolytic cascades, where one protease activates one or several others in sequences that finally regulate hydrolysis of peptide and protein substrates, which is called protease signaling.[10] For example, secreted cathepsins can be considered as initiators of extracellular matrix (ECM)-degrading cascades during cell invasion, by cleaving and activating serine proteases, and modifying the tumor microenvironment by cleaving ECM proteins, shedding cell-cell adhesion molecules and processing relevant cytokines and growth factors to enhance tumor progression.[8,11,12] On the other hand, cathepsins may also possess tumor-suppressive roles[13], depending on the cellular context, which emphasizes the importance of *in vivo* analysis to understand functions of cathepsins in GBM pathobiology.[14] We have extensively investigated expression of cathepsins B, L an S at the mRNA and protein levels[15,16] and found considerable differences in the correlation between expression of cathepsins B, L or S in specific end-points of GBM progression. For example, cathepsin B is involved in GBM cell invasion[7], whereas the nuclear fraction of cathepsin L plays a role in apoptotic threshold regulation in GBM cells.[9,10] Cathepsin S also contributes to GBM progression *in vitro*[17], although its inhibition did not impair GBM cell invasion.[7] Very little is known about the expression and the role of two other cathepsins, *i.e.* cathepsins K and X, in GBM progression.

Cathepsin K has recently been identified as one of the most differentially-expressed proteases in GBM tissue and cell lines as compared to normal counterparts.[18] Cathepsin K belongs to the cathepsin L-like cluster of the C1A family. Highly-positive charged basic residues in its structure allow allosteric accommodation of negatively-charged resident glycosaminoglycans, enabling formation of complexes with unique collagenolytical activity, and unwinding of triple helical collagens[19], thereby participating in ECM degradation, in particular in bone metastasis.[20] Cathepsin K as a monomer also degrades growth factors and chemokines, such as stromal-derived factor 1α (SDF-1α)[21,22], thereby indirectly affecting signaling pathways and migration.

The structure and activity of cathepsin X (also called cathepsin Z) show several unique features that distinguish it from other cysteine cathepsins.[23] Cathepsin X exhibits solely carboxypeptidase activity and is activated by other lysosomal endopeptidases. Cathepsin X expression seems to be restricted to cells of the immune system and it regulates their proliferation, maturation, migration, adhesion, phagocytosis and signal transduction.[24] Various molecular targets of cathepsin X exopeptidase activity have been identified, including the β-chain of integrin receptors, y-enolase, profilin-1, chemokine SDF-1α and others.[23,24] Furthermore, cathepsin X has been detected in the brain where it is localized in neurons, glial cells and ependymal cells.[23,25] Increased cathepsin X expression has been associated with various types of cancer, such as lung, colorectal and gastric cancers.[26-28]

Cathepsins have been reported to be involved in migration and self-renewal of tumor-initiating and therapy-resistant GBM stem cells (GSCs).[29,30] GSC stemness and malignancy are maintained in specific microenvironments, so-called GSC niches, where these cells are protected from the immune system and therapy.[4,31,32] The final goal of GSC niche targeting as a new anti-GBM approach is to disintegrate GSC niches to increase GBM therapeutic sensitivity.[22] Since cathepsins are potent modifiers of the tumor microenvironment, we speculate that they may exert specific functions in GSC niches by modifying ECM and processing cytokines and growth factors.

The aim of this study was to explore expression patterns of cathepsins K and X in GBM tissue at the mRNA and protein level. At the transcriptome level, the data were obtained from publicly-available databases to determine if there is any association with survival of GBM patients. At the protein level, the immunohistochemistry was performed on serial sections of 21 human GBM samples, focusing on cathepsin localization in peri-arteriolar GSC niches. Moreover, we aimed to find correlations between gene expression of cathepsins K and X and GSC niche markers in GBM tissue samples.

Materials and methods

Expression of cathepsins K and X at the mRNA level and correlations with glioma stages and survival of glioma patients

Analysis of expression of cathepsin K and X mRNA in glioma tissue and its association with patient survival was performed using the publically-available GlioVis data portal.[36,37] Briefly, two datasets (RNA-seq) were used, TCGA_LGGGBM (RNA-seq platform) to compare expression of cathepsins in glioma grades II-IV and TCGA_GBM (RNA-seq platform) for all the other analyses. Two hundred twenty-six (226) patients with grade II, 244 patients with grade III, 156 patients with GBM (grade IV) and 4 non-tumor patients were included in the query. All statistical analyses were performed in GlioVis data portal using pairwise comparisons between group levels with corrections for multiple testing (p-values with Bonferroni correction), and the log-rank test for Kaplan-Meier survival curve analysis. Correlation analyses (Pearson correlation coefficient, r) were performed between mRNA expression of cathepsins and the mRNA expression of GSC niche markers.

Patients and brain tumor samples

Paraffin-embedded tissue sections were obtained from biopsies of GBM patients, who were operated at the Department of Neurosurgery, University Clinical Centre of Ljubljana, Slovenia in the period 2013–2016. The study was approved by the National Medical Ethics Committee of the Republic of Slovenia (Approval No. 92/06/13). All procedures followed the Helsinki Declaration. Altogether, 21 patients with newly diagnosed glioblastoma (WHO grade IV) before radio and/or chemotherapy were included in this study. All patients gave informed consent to be included in the study. The histological diagnosis was established by standard protocols at the Institute of Pathology, Medical Faculty, University of Ljubljana. Diagnoses and tumor sample data are shown in Table S1.

Immunohistochemistry

Immunohistochemistry was performed on serial GBM paraffin sections. Five μm-thick sections of GBM biopsy samples were prepared according to routine procedures of the Institute of Pathology, University of Ljubljana. Paraffin sections were dewaxed in 100% xylene (3 min) and then rehydrated in 100%, 96%, 50% and 0% ethanol (in each ethanol dilution for 3 min). Heat-mediated antigen retrieval was achieved with sodium citrate buffer (pH 6.0). Blockage of endogenous peroxidase activity in the tissue was performed by incubation with 3% H_2O_2 in 100% methanol for 30 min at room temperature. To reduce non-specific background staining, sections were incubated with 10% goat or rabbit normal serum (Sigma) in phosphate-buffered saline containing 0.1% bovine serum albumin. After tapping off the serum-containing buffer, sections were incubated overnight at 4°C with primary antibodies: rabbit anti-SMA (1:200; Abcam, ab5694), mouse anti-CD133 (1:10; Miltenyi Biotec, W6B3C1), rabbit anti-SDF-1α (1:200; Abcam, ab9797), mouse anti-CD68 (1:50; Dako, EBM 11), rabbit anti-cathepsin K (1:200; Abcam, ab19027) and goat anti-cathepsin X (1:200; R&D Systems, AF934). This step was followed by incubation with the anti-mouse, anti-rabbit or anti-goat secondary horseradish peroxidase–conjugated antibodies (1:200; Dako) for 1 h. Protein expression was detected using DAB (Abcam) or AEC (Vector Laboratories) as peroxidase substrate, and hematoxylin was used for counterstaining. The negative-control staining was performed in the absence of primary antibodies (Figure S2). All sections were analyzed by light microscopy and images were taken using a Ti Eclipse inverted microscope (Nikon) and NIS elements software (Nikon). Expression of cathepsins is presented as percentage (%) of immunostained areas of tumor sections. Twenty visual fields per tumor section (20x magnification) in non-necrotic areas were quantified using ImageJ software (https://imagej.nih.gov/ij/) and the Immunohistochemistry Image Analysis Toolbox.[6,38,39]

Statistical analyses

All statistical analyses were performed using R and GraphPad Prims 7. Overall survival of GBM patients was calculated from the date of surgery to the date of death or last follow-up. Survival analyses were estimated by Kaplan-Meier survival curves and these curves were compared with log-rank tests. A p value of < 0.05 was considered to indicate statistically significant differences.

Results

Expression of cathepsins K and X at the mRNA level is upregulated in glioblastoma as compared with low grade gliomas and normal brain tissue

Expression of cathepsins K and X in GBM was compared with expression in lower grade gliomas

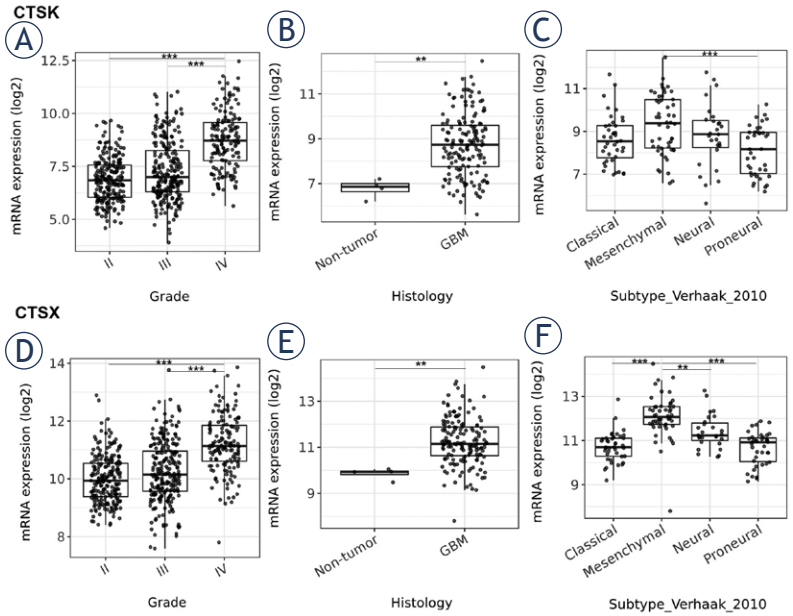

FIGURE 1. mRNA expression of cathepsins K and X in gliomas of different grades and GBM subtypes. Public transcriptomic datasets were used as described in Materials and methods. Higher cathepsin K and X mRNA expression was found in GBM (grade IV glioma) versus grade II and III glioma **(A, D)**, in GBM versus normal brain **(B, E)**, and in the mesenchymal subtype of GBM versus the classical, proneural and neural subtypes, as classified according to Verhaak et al.[39] **(C, F)**. Boxplots show the distribution of mRNA expression (log2) in glioma grade II and III and GBM. Data were retrieved from GlioVis portal.[37] The significance was set at $p < 0.01$ (**), $p < 0.001$ (***).

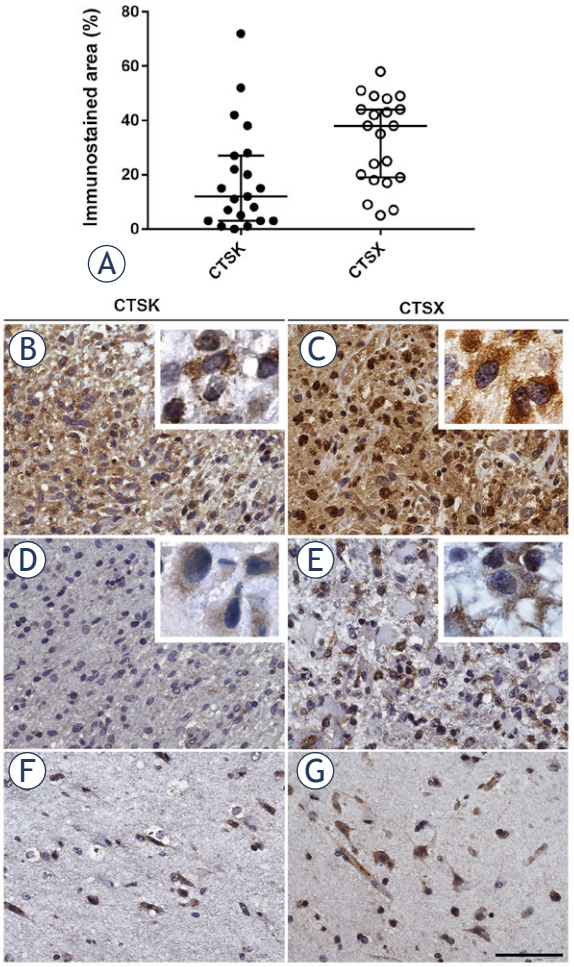

FIGURE 2. Immunohistochemical staining of cathepsins K and X in serial paraffin-embedded GBM sections. The expression of cathepsins K and X in 21 GBM samples, quantified as percentage (%) of immunostained areas and box plots show the distribution of cathepsin expression in GBMs **(A)**. Heterogeneous imunohistochemical staining was found in different parts of GBM samples for cathepsin K **(B, D)** and for cathepsin X **(C, E)**. Inserts present high magnification images of GBM cells containing cathepsin K and X protein. Cathepsin K **(F)** and cathepsin X **(G)** expression was present in specific cells in normal brain tissue of GBM patients. These cells were not further identified. Immunohistochemical labelling of cathepsins was performed with DAB as substrate (brown color). Cell nuclei were stained using hematoxylin (blue/purple). Scale bar = 50 µm.

(WHO II and III), as well as with expression in normal brain tissue in publically-available transcriptomic datasets (The Cancer Genom Atlas –TCGA) using the GlioVis data portal.[36,37] We found higher cathepsin mRNA expression in GBM (WHO grade IV) than in lower-grade gliomas (WHO grade II and III) (Figure 1A,D) and higher cathepsin K and X mRNA expression in GBM as compared to normal brain (Figure 1B,E). Furthermore, we observed overexpression of both cathepsins in the mesenchymal subtype (Figure 1C,F), which has been reported in the literature as being therapy-resistant and a more aggressive subtype of GBM.[40] Expression of cathepsin K and X mRNA was lowest in the classical and the proneural GBM subtype (Figure 1C,F).

Inter- and intratumoral heterogeneity of cathepsin K and X protein expression in GBM tissues

To determine protein expression of cathepsins K and X in GBM, we performed semi-quantitative immunohistochemistry on serial sections of 21 paraffin-embedded GBM samples. We observed that the expression of cathepsin X in GBM tissue was higher (38.0% of immunostained areas), as compared to that of cathepsin K (11.6% of immunostained areas) (Figure 2A). Protein expression of both cathepsins was heterogeneous across tumors as well as within the same tumor (Figure 2B-G). Cathepsin K and X proteins were detected in cancer cells and stromal cells of the tumor microenvironment (Figure 2B-G).

Predictive value of mRNA expression of cathepsins K and X is GBM-subtype dependent

In order to evaluate the predictive value of expression of cathepsins K and X at the mRNA level in GBM, we performed Kaplan-Maier survival analysis, using public GBM cDNA microarray datasets. Cathepsin K mRNA expression did not correlate with survival of all GBM patients (Figure 3A). When the GBMs were stratified into different GBM subtypes according to Verhaak *et al.*[41], again no correlation of cathepsin K mRNA expression and patient survival was found (data not shown). In contrast, significant differences in survival were found in GBMs with different cathepsin X mRNA levels. Kaplan-Meier estimates of median patient survival was 11.8 months for high cathepsin X tumors and 14.9 months for low cathepsin X tumors (log-rank p = 0.027) (Figure 3B). This correlation was dependent on the GBM subtype, as high mRNA levels of cathepsin X correlated only with the shorter survival of GBM patients of the classical subtype (median survival being 10.8 months for cathepsin X high-expressing tumors and 15.8 months for cathepsin X low-expressing tumors, log-rank p = 0.049). In mesenchymal and proneural GBM subtypes, the cathepsin X mRNA expression did not have predictive value for patient survival (Figure 3C).

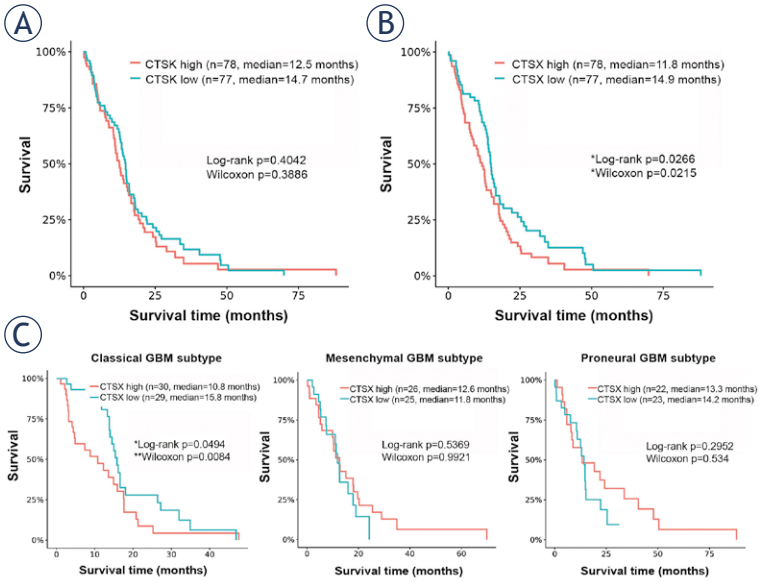

FIGURE 3. Kaplan-Meier survival curves of overall survival in relation to cathepsin K and X mRNA expression. Cathepsin K mRNA expression did not correlate with survival of all GBM patients **(A)**, whereas patients with tumors expressing high cathepsin X mRNA levels exhibited poorer survival than patients with low cathepsin X mRNA expression **(B).** When we stratified GBMs in the different subtypes, cathepsin X mRNA expression had predictive value in the classical GBM subtype only (p = 0.049 by log-rank and p = 0.0084 by Wilcoxons' test) **(C).** Data for the Kaplan-Maier survival curves were obtained from GlioVis data portal.[36,37] GBM tumors were stratified into two groups, tumors with high and with low cathepsin K or X mRNA expression, using median values as cutoff.

Cathepsins K and X in peri-arteriolar GSC niches

Cathepsins K and X were not only present in GBM cells (Figure 2), but also in stromal cells, such as endothelial cells of the tumor vasculature (Figure 4). Furthermore, the expression of both cathepsins was

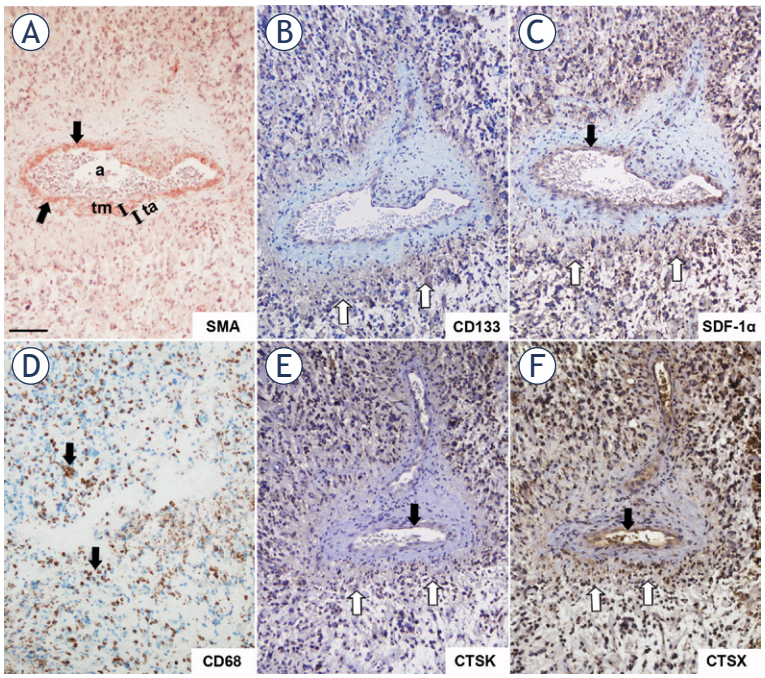

FIGURE 4. Serial GBM sections immunohistochemically stained for peri-arteriolar GSC niche markers and cathepsins K and X. SMA-positive smooth muscle cells were present in the tunica media of the arteriolar wall as indicated by black arrows **(A).** CD133- and SDF-1α-positive cells **(B, C)** were present in the cellular layers adjacent to the tunica adventitia of the arteriole. CD68-positive macrophages and microglia were found in peri-arteriolar regions as indicated by black arrows **(D).** Cathepsins K **(E)** and X **(F)** were expressed in a CD133-, SDF-1α- and CD68-positive areas around the arteriole and their expression overlapped that of CD133-positive cells as indicated by white arrows **(B, E, F).** Cathepsins and SDF-1α were present in the endothelial cells of arterioles as indicated by black arrows **(C, E, F).** Immunohistochemical labelling of SMA **(A)** was performed with AEC as substrate (red color) and of the other proteins **(B-F)** with DAB as substrate (brown color). Cell nuclei were stained using hematoxylin (blue/purple). a, lumen of arteriole; ta, tunica adventitia; tm, tunica media. Scale bar = 100 μm.

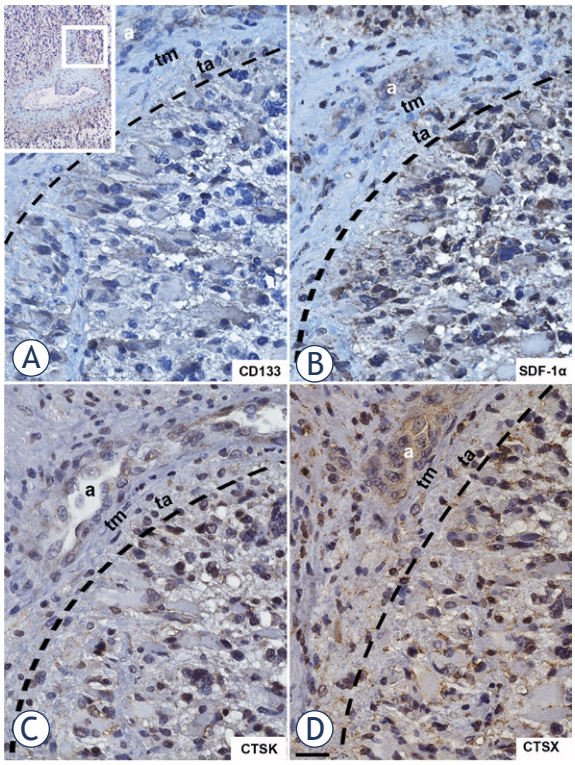

FIGURE 5. High-magnification images of serial GBM sections labelled for CD133, SDF-1a and cathepsins K and X. The region around the arteriole as shown in upper left corner of the Figure was magnified. CD133- **(A)**, SDF-1a- **(B)**, cathepsin K- **(C)** and cathepsin X- **(D)** positive cells were adjacent to the tunica adventitia of the arteriole. Immunohistochemical labelling of proteins was performed with DAB as substrate (brown color). Cell nuclei were stained using hematoxylin (blue/purple). a, lumen of arteriole; ta, tunica adventitia; tm, tunica media. The interrupted black line indicates the outer border of the tunica adventitia. Scale bar = 20 μm.

found in special regions of GBM tumors adjacent to the tunica adventitia of arterioles, in peri-arteriolar GSC niches, as identified by immunohistochemical localization of CD133/Prominin1 as the most-widely used GSC marker, α-smooth muscle actin (SMA) as smooth muscle cell marker, and SDF-1α/CXCL12, which have been shown to be present in GSC niches (Figure 4).[22,34,35] Briefly, CD133 is localized on GSC plasma membranes[42], SMA is specifically localized in smooth muscle cells in the tunica media of arteriolar and venular walls[34,35], whereas SDF-1α, a chemotactic cytokine, is produced by endothelial cells and is involved in angiogenesis[43] and in the retention of GSCs within their niches adjacent to the tunica adventitia of arterioles.[22,44] We also show here that macrophages and/or microglia cells were present in the regions of GSC niches around arterioles using the macrophage and microglia marker CD68 (Figure 4A-D).

Cathepsins K and X were localized in CD133-, SDF-1α- an CD68-positive regions around arterioles, defined by the tunica media containing SMA-positive smooth muscle cells (Figure 4). Cathepsins were present in astrocyte-like cells and endothelial cells (Figure 4) as well as extracellularly (Figure 5) in regions of GSC niches adjacent to the tunica adventitia of arterioles (Figure 5). Overlap of CD133, cathepsin K and cathepsin X immunostaining in GSC niches was observed (Figure 4B,E,F). Higher magnification images of CD133, SDF-1α, cathepsin K and X staining are shown in Figure 5. Taken together, GSC marker CD133, cytokine SDF-1α and macrophage marker CD68 are localized around arterioles where cathepsins K and X are also present.

Correlation between gene expression of cathepsin K and X, selected GSC markers and peri-arteriolar GSC niche markers

The statistical correlation between gene expression levels of cathepsins K and X and gene expression levels of GSC markers and peri-arteriolar GSC niche markers was determined using public microarray datasets as describe in Materials and methods.[36,37] We analyzed gene expression of GSC markers CD133/PROM1 and SOX2, endothelial cell marker CD31/PECAM1, α-smooth muscle actin SMA/ACTA2, chemotactic cytokine SDF-1α/CXCL12 and its receptor CXCR4 and macrophage/microglia markers CD68 and Iba1/AIF1. Cathepsin K mRNA expression correlated negatively with GSC marker SOX2 (Pearson's r = -0.38, *** $p < 0.001$) and positively with several GSC niche markers: PECAM1 (Pearson's r = 0.40, *** $p < 0.001$), ACTA2 (Pearson's r = 0.23, *** $p < 0.001$), CXCL12 (Pearson's r = 0.35, ** $p < 0.01$), CXCR4 (Pearson's r = 0.23, *** $p < 0.001$), CD68 (Pearson's r = 0.22, *** $p < 0.001$) and AIF1 (Pearson's r = 0.29, *** $p < 0.001$) (Figure 6). On the other hand, cathepsin X negatively correlated with GSC markers PROM1 (Pearson's r = -0.18, * $p < 0.05$) and SOX2 (Pearson's r = -0.23, *** $p < 0.001$). A strong positive correlation was observed between cathepsin X gene expression and the endothelial cell markers PECAM1 (Pearson's r = 0.49, *** $p < 0.001$) and ACTA2 (Pearson's r = 0.45, *** $p < 0.001$), CXCL12 (Pearson's r = 0.45, *** $p < 0.001$) and CXCR4 (Pearson's r = 0.46, *** $p < 0.001$). The strongest positive correlation was found for cathepsin X and the macrophage and microglia marker CD68 (Pearson's r = 0.80, *** $p < 0.001$) and AIF1 (Pearson's r = 0.65, *** $p < 0.001$) (Figure 7). Taken

together, gene expression of cathepsins K and X negatively correlated with gene expression of GSC markers and positively correlated with several markers of GSC niches. The positive correlation between gene expression of cathepsin X and GSC niche markers was much stronger than that of cathepsin K and GSC niche markers.

Discussion

Despite intensive research and the introduction of multimodal therapy with surgery, irradiation and chemotherapy, GBM patients survival has not significantly increased.[45] A better understanding of GBM pathobiology and the discovery of cancer biomarkers with predictive value are thus crucial for the improvement of GBM treatment. Such markers may become targets for personalized therapy. In the search for new biomarkers, "omics" analyses, followed by molecular validation is the usual approach. Immunohistochemistry is the most common type of analysis in oncology, due to its relative simplicity in the assessment of biomarkers for diagnosis, prognosis and prediction of responses to therapy. Therefore, we attempted to assess the predictive value of two potential protease biomarkers, cysteine cathepsins K and X. The selection of these cathepsins was based on the fact that a related protease cathepsin B has been consistently found to be predictive at the mRNA and protein level in various types of cancer, including gliomas and GBM.[6,46] High cathepsin B expression in the endothelial cells correlated with low survival rate of glioma patients and enables the identificaton of patients at higher risk in order to follow these patients more carefully or treat them more aggressively. Although cathepsin B is involved in cancer cell and endothelial cell migration and invasion[15], it is unlikely candidate as selective treatment target because it is widely distributed in normal cells.

The high cathepsin K expression as was found in the present study confirmed our previous findings on cathepsin K mRNA upregulation in GBM cells and tissues as compared to their normal counterparts.[18] However, we did not find any association of cathepsin K mRNA expression with survival of GBM patients, as was shown for various other types of cancers, such as lung carcinoma and squamous cell carcinoma.[19] Similar results have been reported for the cysteine cathepsin L by Strojnik and co-workers[47], showing high cathepsin L expression in astrocytomas and GBM, but these high levels were not predictive. We have also shown that cathepsin K is expressed in normal brain cells as has been reported for all brain regions of wild type mice[48] where it has been associated with neurobehavioral disorders such as schizophrenia.[49] At the protein level, cathepsin K was detected in vesicles of neuronal and non-neuronal cells throughout the mouse brain and its deficiency was associated with a marked decrease in differentiated astrocytes, indicating a possible role of cathepsin K in stem cell differentiation.

Cathepsin X has been linked to cancer progression as its upregulation has been found in several types of cancer.[23,28] Previously, high cathepsin X levels in serum and cancer tissues of patients with colorectal cancer and hepatocellular carcinoma, respectively, have been associated with shorter overall survival.[28,50] In present study, we confirmed the same trend for cathepsin X mRNA levels in 156 GBM patients. When GBM were stratified according to subtype[41], high cathepsin X expression in

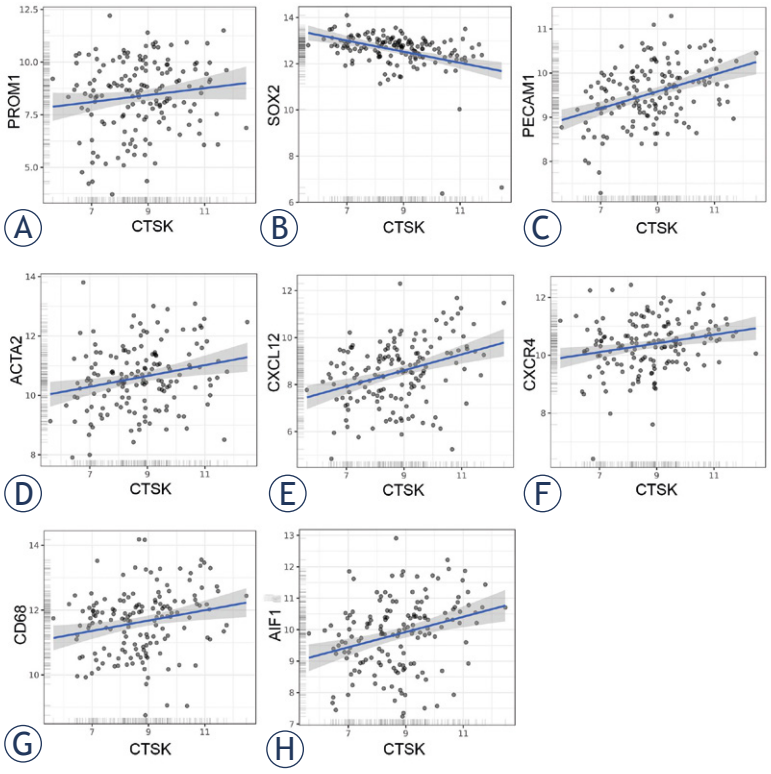

FIGURE 6. Correlation of microarray-based gene expression levels of cathepsin K and GSC niche markers. Cathepsin K did not correlate with GSC marker CD133/PROM1 **(A)**, but negatively correlated with GSC marker SOX2 **(B)** and positively correlated with GSC niche markers CD31/PECAM1 **(C)**, a-smooth muscle actin SMA/ACTA2 **(D)**, chemotactic cytokine SDF-1a/CXCL12 **(E)** and its receptor CXCR4 **(F)**, as well as with macrophage/microglia markers CD68 **(G)** and Iba1/AIF1 **(H)**. Trend lines indicate linear regression estimates. Log2-transformed mRNA expression data were obtained via GlioVis portal.

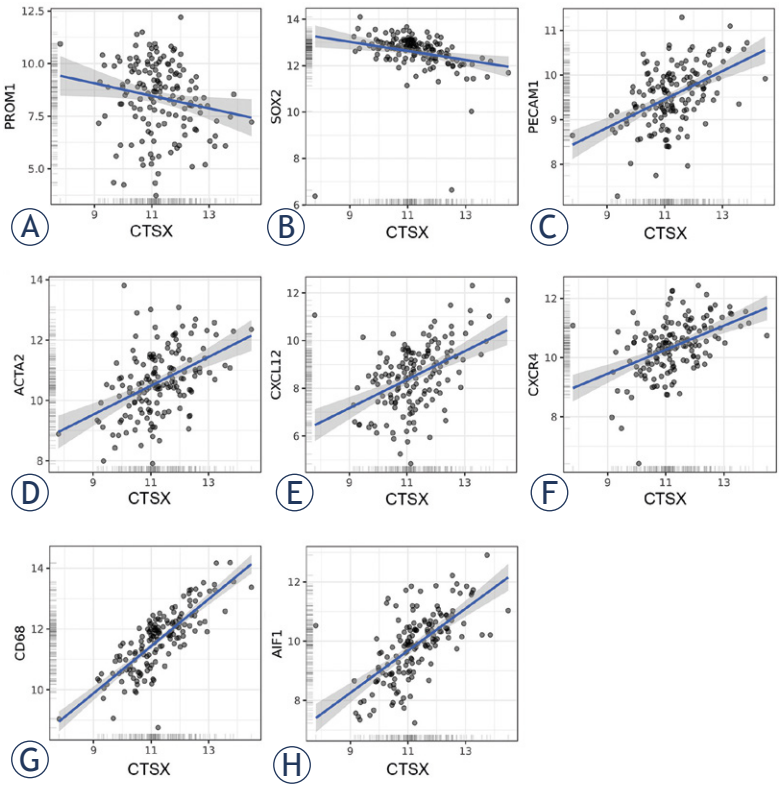

FIGURE 7. Correlation of microarray-based gene expression levels of cathepsin X and GSC niche markers. Cathepsin X negatively correlated with GSC markers CD133/PROM1 **(A)** and SOX2 **(B)** and positively correlated with GSC niche markers CD31/PECAM1 **(C)**, a-smooth muscle actin SMA/ACTA2 **(D)**, chemotactic cytokine SDF-1a/CXCL12 **(E)** and its receptor CXCR4 **(F)**, as well as with macrophage/microglia markers CD68 **(G)** and Iba1/AIF1 **(H)**. Trend lines indicate linear regression estimates. Log2-transformed mRNA expression data were obtained via GlioVis portal.

classical GBM subtype showed predictive potential for poor survival.

Cathepsin X promotes tumor processes by enhancing epithelial-to-mesenchymal transition (EMT) and by cleaving integrin receptors and profilin 1.[23,51,52] Moreover, invasion-promoting functions of cancer cell- and stromal cell-derived cathepsin X are mediated via RGD motifs in the protease prodomain, that binds to integrins and the ECM.[53] This is the first observation that cathepsin X gene expression is significantly higher in GBM than in lower-grade gliomas and in normal brain, which is in line with studies in other types of cancer, such as hepatocellular carcinoma and melanoma, revealing the correlation between cathepsin X overexpression in cancer tissue and advanced tumor stages.[50] In addition to the presence of cathepsin X in cancer cells in GBM tissues, its high levels were detected in endothelial cells of the tumor vasculature as well, which implies the involvement of cathepsin X in GBM angiogenesis, as has been found for cathepsin B.[46] Interestingly, highest cathepsin X expression was observed in the mesenchymal subtype of GBM, which represents the most aggressive and therapy-resistant GBM subtype.[40,41]

As already mentioned, GBM is heterogeneous at the molecular and cellular levels. Cathepsin K and X expression exhibited high inter- and intratumoral heterogeneity, which may be explained by differential infiltration rates of stromal cells, such as macrophages, endothelial cells, fibroblasts and lymphocytes that are also important sources of proteases.[11] In addition, GBM subtypes may significantly differ in their microenvironment, for example, the mesenchymal GBM subtype exhibits a higher immune cell infiltration than all other subtypes.[41,54] At present, the only organized multicellular structures where cathepsins K and X have been found to be clustered, are the peri-arteriolar regions that function as GSC niches.[22,33-35] In these niches, GSCs are surrounded predominantly by endothelial cells, pericytes, smooth muscle cells, fibroblasts and macrophages.[4,55] In particular, cross-talk between endothelial cells and cancer cells is crucial for GSC propagation within the niches.[55,56] Furthermore, the chemotactic cytokine SDF-1α and its receptors CXCR4 and CXCR7 are important for the retention and maintenance of GSCs in their niches as well as for their radiotherapy resistance.[44,57] We localized cathepsin K and X in peri-arteriolar regions, positive for GSC marker CD133, smooth muscle cell marker SMA, SDF-1α and macrophage marker CD68. Thus, we confirmed our previous observations that cathepsin K is present in GSC niche regions and proposed that it is involved in GSC trafficking in/out of niches by proteolytic processing and inactivation of SDF-1α.[22] Interestingly, we found an inverse correlation between cathepsin K and X mRNA expression and mRNA expression of GSC markers CD133 and SOX2 in GBM tissues. This is in line with our previous data[58], showing an inverse correlation between CD133 mRNA levels and mRNA levels and activity of cathepsins B, L and S in isolated primary CD133-positive versus CD133-negative GBM cells. On the other hand, a positive correlation was found between the expression of cathepsins K and X and that of other GSC niche markers. Based on these results and the fact that cathepsin K cleavage of SDF-1α inhibits its chemotactic activity towards CXCR4-positive GSCs, we speculate that cathepsins K and X may both enhance GSC migration out of their niches. This is a similar scenario that was reported by Kollet *et al.*[59] for the mobilization

of hematopoietic progenitor cells from bone marrow niches.

In conclusion, our data support the concept that cathepsins K and X are associated with glioma progression, as both are progressively upregulated from low grade to high grade glioma GBM, as we demonstrated by their significantly increased mRNA expression. High expression of cathepsin X on the mRNA level had predictive value for the survival of GBM patients. Furthermore, we have shown that cathepsin K and X proteins clustered in regions of peri-arteriolar GSC niches, and their mRNA expression levels correlated with expression of niche markers, implying a role of these two cathepsins in maintaining/trafficking of GSCs in or out of niches. The results of this study have to be confirmed in a further prospective study.

Acknowledgements

This work was supported by the Slovenian Research Agency (ARRS), Program P1-0245 (TTL) and ARRS young researcher grant (BB), and the European Program of Cross-Border Cooperation for Slovenia-Italy Interreg TRANS-GLIOMA.

Authors' contributions

All authors revised the manuscript and approved the final version of the manuscript. Specifically, BB designed the study, performed experiments, analyzed and interpreted the data and wrote the manuscript; CL provided GBM sections and optimized the immunohistochemical experiments; MKK performed experiments and analyzed the data; AB contributed to statistical analyses and interpretation of the data; AP, JK, RB provided GBM samples/patients data/sections/antibodies, analyzed and interpreted the data; TTL and CJFVN conceived and designed the study, analyzed and interpreted the data and wrote the final version of the manuscript.

References

1. Louis DN, Perry A, Reifenberger G, von Deimling A, Figarella-Branger D, Cavenee WK, et al. The 2016 World Health Organization classification of tumors of the central nervous system: a summary. *Acta Neuropathol* 2016; **131:** 803-20. doi: 10.1007/s00401-016-1545-1
2. Czarnek N, Clark K, Peters KB, Mazurowski MA. Algorithmic three-dimensional analysis of tumor shape in MRI improves prognosis of survival in glioblastoma: a multi-institutional study. *J Neurooncol* 2017; **132:** 55-62. doi: 10.1007/s11060-016-2359-7
3. Cuddapah VA, Robel S, Watkins S, Sontheimer H. A neurocentric perspective on glioma invasion. *Nat Rev Neurosci* 2014; **15:** 455-65. doi: 10.1038/nrn3765
4. Roos A, Ding Z, Loftus JC, Tran NL. Molecular and microenvironmental determinants of glioma stem-like cell survival and invasion. *Front Oncol* 2017; **7:** 120. doi: 10.3389/fonc.2017.00120
5. Mentlein R, Hattermann K, Held-Feindt J. Lost in disruption: role of proteases in glioma invasion and progression. *Biochim Biophys Acta* 2012; **1825:** 178-85. doi: 10.1016/j.bbcan.2011.12.001
6. Colin, C, Voutsinos-Porche B, Nanni I, Fina F, Metellus P, Intagliata D, et al. High expression of cathepsin B and plasminogen activator inhibitor type-1 are strong predictors of survival in glioblastomas. *Acta Neuropathol* 2009; **118:** 745-54. doi: 10.1007/s00401-009-0592-2
7. Gole B, Huszthy PC, Popović M, Jeruc J, Ardebili YS, Bjerkvig R, et al. The regulation of cysteine cathepsins and cystatins in human gliomas. *Int J Cancer* 2012; **131:** 1779-89. doi: 10.1002/ijc.27453
8. Olson OC, Joyce JA. Cysteine cathepsin proteases: regulators of cancer progression and therapeutic response. *Nat Rev Cancer* 2015; **15:** 712-29. doi: 10.1038/nrc4027
9. Kenig S, Frangež R, Pucer A, Lah T. Inhibition of cathepsin L lowers the apoptotic threshold of glioblastoma cells by up-regulating p53 and transcription of caspases 3 and 7. *Apoptosis* 2011; **16:** 671-82. doi: 10.1007/s10495-011-0600-6
10. Lankelma JM, Voorend DM, Barwari T, Koetsveld J, Van der Spek AH, De Porto AP, et al. Cathepsin L, target in cancer treatment? *Life Sci* 2010; **86:** 225-33. doi: 10.1016/j.lfs.2009.11.016
11. Breznik B, Motaln H, Turnšek TL. Proteases and cytokines as mediators of interactions between cancer and stromal cells in tumours. *Biol Chem* 2017; **398**: 709-19. doi: 10.1515/hsz-2016-0283
12. Kramer L, Turk D, Turk B. The future of cysteine cathepsins in disease management. *Trends Pharmacol Sci* 2017; **38:** 873-98. doi: 10.1016/j.tips.2017.06.003
13. López-Otín C, Matrisian LM. Emerging roles of proteases in tumour suppression. *Nat Rev Cancer* 2007; **7:** 800-8. doi: 10.1038/nrc2228
14. Quail DF, Joyce JA. The microenvironmental landscape of brain tumors. *Cancer Cell* 2017; **31:** 326-41. doi: 10.1016/j.ccell.2017.02.009
15. Lah TT, Duran Alonso MB, Van Noorden CF. Antiprotease therapy in cancer: hot or not? *Expert Opin Biol Ther* 2006; **6:** 257-79. doi: 10.1517/14712598.6.3.257
16. Lah TT, Obermajer N, Duran Alonso MB, Kos J. Cysteine cathepsins and cystatins as cancer biomarkers. In: Edwards D, Hoyer-Hansen G, Blasi F, Sloane BF, editors. *The cancer degradome: proteases and cancer biology.* New York: Springer; 2008. p. 575-613.
17. Flannery T, McQuaid S, McGoohan C, McConnell RS, McGregor G, Mirakhur M, et al. Cathepsin S expression: an independent prognostic factor in glioblastoma tumours - a pilot study. *Int J Cancer* 2006; **119:** 854-60. doi: 10.1002/ijc.21911
18. Verbovšek U, Motaln H, Rotter A, Atai NA, Gruden K, Van Noorden CJ, et al. Expression analysis of all protease genes reveals cathepsin K to be overexpressed in glioblastoma. *PLoS One* 2014; **9:** e111819. doi: 10.1371/journal.pone.0111819
19. Verbovšek U, Van Noorden CJ, Lah TT. Complexity of cancer protease biology: cathepsin K expression and function in cancer progression. *Semin Cancer Biol* 2015; **35:** 71-84. doi: 10.1016/j.semcancer.2015.08.010
20. Novinec M, Lenarčič B. Cathepsin K: a unique collagenolytic cysteine peptidase. *Biol Chem* 2013; **394:** 1163-79. doi: 10.1515/hsz-2013-0134
21. Staudt ND, Maurer A, Spring B, Kalbacher H, Aicher WK, Klein G. Processing of CXCL12 by different osteoblast-secreted cathepsins. *Stem Cells Dev* 2012; **21:** 1924-35. doi: 10.1089/scd.2011.0307
22. Hira VV, Verbovšek U, Breznik B, Srdič M, Novinec M, Kakar H, et al. Cathepsin K cleavage of SDF-1α inhibits its chemotactic activity towards glioblastoma stem-like cells. *Biochim Biophys Acta* 2017; **1864:** 594-603. doi: 10.1016/j.bbamcr.2016.12.021
23. Kos J, Vižin T, Fonović UP, Pišlar A. Intracellular signaling by cathepsin X: molecular mechanisms and diagnostic and therapeutic opportunities in cancer. *Semin Cancer Biol* 2015; **31:** 76-83. doi: 10.1016/j.semcancer.2014.05.001

24. Kos J, Jevnikar Z, Obermajer N. The role of cathepsin X in cell signaling. *Cell Adh Migr* 2009; **3:** 164-6.

25. Wendt W, Zhu XR, Lübbert H, Stichel CC. Differential expression of cathepsin X in aging and pathological central nervous system of mice. *Exp Neurol* 2007; **204:** 525-40. doi: 10.1016/j.expneurol.2007.01.007

26. Nägler DK, Krüger S, Kellner A, Ziomek E, Menard R, Buhtz P, et al. Up-regulation of cathepsin X in prostate cancer and prostatic intraepithelial neoplasia. *Prostate* 2004; **60:** 109-19. doi: 10.1002/pros.20046

27. Krueger S, Kalinski T, Hundertmark T, Wex T, Küster D, Peitz U, et al. Up-regulation of cathepsin X in Helicobacter pylori gastritis and gastric cancer. *J Pathol* 2005; **207:** 32-42. doi: 10.1002/path.1820

28. Vizin T, Christensen IJ, Nielsen HJ, Kos J. Cathepsin X in serum from patients with colorectal cancer: relation to prognosis. *Radiol Oncol* 2012; **46:** 207-12. doi: 10.2478/v10019-012-0040-0

29. Gopinath S, Malla R, Alapati K, Gorantla B, Gujrati M, Dinh DH, et al. Cathepsin B and uPAR regulate self-renewal of glioma-initiating cells through GLI-regulated Sox2 and Bmi1 expression. *Carcinogenesis* 2013; **34:** 550-9. doi: 10.1093/carcin/bgs375

30. Alapati K, Kesanakurti D, Rao JS, Dasari VR. uPAR and cathepsin B-mediated compartmentalization of JNK regulates the migration of glioma-initiating cells. *Stem Cell Res* 2014; **12:** 716-29. doi: 10.1016/j.scr.2014.02.008

31. Lathia JD, Mack SC, Mulkearns-Hubert EE, Valentim CL, Rich JN. Cancer stem cells in glioblastoma. *Genes Dev* 2015; **29:** 1203-17. doi: 10.1101/gad.261982.115

32. Godlewski J, Ferrer-Luna R, Rooj AK, Mineo M, Ricklefs F, Takeda YS, et al. MicroRNA Signatures and molecular subtypes of glioblastoma: the role of extracellular transfer. *Stem Cell Reports* 2017; **8:** 1497-505. doi: 10.1016/j.stemcr.2017.04.024

33. Hira VV, Ploegmakers KJ, Grevers F, Verbovšek U, Silvestre-Roig C, Aronica E, et al. CD133+ and nestin+ glioma stem-like cells reside around CD31+ arterioles in niches that express SDF-1α, CXCR4, osteopontin and cathepsin K. *J Histochem Cytochem* 2015; **63:** 481-93. doi: 10.1369/0022155415581689

34. Hira VVV, Aderetti DA, van Noorden CJF. Glioma stem cell niches in human glioblastoma are periarteriolar. *J Histochem Cytochem* 2018; **66:** 349-58. doi: 10.1369/0022155417752676

35. Hira VVV, Wormer JR, Kakar H, Breznik B, van der Swaan B, Hulsbos R, et al. Periarteriolar glioblastoma stem cell niches express bone marrow hematopoietic stem cell niche proteins. *J Histochem Cytochem* 2018; **66:** 155-73. doi: 10.1369/0022155417749174

36. GlioVis: Data visualization tools for brain tumor datasets. 2017. [cited 20 Sep 2017]. Available from: http://gliovis.bioinfo.cnio.es/.

37. Bowman RL, Wang Q, Carro A, Verhaak RG, Squatrito M. GlioVis data portal for visualization and analysis of brain tumor expression datasets. *Neuro Oncol* 2017; **19:** 139-41. doi: 10.1093/neuonc/now247

38. Završnik J, Butinar M, Trstenjak Prebanda M, Krajnc A, Vidmar R, Fonović M, et al. Cystatin C deficiency suppresses tumor growth in a breast cancer model through decreased proliferation of tumor cells. *Oncotarget* 2017; **8:** 73793-809. doi: 10.18632/oncotarget.17379

39. Chieco P, Jonker A, De Boer BA, Ruijter JM, Van Noorden CJ. Image cytometry: protocols for 2D and 3D quantification in microscopic images. *Prog Histochem Cytochem* 2013; **47:** 211-333. doi: 10.1016/j.proghi.2012.09.001

40. Segerman A, Niklasson M, Haglund C, Bergström T, Jarvius M, Xie Y, et al. Clonal variation in drug and radiation response among glioma-initiating cells is linked to proneural-mesenchymal transition. *Cell Rep* 2016; **17:** 2994-3009. doi: 10.1016/j.celrep.2016.11.056

41. Verhaak RG, Hoadley KA, Purdom E, Wang V, Qi Y, Wilkerson MD, et al; Cancer Genome Atlas Research Network. Integrated genomic analysis identifies clinically relevant subtypes of glioblastoma characterized by abnormalities in PDGFRA, IDH1, EGFR, and NF1. *Cancer Cell* 2010; **17:** 98-110. doi: 10.1016/j.ccr.2009.12.020

42. Zeppernick F, Ahmadi R, Campos B, Dictus C, Helmke BM, Becker N, et al. Stem cell marker CD133 affects clinical outcome in glioma patients. *Clin Cancer Res* 2008; **14:** 123-9. doi: 10.1158/1078-0432.CCR-07-0932

43. Kenig S, Alonso MB, Mueller MM, Lah TT. Glioblastoma and endothelial cells cross-talk, mediated by SDF-1, enhances tumour invasion and endothelial proliferation by increasing expression of cathepsins B, S, and MMP-9. *Cancer Lett* 2010; **289:** 53-61. doi: 10.1016/j.canlet.2009.07.014

44. Plaks V, Kong N, Werb Z. The cancer stem cell niche: how essential is the niche in regulating stemness of tumor cells? *Cell Stem Cell* 2015; **16:** 225-38. doi: 10.1016/j.stem.2015.02.015

45. Saito K, Hirai T, Takeshima H, Kadota Y, Yamashita S, Ivanova A, Yokogami K. Genetic factors affecting intraoperative 5-aminolevulinic acid-induced fluorescence of diffuse gliomas. *Radiol Oncol* 2017; **51**:142-50. doi: 10.1515/raon-2017-0019

46. Strojnik T, Kos J, Zidanik B, Golouh R, Lah T. Cathepsin B immunohistochemical staining in tumor and endothelial cells is a new prognostic factor for survival in patients with brain tumors. *Clin Cancer Res* 1999; **5:** 559-67.

47. Strojnik T, Kavalar R, Trinkaus M, Lah TT. Cathepsin L in glioma progression: comparison with cathepsin B. *Cancer Detect Prev* 2005; **29:** 448-55. doi: 10.1016/j.cdp.2005.07.006

48. Dauth S, Schmidt MM, Rehders M, Dietz F, Kelm S, Dringen R, et al. Characterisation and metabolism of astroglia-rich primary cultures from cathepsin K-deficient mice. *Biol Chem* 2012; **393:** 959-70. doi: 10.1515/hsz-2012-0145

49. Dauth S, Sîrbulescu RF, Jordans S, Rehders M, Avena L, Oswald J, et al. Cathepsin K deficiency in mice induces structural and metabolic changes in the central nervous system that are associated with learning and memory deficits. *BMC Neurosci* 2011; **12:** 74. doi: 10.1186/1471-2202-12-74

50. Wang J, Chen L, Li Y, Guan XY. Overexpression of cathepsin Z contributes to tumor metastasis by inducing epithelial-mesenchymal transition in hepatocellular carcinoma. *PLoS One* 2011; **6:** e24967. doi: 10.1371/journal.pone.0024967

51. Sevenich L, Schurigt U, Sachse K, Gajda M, Werner F, Müller S, et al. Synergistic antitumor effects of combined cathepsin B and cathepsin Z deficiencies on breast cancer progression and metastasis in mice. *Proc Natl Acad Sci U S A* 2010; **107:** 2497-502. doi: 10.1073/pnas.0907240107

52. Mitrović A, Pečar Fonović U, Kos J. Cysteine cathepsins B and X promote epithelial-mesenchymal transition of tumor cells. *Eur J Cell Biol* 2017; **96:** 622-31. doi: 10.1016/j.ejcb.2017.04.003

53. Akkari L, Gocheva V, Kester JC, Hunter KE, Quick ML, Sevenich L, et al. Distinct functions of macrophage-derived and cancer cell-derived cathepsin Z combine to promote tumor malignancy via interactions with the extracellular matrix. *Genes Dev* 2014; **28:** 2134-50. doi: 10.1101/gad.249599.114

54. Euskirchen P, Radke J, Schmidt MS, Schulze Heuling E, Kadikowski E, Maricos M, et al. Cellular heterogeneity contributes to subtype-specific expression of ZEB1 in human glioblastoma. *PLoS One* 2017; **12:** e0185376. doi: 10.1371/journal.pone.0185376

55. Calabrese C, Poppleton H, Kocak M, Hogg TL, Fuller C, Hamner B, et al. A perivascular niche for brain tumor stem cells. *Cancer Cell* 2007; **11:** 69-82. doi: 10.1016/j.ccr.2006.11.020

56. Zhu TS, Costello MA, Talsma CE, Flack CG, Crowley JG, Hamm LL, et al. Endothelial cells create a stem cell niche in glioblastoma by providing NOTCH ligands that nurture self-renewal of cancer stem-like cells. *Cancer Res* 2011; **71:** 6061-72. doi: 10.1158/0008-5472.CAN-10-4269

57. Goffart N, Lombard A, Lallemand F, Kroonen J, Nassen J, Di Valentin E, et al. CXCL12 mediates glioblastoma resistance to radiotherapy in the subventricular zone. *Neuro Oncol* 2017; **19:** 66-77. doi: 10.1093/neuonc/now136

58. Ardebili SY, Zajc I, Gole B, Campos B, Herold-Mende C, Drmota S, et al. CD133/prominin1 is prognostic for GBM patient's survival, but inversely correlated with cysteine cathepsins' expression in glioblastoma derived spheroids. *Radiol Oncol* 2011; **45:** 102-15. doi: 10.2478/v10019-011-0015-6

59. Kollet O, Dar A, Shivtiel S, Kalinkovich A, Lapid K, Sztainberg Y, et al. Osteoclasts degrade endosteal components and promote mobilization of hematopoietic progenitor cells. *Nat Med* 2006 ;**12:** 657–64. doi: 10.1038/nm1417

60. MEROPS database: The peptidase database. [cited 15 Dec 2017]. Available at https://www.ebi.ac.uk/merops/index.shtml.

research article

Dendritic cell profiles in the inflamed colonic mucosa predict the responses to tumor necrosis factor alpha inhibitors in inflammatory bowel disease

Natasa Smrekar[1], David Drobne[1], Lojze M. Smid[1], Ivan Ferkolj[1], Borut Stabuc[1], Alojz Ihan[2], Andreja Natasa Kopitar[2]

[1] Department of Gastroenterology and Hepatology, University Medical Centre, Ljubljana, Slovenia
[2] Institutes of Microbiology and Immunology, Faculty of Medicine, University of Ljubljana, Slovenia

Radiol Oncol 2018; 52(4): 443-452.

Received 12 September 2018
Accepted 25 October 2018

Correspondence to: Assist. Prof. Andreja Nataša Kopitar, Institute of Microbiology and Immunology, Faculty of Medicine, University of Ljubljana, Zaloška 4, SI-1000 Ljubljana, Slovenia. Phone: +386 1 543 74 84, Fax: +386 1 543 74 85; E-mail: andreja-natasa.kopitar@mf.uni-lj.si

Disclosure: No potential conflicts of interest were disclosed.

Background. Dendritic cells play crucial roles in the control of inflammation and immune tolerance in the gut. We aimed to investigate the effects of tumor necrosis factor alpha (TNFa) inhibitors on intestinal dendritic cells in patients with inflammatory bowel disease and the potential role of intestinal dendritic cells in predicting the response to treatment.

Patients and methods. Intestinal biopsies were obtained from 30 patients with inflammatory bowel disease before and after treatment with TNFa inhibitors. The proportions of *lamina propria* dendritic cell phenotypes were analysed using flow cytometry. Disease activity was endoscopically assessed at baseline and after the induction treatment.

Results. At baseline, the proportion of conventional dendritic cells was higher in the inflamed mucosa (7.8%) compared to the uninflamed mucosa (4.5%) ($p = 0.003$), and the proportion of $CD103^+$ dendritic cells was lower in the inflamed mucosa (47.1%) versus the uninflamed mucosa (57.3%) ($p = 0.03$). After 12 weeks of treatment, the proportion of conventional dendritic cells in the inflamed mucosa decreased from 7.8% to 4.5% ($p = 0.014$), whereas the proportion of $CD103^+$ dendritic cells remained unchanged. Eighteen out of 30 (60%) patients responded to their treatment by week 12. Responders had a significantly higher proportion of conventional dendritic cells (9.16% *vs* 4.4%, $p < 0.01$) with higher expression of HLA-DR (median fluorescent intensity [MFI] 12152 *vs* 8837, $p = 0.038$) in the inflamed mucosa before treatment compared to nonresponders.

Conclusions. A proportion of conventional dendritic cells above 7% in the inflamed inflammatory bowel disease mucosa before treatment predicts an endoscopic response to TNFa inhibitors.

Key words: inflammatory bowel disease; dendritic cells; tumor necrosis factor-alpha inhibitors; colon cancer

Introduction

Inflammatory bowel disease (IBD) is a chronic progressive disorder of the gastrointestinal tract with multifactorial pathogenesis. It results from a complex interplay between genetic susceptibility, environmental factors, epithelial barrier defects and altered gut microbiota, which together lead to a dysregulated immune response.[1]

Dendritic cells (DCs) play a central role in the pathogenesis of IBD by maintaining immune homeostasis by regulating the intestinal T-cell response.[2-5] DC activation and maturation occurs after exposure to microbial stimuli or proinflammatory cytokines, such as tumor necrosis factor alpha (TNFa).[6-8] Stimulation is followed by the upregulation of the expression of the costimulatory and activation molecules CD80, CD86, CD83, and HLA-DR

and the promotion of inflammation by the release of various cytokines.[6-10] DCs obtain the ability to polarize naive T-cells into type 1 T helper (Th1), type 2 T helper (Th2), type 17 T helper (Th17) or T-regulatory (Treg) cells after maturation.[11] The inflammatory microenvironment (immune cells and cytokines, such as TNFa) in IBD has many similarities to the cancer microenvironment. The interaction between cytokines and the immune response plays major roles in inflammation and colitis-associated cancer.[12]

The gastrointestinal mucosa contains an extensive network of conventional dendritic cells (cDCs) and plasmacytoid dendritic cells (pDCs) that maintain immune tolerance towards luminal antigens in the healthy mucosa.[4,13-16] It is hypothesized that disturbances in the proportions of pDCs and cDCs and changes in their phenotypes drive uncontrolled inflammation in IBD. Several studies have shown a lack of immature DCs in the peripheral blood of IBD patients and an increased number of activated DCs in the inflamed gut tissue.[17-20] A high concentration of TNFa in the inflamed mucosa drives the activation of DCs.[21-23] TNFa inhibitors, such as infliximab and adalimumab, induce mucosal healing in patients with IBD by suppressing TNFa driven DC activation.[24,25]

Current treatment goals are the induction and maintenance of remission to provide a better quality of life, to reduce the need for long-term corticosteroid use and to reduce the incidence of negative long-term outcomes such as colorectal carcinoma (CRC).[26] Over the past thirty years, the overall risk of IBD-associated CRC has declined, and one of the reasons may be effective medical therapy for IBD.[27] Therefore, it has been proposed that effective disease control and successful mucosal healing may reduce the CRC risk in individual patients with IBD.[26]

TNFa inhibitors have revolutionized the treatment of IBD. They are able to induce and maintain mucosal healing in patients with IBD and therefore may provide additional chemoprevention by reducing long-standing chronic inflammation. However, up to 40% of patients fail to respond to this therapy[28] and the mechanism of primary resistance is not known. We have therefore focused our study on the role of DCs in primary resistance to TNFa inhibitors. We also believe that understanding primary resistance to TNFa inhibitors is important for the prevention of IBD-associated CRC.

The primary aim of our study was to evaluate the impact of TNFa inhibitors on the proportions and phenotypes of DCs in the colonic mucosa in IBD. Furthermore, we also studied whether patients who respond to treatment have different proportions and phenotypes of DCs in the mucosa before or after treatment compared with those who do not respond.

Patients and methods

Patients

In this prospective study, we included 30 consecutive patients with IBD (16 Crohn's disease (CD) and 14 ulcerative colitis (UC) patients) and 10 healthy individuals (with a normal ileocolonoscopy performed for colorectal cancer screening without any clinical, biochemical or endoscopic signs of inflammation).

All included IBD patients were refractory or intolerant to conventional immunesuppressives, such as thiopurines or methotrexate and were also naïve to TNFa inhibitors at the time of inclusion (Table 1). Disease activity was assessed clinically (simple clinical colitis activity index [SCCAI] for ulcerative colitis and the Harvey Bradshaw severity index [HBSI] for Crohn's disease), biochemically and endoscopically at baseline and again after completing treatment at week 12.[29-32] Active disease was defined for ulcerative colitis as a SCCAI score ^{3} 3 and for Crohn's disease as an HBSI $\geq$ 5. Biochemical activity assessment included the measurement of C-reactive protein (CRP) (ADVIA 1800 Chemistry System, Siemens) and faecal calprotectin levels (Calprest assay with a range from 15.6 mg/kg - 500 mg/kg, Eurospital, Trieste, Italy). Endoscopic disease activity (defined as SES-CD $\geq$ 3 or Mayo endoscopic score $\geq$ 2) was confirmed in all patients with ileocolonoscopies at the time of inclusion.[33,34]

Induction treatment and the assessment of responses

All included patients received induction treatment with TNFa inhibitors (infliximab in 13 patients and adalimumab in 17 patients). Infliximab was administered intravenously at a dose of 5 mg/kg at baseline, followed by infusions at week 2 and week 6. Adalimumab was administered subcutaneously at a dose of 160 mg at baseline, followed by 80 mg at week 2 and 40 mg every other week thereafter.[35] The doses of the TNFa inhibitors were not optimized during induction. The dose of azathioprine was kept stable during induction, but corticoster-

TABLE 1. Demographic data of the patients and healthy controls enrolled in the study

	Number (n)	Mean (SD)
Number	40	
Crohn's disease	16	
Female/male	8/8	
Age (years)		38.6 (13.7)
Disease duration (years)		7.1 (6.5)
Age at diagnosis (years)		31.4 (14.5)
Smokers	5	
Ex-smokers	3	
Nonsmokers	8	
Location of Crohn's disease I. L1 (ileal) II. L2 (colonic) III. L3 (ileocolonic) IV. L4 (isolated upper disease)	16 0 7 9 0	
Concomitant medications I. Aminosalicylates II. Corticosteroid III. Azathioprine IV. Azathioprine + corticosteroids V. None	13 0 1 9 3 3	
Ulcerative colitis	14	
Female/male	8/6	
Age (years)		39.2 (12)
Disease duration (years)		5.6 (2.8)
Age at diagnosis (years)		33.5 (11.7)
Smokers	1	
Ex-smokers	3	
Nonsmokers	10	
Extent of ulcerative colitis I. E1 (proctitis) II. E2 (left sided) II. E3 (extensive)	14 1 5 8	
Concomitant medications I. Aminosalicylates II. Corticosteroid III. Azathioprine IV. Azathioprine + corticosteroids V. None	14 3 5 3 3 0	
Healthy controls	10	
Female	6	
Male	4	
Age (years)		58.3 (9.4)

oid doses were tapered after starting the TNFa inhibitors.

An endoscopic response to induction at week 12 was defined by a Mayo endoscopic sub score of 0 to 1 in ulcerative colitis or ≥ 50% decrease in the SES-CD from the baseline colonoscopy in Crohn's disease.

Mucosal biopsies and the characterization of the *lamina propria* dendritic cells

In total, 40 pinch biopsies were obtained from each IBD patient during the study. Twenty were collected during the baseline colonoscopy (10 biopsies from the inflamed colonic mucosa and 10 from the uninflamed mucosa). The remaining 20 biopsies were obtained from the same colonic segments on week 12 after the induction treatment was completed.

One colonoscopy was performed on each healthy control. We performed 10 biopsies per colonoscopy from all colonic segments.

All colonic tissue samples were obtained with biopsy forceps and placed in containers with normal saline. We started the dissociation of DCs within 3 hours of sample collection. The intestinal biopsies were dissociated into single-cell suspensions by combining mechanical dissociation with enzymatic degradation as previously described.[36] Briefly, the intraepithelial cells were isolated by incubating the biopsies for 20 min at 37°C with HBSS-EDTA two times (Gibco, Paisley, Scotland, UK) (HBSS without Ca2+ or Mg2+ and containing 5% FCS, 10 mM Hepes, 5 mM EDTA and 1 mM DTT) (Sigma-Aldrich, St. Louis, USA). The *lamina propria* (LP) mononuclear cells (LPMCs) were isolated by digesting the biopsies in HBSS containing 5% FCS, 1.25 mg/ml collagenase D (Roche, Basel, Switzerland), 1 mg/ml collagenase VIII (Sigma-Aldrich, St. Louis, USA), 1 mg/ml DNase I (Roche, Basel, Switzerland), and 1 mg/ml Dispase (Invitrogen, Oslo, Norway) for 30 min at 37°C with agitation. Following the digestion, the biopsies were further disrupted using a GentleMACS® dissociator (Miltenyi Biotec, Bergisch Gladbach, Germany). The supernatants were collected by filtering the cell suspensions through nylon mesh, and single-cell suspensions of *lamina propria* MNCs were enriched for CD45+ cells by magnetic-activated cell sorting (MACS) (Miltenyi Biotec, Bergisch Gladbach, Germany). The cells were washed twice in staining buffer (BD Pharmingen, San Diego, USA) and stained with fluorochrome-conjugated antibodies for 30 min at 4°C in the dark.

We used the following antibodies: anti-HLA-DR APC-Cy7/FITC, anti-CD3 PerCP Cy5.5, anti-CD19 PerCP Cy5.5, anti-CD16 PerCP Cy5.5, anti-CD14 PerCP Cy5.5, anti-CD11c PE/APC, anti-CD11b PE, anti-CD123 PE/PE Cy7, anti-CD303 FITC, anti-CD103 FITC, anti-CD80 FITC/APC, anti-CD83 PE, and anti-CD86 BD Horizon V450/PE-Cy7. All antibodies were obtained from BD Biosciences

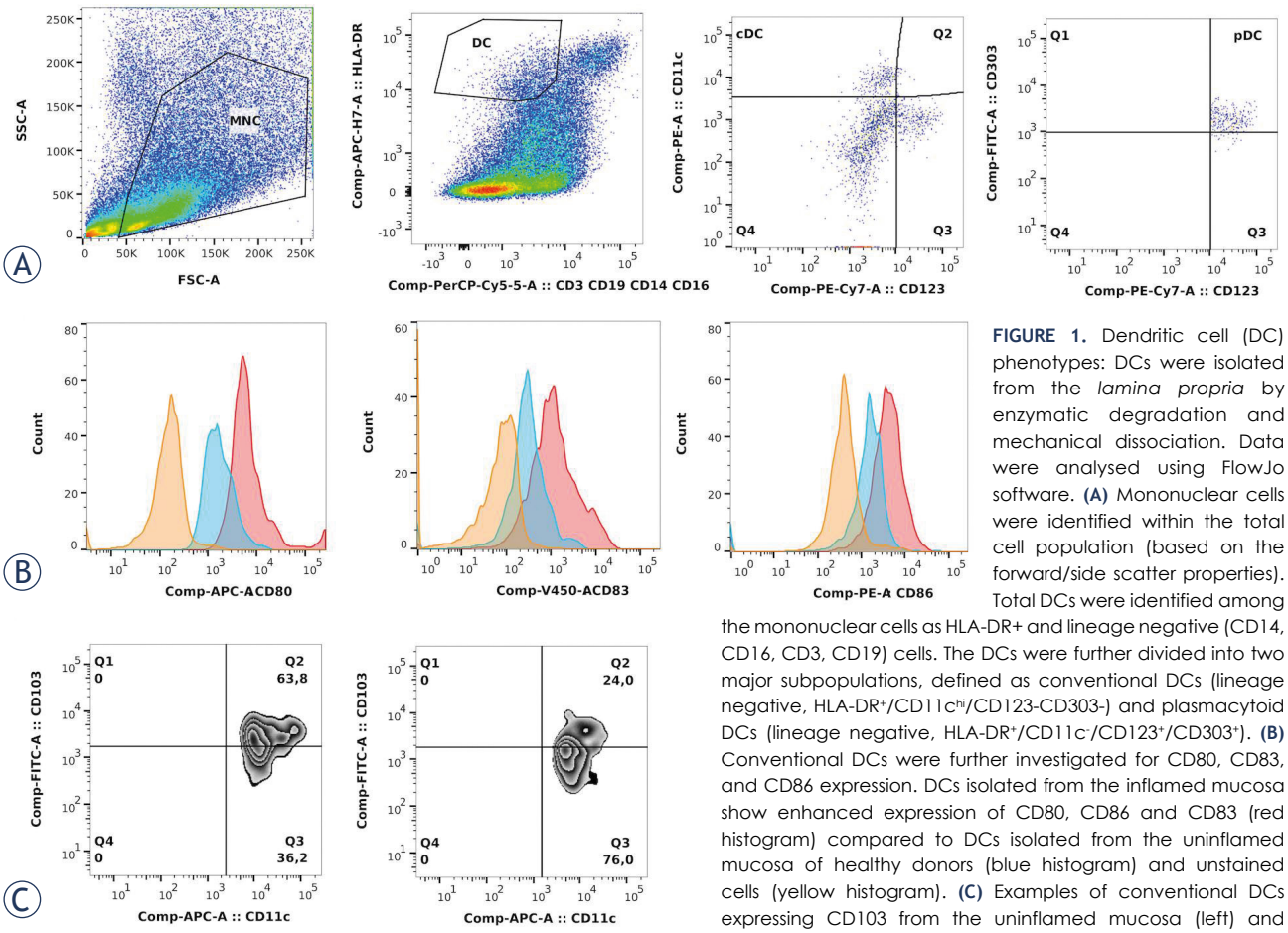

FIGURE 1. Dendritic cell (DC) phenotypes: DCs were isolated from the *lamina propria* by enzymatic degradation and mechanical dissociation. Data were analysed using FlowJo software. **(A)** Mononuclear cells were identified within the total cell population (based on the forward/side scatter properties). Total DCs were identified among the mononuclear cells as HLA-DR+ and lineage negative (CD14, CD16, CD3, CD19) cells. The DCs were further divided into two major subpopulations, defined as conventional DCs (lineage negative, HLA-DR$^+$/CD11c^{hi}/CD123-CD303-) and plasmacytoid DCs (lineage negative, HLA-DR$^+$/CD11c$^-$/CD123$^+$/CD303$^+$). **(B)** Conventional DCs were further investigated for CD80, CD83, and CD86 expression. DCs isolated from the inflamed mucosa show enhanced expression of CD80, CD86 and CD83 (red histogram) compared to DCs isolated from the uninflamed mucosa of healthy donors (blue histogram) and unstained cells (yellow histogram). **(C)** Examples of conventional DCs expressing CD103 from the uninflamed mucosa (left) and inflamed mucosa (right).

(San Diego, USA) except the anti-CD103 (Dako, Glostrup, Denmark), anti-CD80, anti-CD83, and anti-CD303 (Miltenyi Biotec, Bergisch Gladbach, Germany) antibodies.

Lamina propria DCs were analysed on a BD Canto II flow cytometer (BD Biosciences, San Diego, USA) using DIVA software (BD Biosciences, San Diego, USA). The proportion of cells positive for a given marker was determined by referencing unstained cells. FMO (fluorescence minus one) controls were used to identify and gate cells. A total of 50000 cells were acquired. The data analysis was performed using FlowJo version 10.1 software (TreeStar, Ashland, USA) as previously described.[37] *Lamina propria* DCs were identified as HLA-DR-positive and lineage cocktail (CD3/CD14/CD16/CD19)-negative cells. The data for pDCs and cDCs are presented as the frequency within the *lamina propria* mononuclear cells. CD103$^+$/CD103$^-$ DC data is presented as the frequency among the cDCs. The expression of HLA-DR, CD86, CD80 and CD83 on cDCs is given as the median fluorescent intensity (MFI) (Figure 1). Table 2 describes the surface markers of the measured DC populations.

Statistical analysis

SPSS 17.0 software (IBM) and GraphPad Prism 6.0 software (GraphPad Software) were used to perform all appropriate statistical analyses. The data are presented as the mean and standard error of the mean. Differences between independent groups were analysed with an unpaired Student's t-test. Predictive cut-off values were identified using receiver operating characteristics (ROC) curve analysis. A p value < 0.05 was considered statistically significant.

Ethical considerations

All patients and volunteers gave informed consent for the study. The National Ethics Committee approved the study protocol with the registration number 129/06/13.

TABLE 2. Phenotypes of the measured dendritic cells (DC)

	Abbreviation	Phenotype
Plasmacytoid DC	pDC	HLA-DR$^+$, CD123$^+$, CD303$^+$, CD11c$^-$, CD3$^-$, CD14$^-$, CD16$^-$, CD19$^-$
Conventional DC	cDC	HLA-DR$^+$, CD11c$^+$, CD123$^-$, CD303$^-$, CD3$^-$, CD14$^-$, CD16$^-$, CD19$^-$
Mature conventional DC	CD86$^+$ DC	CD80$^+$, CD86$^+$, CD83$^+$, HLA-DR$^+$, CD11c$^+$, CD123$^-$, CD303$^-$, CD3$^-$, CD14$^-$, CD16$^-$, CD19$^-$
Activated mature conventional DC	HLA-DR DC	HLA-DR^{hi}, CD83$^+$, CD80$^+$, CD86$^+$, CD11c$^+$, CD123$^-$, CD303$^-$, CD3$^-$, CD14$^-$, CD16$^-$, CD19$^-$
Intestinal CD103$^+$ DCs important in maintaining intestinal immune homeostasis	CD103$^+$ DC	CD103$^+$, HLA-DR$^+$, CD11c$^+$, CD123$^-$, CD303$^-$, CD3$^-$, CD14$^-$, CD16$^-$, CD19$^-$

Results

Clinical outcomes

An endoscopic response to treatment was observed in 7/14 (50%) patients with UC and 11/16 (69%) CD patients at week 12 (Table 3). CRP and faecal calprotectin concentrations decreased following the induction treatment. However, neither the baseline CRP nor the baseline faecal calprotectin concentration was predictive of the response to treatment, data not shown.

TABLE 3. Clinical, biochemical and endoscopic data of the patients before and after treatment with TNFa inhibitors

	Before treatment (week 0)	After treatment (week 12)
ULCERATIVE COLITIS (n = 14)		
SCCAI	8.4 (0.9)	3.1 (0.5)
CRP (mg/l)	8.8 (2.9)	7.8 (2.4)
Fecal calprotectin (mg/kg)	351 (41.7)	254 (58.2)
Endoscopic Mayo Score	2.4 (0.1)	1.5 (0.3)
CROHN'S DISEASE (n = 16)		
HBSI	9.5 (1.3)	3.3 (0.8)
CRP (mg/l)	17.5 (3.1)	10.5 (3.6)
Fecal calprotectin (mg/kg)	341 (40)	209 (48)
SES-CD	12.9 (1.1)	5.5 (1.8)

The data are presented as the mean and standard error of the mean.
CRP = C-reactive protein; HBSI = Harvey Bradshaw severity index; SCCAI = simple clinical colitis activity index; SES-CD = simple endoscopic score for Crohn disease

Proportions of dendritic cells in the colonic mucosa

We analysed biopsies from 59 colonoscopies from 30 patients (29 patients had colonoscopies performed before and after treatment, while one patient only had a baseline endoscopy performed). The proportions of the pDC, cDC and CD103$^-$ DC subsets were higher in the inflamed mucosa of IBD patients compared to the mucosa of healthy controls. However, the proportion of the CD103$^+$ subset was lower in the inflamed mucosa than in the mucosa of healthy controls (Table 4).

At baseline, the proportion of cDCs was higher in the inflamed mucosa compared to the uninflamed mucosa of IBD patients, but the proportion of the CD103$^+$ DCs subset was lower in the inflamed mucosa (Table 5).

When comparing the pretreatment inflamed mucosa of UC and CD patients, we found no differences in the proportions of the pDC, cDC, CD103$^+$ and CD103$^-$ DCs subsets, and we did not observe any differences in the expression of the costimulatory molecule CD86.

TABLE 4. Subpopulations of dendritic cells (DC) in the inflamed inflammatory bowel disease (IBD) mucosa and the mucosa of healthy controls (HC) before the treatment with TNFa inhibitors

	IBD-inflamed	HC	p value
pDC (%)	1.7 (0.3)	0.3 (0.1)	**0.005**
cDC (%)	7.8 (0.9)	0.5 (0.1)	**< 0.001**
CD86 (MFI)	1248 (231)	430 (43)	**0.04**
HLA-DR (MFI)	10918 (767)	11808 (711)	0.52
CD103$^+$ (%)	47.1 (3.1)	66.3 (3.3)	**0.002**
CD103$^-$ (%)	52.8 (3.2)	32.1 (4.1)	**0.001**

Proportion and median fluorescence intensity (MFI) of plasmacytoid DCs (pDCs) and conventional DCs (cDCs) in the inflamed IBD mucosa (n = 30) and the mucosa of healthy controls (HC) (n = 10) before the treatment with TNFa inhibitors. The results are presented as the mean with the standard error of the mean (SEM). To compare means, we used an unpaired Student's t-test.

Effect of the treatment with TNFa antagonists on DC expression patterns

The proportion of cDCs decreased after the treatment with TNFa inhibitors in the inflamed mucosa, while the proportions of the pDC and CD103$^+$ DC subsets remained unchanged (Table 6).

Responders to the treatment had a significantly higher proportion of cDCs in the inflamed mucosa

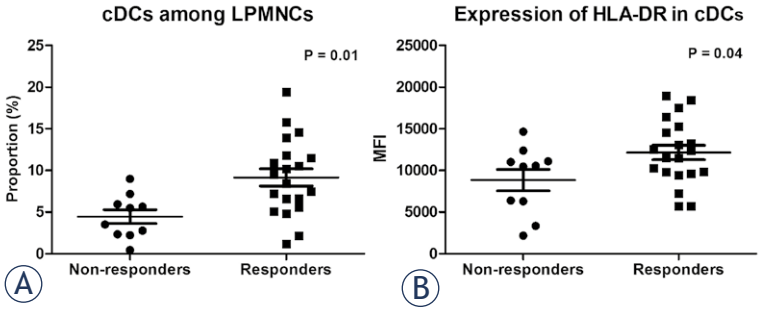

FIGURE 2. Predictors of the response to treatment. Inflammatory bowel disease patients who responded to TNFa inhibitors had a significantly higher proportion of **(A)** conventional dendritic cells (cDCs) with **(B)** higher expression of HLA-DR in the inflamed mucosa before treatment compared to nonresponders. cDC values are given as the percentage of cDCs among the *lamina propria* mononuclear cells and the expression of HLA-DR is shown as the mean fluorescence intensity (MFI) among cDCs. Horizontal lines indicate mean levels.

TABLE 5. Subpopulations of dendritic cells (DCs) in the uninflamed and inflamed inflammatory bowel disease (IBD) mucosa before the treatment with TNFa inhibitors

	IBD-uninflamed	IBD-inflamed	p value
pDC (%)	1.7 (0.2)	1.7 (0.3)	0.9
cDC (%)	4.5 (0.6)	7.8 (0.9)	**0.003**
CD86 (MFI)	1483 (212)	1248 (231)	0.53
HLA-DR (MFI)	11965 (767)	10918 (767)	0.33
CD103⁺ (%)	57.3 (3.5)	47.1 (3.1)	**0.03**
CD103⁻ (%)	42.3 (3.4)	52.8 (3.2)	**0.02**

Proportion and median fluorescence intensity (MFI) of plasmacytoid DCs (pDCs) and conventional DCs (cDCs) in the inflamed and uninflamed IBD mucosa (n = 30) before the treatment with TNFa inhibitors. The results are presented as the mean with the standard error of the mean (SEM).

TABLE 6. Subpopulations of dendritic cells (DCs) in inflamed inflammatory bowel disease (IBD) mucosa before and after the treatment with TNFa inhibitors

	IBD-before	IBD-after	p value
pDC (%)	1.7 (0.3)	1.3 (0.2)	0.32
cDC (%)	7.8 (0.9)	4.5 (0.9)	**0.01**
CD86 (MFI)	1248 (231)	826 (219)	0.29
HLA-DR (MFI)	10918 (767)	12141 (616)	0.09
CD103⁺ (%)	47.1 (3.1)	48.1 (4.5)	0.86
CD103⁻ (%)	52.8 (3.2)	50.7 (4.8)	0.75

Proportion and median fluorescence intensity (MFI) of plasmacytoid DCs (pDCs) and conventional DCs (cDCs) in the inflamed IBD mucosa (n = 29) before and after the treatment with TNFa inhibitors. The results are presented as the mean with the standard error of the mean (SEM). To compare means, we used a paired Student's t-test.

before treatment compared to nonresponders. The expression of HLA-DR was also higher in the responders (Figure 2, Table 7).

There were no differences in these parameters between the two IBD types; however, only UC responders had a higher proportion of the CD103⁺ DCs subset in the inflamed mucosa before the treatment compared to nonresponders (Table 8).

Patients with a higher proportion of cDCs in the inflamed mucosa before treatment were more likely to respond to the TNFa inhibitors. A total of 93% of patients with a proportion of cDCs above 7% responded to the therapy. The cut-off value of 6% was still 100% specific and 88% sensitive for the response to TNF-α inhibitors (Figure 3). Similarly, an HLA-DR MFI > 12450 had 90% specificity and 45% sensitivity for the response (Figure 4).

Discussion

We prospectively investigated the in vivo effects of TNFa inhibitors on mucosal DCs in 30 IBD patients. This study confirmed previous observations on cDC changes after treatment with TNFa inhibitors.[38] Our most important finding was that a proportion of cDCs above 7% in the inflamed IBD mucosa before treatment reliably predicted an endoscopic response to TNFa inhibitors, as 93% of the patients with a proportion of cDC above this threshold responded to treatment.

To the best of our knowledge, this is the first study that investigates primary resistance to treatment with TNFα inhibitors from the perspective of DCs. Primary resistance to TNFa inhibitors is observed in up to 40% of patients with IBD and is associated with poor outcomes.[28] Ineffective induction treatment can lead to serious adverse effects and high costs.[28,39] Therefore, the identification of predictors of patient responsiveness to TNFa inhibitors, which would guide the selection of patients most likely to benefit from this therapy, is eagerly awaited.

The results of our study add important knowledge to this field as we identified significant differences in DC profiles in the pretreatment colonic mucosa of patients with primary resistance compared to that of patients who responded to the induction treatment with TNF-α inhibitors. The proportion of cDCs in the pretreatment colonic mucosa was higher in responders to TNFa inhibitors compared to nonresponders. Furthermore, in patients with primary resistance, there was a lack of activated cDCs, as evidenced by the lower expression of the activation marker HLA-DR. We also observed that responding patients had a higher proportion of the CD103+ DC subset. This was particularly pronounced in patients with UC. We predicted the response to TNFa inhibitors with 93% specificity

based on the DC profile of the pretreatment mucosa. Our results, if confirmed in a larger cohort, are likely to guide treatment decisions. Patients with an unfavourable DC profile could expect a greater benefit from other non-TNFa-based treatments for IBD, such as ustekinumab or vedolizumab.[40,41]

The strengths of our study are the prospective inclusion of patients with endoscopically confirmed inflammation in the colonic mucosa at baseline and the use of the robust endpoint of mucosal healing after induction treatment, which has been shown to be associated with long-term remission in patients with IBD.[42,43] These conclusions are further strengthened by our finding that objective markers of inflammation (CRP and faecal calprotectin concentrations) before treatment had no predictive value for the response to TNFα inhibitors. Therefore, we believe that changes in the DC profile after the successful induction of mucosal healing with TNFa inhibitors predict long-term control of disease.

Our data also showed that CD and UC patients display the same DC imbalance in the inflamed intestinal mucosa compared to mucosa of healthy controls, which is consistent with previously published data.[44]

The inclusion of healthy controls enabled us to study differences in healthy and diseased colonic mucosa. We observed a higher frequency of the $CD103^-$ DC subset and an inverse ratio of the $CD103^+/CD103^-$ DC subsets in the inflamed mucosa compared to the mucosa of the healthy controls. The reduced proportion of the $CD103^+$ DC subset reflects the disturbance in gut tolerance and explains the high levels of proinflammatory cytokines, such as IL-12 and IL-23, in the inflamed mucosa of patients with IBD.[45-50] In line with this, we observed a shift towards a more favorable $CD103^+/CD103^-$ ratio in UC responders compared to UC nonresponders. The successful induction of mucosal healing in patients with CD was not associated with changes in the $CD103^+/CD103^-$ DC ratio. This underlines the different pathological mechanisms of the two diseases.[5,14,51]

In our study, patients with more activated cDCs in the pretreatment colonic mucosa responded better to TNFa inhibitors than patients with a lower proportion of cDCs in the colonic mucosa. The increased amount of activated cDCs in responders could be a reflection of a higher local amount of mucosal TNFa in responders compared to nonresponders. A possible explanation for the favourable response to TNFa inhibitors in patients with a high local concentration of TNFa was provided by Yarur *et al.*[52], who observed increased local accumulation of TNFa inhibitors in patients with more TNFa expression in inflamed colonic tissue. In our patients who did not respond, inflammation could be driven by non-TNFa mediators, such as IL-23. In such cases, IL-23, which maintains chronic inflammation through the Th17 cell pathway, could be a better treatment target.[40,53] Interestingly, many genetic polymorphisms linked to primary resistance to TNFa inhibitors have been identified in the Th17 pathway.[54]

The CD86 costimulatory molecule primes T cells during antigen presentation and represents a marker of DC maturation.[55] It is therefore not surprising that we confirmed higher expression of this molecule in IBD patients compared to healthy controls.[56] This is also in agreement with our observation that CD86 expression decreased more

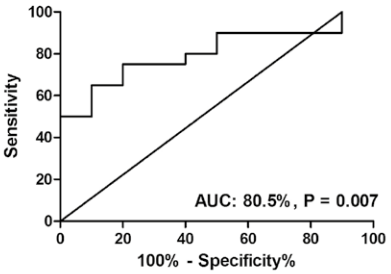

FIGURE 3. ROC curve analysis identified the proportion of conventional dendritic cells as a predictor of the response to TNFa inhibitors. Patients with a proportion of conventional dendritic cells above 7% responded to treatment.

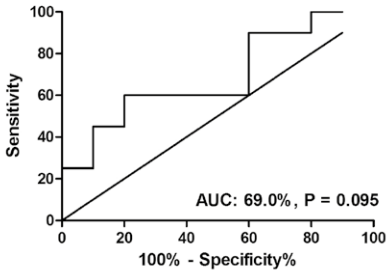

FIGURE 4. ROC curve analysis of conventional dendritic cell HLA-DR expression in the colonic mucosa before treatment for the prediction of the response to the induction treatment with TNF-a inhibitors. All patients with an HLA-DR MFI above 12450 responded to the treatment.

TABLE 7. Subpopulations of dendritic cells (DCs) in the inflamed inflammatory bowel disease (IBD) mucosa in responders and nonresponders before the treatment with TNFa inhibitors

	Responders	Nonresponders	p value
IBD			
pDC (%)	1.9 (0.4)	1.3 (0.4)	0.3
cDC (%)	9.2 (1.0)	4.4 (0.8)	**0.01**
CD86 (MFI)	1436 (332)	785 (177)	0.2
HLA-DR (MFI)	12152 (868)	8838 (1286)	**0.04**
$CD103^+$ (%)	51.0 (3.7)	42.5 (5.5)	0.2
$CD103^-$ (%)	48.8 (3.8)	57.5 (5.5)	0.2

Proportion and median fluorescence intensity (MFI) of plasmacytoid DCs (pDCs) and conventional DCs (cDCs) in the inflamed IBD mucosa of responders and nonresponders (n = 29) before the treatment with TNFa inhibitors. The results are presented as the mean with the standard error of the mean (SEM). To compare means, we used an unpaired Student's t-test.

TABLE 8. Subpopulations of dendritic cells (DCs) in the inflamed ulcerative colitis and Crohn's disease mucosa in responders and nonresponders before the treatment with TNFa inhibitors

	Responders	Nonresponders	p value
Ulcerative colitis			
pDC (%)	2.5 (0.6)	1.7 (0.6)	0.9
cDC (%)	10.1 (1.5)	4.7 (1.2)	**0.04**
CD86 (MFI)	1595 (523)	552 (40)	0.2
HLA-DR (MFI)	12182 (3613)	6693 (3614)	**0.01**
CD103$^+$ (%)	61.4 (7.0)	34.8 (6.5)	**0.02**
CD103$^-$ (%)	38.4 (7.1)	65.2 (2.7)	**0.02**
Crohn's disease			
pDC (%)	1.6 (0.4)	0.9 (0.3)	0.2
cDC (%)	9.7 (1.6)	4.2 (1.0)	**0.04**
CD86 (MFI)	1452 (434)	1019 (335)	0.5
HLA-DR (MFI)	13152 (1319)	10983 (1368)	0.3
CD103$^+$ (%)	50.8 (4.9)	50.2 (9.9)	0.9
CD103$^-$ (%)	49.2 (4.5)	49.8 (9.9)	0.9

Proportion and median fluorescence intensity (MFI) of plasmacytoid DCs (pDCs) and conventional DCs (cDCs) in the inflamed inflammatory bowel disease (IBD) mucosa of responders and nonresponders with ulcerative colitis and Crohn's disease (n = 29) before the treatment with TNFa inhibitors. The results are presented as the mean with the standard error of the mean (SEM). To compare means, we used an unpaired Student's t-test.

in responders to TNFa inhibitors compared to nonresponders (although our finding needs further conformation due to the limited sample size, which possibly prevented us from reaching statistical significance).[57] Interestingly, we also found increased expression of CD86 in macroscopically uninflamed segments of colon from patients with IBD compared to those from healthy controls – a finding that underlines that chronic inflammation is also present in colonic segments that appear endoscopically normal (Table 4).

In our study, we confirmed more pDCs in patients with CD and UC compared to healthy controls.[20,58-60] However, we did not observe any differences in the amount of pDCs in the inflamed mucosa compared to the uninflamed mucosa in patients with IBD. Additionally, TNFa inhibitors did not affect the proportion of pDCs in the colonic mucosa.

The small number of patients included in this study represents a limitation, which we tried to mitigate by assessing the treatment with the robust and objective criteria of mucosal healing instead of clinical parameters. This eliminated the placebo effect, which has been observed in many IBD studies in up to 30% of patients. Fifty-seven percent of our patients were being treated with concomitant immunosuppressants at the time of study inclusion. This could have influenced our results; however, the dose of the immunosuppressants was stable during the induction treatment up to the time point of the evaluation endoscopy. Additionally, a recent meta-analysis did not show any impact of immunosuppressants on DC maturation.[61]

The second limitation of our study is that the IBD group (on average 39 yrs old) and healthy controls (on average 58 yrs old) were not completely age-matched. There are very few reports evaluating age-related DC numbers in intestinal tissue. In children, Teig *et al*.[62] reported a change in the numbers of different DC subpopulations according to age. However, Bella *et al*.[63] did not find any significant age-related changes in the numbers of DC subpopulations, but DCs from elderly individuals (older than 60 yrs) were more mature and impaired in the production of IL-12 compared to those from younger individuals. In our study, DCs from the healthy control group expressed fewer markers of maturation (CD86). We believe that age differences between our groups did not influence the proportions and phenotypes of the DCs.

Our findings are limited to colonic DCs since we did not include small bowel biopsies in the analysis. This is important to note, as it has been shown that ileal involvement represents a distinct IBD phenotype.[64,65]

In conclusion, we prospectively investigated the effect of TNFa inhibitors on colonic DC profiles in 30 IBD patients. Our findings of differential pretreatment DC profiles and differential expression of HLA-DR in responders compared to nonresponders to TNFa inhibitors add important additional insight into the mechanism of primary resistance to TNFa inhibitors.

We identified a pretreatment mucosal DC profile that was linked to successful mucosal healing after induction therapy with TNFa inhibitors. According to this profile, we were able to predict the response to TNFa inhibitors with 93% specificity and 88% sensitivity.

The pretreatment mucosal DC profile may be a powerful tool to predict the response to TNFa inhibitors and thus assist clinicians in choosing the most effective treatment for individual patients.

Acknowledgement

The study was supported by the Slovene Ministry of Education and Science grant P3-0083.

References

1. Geremia A, Biancheri P, Allan P, Corazza GR, Di Sabatino A. Innate and adaptive immunity in inflammatory bowel disease. *Autoimmun Rev* 2014; **13:** 3-10. doi: 10.1016/j.autrev.2013.06.004
2. Kmiec Z, Cyman M, Slebioda TJ. Cells of the innate and adaptive immunity and their interactions in inflammatory bowel disease. *Adv Med Sci* 2017; **62:** 1-16. doi: 10.1016/j.advms.2016.09.001
3. Niess JH. Role of mucosal dendritic cells in inflammatory bowel disease. *World J Gastroenterol* 2008; **14:** 5138-48. doi: 10.3748/wjg.14.5138
4. Rutella S, Locatelli F. Intestinal dendritic cells in the pathogenesis of inflammatory bowel disease. *World J Gastroenterol* 2011; **17:** 3761-75. doi: 10.3748/wjg.v17.i33.3761
5. Cader MZ, Kaser A. Recent advances in inflammatory bowel disease: mucosal immune cells in intestinal inflammation. *Gut* 2013; **62:** 1653-64. doi: 10.1136/gutjnl-2012-303955
6. Kushwah R, Hu J. Complexity of dendritic cell subsets and their function in the host immune system. *Immunology* 2011; **133:** 409-19. doi: 10.1111/j.1365-2567.2011.03457.x
7. Alloatti A, Kotsias F, Magalhaes JG, Amigorena S. Dendritic cell maturation and cross-presentation: timing matters! *Immunol Rev* 2016; **272:** 97-108. doi: 10.1111/imr.12432
8. Stockwin LH, McGonagle D, Martin IG, Blair GE. Dendritic cells: immunological sentinels with a central role in health and disease. *Immunol Cell Biol* 2000; **78:** 91-102. doi: 10.1046/j.1440-1711.2000.00888.x
9. Abbas A, Lichtman A, Pillai S. *Basic immunology: functions and disorders of the immune system.* 5th Edition. St. Louis, Missouri: Elsevier; 2015.
10. Sallusto F, Lanzavecchia A. The instructive role of dendritic cells on T-cell responses. *Arthritis Res* 2002; **4:** S127-32. doi: 10.1186/ar567
11. Blanco P, Palucka AK, Pascual V, Banchereau J. Dendritic cells and cytokines in human inflammatory and autoimmune diseases. *Cytokine Growth Factor Rev* 2008; **19:** 41-52. doi: 10.1016/j.cytogfr.2007.10.004
12. Axelrad JE, Lichtiger S, Yajnik V. Inflammatory bowel disease and cancer: the role of inflammation, immunosuppression, and cancer treatment. *World J Gastroenterol* 2016; **22:** 4794-801. doi: 10.3748/wjg.v22.i20.4794
13. Coombes JL, Powrie F. Dendritic cells in intestinal immune regulation. *Nat Rev Immunol* 2008; **8:** 435-46. doi: 10.1038/nri2335
14. Choy MC, Visvanathan K, De Cruz P. An overview of the innate and adaptive immune system in inflammatory bowel disease. *Inflamm Bowel Dis* 2017; **23:** 2-13. doi: 10.1097/mib.0000000000000955
15. Persson EK, Scott CL, Mowat AM, Agace WW. Dendritic cell subsets in the intestinal lamina propria: ontogeny and function. *Eur J Immunol* 2013; **43:** 3098-107. doi: 10.1002/eji.201343740
16. Schiavi E, Smolinska S, O'Mahony L. Intestinal dendritic cells. *Curr Opin Gastroenterol* 2015; **31:** 98-103. doi: 10.1097/mog.0000000000000155
17. Vitale S, Strisciuglio C, Pisapia L, Miele E, Barba P, Vitale A, et al. Cytokine production profile in intestinal mucosa of paediatric inflammatory bowel disease. *PLoS One* 2017; **12:** e0182313. doi: 10.1371/journal.pone.0182313
18. Baumgart DC, Metzke D, Schmitz J, Scheffold A, Sturm A, Wiedenmann B, et al. Patients with active inflammatory bowel disease lack immature peripheral blood plasmacytoid and myeloid dendritic cells. *Gut* 2005; **54:** 228-36. doi: 10.1136/gut.2004.040360
19. Middel P, Raddatz D, Gunawan B, Haller F, Radzun HJ. Increased number of mature dendritic cells in Crohn's disease: evidence for a chemokine mediated retention mechanism. *Gut* 2006; **55:** 220-7. doi: 10.1136/gut.2004.063008
20. Baumgart DC, Metzke D, Guckelberger O, Pascher A, Grotzinger C, Przesdzing I, et al. Aberrant plasmacytoid dendritic cell distribution and function in patients with Crohn's disease and ulcerative colitis. *Clin Exp Immunol* 2011; **166:** 46-54. doi: 10.1111/j.1365-2249.2011.04439.x
21. Sanchez-Munoz F, Dominguez-Lopez A, Yamamoto-Furusho JK. Role of cytokines in inflammatory bowel disease. *World J Gastroenterol* 2008; **14:** 4280-8. doi: 10.3748/wjg.14.4280
22. Van Deventer SJ. Tumour necrosis factor and Crohn's disease. *Gut* 1997; **40:** 443-8. doi: 10.1136/gut.40.4.443
23. Sands BE, Kaplan GG. The role of TNFalpha in ulcerative colitis. *J Clin Pharmacol* 2007; **47:** 930-41. doi: 10.1177/0091270007301623
24. Levin AD, Wildenberg ME, van den Brink GR. Mechanism of action of anti-TNF therapy in inflammatory bowel disease. *J Crohns Colitis* 2016; **10:** 989-97. doi: 10.1093/ecco-jcc/jjw053
25. Nielsen OH, Ainsworth MA. Tumor necrosis factor inhibitors for inflammatory bowel disease. *N Engl J Med* 2013; **369:** 754-62. doi: 10.1056/NEJMct1209614
26. Chapman CG, Rubin DT. The potential for medical therapy to reduce the risk of colorectal cancer and optimize surveillance in inflammatory bowel disease. *Gastrointest Endosc Clin N Am* 2014; **24:** 353-65. doi: 10.1016/j.giec.2014.03.008
27. Andersen NN, Jess T. Has the risk of colorectal cancer in inflammatory bowel disease decreased? *World J Gastroenterol* 2013; **19:** 7561-8. doi: 10.3748/wjg.v19.i43.7561
28. Kopylov U, Seidman E. Predicting durable response or resistance to anti-tumor necrosis factor therapy in inflammatory bowel disease. *Therap Adv Gastroenterol* 2016; **9:** 513-26. doi: 10.1177/1756283x16638833
29. Gomollon F, Dignass A, Annese V, Tilg H, Van Assche G, Lindsay JO, et al. 3rd European evidence-based consensus on the diagnosis and management of Crohn's disease 2016: part 1: diagnosis and medical management. *J Crohns Colitis* 2017; **11:** 3-25. doi: 10.1093/ecco-jcc/jjw168
30. Magro F, Gionchetti P, Eliakim R, Ardizzone S, Armuzzi A, Acosta MB, et al. Third european evidence-based consensus on diagnosis and management of ulcerative colitis. Part 1: definitions, diagnosis, extra-intestinal manifestations, pregnancy, cancer surveillance, surgery, and ileo-anal pouch disorders. *J Crohns Colitis* 2017; **11:** 649-70. doi: 10.1093/ecco-jcc/jjx008
31. Best WR. Predicting the Crohn's disease activity index from the Harvey-Bradshaw Index. *Inflamm Bowel Dis* 2006; **12:** 304-10. doi: 10.1097/01.MIB.0000215091.77492.2a
32. Walmsley RS, Ayres RC, Pounder RE, Allan RN. A simple clinical colitis activity index. *Gut* 1998; **43:** 29-32. doi: 10.1136/gut.43.1.29
33. Daperno M, D'Haens G, Van Assche G, Baert F, Bulois P, Maunoury V, et al. Development and validation of a new, simplified endoscopic activity score for Crohn's disease: the SES-CD. *Gastrointest Endosc* 2004; **60:** 505-12. doi: 10.1016/S0016-5107(04)01878-4
34. Buchner AM, Lichtenstein GR. How to assess and document endoscopies in IBD patients by including standard scoring systems. *Inflamm Bowel Dis* 2016; **22:** 1010-9. doi: 10.1097/mib.0000000000000649
35. Côté-Daigneault J, Bouin M, Lahaie R, Colombel JF, Poitras P. Biologics in inflammatory bowel disease: what are the data? *United Eur Gastroenterol J* 2015; **3:** 419-28. doi: 10.1177/2050640615590302
36. Scott CL, Wright PB, Milling SW, Mowat AM. Isolation and identification of conventional dendritic cell subsets from the intestine of mice and men. *Methods Mol Biol* 2016; **1423:** 101-18. doi: 10.1007/978-1-4939-3606-9_7
37. Roe MM, Swain S, Sebrell TA, Sewell MA, Collins MM, Perrino BA, et al. Differential regulation of CD103 (alphaE integrin) expression in human dendritic cells by retinoic acid and Toll-like receptor ligands. *J Leukoc Biol* 2017; **101:** 1169-80. doi: 10.1189/jlb.1MA0316-131R
38. Dige A, Magnusson MK, Ohman L, Hvas CL, Kelsen J, Wick MJ, et al. Reduced numbers of mucosal DR(int) macrophages and increased numbers of CD103(+) dendritic cells during anti-TNF-alpha treatment in patients with Crohn's disease. *Scand J Gastroenterol* 2016; **51:** 692-9. doi: 10.3109/00365521.2015.1134649
39. Zampeli E, Gizis M, Siakavellas SI, Bamias G. Predictors of response to anti-tumor necrosis factor therapy in ulcerative colitis. *World J Gastrointest Pathophysiol* 2014; **5:** 293-303. doi: 10.4291/wjgp.v5.i3.293
40. Feagan BG, Sandborn WJ, Gasink C, Jacobstein D, Lang Y, Friedman JR, et al. Ustekinumab as induction and maintenance therapy for Crohn's disease. *N Engl J Med* 2016; **375:** 1946-60. doi: 10.1056/NEJMoa1602773
41. McLean LP, Shea-Donohue T, Cross RK. Vedolizumab for the treatment of ulcerative colitis and Crohn's disease. *Immunotherapy* 2012; **4:** 883-98. doi: 10.2217/imt.12.85
42. Colombel JF, Rutgeerts P, Reinisch W, Esser D, Wang Y, Lang Y, et al. Early mucosal healing with infliximab is associated with improved long-term clinical outcomes in ulcerative colitis. *Gastroenterology* 2011; **141:** 1194-201. doi: 10.1053/j.gastro.2011.06.054

43. Baert F, Moortgat L, Van Assche G, Caenepeel P, Vergauwe P, De Vos M, et al. Mucosal healing predicts sustained clinical remission in patients with early-stage Crohn's disease. *Gastroenterology* 2010; **138:** 463-8. doi: 10.1053/j.gastro.2009.09.056

44. Magnusson MK, Brynjólfsson SF, Dige A, Uronen-Hansson H, Börjesson LG, Bengtsson JL, et al. Macrophage and dendritic cell subsets in IBD: ALDH(+) cells are reduced in colon tissue of patients with ulcerative colitis regardless of inflammation. *Mucosal Immunol* 2016; **9:** 171-82. doi: 10.1038/mi.2015.48

45. Annacker O, Coombes JL, Malmstrom V, Uhlig HH, Bourne T, Johansson-Lindbom B, et al. Essential role for CD103 in the T cell-mediated regulation of experimental colitis. *J Exp Med* 2005; **202:** 1051-61. doi: 10.1084/jem.20040662

46. Scott CL, Aumeunier AM, Mowat AM. Intestinal CD103+ dendritic cells: master regulators of tolerance? *Trends Immunol* 2011; **32:** 412-9. doi: 10.1016/j.it.2011.06.003

47. del Rio ML, Bernhardt G, Rodriguez-Barbosa JI, Forster R. Development and functional specialization of CD103+ dendritic cells. *Immunol Rev* 2010; **234:** 268-81. doi: 10.1111/j.0105-2896.2009.00874.x

48. Cerovic V, Houston SA, Scott CL, Aumeunier A, Yrlid U, Mowat AM, et al. Intestinal CD103(-) dendritic cells migrate in lymph and prime effector T cells. *Mucosal Immunol* 2013; **6:** 104-13. doi: 10.1038/mi.2012.53

49. Ruane DT, Lavelle EC. The role of CD103(+) dendritic cells in the intestinal mucosal immune system. *Front Immunol* 2011; **2:** 25. doi: 10.3389/fimmu.2011.00025

50. Iliev ID, Spadoni I, Mileti E, Matteoli G, Sonzogni A, Sampietro GM, et al. Human intestinal epithelial cells promote the differentiation of tolerogenic dendritic cells. *Gut* 2009; **58:** 1481-9. doi: 10.1136/gut.2008.175166

51. Annaházi A, Molnár T. Pathogenesis of ulcerative colitis and Crohn's disease: similarities, differences and a lot of things we do not know yet. *J Clin Cell Immunol* 2014; **5:** 253. doi: 10.4172/2155-9899.1000253

52. Yarur AJ, Jain A, Sussman DA, Barkin JS, Quintero MA, Princen F, et al. The association of tissue anti-TNF drug levels with serological and endoscopic disease activity in inflammatory bowel disease: the ATLAS study. *Gut* 2016; **65:** 249-55. doi: 10.1136/gutjnl-2014-308099

53. Abraham C, Dulai PS, Vermeire S, Sandborn WJ. Lessons learned from trials targeting cytokine pathways in patients with inflammatory bowel diseases. *Gastroenterology* 2017; **152:** 374-88. doi: 10.1053/j.gastro.2016.10.018

54. Prieto-Perez R, Almoguera B, Cabaleiro T, Hakonarson H, Abad-Santos F. Association between genetic polymorphisms and response to anti-TNFs in patients with inflammatory bowel disease. *Int J Mol Sci* 2016; **17:** 225. doi: 10.3390/ijms17020225

55. Radwan P, Radwan-Kwiatek K, Tabarkiewicz J, Radej S, Rolinski J. Enhanced phenotypic and functional maturation of monocyte-derived dendritic cells from patients with active Crohn's disease and ulcerative colitis. *J Physiol Pharmacol* 2010; **61:** 695-703. PMID: 21224500

56. Vuckovic S, Florin TH, Khalil D, Zhang MF, Patel K, Hamilton I, et al. CD40 and CD86 upregulation with divergent CMRF44 expression on blood dendritic cells in inflammatory bowel diseases. *Am J Gastroenterol* 2001; **96:** 2946-56. doi: 10.1111/j.1572-0241.2001.04686.x

57. Hart AL, Al-Hassi HO, Rigby RJ, Bell SJ, Emmanuel AV, Knight SC, et al. Characteristics of intestinal dendritic cells in inflammatory bowel diseases. *Gastroenterology* 2005; **129:** 50-65. doi: 10.1053/j.gastro.2005.05.013

58. Lombardi VC, Khaiboullina SF. Plasmacytoid dendritic cells of the gut: relevance to immunity and pathology. *Clin Immunol* 2014; **153:** 165-77. doi: 10.1016/j.clim.2014.04.007

59. Hostmann A, Kapp K, Beutner M, Ritz JP, Loddenkemper C, Ignatius R, et al. Dendritic cells from human mesenteric lymph nodes in inflammatory and non-inflammatory bowel diseases: subsets and function of plasmacytoid dendritic cells. *Immunology* 2013; **139:** 100-8. doi: 10.1111/imm.12060

60. Knight SC. Dendritic cell-T-cell circuitry in health and changes in inflammatory bowel disease and its treatment. *Dig Dis* 2016; **34:** 51-7. doi: 10.1159/000442926

61. Lagaraine C, Lebranchu Y. Effects of immunosuppressive drugs on dendritic cells and tolerance induction. *Transplantation* 2003; **75:** 37s-42s. doi: 10.1097/01.tp.0000067950.90241.1d

62. Teig N, Moses D, Gieseler S, Schauer U. Age-related changes in human blood dendritic cell subpopulations. *Scand J Immunol* 2002; **55:** 453-7. doi: 10.1046/j.1365-3083.2002.01068.x

63. Bella SD, Bierti L, Presicce P, Arienti R, Valenti M, Saresella M, et al. Peripheral blood dendritic cells and monocytes are differently regulated in the elderly. *Clin Immunol* 2007; **122:** 220-8. doi: 10.1016/j.clim.2006.09.012

64. Dzutsev A, Hogg A, Sui Y, Solaymani-Mohammadi S, Yu H, Frey B, et al. Differential T cell homing to colon vs. small intestine is imprinted by local CD11c(+) APCs that determine homing receptors. *J Leukoc Biol* 2017; **102:** 1381-8. doi: 10.1189/jlb.1A1116-463RR

65. Cleynen I, Boucher G, Jostins L, Schumm LP, Zeissig S, Ahmad T, et al. Inherited determinants of Crohn's disease and ulcerative colitis phenotypes: a genetic association study. *Lancet* 2016; **387:** 156-67. doi: 10.1016/s0140-6736(15)00465-1

research article

Locoregional disease control after external beam radiotherapy in 91 patients with differentiated thyroid carcinoma and pT4 tumor stage - a single institution experience

Nikola Besic[1], Marta Dremelj[2], Gasper Pilko[1]

[1] Department of Surgical Oncology, Institute of Oncology Ljubljana, Ljubljana, Slovenia
[2] Department of Radiotherapy, Institute of Oncology Ljubljana, Ljubljana, Slovenia

Radiol Oncol 2018; 52(4): 453-460.

Received 04 May 2018
Accepted 23 May 2018

Correspondence to: Prof. Nikola Bešić, M.D., Ph.D., Department of Surgical Oncology, Institute of Oncology Ljubljana, Zaloška 2, SI-1000 Ljubljana, Slovenia. Phone:+386 1 5879 994; Fax: +386 1 5879 998; E-mail: nbesic@onko-i.si

Disclosure: No potential conflict of interest were disclosed.

Background. Locoregional recurrence is common in patients with locally advanced differentiated thyroid carcinoma (DTC). Our aim was to find out the rate of locoregional control of the disease after external beam radiotherapy (EBRT) of the neck and mediastinum in patients with DTC and pT4 tumor.

Patients and methods. Altogether 91 patients (47 males, 44 females, median age 61 years) with DTC had EBRT of the neck and mediastinum as part of the multimodal treatment of pT4 tumor (63 cases pT4a, 28 cases pT4b) from the year 1973 to 2015. Data on clinical factors, histopathology and recurrence were collected. Disease-free, disease-specific and overall survival was calculated.

Results. Median tumor size was 5 cm (range 1–30 cm). Out of 91 patients, 23 had distant and 38 regional metastases. A total or near-total thyroidectomy, lobectomy, subtotal thyroidectomy and lymph node dissection was performed in 70%, 14%, 2% and 30% of cases, respectively. Thirteen percent of patients were not treated with surgery. All patients had EBRT and 39 had chemotherapy. Radioiodine (RAI) ablation of thyroid remnant and RAI therapy was applied in 90% and 40% of cases, respectively. Recurrence was diagnosed in 29/64 patients without a persistent disease: locoregional and distant in 16 and 13 cases, respectively. Five-year and ten-year disease-free survival rate was 64% and 48%, respectively.

Conclusions. The majority of patients with DTC and pT4 tumors who were treated with EBRT of the neck and mediastinum region as part of multimodal treatment have long-lasting locoregional control of the disease.

Key words: thyroid carcinoma; radiotherapy; survival; pathology; locoregional recurrence

Introduction

The majority of patients with papillary and follicular carcinoma, *i.e.*, differentiated thyroid carcinoma (DTC), are successfully treated by a combination of surgery, radioiodine and L-thyroxin therapy.[1] However, 5 to 20 % of patients with differentiated thyroid carcinomas have local or regional recurrences.[1] Local or lymph nodes relapses are associated with worse survival of patients with differentiated thyroid carcinoma, so every effort should be made to minimize local or regional relapse.[2] Apart from surgery, postoperative radioactive iodine (RAI) and external beam radiotherapy (EBRT) can reduce locoregional relapse, especially in patients with the postoperative locoregional residual disease.[2,3]

Only a limited number of series have been published about results of EBRT treatment in patients with locally advanced differentiated thyroid carcinoma.[2,4-14] Management of about 10% of patients with the locally advanced disease remains contro-

versial.[12] Our aim was to find out the rate of locoregional control of the disease after external beam radiotherapy (EBRT) of the neck and mediastinum in patients with DTC and pT4 tumor treated in a comprehensive tertiary cancer center.

Patients and methods

The Cancer Registry of the Republic of Slovenia is one of the oldest population-based registries in Europe. It was founded in 1950 at the Institute of Oncology in Ljubljana (IOL) as a special service for collecting and processing data on cancer incidence and cancer patients' survival. According to data from the Cancer Registry 3,566 patients were treated for thyroid carcinoma in Republic of Slovenia during the period from 1973 to 2015.[15] All patients with thyroid carcinoma from our country are treated at IOL, which is the only comprehensive cancer center with the only radiotherapy facility equipped with the equipment and systems to plan, carry out and ensure the quality of ionizing radiation treatment in Slovenia. Among 3146 patents with DTC 91 patients (47 males, 44 females; median age 61 years, range 19–87 years) with DTC had EBRT of the neck and mediastinum as part of the multimodal treatment of DTC and pT4 tumor from the year 1973 to 2015. The mean tumor diameter was 6.3 cm (range 1–30 cm). Follicular, papillary and Hürthle cell carcinoma was diagnosed in 27, 53 and 11 cases, respectively.

Approval for the study was obtained from The Medical Ethics Committee of the Republic of Slovenia, the Protocol Review Board (MZ 32/12/11), and Protocol Review Board Ethics Committee of the Institute of Oncology (KSOPKR/18/11/10). The trial was retrospectively registered in ISRCTN registry - Study number 34641. The study was conducted in accordance with the ethical standards laid down in an appropriate version of the 1964 Declaration of Helsinki. The study was conducted with the understanding and the consent of the subjects. All patients are asked upon their first admission to the IOL or during a follow-up visit to give consent for the study of her/his chart and/or bioptic material for scientific purposes. Since the Institutional Review Board of the IOL approved this specific study, the patients were not asked to give their written consent for this specific study.

All histological slides of our patients with DTC were reexamined by the pathologist experienced in thyroid pathomorphology. DTC was diagnosed on the histological criteria defined by Rosai and LiVolsi.[16,17] The diagnosis of malignancy of follicular and Hürthle cell carcinoma was based on histologic evidence of transcapsular and/or vascular invasion, extrathyroidal local tissue invasion by the primary tumor, or presence of nodal or distant metastasis. An oncocyte was characterized by the presence of acidophilic, granular cytoplasm and hyperchromatic or vesicular nuclei with a large nucleolus. Only lesions demonstrating more than 75% of follicular cells with oncocytic characteristics were classified as Hürthle cell carcinoma. All patients with Hürthle cell neoplasms with cells containing typical nuclear features of papillary carcinoma were classified as Hürthle cell papillary thyroid carcinoma.

The charts were reviewed, and data on patients' age, gender, disease history, the extent of disease, histomorphological characteristics, modalities of therapy, outcome, and survival were collected. Demographic and clinical characteristics, treatment, and patient outcome are presented in Table 1 and Table 2. Disease-specific survival, overall survival, disease-free survival, locoregional relapse free survival, disease-specific survival according to T4a and T4b tumor stage and disease-specific survival according to distant metastases are presented in Figures 1 to 4. According to TNM classification, T4a tumors have gross extra-thyroid extension in soft tissue, larynx, trachea, esophagus or recurrent laryngeal nerve, while T4b tumors have gross extra-thyroid extension in prevertebral fascia or encasing the carotid artery or gross mediastinal vessels.[18]

The tumor stage, presence of regional and/or distant metastases, as well as a residual tumor after surgery were assessed by the TNM clinical classification according to the 7th edition of UICC criteria from 2009.[18] The initial diagnostic work-up in all patients with DTC included ultrasound (US) of the neck region and a chest X-ray. The criteria for disease-free survival after thyroid surgery and RAI ablation of thyroid remnant were: thyroglobulin (Tg) levels of less than 1 ng/mL, negative whole-body RAI scans, and the exclusion of cervical lymph node metastases by the US. Additional diagnostic work-up was conducted whenever the medical history, physical examination, laboratory findings, and/or radioiodine (RAI) uptake indicated recurrence and/or distant metastases. It comprised X-ray investigation, US investigation, computed tomography, magnetic resonance imaging, bone scintigraphy, scintigraphy with MIBI and/or PET-CT.

All patients with DTC had a follow-up exam at our Institute at least once per year, while for all

patients with a recurrence or distant metastases follow-ups were performed at least twice per year. This consisted of meticulously taking their medical history, a physical examination, and determining serum Tg concentration. Imaging was also conducted whenever Tg concentration increased, or clinical symptoms or signs suggested that the disease had recurred and/or progressed.

Treatment

Surgical treatment of primary tumor, locoregional recurrences, and distant metastases was not uniform during the 42-year period; neither was the proportion of patients treated by RAI ablation of thyroid remnant tissue, EBRT, chemotherapy and/or RAI therapy.

Surgery is the mainstay of DTC treatment. Among surgically treated patients, 84% had primary surgery at the IOL and 16% elsewhere, while all other specific therapies (surgery for locoregional recurrence, RAI, EBRT and/or chemotherapy) were applied and follow-ups were conducted for all patients at the IOL. After surgery, all patients received a thyroid hormone replacement titrated to suppress thyroid stimulating hormone (TSH) production.

The data on the type of surgery for primary tumors are listed in Table 1 and Table 2. Total or near-total thyroidectomy is considered an appropriate surgical procedure for DTC. Generally, after an inadequate surgical procedure, a completion thyroidectomy is performed. However, in our study group, this was performed in only five of 21 patients with inadequate surgery. It was not performed if the patient had a recurrent nerve injury (N = 7), preferred treatment with RAI (N = 5), if the patient was very old or with severe comorbidities (N = 3) or the patient refused another surgical procedure (N = 1). Metastases in regional lymph nodes were treated surgically by functional radical neck dissection in 29 patients as part of primary treatment. Twelve of our patients had surgically unresectable tumor because it encasted the carotid artery or gross mediastinal vessels, so they were treated by other treatment modalities.

The initial treatment in 13 patients with a locally advanced tumor was neoadjuvant chemotherapy; of these three patients received concomitant EBRT. Before surgery two patients were treated with preoperative EBRT only. Tumor size decreased in all of these patients, and in five of 15 patients, the largest tumor diameter decreased by more than 30%. Neoadjuvant chemotherapy consisted of long infusion of low dose vinblastine (2 mg in 12-hour or 24-hour) in five patients and vinblastine and doxorubicin (20 mg in 2-hour infusion) in three patients. Neoadjuvant chemotherapy consisted of vinblastine and cis-platinum in one patient, of vinblastine, doxorubicin, and mitoxantrone in one patient, while in three patients more than three cytostatic drugs were used. Altogether 39 patients were treated with chemotherapy. Tyrosine kinase inhibitors were used in two patients included in this study.

RAI was used to ablate thyroid remnant tissue in 82 (90%) patients. Altogether 20 of 27 patients

TABLE 1. Clinical data and outcome of 91 patients with pT4 tumor stage

Characteristic	Subgroup	Number of patients
Gender	Female	44
	Male	47
Patient's age	44 or less	15
	45 or more	76
Tumor diameter (cm)	1-9	75
	9.1-30	16
T stage	pT4a	63
	pT4b	28
Lymph nodes metastases	No	53
	Yes	38
Distant metastases	No	68
	Yes	23
Residual tumor after surgery	R0	27
	R1	47
	R2	5
	No surgery	12
Recurrence	No	39
	Yes-distant	13
	Yes-locoregional	16
	Disease present permanently	23
Outcome	Alive	44
	Dead of distant disease	29
	Dead of local disease	1
	Dead of local and distant disease	4
	Dead of other causes	10
	Lost from follow-up	3

TABLE 2. Treatment of patients

Characteristic	Subgroup	Number of Patients
Surgery of the thyroid	Lobectomy or less	15
	Total or near-total thyroidectomy	64
	Without surgery	12
Neck dissection	No	64
	Yes	27
Radioiodine ablation	No	9
	Yes	82
Therapy with radioiodine	No	54
	Yes	37
Radiotherapy - Neck region	No	0
	Yes	91
Chemotherapy	No	52
	Yes	39
Tyrosine kinase inhibitors	No	89
	Yes	2

(74%) with non-adequate surgery had the ablation of thyroid remnant tissue. The ablation dose was 3.4–4.8 GBq (92–129 mCi) of RAI. RAI was also used for the treatment of distant metastases and/or inoperable locoregional disease with an empiric dose of 3.7–7.4 GBq (100–200 mCi). Patients with distant metastases underwent total thyroidectomy before treatment with RAI to increase the uptake of iodine in metastases and to speed up the treatment whenever possible. Before 2002, serum concentration of TSH of > 30 mU/L was achieved by a 4–6 week withdrawal of L-thyroxin suppression therapy. Since 2002, recombinant human TSH (rhTSH)-aided RAI therapy has been used in altogether 13 patients who were elderly and had concomitant diseases, had a history of severe hypothyroid or compressive symptoms and/or evidence of tumor progression during thyroid hormone withdrawal.[19]

All 91 patients included in this report had EBRT to the neck and superior mediastinum. Six patients were treated preoperatively with EBRT, four of them with concomitant chemotherapy and two with EBRT only. Even 63 (69%) of our patents were irradiated using antero-posterior opposed fields in the supine position with an extended neck. The target volume extended from mastoid tips cranially to tracheal bifurcation caudally and to the coracoids laterally, to cover neck lymph nodes regions I–VI, thyroid bed, and superior mediastinal lymph nodes. The two beams, using Cobalt unit or 6 MV photon beams, were weighted anteriorily; dose from the anterior field was 1.2 Gray (Gy) and from posterior field 0.6 Gy per fraction, 5 fractions per week. The apices of the lungs were shielded; after the received dose of 39.6 Gy. The spinal cord was also shielded from the posterior field, so the dose to the spinal cord was kept bellow 45 Gy. The prescribed dose to the midplane in the vast majority of postoperative patients was 50.4 Gy. A boost dose of 6–16 Gy with 1.8–2 Gy per fraction was delivered to some patients with the macroscopic remnant of disease using photon beams or electron beams avoiding spinal cord. Eight patients were irradiated by 3D technique (TD 50.4–70 Gy, median 63.5 Gy) and 20 patients by intensity-modulated radiotherapy technique (IMRT) to the whole neck and mediastinum (TD 56–70 Gy, median 64 Gy), while only one patient had only thyroid bed irradiation. The five of six patients treated with EBRT before surgery received 36 Gy before surgery and 14 Gy after surgery, while one patient treated with EBRT before surgery received 50 Gy with IMRT technique.

EBRT toxicity was difficult to estimate since in some patients it was inadequately documented. Ten patients had radiotherapy interrupted for one to three weeks because of acute mucositis or dermatitis, but eventually finished the prescribed therapy. One patient stopped postoperative radiotherapy at 16 Gy due to reported side effects, received further radioiodine therapy and progressed two years later at a distant site. Among 28 patients treated with IMRT or 3D technique Grade 3 mucositis or Grade 3 dermatitis was reported in 10 patients. Furthermore, a weight loss above 5 kg was detected in eight patients who also needed hospitalization for parenteral therapy, in two of them a nasogastric tube was placed, while in one patient a tracheostomy was done. Of the late effects, a grade 2–3 neck fibrosis was documented in two patients and Lhermitte's sign in one patient. One patient had tracheal stricture after partial resection of the trachea which was resolved with laser therapy, and the patient is alive with very slowly progressing regional and distant disease recurrence 17 years after the beginning of treatment.

Survival

Disease-specific survival was defined as the period from primary treatment (surgery, chemotherapy or EBRT) to death or the last follow-up. Disease-free survival was defined as the period from primary surgical treatment to the radiologic or morphologic diagnosis of locoregional recurrence, distant metastases or the last follow-up. Locoregional relapse free survival was analyzed in patients without gross residual tumor. Locoregional relapse free survival was defined as the period from primary surgical treatment to the radiologic or morphologic diagnosis of locoregional recurrence or the last follow-up.

Overall survival was defined from the period of primary treatment to death of any cause or the last follow-up. The median duration of follow-up was 5.1 years (range 0.5–25.7 years).

Statistical analysis

The Student t-test or the Mann–Whitney U-test was used according to data distribution. The association between categorical variables was tested by the chi-square test or Fisher's exact test, as appropriate. All comparisons were two-sided and a p-value < 0.05 was considered statistically significant. The statistical correlation between possible prognostic factors and cause-specific survival was analyzed by chi-square test and log-rank analysis. The estimated survival curves were calculated ac-

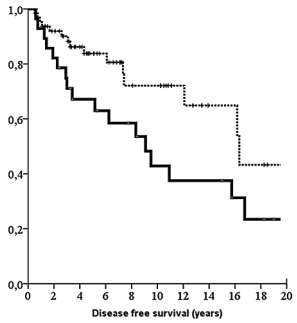

FIGURE 1. Disease-specific survival according to T4a and T4b tumor stage (p = 0.07) (bold line, T4b; dotted line, T4a).

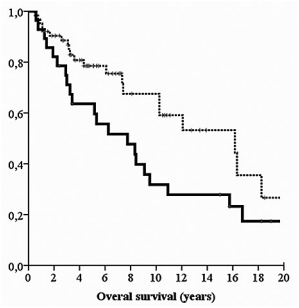

FIGURE 2. Overall survival according to T4a and T4b tumor stage (p = 0.08) (bold line, T4b; dotted line, T4a).

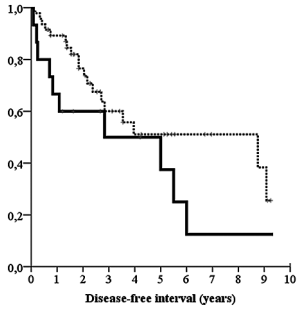

FIGURE 3. Disease-free survival according to T4a and T4b tumor stage in 64 patients without persistent disease (p = 0.122) (bold line, T4b; dotted line, T4a).

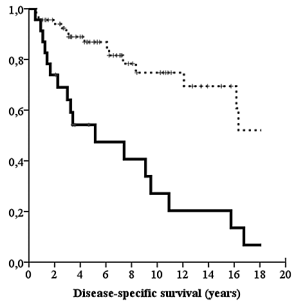

FIGURE 4. Patients without distant metastases had longer disease-specific survival than those without distant metastases (p < 0.001) (bold line, with metastases; dotted line, without metastases).

cording to the Kaplan-Meier method. Multivariate statistical analysis was not performed because of the small number of patients. The statistical package PASW 18 (SPSS Inc., Chicago, IL, USA) was used for the analysis.

Results

Follicular, papillary and Hürthle cell carcinoma was diagnosed in 27, 53 and 11 cases, respectively. Median tumor size was 5 cm (range 1–30 cm). Of 91 patients, 23 had distant and 38 regional metastases (Table 1). A total or near-total thyroidectomy, lobectomy, subtotal thyroidectomy and lymph node dissection was performed in 70%, 14%, 2% and 30% of cases, respectively. 13% of patients were not treated with surgery. All patients had EBRT and 39 had chemotherapy. Radioiodine (RAI) ablation of remnant thyroid tissue and RAI therapy was done in 90% and 40% of cases, respectively (Table 2).

Locoregional control of disease

The follow-up period was 6 to 308 (median 61) months. Recurrence was diagnosed in 29/68 (43%) patients without a persistent disease: locoregional and distant in 16 and 13 cases, respectively. Five-year and 10-year recurrence-free survival was in 64% and 48%, respectively. Locoregional control of disease was achieved in 49/64 (77%) of patients.

Locoregional recurrence or progression of residual locoregional carcinoma was detected in 21% of patients after R1 resection, 30% after R2 resection and 33.3% of patients with unresectable disease. Of the 18 patients who had gross residual neck disease without distant metastases after a surgical procedure, 7 demonstrated complete response, 6 had locoregional progression (after 6, 17, 26, 49, 68 and 144 months) and 5 only distant progression of the disease.

Survival

By the end of the study, 44 patients were still alive (28 with no evidence of disease, 16 alive with the disease), 3 were lost to follow-up, 34 patients died of thyroid carcinoma (29 of distant metastases, 1 of locoregional disease, and 4 of locoregional disease and distant metastases), while 10 died of causes unrelated to the primary disease.

The median survival of follicular, Hürthle cell and papillary carcinoma was 62, 131 and 240 months, respectively. Estimated locoregional relapse-free survival, disease-specific survival, and overall survival at 4 years were 71%, 79%, and 75%, respectively. Five-year and 10-year cancer-specific survival in patients with T4a and T4b tumors was 77% and 60% (Figure 1). Five-year and 10-year overall survival in patients with T4a and T4b tumors was 72% and 49% (Figure 2). Five-year and 10-year disease-free survival in patients with T4a and T4b tumors was 64% and 48% (Figure 3). Figure 4 shows that patients without distant metastases had longer disease-specific survival than those with distant metastases (p < 0.001).

Of the 18 patients who had gross residual neck disease without distant metastases after surgical procedure, 7 are alive (29, 37, 40, 57, 97, 153 and 228 months) and 4 died of other causes (39, 64, 123 and 219 months), while 6 died of distant metasta-

ses after 2, 6, 17, 26, 31 and 52 months and one is lost from follow-up.

Ten of 12 patients who were not surgically treated are dead, and 8 of 10 died of DTC. They were alive for 9, 11, 17, 17, 27, 39, 62, 114 and 194 months. Locoregional control of disease was achieved in 5 of 8 patients. Five patients died of distant metastases, one of the locally progressive tumor, while two patients died of distant and locoregional disease.

Discussion

In a cohort of 1,297 patients, Chow *et al.* reported that 100 patients died because of thyroid cancer.[9] The uncontrolled locoregional disease was the cause of death in as many as 59/100 patients.[9] Locoregional recurrence of DTC is a heavy burden for individual patients, as well as for the health care system. Locoregional recurrence in the majority of cases necessitates reoperation, with significant consequential morbidity and costs.[12] Furthermore, recurrences located in the thyroid bed with soft tissue infiltration are less likely to be iodine avid so that they can be rarely cured with radioiodine.[20] Moreover, not all patients with recurrence can be successfully saved. Therefore, prevention of locoregional recurrence is very reasonable. Our aim was to find out the rate of locoregional control of the disease after EBRT of the neck and mediastinum in patients with DTC and pT4 tumor treated in a tertiary cancer comprehensive center.

Adjuvant therapy is administered in addition to the primary, main, or initial therapy to maximize its effectiveness. Adjuvant systemic therapy and radiotherapy are often applied following surgery for many types of cancer, including colon cancer, lung cancer, pancreatic cancer, breast cancer, prostate cancer, and some gynecological cancers.[21] In patients with DTC, adjuvant therapy and therapy for the residual disease may include chemotherapy, EBRT, radioiodine treatment and/or suppressive L-thyroxin therapy.[3,4,22,23]

We believe that chemotherapy may be an effective adjuvant treatment in patients with high risk of recurrence, so it was used in as many as 43% of our patients treated at IOL. Interestingly, this mode of therapy was seldom used in other centers. Schwartz *et al*. from MD Anderson Cancer Center reported that chemotherapy was used in only 6 of 126 patients (5%) who were treated with EBRT.[12]

Adjuvant EBRT is another rarely used treatment in locally advanced DTC disease to prevent a locoregional recurrence. So only a limited number of series have been published reporting the results of EBRT treatment in patients with locally advanced DTC.[2,4-14] To our knowledge, only one randomized study about ERBT is reported in the literature.[13] The Multicenter Study on Differentiated Thyroid Cancer (MSDS) was planned as a prospective multicenter trial on the benefit of adjuvant EBRT in patients with DTC and pT4, with or without lymph node metastases and no known distant metastases.[13] However, only 45 of planned 311 patients were randomized. Not surprisingly, only a weak benefit of EBRT regarding local control was observed that did not reach statistical significance.[13]

Gross, the unresectable residual disease is accepted as an indication for adjuvant radiotherapy in the 2015 American Thyroid Association Management Guidelines for Adult Patients with Thyroid Nodules and Differentiated Thyroid Cancer.[23] Schwartz *et al.* reported that a total of 15 patients received EBRT for gross unresectable or residual disease.[12] After EBRT of the 15 patients, 4 demonstrated a complete response, 3 had a partial response, 6 had stable disease, and 2 progressed through treatment.[12] Our multimodal treatment resulted in better locoregional control and longer survival in 8 of 12 (67%) patients who were not surgically treated because of unresectable disease. Of the 18 patients who had gross residual disease after the surgical procedure and were without distant metastases, 7 demonstrated a complete response, 5 had only distant progression, while 6 had locoregional progression after 6, 17, 26, 49, 68 and 144 months.

EBRT in the neck region is a very difficult task because of its concave shape.[12] An additional difficulty is the close proximity of the thyroid bed to critical normal structures, which makes it challenging to deliver high doses.[12] The proximity of the esophagus, trachea, larynx, lungs, spinal cord, and, in cases with the disease in cervical regions I and II also parotid glands, results in considerable toxicity after conventional radiotherapy.[12] The majority of patients (69%) from our study were treated with conventional two-field EBRT. This dose was effective in preventing locoregional recurrence or progression of residual tumor in 49/65 (75%) patients: 80% after R1 resection and 70% after R2 resection. None of our patients treated with two-field EBRT needed hospitalization due to side effects or placement of a nasogastric feeding tube. Mild or moderate dysphagia or xerostomia was present in some patients, while Lhermitte's sign was reported in only one patient. A probable explanation for this is a lower dose (median 50.4 Gy) which was used in our patients treated with conventional EBRT.

However, one should take into account the retrospective nature of our study, so not all side effects were documented and were probably under-reported.

Rosenbluth *et al*. from Memorial Sloan-Kettering reported the results of a pilot study about IMRT used in 20 patients with differentiated or medullary thyroid cancer.[8] They reported Grade 3 mucositis in 7 patients, Grade 3 pharyngitis in 3 patients, Grade 3 acute laryngeal toxicity in 2 patients, and Grade 3 skin toxicity in 2 patients. Eleven of their patients received percutaneous endoscopic gastrostomy. However, acute toxicity was mostly self-limited.[8] In our 20 patients treated with IMRT technique a Grade 3 mucositis or Grade 3 dermatitis was reported in 7 patients. Furthermore, weight loss larger than 5 kg was detected in six patients who also needed hospitalization for parenteral therapy. In one of our patient's tracheostomy was done. Lower proportion of side effects in our patients in comparison to patients from Memorial Sloan-Kettering may be explained by a lower dose in our patients (median 64 Gy versus 66 Gy, respectively). On the other hand, the larger volumes of irradiated tissue come at the cost of higher toxicity, so it is important that the volume at risk of relapse is carefully considered.[24] Brierley reported that they frequently use a more limited volume and the locoregional relapse rate was only 7% in selected patients with extrathyroidal extension and no gross residual disease. He concluded that more information is required to ascertain which patients require extended field EBRT, as well as the risk of higher acute and late toxicities.[24]

The limitation of our study is that the results of treatment and survival from a single institution are reported. Another limitation is that not all our patients were treated uniformly. During a 42-year time frame, they were treated by many surgeons and oncologists. Our study is observational and not randomized, thus it is not possible to draw conclusions about the impact of a treatment's specific modality on recurrence rates or patients' survival. Due to the retrospective nature of our study side effects of EBRT and IMRT were not completely documented and are probably under-reported.

Our view is that all patients with non-favorable prognoses and/or a high risk of structural disease recurrence should be treated by a multidisciplinary team consisting of a surgeon, a nuclear medicine specialist, a radiotherapist and a medical oncologist. Appropriate surgical procedures consisting of a total thyroidectomy and lymph node dissection of affected compartments should be followed by a radioiodine ablation of remnant thyroid tissue whenever possible. Our results prove that long-term survival can also be obtained in patients with locoregionally advanced DTC and a distant metastatic disease if they are treated multidisciplinary. Chemotherapy before surgical procedures may be effective to decrease the size of the primary tumor in DTC.[25-27] Concomitant chemotherapy with EBRT in locoregionally advanced DTC can result in complete and very long locoregional control.[4] Failure to obtain a locoregional control of disease may cause a dismal course of thyroid carcinoma.[9,28] Since residual tumors after thyroid surgery are an independent prognostic factor for disease-specific as well as disease-free survival, an effective locoregional therapy is mandatory. Our view is that the use of adjuvant EBRT can postpone or prevent treatment with kinase inhibitors which are very expensive and have many very unpleasant and also serious side effects. On the other hand, also IMRT technique of EBRT has serious acute side effects. However, in the majority of patients, acute side effects last only about one month and are self-limiting. Furthermore, the late toxicity of EBRT is rare. Therefore, EBRT should be used in cases of residual tumors and as adjuvant therapy in patients with a high risk of structural disease recurrence.

Conclusions

The majority of patients with DTC and pT4 tumors who were treated with EBRT of the neck and mediastinum region as part of multimodal treatment have long-lasting locoregional control of the disease. Locoregional recurrence or progression of residual locoregional carcinoma was detected in 21% of patients after R1 resection, 30% after R2 resection and 33.3% of patients with unresectable disease.

Acknowledgements

The paper was supported by a research program, P3-0289, by the Ministry of Higher Education, Science and Sport of Slovenia.

References

1. Schlumberger MJ. Papillary and follicular thyroid carcinoma. *N Engl J Med* 1998; **338:** 297-306. doi: 10.1056/NEJM199801293380506

2. Chow SM, Law SCK, Mendenhall WM, Au SK, Chan PT, Leung TW, et al. Papillary thyroid carcinoma: prognostic factors and the role of radioiodine and external radiotherapy. *Int J Radiat Oncol Biol Phys* 2002; **52:** 784-95. doi: org/10.1016/S0360-3016(01)02686-4

3. Brierley J, Tsang R, Panzarella T, Bana N. Prognostic factors and the effect of treatment with radioactive iodine and external beam radiation on patients with differentiated thyroid cancer seen at a single institution over 40 years. *Clin Endocrinol (Oxf)* 2005; **63:** 418-27. doi: 10.1111/j.1365-2265.2005.02358.x

4. Kim JH, Leeper RD. Treatment of locally advanced thyroid carcinoma with combination doxorubicin and radiation therapy. *Cancer* 1987; **60:** 2372-5.

5. Philips P, Hanzen C, Andry G, Van Houtte P, Früuling J. Postoperative irradiation for thyroid cancer. *Eur J Surg Oncol* 1993; **19:** 399-404.

6. Farahati J, Reiners C, Stuschke M, Müller SP, Stüben G, Sauerwein W, Sack H. Differentiated thyroid cancer. Impact of adjuvant external radiotherapy in patients with perithyroidal tumor infiltration (stage pT4). *Cancer* 1996; **77:** 172-80. doi: 10.1002/(SICI)1097-0142(19960101)77:1<172::AID-CNCR28>3.0.CO;2-1

7. Tsang RW, Brierley JD, Simpson WJ, Panzarella T, Gospodarowicz MK, Sutcliffe SB. The effects of surgery, radioiodine, and external radiation therapy on the clinical outcome of patients with differentiated thyroid carcinoma. *Cancer* 1998; **82:** 375-88.

8. Rosenbluth BD, Serrano V, Happersett L, Shaha AR, Tuttle RM, Narayana A, et al. Intensity-modulated radiation therapy for the treatment of nonanaplastic thyroid cancer. *Int J Radiat Oncol Biol Phys* 2005; **63:** 1419-26. doi: 10.1016/j.ijrobp.2005.05.043

9. Chow SM, Yau S, Kwan CK, Poon PC, Law SC. Local and regional control in patients with papillary thyroid carcinoma: specific indications of external radiotherapy and radioactive iodine according to T and N categories in AJCC 6th edition. *Endocr Relat Cancer* 2006; **13:** 1159-72. doi: 10.1677/erc.1.01320

10. Azrif M, Slevin NJ, Sykes AJ, Swindell R, Yap BK. Patterns of relapse following radiotherapy for differentiated thyroid cancer: implication for target volume delineation. *Radiother Oncol* 2008; **89:** 105-13. doi: 10.1016/j.radonc.2008.05.023

11. Terezakis SA, Lee KS, Ghossein RA, Rivera M, Tuttle RM, Wolden SL, et al. Role of external beam radiotherapy in patients with advanced or recurrent nonanaplastic thyroid cancer: Memorial Sloan-Kettering Cancer Center experience. *Int J Radiat Oncol Biol Phys* 2009; **73:** 795-801. doi: 10.1016/j.ijrobp.2008.05.012

12. Schwartz DL, Lobo MJ, Ang KK, Morrison WH, Rosenthal DI, Ahamad A, et al. Postoperative external beam radiotherapy for differentiated thyroid cancer: outcomes and morbidity with conformal treatment. *Int J Radiat Oncol Biol Phys* 2009; **74:** 1083-91. doi: 10.1016/j.ijrobp.2008.09.023

13. Biermann M, Pixberg M, Riemann B, Schuck A, Heinecke A, Schmid KW, et al; MSDS study group. Clinical outcomes of adjuvant external-beam radiotherapy for differentiated thyroid cancer - results after 874 patient-years of follow- up in the MSDS-trial. *Nuklearmedizin* 2009; **48:** 89-98. doi: 10.3413/nukmed-0221

14. Kim TH, Chung KW, Lee YJ, Park CS, Lee EK, Kim TS, et al. The effect of external beam radiotherapy volume on locoregional control in patients with locoregionally advanced or recurrent nonanaplastic thyroid cancer. *Radiat Oncol* 2010; **5:** 69. doi: 10.1186/1748-717X-5-69

15. Cancer in Slovenia 2014. Ljubljana: Institute of Oncology Ljubljana, Epidemiology and Cancer Registry, Cancer Registry of Republic of Slovenia, 2017. [cited 2018 April 15]. Available from: https://www.onko-i.si/fileadmin/onko/datoteke/dokumenti/RRS/LP_2014.pdf

16. Rosai J. Tumors of thyroid gland. In: Rosai J, Carcangiu ML, DeLellis RA, editors. Atlas of tumor pathology. Washington: Armed Forces Institute of Pathology; 1992. p. 31-50.

17. LiVolsi VA, Baloch ZW. Follicular neoplasms of the thyroid: view, biases, and experiences. *Adv Anat Pathol* 2004; **11:** 279-87. doi: 10.1097/01.pap.0000138143.34505.02

18. Sobin LH, Gospodarowicz MK, Wittekind C. Thyroid gland (ICD-O C73). In: Sobin LH, Gospodarowicz MK, Witekind C, editors. *TNM classification of malignant tumours.* 7th Edition. New York: Wiley Blackwell; 2009. p. 58-62.

19. Zagar I, Schwarzbartl-Pevec A, Vidergar-Kralj B, Horvat R, Besic N. Recombinant human thyrotropin-aided radioiodine therapy in patients with metastatic differentiated thyroid carcinoma. *J Thyroid Res* 2012**;** 670180. doi: 10.1155/2012/670180

20. Vassilopoulou-Sellin R, Schultz PN, Haynie TP. Clinical outcome of patients with papillary thyroid carcinoma who have recurrence after initial radioactive iodine therapy. *Cancer* 1996; **78**: 493-501. doi: 10.1002/(SICI)1097-0142(19960801)78:3<493::AID-CNCR17>3.0.CO;2-U

21. Feig BW, Ching DC editors. *The MD Anderson surgical oncology handbook.* Philadelphia: Lippincott Williams & Wilkins; 2012.

22. Santini F, Bottici V, Elisei R, Montanelli L, Mazzeo S, Basolo F, et al. Cytotoxic effects of carboplatinum and epirubicin in the setting of an elevated serum thyrotropin for advanced poorly-differentiated thyroid cancer. *J Clin Endocrinol Metab* 2002; **87:** 4160-5. doi: 10.1210/jc.2001-011151

23. Haugen BR, Alexander EK, Bible KC, Doherty GM, Mandel SJ, Nikiforov YE, et al. 2015 American Thyroid Association Management Guidelines for Adult Patients with Thyroid Nodules and Differentiated Thyroid Cancer. *Thyroid* 2016; **26:** 1-133. doi: 10.1089/thy.2015.0020

24. Brierley JD. Update on external beam radiation therapy in thyroid cancer. *J Clin Endocrinol Metab* 2011; **96:** 2289-95. doi: 10.1210/jc.2011-1109

25. Besic N, Auersperg M, Gazic B, Dremelj M, Zagar I. Neoadjuvant chemotherapy in 29 patients with locally advanced follicular or Hürthle cell thyroid carcinoma: a phase 2 study. *Thyroid* 2012; **22:** 131-7. doi: 10.1089/thy.2011.0243

26. Besic N, Auersperg M, Dremelj M, Vidergar-Kralj B, Gazic B. Neoadjuvant chemotherapy in 16 patients with locally advanced papillary thyroid carcinoma. *Thyroid* 2013; **23:** 178-84. doi: 10.1089/thy.2012.0194

27. Besic N, Dremelj M, Schwartzbartl-Pevec A, Gazic B. Neoadjuvant chemotherapy in 13 patients with locally advanced poorly differentiated thyroid carcinoma based on Turin proposal - a single institution experience. *Radiol Oncol* 2015; **49:** 271-8. doi: 10.1515/raon-2015-0001

28. Vogrin A, Besic H, Besic N, Music MM. Recurrence rate in regional lymph nodes in 737 patients with follicular or Hürthle cell neoplasms. *Radiol Oncol* 2016; **50:** 269-73. doi: 10.1515/raon-2016-0025

research article

Image guided high-dose-rate brachytherapy versus volumetric modulated arc therapy for head and neck cancer: A comparative analysis of dosimetry for target volume and organs at risk

Hironori Akiyama[1,2], Csilla Pesznyák[1], Dalma Béla[1], Örs Ferenczi[1], Tibor Major[1], Csaba Polgár[1,3], Zoltán Takácsi-Nagy[1,3]

[1] Center of Radiotherapy, National Institute of Oncology, Budapest, Hungary
[2] Department of Oral Radiology, Osaka Dental University, Osaka, Japan
[3] Department of Oncology, Semmelweis University, Budapest, Hungary

Radiol Oncol 2018; 52(4): 461-467.

Received 19 June 2018
Accepted 6 October 2018

Correspondence to: Hironori Akiyama, Department of Oral Radiology, Osaka Dental University, 1-5-17 Otemae Chuo-Ku, 5400008, Osaka, Japan. Phone: +81-90-5894-3937; E-mail: ddiisbt@gmail.com

Disclosure: No potential conflicts of interest were disclosed.

Background. The aim of the study was to present dosimetric comparison of image guided high-dose-rate brachytherapy (IGBT) with volumetric modulated arc therapy (VMAT) for head and neck cancer regarding conformity of dose distribution to planning target volume (PTV) and doses to organs at risk (OARs).

Patients and methods. Thirty-eight consecutive patients with T1-4 mobile tongue, floor of mouth and base of tongue cancer treated with IGBT were selected. For these patients additional VMAT treatment plans were also prepared using identical computed tomography data. OARs and PTV related parameters (*e.g.* V98, D0.1cm^3, Dmean, *etc.*) were compared.

Results. Mean V98 of the PTV was 90.2% *vs.* 90.4% ($p > 0.05$) for IGBT and VMAT, respectively. Mean D0.1cm^3 to the mandible was 77.0% *vs.* 85.4% ($p < 0.05$). Dmean to ipsilateral and contralateral parotid glands was 4.6% *vs.* 4.6% and 3.0% *vs.* 3.9% ($p > 0.05$). Dmean to ipsilateral and contralateral submandibular glands was 16.4% *vs.* 21.9% ($p > 0.05$) and 8.2% *vs.* 16.9% ($p < 0.05$), respectively.

Conclusions. Both techniques showed excellent target coverage. With IGBT dose to normal tissues was lower than with VMAT. The results prove the superiority of IGBT in the protection of OARs and the important role of this invasive method in the era of new external beam techniques.

Key words: head and neck cancers; image guided high-dose-rate brachytherapy; volumetric modulated arc therapy; dosimetric comparison

Introduction

Head and neck (H&N) cancer is an excellent indication for radiation therapy (RT) which is an organ preserving method maintaining the quality of life of patients. Brachytherapy (BT) with or without external beam RT (EBRT) can play an essential role in the treatment of certain tumor localizations in the H&N area except cases with bone invasion or proximity of large vessels, delivering an ablative dose to the target volume while sparing the critical and normal tissues - due to the rapid dose fall-off - which is not safely feasible with EBRT alone.[1-3] Image guided high-dose-rate BT (IGBT) with computed tomography (CT) and/or magnetic resonance imaging (MRI) has been implemented improving the effica-

cy of BT.[4] IGBT decreases irradiated doses to critical structures without compromising target coverage.[5] However, IGBT is an invasive procedure requiring special skills and interdisciplinary co-operation with a H&N surgeon, as well as patience on the part of patients who have to endure e the insertion of catheters.[6,7] Recently, intensity modulated RT (IMRT) has been introduced in clinical practice and achieved higher dose conformity with better organs at risk (OARs) sparing compared to 3-dimensional conformal radiation therapy.[8] Volumetric modulated arc therapy (VMAT), an improved technique of IMRT offers reduced irradiation time compared to IMRT.[9] Nowadays IGBT meets the challenge of high precision EBRT such as VMAT, which is a non-invasive modality and does not require special skills to deliver a high conformal dose to the target volume while saving critical normal structures. To our knowledge no detailed dosimetric comparisons of IGBT with VMAT have so far been reported in the H&N region, such publications are available only for breast and cervical cancer.[10,11]

The purpose of this study is to present a dosimetric analysis regarding planning target volume (PTV) and OARs with the comparison of IGBT and VMAT for localized H&N cancer using identical CT data and contours.

Patients and methods

Patients' characteristics

Thirty-eight consecutive patients with T1-4 mobile tongue (n = 17), floor of mouth (n = 9) and base of tongue (n = 12) cancer treated between January 2013 and March 2017 at the National Institute of Oncology, Budapest, Hungary were selected for this study (Table 1). Primary lesions or tumor bed were treated with CT image based IGBT alone (n = 22) or after EBRT as a boost (n = 16). All T3-4 cases (n = 12) were base of tongue cancer treated exclusively with radiotherapy (EBRT + BT boost). The T4 tumors invaded the deep muscles of the tongue, without invasion into the mandible or other regions. Tumor excision was carried out in 18 patients. Ipsi- and contralateral submandibular glands (15 and 1) (iSMGs, cSMGs) were removed during surgery.

TABLE 1. Dosimetry of PTV

Parameters	IGBT n=38		VMAT n=38		p-value
	mean	S.D.	mean	S.D.	
V95 (%)	92.1	3.0	98.4	0.9	<0.05
V98 (%)	90.2	3.2	90.4	3.7	>0.05
V100 (%)	89.0	3.4	76.7	8.9	<0.05
D90 (%)	98.6	4.7	98.2	0.8	<0.05
D100 (%)	58.6	9.0	87.0	3.2	<0.05

DX = minimum relative dose of the planning dose delivered to X% of the PTV; IGBT = image guided high-dose-rate brachytherapy; n = number of patients for analysis; PTV = planning target volume; S.D. = standard deviation; VMAT = volumetric modulated arc therapy; VX = relative volume of the PTV receiving at least X% of the panning dose

Brachytherapy planning

The process of BT planning was described in details in our previous publication.[12] Under general anesthesia in the operating theatre plastic catheters (median 7, range 3–12) were implanted into the target volume located in 17 patients on the left, in 18 on the right side, and in 3 in the central region of the tongue/ floor of mouth/base of tongue. After implantation, all patients underwent CT imaging with 3 mm slice thickness including the primary tumor or tumor bed, the spinal cord, parotid glands (PAGs) on both sides and SMGs. The images were transferred to the Oncentra Brachy v4.3 (Elekta, Brachytherapy, Veenendaal, The Netherlands) treatment planning system. Gross tumor volume (GTV), clinical target volume (CTV) and PTV were contoured on CT images as follows. In non-surgical cases (definitive) palpation, visual inspection and MR images without CT-MRI fusion were used to determine GTV in the patients. CTV was defined as GTV + 5mm limited to mandible. In postoperative cases CTV was directly defined similarly to definitive cases using the preoperative MRI. For all cases PTV was the same as CTV without using any margin. Based on CT image sets, the mandible, the spinal cord, PAGs on both sides and SMGs - as OARs - were delineated. Mandible was not part of the PTV. After catheter reconstruction, treatment plans were made with geometrical optimization, complemented with graphical optimization by adjusting the isodose line in order to appropriately cover the PTV by the prescribed dose (PD) and keep the doses to OARs as low as possible.[13] Our aim was to obtain less than 0.40 for the dose non-uniformity ratio (DNR), the ratio of volumes receiving 1.5 times the PD and those receiving the PD, (V_{150}/V_{100}). At our institute the fractionation schedule was 15 x 3 Gy (45 Gy) for IGBT alone and 7 x 3 Gy (21 Gy) for IGBT after 50 Gy EBRT.

VMAT planning

For VMAT plans the same CT images and structure set were used as for IGBT. The contours applied for

IGBT plans were transferred from the Oncentra Brachy to the Eclipse v11 (Varian Medical Systems, Palo Alto, CA) treatment planning system using DICOM RT protocol. Due to this process, all contours of PTV and OARs were identical in both planning systems. In case of IGBT alone patients VMAT was set up for a total dose of 70 Gy (35 x 2 Gy), and for EBRT+IGBT patients a total dose of 20 Gy (10 x 2 Gy) was planned as a boost. VMAT plans were created with 6 MV photon energy beams using double partial arcs from gantry angle 110° to 250° to ensure the homogeneity of PTV dose coverage. As regards the dose constraints for OARs and target volume coverage, VMAT plans were optimized using the Varian RapidArc progressive resolution optimization algorithm (PRO) and AAA dose calculation algorithm. The objective for PTV was to deliver a dose of 95–107% of the PD. The dose constraints for PTV70Gy were as follows: V98% > 90%, V95% > 95%, V50% = 100%, V2% < 107%, for the spinal cord V2% < 45 Gy, for parotid glands Dmean < 24 Gy, for mandible V0.03cc < 70 Gy.

Dosimetric analysis

Based on dose-volume-histograms (DVHs), treatment plans of both techniques were dosimetrically analyzed. For evaluating conformity of dose distribution to PTV, the relative volume of the PTV receiving at least 95, 98 and 100% of the PD (V95, V98 and V100) and the minimum relative dose of the PD delivered to 90 and 100% of the PTV (D90 and D100) were calculated. The minimum relative doses of the PD delivered to the most exposed 0.1, 1 and 2 cm^3 of the organs (D0.1cm^3, D1cm^3 and D2 cm^3) were quantified for the assessment of doses to OARs. The salivary glands were classified as ipsilateral or contralateral based on the tumor location, and were dosimetrically evaluated. For the salivary glands, additional parameters such as the mean relative dose of the PD delivered to the organs (Dmean), D10, D30, D50, V10, V30 and V50 were also quantified. The dosimetric data for the parotid and submandibular glands were not evaluated for all patients, because in some cases the glands were excluded from the field-of-view of the CT scans, the volume was too small (for D1 and D2cm^3 calculation), or the target volume (tumor or tumor bed) was centrally located (Tables 4 and 5). The spinal cord was not detected in one case because it was excluded from the field-of-view of the CT scans (Table 3).

The mean value with standard deviation was used to describe dosimetric parameters for both

TABLE 2. Dosimetry of mandible and spinal cord

Parameters	IGBT		VMAT		*p*-value
	mean	S.D.	mean	S.D.	
Mandible, n=38					
D0.1cm^3 (%)	77.0	17.2	85.4	7.9	<0.05
D1cm^3 (%)	56.9	13.4	74.5	9.6	<0.05
D2cm^3 (%)	48.4	12.2	68.4	9.5	<0.05
Spinal cord, n=37*					
D0.1cm^3 (%)	9.7	2.6	12.3	4.1	<0.05
D1cm^3 (%)	6.8	2.0	10.8	3.7	<0.05
D2cm^3 (%)	5.9	1.9	10.0	3.6	<0.05

DXcm^3 = minimum relative dose of the planning dose delivered to most exposed X cm^3 of the organs; IGBT = image guided high-dose-rate brachytherapy; n = number of patients for analysis; S.D. = standard deviation; VMAT = volumetric modulated arc therapy.

* in one patient the spinal cord was not detected because it was excluded from the field-of-view of the CT scans

TABLE 3. Dosimetry of parotid gland

Parameters	IGBT		VMAT		*p*-value
	mean	S.D.	mean	S.D.	
ipsilateral side (n=34*)					
Dmean (%)	4.6	1.4	4.6	2.6	>0.05
D0.1cm^3 (%)	11.2	2.8	18.0	7.1	<0.05
D1cm^3 (%)	8.1	2.1	12.9	6.3	<0.05
D2cm^3 (%)	7.0	2.0	10.5	5.7	<0.05
D10 (%)	7.3	2.1	11.2	5.6	<0.05
D30 (%)	5.5	1.6	5.5	4.0	>0.05
D50 (%)	4.5	1.3	3.0	3.1	<0.05
V10 (%)	3.1	4.0	18.0	16.9	<0.05
V30 (%)	0.0	0.0	0.7	3.9	N.A.
V50 (%)	0.0	0.0	0.1	0.5	N.A.
contralateral side (n=35**)					
Dmean (%)	3.0	0.9	3.9	2.1	>0.05
D0.1cm^3 (%)	8.9	2.1	15.3	5.9	<0.05
D1cm^3 (%)	5.9	1.6	10.8	5.9	<0.05
D2cm^3 (%)	4.9	1.5	9.1	5.4	<0.05
D10 (%)	5.4	1.3	9.9	4.4	<0.05
D30 (%)	4.0	1.0	4.9	3.7	>0.05
D50 (%)	3.2	0.8	2.2	2.3	<0.05
V10 (%)	0.5	0.3	14.2	13.2	<0.05
V30 (%)	0.0	0.0	0.8	4.7	N.A.
V50 (%)	0.0	0.0	0.2	1.3	N.A.

Dmean = minimum relative dose of the planning dose delivered to the organs; DX = minimum relative dose of the planning dose delivered to X% of the PTV; DXcm^3 = minimum relative dose of the planning dose delivered to most exposed X cm^3 of the organs; IGBT = image guided high-dose-rate brachytherapy; n = number of patients for analysis; N.A. = not available; S.D. = standard deviation; VMAT = volumetric modulated arc therapy; VX = relative volume of the PTV receiving at least X% of the panning dose

* in one patient the parotid gland was not detected because it was excluded from the field-of-view of the CT scans, and in three patients parotid glands were not evaluated because of central implantation

** three patients were not evaluated because of central implantation

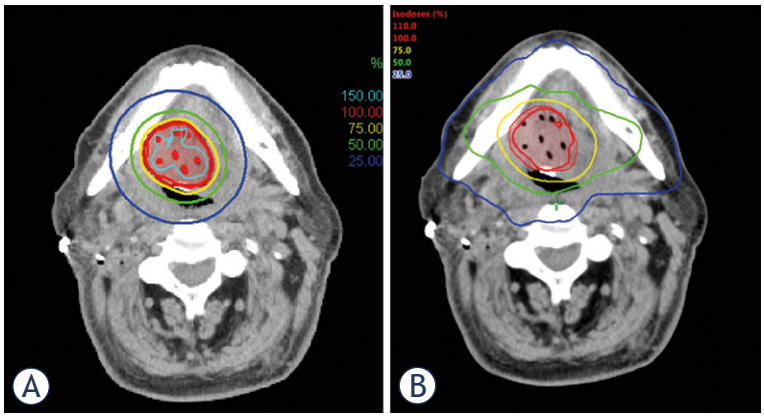

FIGURE 1. Representative dose distribution of **(A)** image guided high-dose-rate brachytherapy (IGBT) and **(B)** volumetric modulated arc therapy (VMAT).

TABLE 4. Dosimetry of submandibular gland

Parameters	IGBT		VMAT		*p*-value
	mean	S.D.	mean	S.D.	
ipsilateral side					
Dmean (%), n=20*	16.4	10.7	21.9	19.9	>0.05
D0.1cm^3 (%), n=20*	27.4	15.6	39.9	23.3	>0.05
D1cm^3 (%), n=18**	19.4	11.2	27.2	17.6	>0.05
D2cm^3 (%), n=17**	16.1	9.4	20.8	14.7	>0.05
D10 (%), n=20*	22.6	13.9	33.2	23.0	>0.05
D30 (%), n=20*	18.3	11.7	25.8	21.9	>0.05
D50 (%), n=20*	15.7	10.4	21.0	20.9	>0.05
V10 (%), n=20*	61.3	38.6	63.9	33.6	>0.05
V30 (%), n=20*	14.5	28.0	30.1	38.7	>0.05
V50 (%), n=20*	1.4	3.7	14.1	27.4	>0.05
contralateral side					
Dmean (%), n=34***	8.2	4.8	16.9	10.8	<0.05
D0.1cm^3 (%), n=34***	13.4	5.3	29.7	12.0	<0.05
D1cm^3 (%), n=32****	9.4	3.2	21.7	8.6	<0.05
D2cm^3 (%), n=32****	8.1	2.9	18.3	8.3	<0.05
D10 (%), n=34***	11.1	5.6	25.3	12.2	<0.05
D30 (%), n=34***	9.2	5.1	20.4	11.4	<0.05
D50 (%), n=34***	8.0	4.7	16.7	11.4	<0.05
V10 (%), n=34***	26.0	30.2	69.9	27.5	<0.05
V30 (%), n=34***	1.2	7.0	14.1	25.1	<0.05
V50 (%), n=34***	0.0	0.0	2.7	12.1	N.A.

Dmean = minimum relative dose of the planning dose delivered to the organs; DX = minimum relative dose of the planning dose delivered to X% of the PTV; DXcm^3 = minimum relative dose of the planning dose delivered to most exposed X cm^3 of the organs; IGBT = image guided high-dose-rate brachytherapy; n = number of patients for analysis; N.A. = not available; S.D. = standard deviation; VMAT = volumetric modulated arc therapy; VX = relative volume of the PTV receiving at least X% of the panning dose

* in fifteen patients the submandibular glands were resected by operation and three patients were not evaluated because of central implantation.

** two and three patients, respectively, were additionally excluded from the analysis of D1cm^3 and D2cm^3 because the volume was too small.

*** in one patient the submandibular gland was resected by operation and three patients were not evaluated because of central implantation.

**** two and two patients, respectively, were additionally excluded from the analysis of D1cm^3 and D2cm^3 because the volume was too small.

techniques, and the data were compared using the non-parametric Mann-Whitney U test with GraphPad Prism version 5.01 for Windows (GraphPad Software, San Diego, CA). The level of statistical significance was set at $p \leq 0.05$.

Results

The dosimetric parameters of PTV are presented in Table 2. Dose distribution of BT and VMAT are presented in Figure 1. The dose conformity was excellent with both techniques. V95 was significantly better with VMAT (98.4% *vs.* 92.1%, $p < 0.05$), but V100 was superior with IGBT (89.0% *vs.* 76.7%, $p < 0.05$). V98 was similar in both techniques (90.2% *vs.* 90.4% for IGBT and VMAT, $p > 0.05$, respectively). Relative dose coverage to PTV, D90 was statistically significantly better with IGBT (98.6% *vs.* 98.2%), probably without clinical consequences. However, D100 showed a reverse result (58.6% *vs.* 87.0%).

As for OARs, the mandible and the spinal cord were better protected by IGBT (Table 3). For doses to small volumes (D0.1cm^3, D1cm^3 and D2cm^3) significantly lower values were obtained with IGBT (*e.g.* D0.1cm^3 was 77.0% *vs.* 85.4% and 9.7% *vs.* 12.3% to the mandible and the spinal cord).

Doses to the salivary glands were generally lower with IGBT (Tables 4 and 5). Six parameters of ipsilateral PAGs (iPAGs) were significantly lower with IGBT than with VMAT (*e.g.* D0.1cm^3 was 11.2% *vs.* 18.0%, D10 was 7.3% *vs.* 11.2% and V10 was 3.1% *vs.* 18.0%, respectively) (Table 4). Two parameters (Dmean and D30) were identical for the two techniques (4.6% and 5.5%). Parameters of contralateral PAGs (cPAGs) showed the same tendency as iPAGs (Table 4). Dosimetry of iSMGs indicated that doses with IGBT were smaller than with VMAT, but no significant differences were found between the two techniques (Table 5). All dose parameters of cSMGs were significantly smaller with IGBT than with VMAT (*e.g.* Dmean was 8.2% *vs.* 16.9%, D10 was 11.1% *vs.* 25.3% and V10 was 26.0% *vs.* 69.9%, respectively) (Table 5).

Discussion

The comparison of new technologies in the H&N region is a very interesting area of research.[7] Sresty *et al.* compared plans of IGBT and IMRT for mobile tongue cancer directly, and found a very good dose conformity between the two techniques.[14] Our study also revealed good target coverage with both

IGBT and VMAT. Our results confirmed that the volumes irradiated by 100% of the PD were larger and the dose gradient around PTV was higher with IGBT than with VMAT - because of the physical characteristics of BT. Moreover, IGBT yielded better values in D90, but worse in D100. The majority of locoregional treatment failures occur within the target volumes irradiated with high doses by IMRT.[15,16] These regions are thought to represent areas of hypoxia and radiation resistant tumor cells, and may require higher doses to improve local control.[17] These observations might support the theory that the PTV of the primary tumor or tumor bed - if it is technically feasible - can be treated with IGBT.

Owosho *et al.* analyzed oral and oropharyngeal cancer patients and 96% of the osteoradionecrosis (ORN) affected regions of the jaw received doses over 60 Gy, suggesting >60 Gy as a threshold for ORN risk.[18] In the current research mean D0.1cm^3 of the mandible was 85.4% with VMAT, so 0.1cm^3 received at least 59.8 Gy (70 Gy x 0.854). The mandible was significantly better protected with IGBT than with VMAT, due to intensity modulation with stepping source technology avoiding high irradiation of the mandible.[1] IGBT provided safe and secure treatment for the mandible.

For tonsillar cancer patients Stieler *et al.* reported 41.6 Gy and 42.6 Gy as mean maximum dose to the spinal cord with IMRT (9 fields) and VMAT (single arc), respectively, including the neck region in the treatment fields.[19] In the direct comparison of plans of IGBT and IMRT for mobile tongue cancer, Sresty *et al.* reported maximum doses to the spinal cord from 9% to 14% with IGBT, whereas from 15.6% to 24.6% with IMRT.[14] Meanwhile our results of mean D0.1cm^3, which represents the maximum dose to the spinal cord, showed 9.7% (4.4 Gy) with IGBT and 12.3% (8.6 Gy) with VMAT ($p < 0.05$). The results were similar and doses to the spinal cord were acceptable for both techniques in patients, in whom only the primary lesion was irradiated.

Dose to PAGs is important in terms of xerostomia, because they produce up to 70% of the total stimulated saliva.[20-23] Owosho *et al.* analyzed the role of PAGs irradiation in the development of severe xerostomia defined as Grade 4 according to the LENT SOMA scales after IMRT, and reported that xerostomia occurred in a follow-up time of <6 months, when the Dmean to iPAG and cPAG was 43.8 Gy and 24.9 Gy, respectively.[23] They concluded that the incidence of xerostomia could be decreased by limiting the mean dose to both PAGs to values below 25 Gy. In our study the mean doses to iPAG and cPAG were 4.6% (3.2 Gy) and 3.9% (2.7 Gy) with VMAT and 4.6% (2.1 Gy) and 3.0% (1.4 Gy) with IGBT, respectively. Dose delivery to PAGs by both techniques probably has a little impact on xerostomia in patients, whose PTV includes only the primary tumor or tumor bed, but in IGBT the dose to PAGs was somewhat lower. Maintenance of adequate SMG function is also important in the reduction of xerostomia because SMGs produce about 20% to 30% of salivary output, including up to 90% of unstimulated salivary output.[24-27] Wang *et al.* reported SMG dosimetry using IMRT with or without cSMG sparing.[27] In their study the mean doses to iSMGs and cSMGs were 60.8 Gy and 20.4 Gy, in the cSMG-sparing group as opposed to the unspared group, where these parameters were 60.9 Gy and 57.4 Gy, respectively. They observed that xerostomia grades at 2 and 6 months post-IMRT were significantly lower among patients in the cSMG-sparing group than in the unspared group. In our study all parameters of cSMGs were smaller with IGBT than with VMAT ($p < 0.05$). Dmean of cSMGs with VMAT was 16.9% (11.8 Gy). Dmean of cSMGs with IGBT was 8.2% (3.7 Gy), about one third of the value with VMAT, so IGBT had a more significant effect on dose reduction to cSMGs.

A major source of concern with VMAT and IMRT is the higher low dose radiation to surrounding normal tissue, which potentially increases the risk of secondary malignancy.[17] As for our results, V10 with VMAT was appreciably large especially for PAG. Immobilization for precise irradiation and the possibility of tumor repopulation during the long treatment time can also be a problem with VMAT. On the other hand, technique sensitivity is one of the drawbacks of IGBT. However, some measures have been introduced for easy implantation, such as the use of a vinyl template or ultrasound guided technique.[5]

One of the limitations of our study is that the Task Group (TG)-43 formalism, implemented in our planning system for dose calculation, has not taken into consideration tissue heterogeneities.[28] However, Peppa *et al.* revealed that the absolute differences in the parameters are too small to warrant clinical importance in terms of tumor control or complication probabilities.[29] The second drawback is that the catheters in the target have a small tissue inhomogeneity effect. However, according to our investigation the variations in density in small volumes cause less than a 0.5% change in dosimetry. We are aware of that in EBRT the PTV should be larger than in BT, but our aim was to make comparison between two largely different irradiation

techniques, and since the same PTVs were used in plans of both treatment modalities in our study the dosimetric results apply only to the differences between BT and VMAT.

Though this article deals with the dosimetric and not the therapeutic comparison of the above mentioned two techniques, we would like to emphasize that the fractionation schedule, which we used in our BT treatment, was based on the European and American recommendations, where the suggested boost dose is 21-30/3 Gy with HDR after 45–50 Gy EBRT and the definitive dose is 45–60/3 Gy.[2,30] Using alfa/beta = 10 Gy and without taking into consideration the time factor, the calculated biological effective dose (BED) for BT alone (15 x 3 Gy) was 58.5 Gy, for EBRT (25 x 2 Gy) and BT boost (7 x 3 Gy) 87.3 Gy (60 Gy + 27.3 Gy), for EBRT alone (35 x 2 Gy) 84 Gy and for EBRT (25 x 2 Gy) and EBRT boost (10 x 2 Gy) 84 Gy (60 Gy + 24 Gy). We applied lower BT dose for BT alone because of the lack of long-term experiences with HDR BT.

Conclusions

This is the first study with direct dosimetric comparison between IGBT and VMAT for H&N cancer applying various parameters. Both techniques provided excellent target coverage, but IGBT was found superior in protecting OARs. Adverse events, such as xerostomia and osteoradionecrosis, derived from irradiation of OARs could be serious problems in the H&N cancer radiotherapy. Therefore, it is clinically important to keep the dose for OARs as low as possible. In this respect the results confirm the important role of interstitial RT in the era of new external beam RT techniques. To translate the results of these dosimetric findings into clinical practice, more patients and long term follow-up with prospective collection of toxicities are necessary.

References

1. Kovács G. Modern head and neck brachytherapy: from radium towards intensity modulated interventional brachytherapy. *J Contemp Brachytherapy* 2014; **6:** 404-16. doi: 10.5114/jcb.2014.47813
2. Mazeron JJ, Ardiet JM, Haie-Méder C, Kovács G, Levendag P, Peiffert D, et al. GEC-ESTRO recommendations for brachytherapy for head and neck squamous cell carcinomas. *Radiother Oncol* 2009; **91:** 150-6. doi: 10.1016/j.radonc.2009.01.005
3. Takácsi-Nagy Z, Oberna F, Koltai P, Hitre, E, Major T, Fodor J, et al. Long-term outcomes with high-dose-rate brachytherapy for the management of base of tongue cancer. *Brachytherapy* 2013; **12:** 535-41. doi: 10.1016/j.brachy.2013.07.001
4. Major T, Polgár C, Mangel L, Takácsi-Nagy Z, Somogyi A, Németh G. CT based conformal brachytherapy treatment planning. *Magy Onkol* 2000; **44:** 109-15. doi: HUON.2000.44.2.0109
5. Yoshida K, Takenaka T, Akiyama H, Yamazaki H, Yoshida M, Masui K, et al. Three-dimensional image-based high-dose-rate interstitial brachytherapy for mobile tongue cancer. *J Radiat Res* 2014; **55:** 154-61. doi: 10.1093/jrr/rrt079
6. Akiyama H, Yoshida K, Yamazaki H, Takenaka T, Kotsuma, T, Masui, K, et al. High-dose-rate interstitial brachytherapy for mobile tongue cancer: preliminary results of a dose reduction trial. *J Contemp Brachytherapy* 2014; **6:** 10-4. doi: 10.5114/jcb.2014.40726
7. Takácsi-Nagy Z, Martínez-Mongue R, Mazeron JJ, Anker CJ, Harrison LB. American Brachytherapy Society Task Group Report: Combined external beam irradiation and interstitial brachytherapy for base of tongue tumors and other head and neck sites in the era of new technologies. *Brachytherapy* 2017; **16:** 44-58. doi: 10.1016/j.brachy.2016.07.005
8. Gupta T, Agarwal J, Jain S, Phurailatpam R, Kannan S, Ghosh-Laskar S, et al. Three-dimensional conformal radiotherapy (3D-CRT) versus intensity modulated radiation therapy (IMRT) in squamous cell carcinoma of the head and neck: a randomized controlled trial. *Radiother Oncol* 2012; **104:** 343-8. doi: 10.1016/j.radonc.2012.07.001
9. Osborn J. Is VMAT beneficial for patients undergoing radiotherapy to the head and neck? *Radiography* 2017; **23:** 73-6. doi: 10.1016/j.radi.2016.08.008
10. Major T, Stelczer G, Pesznyák C, Mészáros N, Polgár C. Multicatheter interstitial brachytherapy versus intensity modulated external beam therapy for accelerated partial breast irradiation: A comparative treatment planning study with respect to dosimetry of organs at risk. *Radiother Oncol* 2017; **122:** 17-23. doi: 10.1016/j.radonc.2016.08.003
11. Sharma DN, Gandhi AK, Sharma S, Rath GK, Jagadesan P, Julka PK. Interstitial brachytherapy vs. intensity-modulated radiation therapy for patients with cervical carcinoma not suitable for intracavitary radiation therapy. *Brachytherapy* 2013; **12:** 311-6. doi: 10.1016/j.brachy.2012.10.003
12. Akiyama H, Major T, Polgár C, Takácsi-Nagy Z. Dose-volume analysis of target volume and critical structures in computed tomography image-based multicatheter high-dose-rate interstitial brachytherapy for head and neck cancer. *J Contemp Brachytherapy* 2017; **9:** 553-60. doi: 10.5114/jcb.2017.72581
13. Major T, Polgár C. Treatment planning for multicatheter interstitial brachytherapy of breast cancer - from Paris system to anatomy-based inverse planning. *J Contemp Brachytherapy* 2017; **9:** 89-98. doi: 10.5114/jcb.2017.66111
14. Sresty NVNM, Ramanjappa T, Raju AK, Muralidhar KR, Sudarshan G. Acquisition of equal or better planning results with interstitial brachytherapy when compared with intensity-modulated radiotherapy in tongue cancers. *Brachytherapy* 2010; **9:** 235-8. doi: 10.1016/j.brachy.2009.05.006
15. Bussels B, Maes A, Hermans R, Nuyts S, Weltens C, Van den Bogaert W. Recurrences after conformal parotid-sparing radiotherapy for head and neck cancer. *Radiother Oncol* 2004; **72:** 119-27. doi: 10.1016/j.radonc.2004.03.014
16. Chao KSC, Ozyigit G, Tran BN, Cengiz M, Dempsey JF, Low DA. Patterns of failure in patients receiving definitive and postoperative IMRT for head-and-neck cancer. *Int J Radiat Oncol Biol Phys* 2003; **55:** 312-21.
17. Teoh M, Clark CH, Wood K, Whitaker S, Nisbet A. Volumetric modulated arc therapy: a review of current literature and clinical use in practice. *Br J Radiol* 2011; **84:** 967-96. doi: 10.1259/bjr/22373346
18. Owosho AA, Tsai CJ, Lee RS, Freymiller H, Kadempour A, Varthis S, et al. The prevalence and risk factors associated with osteoradionecrosis of the jaw in oral and oropharyngeal cancer patients treated with intensity-modulated radiation therapy (IMRT): The Memorial Sloan Kettering Cancer Center experience. *Oral Oncol* 2017; **64:** 44-51. doi: 10.1016/j.oraloncology.2016.11.015
19. Stieler F, Wolff D, Schmid H, Welzel G, Wenz F, Lohr F. A comparison of several modulated radiotherapy techniques for head and neck cancer and dosimetric validation of VMAT. *Radiother Oncol* 2011; **101:** 388-93. doi: 10.1016/j.radonc.2011.08.023
20. Dawes C, Wood CM. The contribution of oral minor mucous gland secretions to the volume of whole saliva in man. *Arch Oral Biol* 1973; **18:** 337-42.
21. Sreebny LM. Saliva in health and disease: an appraisal and update. *Int Dent J* 2000; **50:** 140-61.

22. Humphrey SP, Williamson RT. A review of saliva: normal composition, flow, and function. *J Prosthet Dent* 2001; **85:** 162-9. doi: 10.1067/mpr.2001.113778

23. Owosho AA, Thor M, Oh JH, Riaz, N, Tsai CJ, Rosenberg H, et al. The role of parotid gland irradiation in the development of severe hyposalivation (xerostomia) after intensity-modulated radiation therapy for head and neck cancer: Temporal patterns, risk factors, and testing the QUANTEC guidelines. *J Craniomaxillofac Surg* 2017; **45:** 595-600. doi: 10.1016/j.jcms.2017.01.020

24. Eisbruch A, Rhodus N, Rosenthal D, Murphy B, Rasch C, Sonis S, et al. How should we measure and report radiotherapy-induced xerostomia? *Semin Radiat Oncol* 2003; **13:** 226-34. doi: 10.1016/S1053-4296(03)00033-X

25. Jellema AP, Doornaert P, Slotman BJ, Leemans CR, Langendijk JA. Does radiation dose to the salivary glands and oral cavity predict patient-rated xerostomia and sticky saliva in head and neck cancer patients treated with curative radiotherapy*? Radiother Oncol* 2005; **77:** 164-71. doi: 10.1016/j.radonc.2005.10.002

26. Dawes C. Rhythms in salivary flow rate and composition. *Int J Chronobiol* 1974; **2:** 253-79.

27. Wang ZH, Yan C, Zhang ZY, Zhang CP, Hu HS, Tu WY, et al. Impact of salivary gland dosimetry on post-IMRT recovery of saliva output and xerostomia grade for head-and-neck cancer patients treated with or without contralateral submandibular gland sparing: a longitudinal study. *Int J Radiat Oncol Biol Phys* 2011; **81:** 1479-87. doi: 10.1016/j.ijrobp.2010.07.1990

28. Nath R, Anderson LL, Luxton G, Weaver KA, Williamson JF, Meigooni AS. Dosimetry of interstitial brachytherapy sources: recommendations of the AAPM Radiation Therapy Committee Task Group No. 43. *Med Phys* 1995; **22:** 209-34. doi: 10.1118/1.597458

29. Peppa V, Pappas E, Major T, Takácsi-Nagy Z, Pantelis E, Papagiannis P. On the impact of improved dosimetric accuracy on head and neck high dose rate brachytherapy. *Radiother Oncol* 2016; **120:** 92-7. doi: 10.1016/j.radonc.2016.01.022

30. Nag S, Cano ER, Demanes DJ, Puthawala AA, Vikram B. The American Brachytherapy Society recommendations for high-dose-rate brachytherapy for head-and-neck carcinoma. *Int J Radiat Oncol Biol Phys* 2001; **50:** 1190-8.

research article

Comparison of anteroposterior and posteroanterior projection in lumbar spine radiography

Erna Alukic[1], Damijan Skrk[2], Nejc Mekis[1]

[1] University of Ljubljana, Faculty of Health Sciences, Medical Imaging and Radiotherapy Department, Ljubljana, Slovenia
[2] Slovenian Radiation Protection Administration, Ljubljana, Slovenia

Radiol Oncol 2018; 52(4): 468-474.

Received 30 January 2018
Accepted 18 April 2018

Correspondence to: Nejc Mekiš, Ph. D., University of Ljubljana, Faculty of Health Sciences, Medical Imaging and Radiotherapy Department, Zdravstvena pot 5, SI-1000 Ljubljana, Slovenia. Phone: +368 1 300 11 51; Fax: +386 1 300 11 19; E-mail: nejc.mekis@zf.uni-lj.si

Disclosure: No potential conflicts of interest were disclosed.

Background. The aim of the study was to compare patient radiation dose and image quality in planar lumbar spine radiography using the PA and AP projection in a large variety of patients of both sexes and different sizes.

Patients and methods. In the first phase data of image field size, DAP, effective dose and image quality were gathered for AP and PA projection in lumbar spine imaging of anthropomorphic phantom. In the second phase, data of BMI, image field size, diameter of the patient's abdomen, DAP, effective dose and image quality were gathered for 100 patients of both sexes who were referred to lumbar spine radiography. The patients were divided into two groups of 50 patients, one of which was imaged using the AP projection while the other the PA projection.

Results. The study on the phantom showed no statistically significant difference in image field size, DAP and image quality. However, the calculated effective dose in the PA projection was 25% lower compared to AP projection ($p = 0.008$). Measurements on the patients showed no statistically significant difference between the BMI and the image field size. In the PA projection, the thickness of abdomen was 10% ($p < 10^{-3}$) lower, DAP 27% lower ($p = 0.009$) and the effective dose 53% ($p < 10^{-3}$) lower than in AP projection. There was no statistically significant difference in image quality between the AP and the PA projection.

Conclusions. The study results support the use of the PA projection as the preferred method of choice in planar lumbar spine radiography.

Key words: lumbar spine radiography; PA projection; dose reduction; image quality

Introduction

In general radiography lumbar spine imaging is one of procedures with the highest patient radiation dose.[1-3] In order to reduce patient dose, one of the methods is the replacement of the conventional anteroposterior (AP) projection with the posterioanterior (PA) projection.[4-11] Even though the reviewed professional literature[12-14] still quotes AP projection as the method of choice for most of the procedures in plane radiography, the dose reduction with the use of PA projection was shown in several articles for a number of procedures, such as imaging of the clavicle[4], sacroiliac joint[5], abdomen[6], knee joint[15] and lumbar spine.[7,8,16]

Mc Entee and Kinsella (2010) noted that the use of PA projection of the clavicle can result in dose decrease of 28% to the eyes, 56% to the breast and 78% to the thyroid. Although the image quality was better in the AP projection by 6.3%, the images performed in the PA projection were diagnostically acceptable. Mekis *et al.*[5] investigated how dose reduction to the patient can be achieved with the use of PA projection in the sacroiliac joint imaging. The results show the reduction of DAP value by 12.6% and the reduction of entrance skin dose (ESD) by

21% when the PA projection is used. The reduction of dose to the patient was also shown in the article by Nic an Ghearr and Brennan[6] when they used PA projection for the imaging of the abdomen. They concluded that a 31% of ESD decrease and 56% decrease in effective dose can be observed when using PA projection with no statistically significant difference in the image quality.

Patient dose reduction in the lumbar spine radiography has already been explored by several authors. Brennan and Madigan[8] investigated the dose reduction to female patients when using PA instead of the conventional AP projection in lumbar spine radiography. They concluded that tissue displacement caused dose reduction with the use of PA projection. In their study the EDS was reduced by 38.6% without statistically significant difference in image quality.

Davey and England[7] reported that with the use of PA projection of lumbar spine, the effective dose can be decreased by 19.8%. The research was performed on the anthropomorphic phantom. They observed a loss of image quality in the PA projection but without statistically significant difference.

Based on the literature the dose reduction in the PA projection is the result of various factors, such as tissue compression (smaller diameter)[8], bone position as the protection of the internal organs and longer distance from the primary source.[7]

The PA imaging process is simple to perform, does not require any additional equipment nor increases the costs, which is often a limiting factor in many diagnostic procedures.[7] However, the PA projection has its limitations and cannot be used in emergency patients with lumbar spine injuries.[12-14]

The previous research regarding comparison between the AP and PA projections of the lumbar spine radiography were conducted on anthropomorphic phantom and on women within the weight range 70 ± 5 kg and 155 to 175 cm height range. No extensive research has yet been conducted on a larger population, including both genders and larger weight range. Therefore, the aim of the study was to determine the impact of PA projection in lumbar spine radiography to patient dose, tissue displacement and influence on image quality in a large variety of patients of both sexes and different sizes.

Patients and methods

Cross-sectional study with the experimental research method was performed in this study. The study was conducted in two phases. In the first phase, the measurements were performed on an anthropomorphic phantom, and in the second phase, on 100 patients that were referred to lumbar spine radiography and were randomly divided into two groups of equal size. One group was imaged using the AP projection while the second group using the PA projection.

In both phases, the measurements were performed at the Radiology Department of the Community Health Centre Ljubljana on the Siemens Axiom Aristos FX Plus system. The grid ratio used in the study was 15:1, with 80 line/cm, the focus-detector distance was 115 cm. Prior to and during the study, the quality assurance test was performed on all parts of the x-ray machine.

Beam positioning in AP and PA projections was performed according to the literature.[12-14,17] The longitudinal line of the central ray was positioned in the centre of the body line and at the transverse line at the lowest point of the rib cage.

For each patient, the image size area was measured to enable the comparison of the image field size between AP and PA projection and to ensure that the image size would not affect the DAP and influence the calculation of dose received by the phantom and the patients.

Dosimetry

The dose area product (DAP) was measured using a built-in DAP which calibration was tested prior to the study.

Phantom measurements

Prior to the patient study, the measurements were carried out on the anthropomorphic phantom PBU60 (Kyotogagaku Co., Ltd, Japan) that has the same attenuation factor as a patient with weight of 50 kg and a height of 165 cm (Figure 1). Measurements on the phantom were performed using the same protocol as in the lumbar spine imaging in the department where the study was conducted. In both projections, the tube voltage was 79 kV and was not changed during the measurements. The central chamber of automatic exposure control (AEC) was used in both projections. The additional copper filtration of 0.1 mm was used in all the exposures. The phantom was imaged 10 times, 5 times in the AP and then 5 times in the PA projection. The phantom and the x-ray system were moved and reset for each exposure, so that the error of the positioning was included in the measurements.

FIGURE 1. Image of the anthropomorphic phantom used in the study.

Patient measurements

The second part of the study was performed on 100 patients who were referred to the lumbar spine radiography. The patients were randomly divided into two groups of 50. All of the patients were measured and weighted and their BMI was calculated. The exposure parameters were the same as in the phantom measurements and did not differ in the AP and PA projection. Before each exposure, the thickness of the patient's abdomen at the part of the transverse beam position (lowest point of the rib cage) was measured to determine whether the PA projection showed flattening of the excess abdomen.

The approval of the National Medical Ethics Committee was obtained prior to the study. All the participants were informed about the purpose of the study and gave a written consent to participate in the study. None of the patients declined the participation in the study.

Image quality

The images were assessed by three experienced radiology specialists working in the Health Community Center Ljubljana, with more than 5 years of experience. A blind randomized study was used, and all images were assessed on the same diagnostic monitor. All 110 radiographs were assessed on a 5-point scale, in the same way as in study conducted by Davey and England[7], where a 5-point Likert score rating was used. The ratings on the scale were as follows: score 1 - insufficient; score 2 - sufficient; score 3 - well; score 4 - very good and the score 5 - excellent.

The images were assessed according to the following criteria, which are listed in the guidelines[18]:

1. Complete visualisation of the lumbar spine and sacrum.
2. Visually sharp imaging, as a single line, of the upper and lower-plate surfaces in the centred beam area.
3. Visualisation of the intervertebral spaces in the centred beam area.
4. Visually sharp imaging of the pedicels, transverse processes, spinous processes and intervertebral joints.
5. Visualisation of the sacroiliac joints
6. Visually sharp imaging of the cortical and trabecular structures

For each criterion, a minimum possible score was 1 and a maximum possible score was 5. Scores were achieved in a way that each image could receive a minimum 6 and a maximum 30 score. Next, the average score of all three evaluators was calculated for each image.

During the assessment, it was not possible to change the contrast of the image or use a magnification or take measurements on the pictures which could indicate a PA projection.

Effective dose calculations

The effective dose was calculated using the Monte Carlo simulation program PCXMC 2.0 (STUK, Radiation and Nuclear Safety Authority in Finland). The image field size, weight and height were inserted into the program for each patient individually. The effective dose calculations were then performed for each patient according to the Monte Carlo simulation and the measured DAP value.

Statistical analysis

All the measurements were processed with the IBM SPSS STATISTICS version 23. Shapiro-Wilk test was used to check the normal distribution of the sample. For the phantom measurements, a non-parametric Mann-Whitney U test was used. For the patient study, the T-test for independent samples and Mann-Whitney U test were performed. Cohen's coefficient Kappa was used to check the level of matching of the assessors. The significance of $p < 0.05$ was used for all the tests. The results DAP and effective dose are presented with relative difference and standard mean error (relative difference ± standard mean error).

TABLE 1. Basic statistical characteristics of the phantom study

Variable	Projection	Mean	Standard deviation	Median	Minimum	Maximum
Imaging field size (cm²)	AP	725.5	120.0	690.1	587.4	913.5
	PA	788.1	66.2	770.3	723.6	874.5
Dose-area product (μGy m²)	AP	26.7	3.6	25.9	22.4	32.1
	PA	28.6	2.0	28.0	26.7	31.0
Effective dose (μSv)	AP	117	18	114	95	144
	PA	85	5	83	80	91
Average image estimation	AP	27.5	1.3	27.0	26.3	29.7
	PA	27.3	1.1	27.7	25.3	28.0

TABLE 2. Results of patient study

Variable	Projection	Mean	Standard deviation	Median	Minimum	Maximum
Body mass index	AP	26.6	3.2	26.3	19.7	35.2
	PA	26.6	4.0	26.6	20.0	35.7
Imaging field size (cm²)	AP	822.8	62.2	832.5	653.4	992.0
	PA	830.8	65.4	848.4	630.9	941.1
Patient's abdominal diameter (cm)	AP	23.6	4.0	24.0	16.0	30.0
	PA	21.2	2.8	22.0	15.5	28.0
Dose-area product (μGy m²)	AP	61.0	30.9	55.4	21.6	137.6
	PA	44.7	19.8	41.4	15.3	94.5
Effective dose (μSv)	AP	169	72	159	55	346
	PA	79	24	77	45	136
Average image estimation	AP	27.4	1.5	27.9	23.3	29.7
	PA	27.5	1.4	28	24.7	29.7

Results

Phantom study

In the phantom study, 10 measurements of DAP and 30 image quality assessments were obtained. The basic statistical characteristics of the measurement (imaging field size, DAP, effective dose and image quality assessment) performed on the phantom are shown in the Table 1. There was no statistically significant difference between imaging filed size ($p = 0.310$), DAP ($p = 0.310$) and image quality assessment ($p = 0.690$). The effective dose calculations showed a 25 ± 5% lower value ($p = 0.008$) when the phantom was imaged in the PA projection.

Patient study

In the second part of the study, a total of 100 BMI, image field size, abdominal diameter, DAP, effective dose and 300 image quality assessments were collected. The results of all the listed values are summarized in the Table 2.

First, an analysis of the imaging filed size and the BMI was performed. The PA and AP group were compared with respect to BMI distribution using the independent samples T test and no statistically significant difference was found between the groups ($p = 0.949$). The image field size analysis using Mann Whitney U test showed the same result, confirming there was no statistically significant difference ($p = 0.391$). According to the obtained results, comparison of all the other values was performed.

The use of a PA projection instead of the standard AP resulted in a decrease of the patient abdominal diameter by 10% (2.4 cm). The results were analysed using independent samples T test that showed a statistically significant difference ($p < 10^{-3}$) between the abdominal thickness of AP and

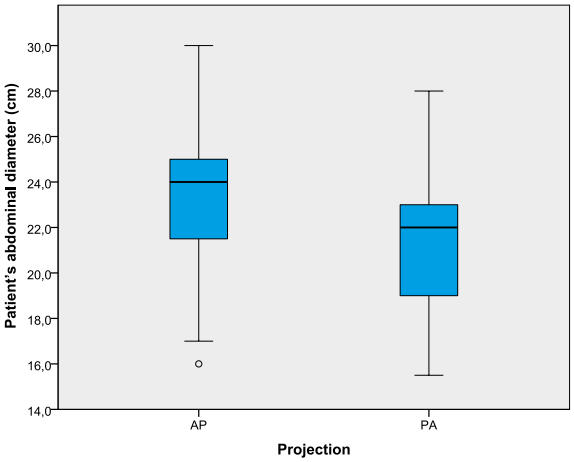

FIGURE 2. The comparison of the patient's abdominal diameter in AP and PA projection.

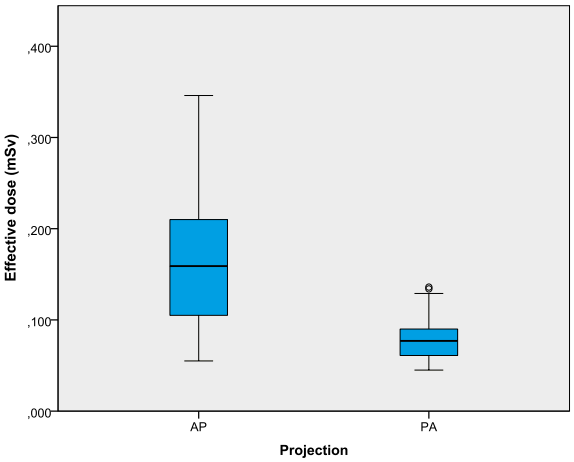

FIGURE 4. The comparison of the effective dose in both projections.

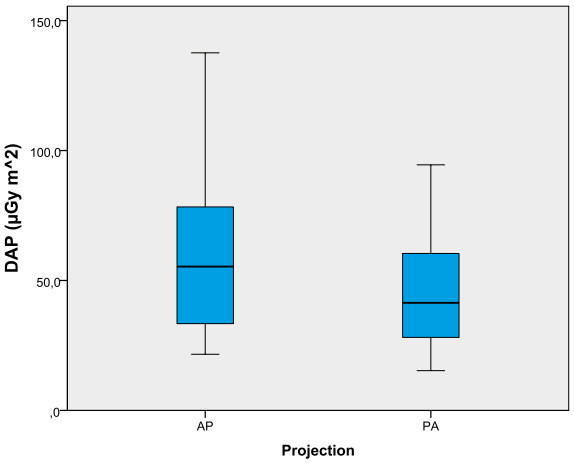

FIGURE 3. The comparison of DAP between the AP and PA projection.

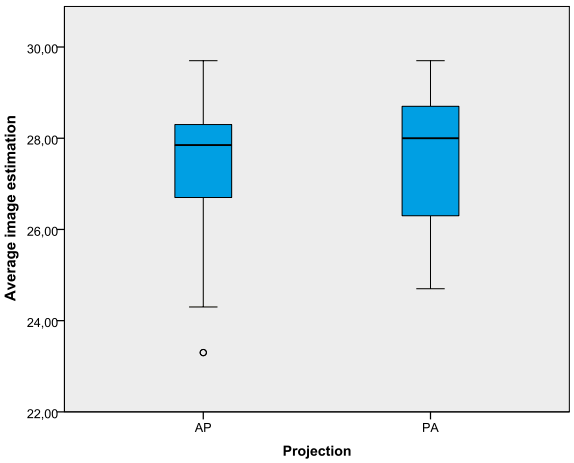

FIGURE 5. Graphical comparison of the average image estimation between the AP and PA projection.

PA projection of lumbar spine (Figure 2). The average DAP value was 16.3 µGym^2 (27 ± 7%) lower in the PA projection. Nonparametric Mann-Whitney U test, showed a statistically significant differences ($p = 0.009$) between the DAP in the AP and PA projections (Figure 3). The average effective dose was 90 µSv (53 ± 3%) lower in PA projection. The Mann Whitney U test shows statistically significant difference of $p < 10^{-3}$ (Figure 4). There was no statistically significant difference between the image quality ($p = 0.690$) in the AP and PA projection (Figure 5).

Cohens Kappa coefficient showed no matching between the assessors, so we also tested the difference between AP and PA projection for each assessor separately and found that there were no statistically significant differences between AP and PA projection in individual assessors ($p = 0.091$; $p = 0.416$; $p = 0.411$).

Discussion

The aim of the study was to compare patient radiation dose and image quality in lumbar spine plane radiography using the PA and AP projection in a large variety of patients of both sexes and different sizes.

We found that the use of PA projection leads to a reduction of DAP and effective dose by 27% and 53% respectively with no statistically significant impact on image quality. The main parameters that influence the dose reduction were BMI[19,20], size of imaging field[21] and the diameter of the patient.[8] As

the difference in the BMI can influence the patient dose, the differences in BMI between the AP and PA projection were explored. In this study, the BMI and the size of imaging field had no statistically significant difference, therefore we can conclude that the dose reduction was due to the use of PA projection.

The differences in the diameter of the abdomen between the patients in AP and PA projection was 10% which is in agreement with the study conducted by Brennan and Madigan[8], where the difference between AP and PA projection was 9.6%.

In the phantom study there was no statistically significant difference between DAP in AP and PA projection. Such results were expected because the phantom is made of a rigid material that cannot be dispersed and consequently the diameter of the phantom does not change. The results of the current and previous studies[8] confirm that the diameter of the patient has a large influence on the patient dose. In the patient study, a statistically significant difference was established between DAP in both projections, with the average DAP value being 27% lower in PA projection. Similar results in DAP reduction were obtained in the research conducted by Mekis *et al.*[5] where an average of 12.6% reduction in sacroiliac joint imaging was reported, and in the study by Nic an Ghearr and Brennan (1998)[6] where an average DAP reduction in imaging of the abdomen by 31% was evidenced.

Statistically significant difference in effective dose between the AP and PA projections were found in both parts of the study. In the phantom study, there was a decrease of effective dose by an average of approximately 27%, while in the patient study, an average 53% decrease was observed. The difference in results obtained in the phantom and the patient is due to tissue redistribution in the patients, leading to reduced thickness of the imaged area. The findings of the current study are consistent with those of previous research.[4,6-8] Nic an Ghearr and Brennan[6] documented that with the use of PA projection the effective dose in abdomen imaging in plane radiography can be reduced by an average of 56%. The results obtained in a phantom study by Davey and England[7] indicate that the effective dose in lumbar spine radiography can be reduced by an average of 19.8%. The difference between the dose to internal organs in both projections was not investigated, as was the case in the study by Davey and England[7], and by which we could confirm additional advantages of the PA projection regarding the patient dose.

No statistically significant difference was found in the comparison of the image quality of radiographs gained with AP and PA projection in both parts of the study. Most of the studies investigating the difference between the AP and PA projection do not identify any difference in the image quality between the projections. Only in the study conducted by Mc Entee and Kinsella[4], an improvement of image quality by 6.3% was reported in the AP projection. The authors, however, claim that despite reduced quality, the images performed in the PA projection were still diagnostically acceptable. Tsuno and Shu[22] argue that the PA projection of the lumbar spine is preferred because of the anatomy of the body part and the curve of the lumbar spine that is imaged better in the PA than in the AP projection.

The decrease of the patient comfort for patients with acute injuries, stomach pains, and respiratory distress are the restrictions for the PA projection of the lumbar spine radiography, which are described by Davey and England[7] and Chaparian *et al.*[11] In certain pathologies, the AP projection cannot be replaced by the PA projection, however, most of the patients can be imaged in the PA projection.

The PA projection is a technique that does not require any additional equipment and therefore brings no additional costs. It can be managed quickly without discomfort to the patient and loss of diagnostically important information with a significant decrease of the dose received by the patient.

Conclusions

The DAP reduction of approximately 27% and effective dose reduction of approximately 53% is achievable by using the PA instead of a standard AP projection in lumbar spine radiography. The change of the projection has no influence on the image quality ($p = 0.690$). The results of the study support the use of the PA projection as the preferred method of choice given that the lumbar spine imaging is one of the procedures in the plane radiography with the highest patient radiation dose.

Acknowledgements

We would like to thank the entire radiology team of the Community Health Centre Ljubljana for enabling the performance of this study, and for their support in carrying out the practical part of research.

References

1. European Commission. *European guidelines on quality criteria for diagnostic reference levels in thirty-six european countries*. Luxembourg; 1996.
2. European Union. Diagnostic Reference Levels in Thirty-six European Countries. Part 272. *Radiat Prot* 2014; **180:** 1-73.
3. Mekis N, Zontar D, Skrk D. The effect of breast shielding during lumbar spine radiography. *Radiol Oncol* 2013; **47:** 26-31. doi: 10.2478/raon-2013-0004
4. Mc Entee MF, Kinsella C. The PA projection of the clavicle: a dose-reducing technique. *Radiat Prot Dosimetry* 2010; **139:** 539-45. doi: 10.1093/rpd/ncp291
5. Mekis N, Mc Entee MF, Stegnar P. PA positioning significantly reduces testicular dose during sacroiliac joint radiography. *Radiography* 2010; **16:** 333-8. doi: 10.1016/j.radi.2010.04.003
6. Nic an Ghearr FA, Brennan PC. The PA projection of the abdomen: A dose reducing technique. *Radiography* 1998; **4:** 195-203. doi: 10.1016/S1078-8174(98)80046-1
7. Davey E, England A. AP versus PA positioning in lumbar spine computed radiography: Image quality and individual organ doses. *Radiography* 2015; **21:** 188-96. doi: 10.1016/j.radi.2014.11.003
8. Brennan PC, Madigan E. Lumbar spine radiology: Analysis of the posteroanterior projection. *Eur Radiol* 2000; **10:** 1197-201. doi: 10.1007/s003309900272
9. Heriard JB, Terry JA, Arnold AL. Achieving dose reduction in lumbar spine radiography. *Radiol Technol* 1993; **65:** 97-103
10. Ben-Shlomo A, Bartal G, Mosseri M, Avraham B, Leitner Y, Shabat S. Effective dose reduction in spine radiographic imaging by choosing the less radiation-sensitive side of the body, Technical Report. *The Spine Journal* 2016; **16:** 558-63. doi: 10.1016/j.spinee.2015.12.012
11. Chaparian A, Kanani A, Baghbanian M. Reduction of radiation risks in patients undergoing some X-ray examinations by using optimal projections: A Monte Carlo program-based mathematical calculation. *J Med Psys* 2014; **39:** 32-9. doi: 10.4103/0971-6203.125500
12. Swallow RA, Naylor E, editors. *Clark's positioning in radiography.* 11th edition. London: Butterworth Heinemann; 1996. p. 166-70.
13. Lipovec V, Mekiš N, Starc T. *Rentgenske slikovne metode in protokoli.* 2. dopolnjena izdaja. Ljubljana: UL, Zdravstvena fakulteta; 2011. p. 253-90.
14. Frank ED, Long BW, Smith BJ. *Merrill's atlas of radiographic positioning & procedures.* 11th edition. St. Louis: Mosby/Elsevier; 2007. p. 371-458.
15. Farrugia Wismayer E, Zarb F. Radiography of the knee joint: A comparative study of the standing partial flexion PA projection and the standing fully extended AP projection using visual grading characteristics (VGC). *Radiography* 2016; **22:** 152-60. doi: 10.1016/j.radi.2015.10.002
16. Frank ED, Stears JG, Gray JE, Winkler NT, Hoffman AD. Use of the posteroanterior projection: A method of reducing x-raw exposure to specific radiosensitive organs. *Radiol Technol* 1983; **54**: 343-7.
17. Bontrager KL. *Textbook of radiographic positioning and related anatomy.* 3rd edition. St. Louis: Mosby Year Book; 1993. p. 241-65.
18. Busch HP, Decker MD, Schilz C, Jockenhöfer A, Busch MD, Anschütz M. Image quality and dose management for digital radiography. *Qual Assur* 2004; p. 24-51.
19. Yanch JC, Behrman RH, Hendricks MJ, McCall JH. Increased radiation dose to overweight and obese patients from radiographic examinations. *Radiology* 2009; **252:** 128-39. doi: 10.1148/radiol.2521080141
20. Mekis N. Vpliv indeksa telesne mase na obsevanost pacientov pri slikanju medenice. *Bilten* 2017; **34**: 21-4.
21. Karami V, Zabihzadeh M. Beam Collimation during lumbar spine radiography: a retrospective. *J Biomed Phys Eng* 2017; **7:** 101-6.
22. Tsuno MM, Shu GJ. Posteroanterior versus anteroposterior lumbar spine radiology. *J Manip physilogical Ther* 1990; **13:** 144-151.

Radiol Oncol 2018; 52(4): 353-364.
doi: 10.2478/raon-2018-0044

Sodobna dognanja v magnetnoresonančni diagnostiki hepatoceličnega raka

Horvat N, Monti S, Oliveira BC, Rocha CCTR, Giancipoli RG, Mannelli L

Izhodišča. Rak jeter je šesti najpogostejši rak na svetu in drugi najpogostejši vzrok umrljivosti za rakom. Kronične jetrne bolezni, povzročene z virusnimi infekcijami, zlorabo alkohola ali drugimi dejavniki lahko vodijo v cirozo. Ciroza je najpomembnejši klinični dejavnik tveganja za hepatocelični rak (HCC), pri čemer se navadna jetrna arhitektura izmenja s fibroznimi septi in različnimi noduli. Spremembe so lahko benigne regenerativne in se stopnjujejo do HCC, ter imajo različne slikovne značilnosti.

Raziskave govorijo v prid veliki občutljivosti in specifičnosti magnetnoresonančnega (MR) slikanja v primerjava z računalniško tomografijo (CT) in ultrazvokom (UZ). Nadgradnje standardnega protokola izboljšujejo detekcijo HCC. Takšne nadgradnje so MR s hepatobiliarnimi kontrastnimi sredstvi, nove sekvence, kot so difuzijsko poudarjeno slikanje z navideznim difuzijskim koeficientom (*DWI with APC*) ter subtrakcijsko slikanje, večravninska meritev in hepatobiliarna faza. Ugotavljamo prednostih takšni preiskav predvsem pri majhnih, dobro-diferenciranih HCC in HCC po zdravljenju.

Zaključki. Sodobne tehnike, kot so kvantificiranje jetrnih in znotrajlezijskih maščob in železa, magnetnoresonančna elastografija, radiomika, radiogenomika in preiskave PET-MR, veliko obetajo. Omogočajo prepoznavo novih slikovnih bioloških označevalcev, ki opisujejo tmorsko mikrookolje. V prihodnje bi lahko pripomogle k boljši izbiri načina zdravljenja HCC.

Radiol Oncol 2018; 52(4): 365-369.
doi: 10.2478/raon-2018-0037

Kriteriji RECIST, prilagojeni za oceno zdravljenja z imunoterapijo (iRECIST) in simptomatski pseudoprogres pri bolnikih z nedrobnoceličnim rakom pljuč

Vrankar M, Unk M

Izhodišča. Nenavadni odzivi med zdravljenjem z imunoterapijo so nov izziv v vsakdanji onkološki praksi. Sprejeta so bila nova merila za oceno odziva na imunoterapijo, t.i. kriteriji iRECIST. Po teh kriterijih poslabšanje stanja zmogljivosti bolnika, pri katerem ugotavljamo pseudoprogres, predstavlja resnično napredovanje maligne bolezni.

Metode. Opravili smo sistematični pregled literature z uporabo več elektronskih podatkovnih baz z naslednjimi iskalnimi kriteriji: simptomatski pseudoprogres, atipični odziv, imunoterapija in pljučni rak.

Rezultati. V literaturi smo našli pet poročil o sedmih bolnikih z rakom pljuč, ki so jih zdravili z imunoterapijo in so izpolnjevali merila za vključitev v analizo. V članku smo predstavili tudi izkušnjo bolnice s pseudoprogresom po le enem odmerku imunoterapije, ki smo jo zdravili na Onkološkem inštitutu v Ljubljani.

Zaključki. Po pregledu literature in na podlagi našega primera ugotavljamo, da kriteriji iRECIST za odgovor na imunoterapijo pri nekaterih bolnikih z nedrobnoceličnim rakom pljuč ne zadoščajo za razlikovanje pravega napredovanja rakave bolezni od pseudoprogresa. Nujno potrebujemo natančnejše metode za ocenjevanje odgovora na zdravljenje z imunoterapijo.

Radiol Oncol 2018; 52(4): 370-376.
doi: 10.2478/raon-2018-0039

Stopnja diagnosticiranega raka ščitnice in z njim povezani dejavniki tveganja pri bolnikih s ščitničnimi vozliči razvrščenimi v kategorijo Bethesda III

Mileva M, Stoilovska B, Jovanovska A, Ugrinska A, Petrushevska G, Kostadinova-Kunovska S, Miladinova D, Majstorov V

Izhodišča. Ultrazvočno vodena aspiracija s tanko iglo (FNA) je standarden postopek v diagnostiki ščitničnih vozličev in odločanja, kateri bolniki potrebujejo kirurško zdravljenje. Atipije nejasnega pomena ali folikularna lezija nedoločenega pomena, kot ju klasificira Sistem za poročane ščitnične citologije Bethesda, je diagnostična kategorija, katere tveganje za malignom je 5–15 %. Namen raziskave je bil pregledati citološke in patološke izvide ter klinične in ultrazvočne podatke ščitničnih vozličev z atipijo nejasnega pomena ali folikularno lezijo nedoločenega pomena ter oceniti stopnjo malignosti ter proučiti dejavnike tveganja, povezane z malignim izidom.

Material in metode. Analizirali smo 112 ščitničnih vozličev z atipijo nejasnega pomena ali folikularno lezijo nedoločenega pomena pri 105 bolnikih. Kirurško smo odstranili 85 (75,9 %) vozličev, s ponavljajočimi FNA smo spremljali 21 (18,8 %), klinično pa 6 (5,3 %) vozličev. Vsakega od vozličev smo uvrstili v skupino ali benigni ali maligni, potem pa smo primerjali klinične podatke bolnikov in ultrazvočne značilnosti vozličev.

Rezultati. Rak smo diagnosticirali v 35 primerih (31,2 %), benignih vozličev pa je bilo 77 (68,8 %). Najpogostejša oblika raka je bila Papilarni rak ščitnice (58,1 %), folikularno obliko papilarnega raka ščitnice pa smo ugotovili v 25,8 %. Statistično značilni dejavniki tveganja za nastanek raka so bili mladost bolnikov, manjša velikost vozličev, hipoehogenost vozličev in prisotnost kalcinacij.

Zaključki. Stopnja malignosti ščitničnih vozličev z atipijo nejasnega pomena ali folikularno lezijo nedoločenega pomena je bila v naši raziskavi višja kot jo ocenjuje sistem Bethesda. Pri odločitvi o zdravljenju bolnikov je potrebno upoštevati klinične in ultrazvočne dejavnike.

Radiol Oncol 2018; 52(4): 377-382.
doi: 10.2478/raon-2018-0047

Ultrazvočna meritev premera ovojnice optičnega živca za oceno tekočinskega stanja bolnic s težko preeklampsijo

Bržan-Šimenc G, Ambrožič J, Prokšelj K, Tul N, Cvijić M, Mirković T, Lackner HK, Lučovnik M

Izhodišča. Eden od najpogostejših življenje ogrožajočih zapletov preeklampsije je pljučni edem. Namen raziskave je bil opredeliti uporabnost ultrazvočne meritve premera optičnega živca kot kazalca tekočinskega stanja in pljučne kongestije pri bolnicah s težko preeklampsijo.

Bolniki in metode. Vključili smo 30 bolnic s težko preeklampsijo. Ultrazvočno meritev premera optičnega živca (3 mm za zrklom) in ultrazvočni pregled pljuč smo opravili v 24 urah do poroda. Analizirali smo povezavo med premerom ovojnice optičnega živca in vsoto B-linij (»*kometov*«) v parasternalnih medrebrnih prostorih obojestransko. Za statistično analizo smo uporabili Pearsonov koeficient korelacije; vrednost $p < 0,05$ je bila statistično značilna.

Rezultati. Srednja vrednost premera optičnega živca je bila 5,7 mm (razpon 3,8 do 7,5 mm). Srednja vrednost vsote B linij v parasternalnih medrebrnih prostorih je bila 19 (razpon 0 do 24). Premer optičnega živca je bil statistično značilno povezan s količino B linij parasternalno ($r2 = 0,464$; $p < 0,001$).

Zaključki. Ultrazvočna meritev premera ovojnice optičnega živca korelira z obsegom pljučne kongestije pri bolnicah s težko preeklampsijo in bi lahko bila uporabna kot hitra neinvazivna metoda za oceno tekočinskega stanja pri teh bolnicah.

Radiol Oncol 2018; 52(4): 383-391.
doi: 10.2478/raon-2018-0041

Ultrazvočne spremembe kot pokazatelj primerne pokritosti tumorja z električnim poljem za učinkovito elektrokemoterapijo jetrnih tumorjev

Boc N, Edhemović I, Kos B, Mušič MM, Brecelj E, Trotovšek B, Bošnjak M, Đokić M, Miklavčič D, Čemažar M, Serša G

Izhodišča. Namen raziskave je bil opredeliti ultrazvočne spremembe med in po elektrokemoterapiji. Želeli smo preveriti pokritost področja ablacije z dovolj visokim električnim poljem, ki zagotavlja uspešnost terapije.

Bolniki in metode. Predstavili smo takojšnje in zakasnjene spremembe, ki jih vidimo na ultrazvočnih slikah metastaz kolorektalnega raka v jetrih po zdravljenju z elektrokemoterapijo.

Rezultati. Izsledki na ultrazvočnih slikah so se ujemali z izsledki slikanja z magnetno resonanco. Tumorje smo zdravili z elektrokemoterapijo na osnovi računalniškega načrtovanja. Na ultrazvočnih slikah so bili nemudoma po elektrokemoterapiji vidni hiperehogeni mikromehurčki vzdolž poti elektrod. V roku nekaj minut so tumorji postali enakomerno hiperehogeni, hkrati pa se je vzpostavil edematozni rob, ki se je kazal kot hipoehogeno področje in je bil na slikah prisoten več ur po zdravljenju. Značilna področja na ultrazvočnih slikah so se ujemala z računsko določeno porazdelitvijo električnega polja v zdravljenih tumorjih, kar kaže na možnost preverjanja zadostne pokritosti ciljnega tkiva z ustreznim električnim poljem.

Zaključki. Ultrazvok predstavlja uporabno orodje za preverjanje ustreznosti postavitve elektrod pri intraoperativni elektrokemoterapiji jetrnih tumorjev, hkrati pa lahko služi tudi kot indikator ustrezne pokritosti tumorjev z ustreznim električnim poljem in tako napove odgovor tumorjev na zdravljenje.

Radiol Oncol 2018; 52(4): 392-398.
doi: 10.2478/raon-2018-0046

Metabolni odtis bevacizumaba pri gliomskih celicah IDH1, ugotovljen z nuklearno magnetno resonanco

Mesti T, Bouchemal N, Banissi C, Triba MN, Carole Marbeuf-Gueye C, Čemažar M, Le Moyec L, Carpentier AF, Savarin P, Ocvirk J

Izhodišča. Maligni gliomi so hitro rastoči tumorji, ki globoko vraščajo v možganovino in imajo slabo napoved poteka bolezni. Namen raziskave je bil ugotoviti metabolno delovanje bevacizumaba na gliomske celice z IDH1 mutacijo, ki jo povezujemo z boljšo napovejo poteka bolezni in boljšim odgovorom na zdravljenje. Znano je, da bevacizumab zavira tumorsko rast z nevtralizacijo biološkega delovanja žilnega endotelialnega rastnega dejavnika (VEGF). Direktno delovanje bevacizumaba na metabolizem tumorskih celic pa ostaja neznan.

Materijali in metode. Imunološka in MTT testiranja smo uporabili za določitev koncentacije izločenega VEGF in celičnega preživetja po izpostavljenosti celic na bevacizumab. Raziskavo celičnega metaboloma smo opravili z uporabo nuklearnomagnetno resonančno spektroskopijo z visoko ločljivostjo (HRMAS).

Rezultati. Celice mIDH1-U87 so izločale VEGF (13 ng/mL). Bevacizumab ni imel citotoksičnega učinka, četudi smo celice izpostavili njegovemu 72-urnemu delovanju z visokimi odmerki do 1 mg/mL. Ne glede na to je razsikava s HRMAS pokazala statistično značilen učinek bevacizumaba (0.1 mg/mL) na metabolični fenotip celic mIDH1-U87 s porastom 2-hidroksglutarata in s spremembami v skupini glutaminskih metabolitov (alanin, glutamat, glicin) in lipidov (polinenasičene maščobne kisline [PUFA], glicerofosfoholin in fosfoholin).

Zaključki. Na celicah mIDH1-U87 smo ugotovili spremembe v skupini glutaminskih metabolitov, ki predstavljajo metabolni označevalec za delovanje bevacizumaba. Naši podatki podpirajo možnost funkcionalnega ciklusa trikarboksilične kisline, ki naj bi potekal v reduktivni smeri kot najverjetnejši mehanizem delovanja bevacizumaba. S tem predlagamo novo tarčno pot za učinkovito zdravljenje malignih gliomov.

Radiol Oncol 2018; 52(4): 399-412.
doi: 10.2478/raon-2018-0036

Randomizirana uvedba samoodvzema vzorca doma za test HPV pri ženskah, ki se ne udeležujejo Državnega presejalnega programa za zgodnje odkrivanje predrakavih sprememb materničnega vratu ZORA. Primerjava treh pristopov.

Ivanuš U, Jerman T, Repše Fokter A, Takač I, Kloboves Prevodnik V, Marčec M, Salobir Gajšek U, Pakiž M, Koren J, Hutter Čelik S, Gornik Kramberger K, Klopčič U, Kavalar R, Šramek Zatler S, Grčar Kuzmanov B, Florjančič M, Nolde N, Novaković S, Poljak M, Primic Žakelj M

Izhodišča. Z randomizirano pilotno raziskavo smo preverili tri pristope za povečanje pregledanosti v Državnem programu za zgodnje odkrivanje predrakavih sprememb ZORA. Neodzivnicam programa iz dveh slovenskih regij smo ponudili možnost samoodvzema brisa za testiranje na okužbo s človeškimi papilomavirusi (HPV).

Bolniki in metode. Neodzivnice stare 30-64 let smo naključno razporedili v eno primerjalno (skupina P, n = 2.600) in dve intervencijski skupini, v prvi so morale odvzemnik za test HPV naročiti (skupina I1, n = 14.400) in v drugi ne (skupina I2, n = 9.556). Na vseh samoodvzetih vzorcih smo opravili test HPV Hybrid Capture 2. HPV-pozitivne ženske so bile povabljene v kolposkopsko ambulanto. Zanimala nas je odzivnost (celokupna in glede na vrsto presejalnega testa) in histopatološki izidi (vključno s pozitivno napovedno vrednostjo testa) glede na pristop, starost žensk, predhodno udeležbo v presejalnem programu in regijo bivališča.

Rezultati. Od 26.556 vključenih žensk, jih je 8.972 (33,8 %) opravilo samoodvzem brisa za test HPV ali odvzem brisa materničnega vratu za citološki pregled pri ginekologu. Odzivnost je bila 37,7 % v skupini I2; 34,0 % v skupini I1 in 18,4 % v skupini P ($p < 0.05$). V skupini I2 je bila cervikalna intraepitelijska neoplazia (CIN)2+ odkrita pri 3,9/1.000 vključenih žensk, v skupini I1 pri 3,4/1.000 in v skupini P pri 3,1/1.000 ($p > 0.05$). Pozitivna napovedna vrednost testa HPV doma za CIN2+ je bila 12,0 % in za CIN3+ 9,6 %. Največja je bila pri ženskah, ki že vsaj deset let niso imele brisa materničnega vratu in so imele pozitiven izvid testa HPV doma in pri ginekologu, in sicer 40,8 % za CIN2+ in 38,8 % za CIN3+.

Zaključki. Ženske, ki se ne udeležujejo redno presejalnih pregledov, se dobro odzovejo tudi, če morajo odvzemnik za test HPV naročiti, če jih ob tem spodbudimo, da lahko naročijo odvzemnik ali opravijo odvzem brisa materničnega vratu za citološki pregled pri ginekologu. Med ženskami s pozitivnim izvidom testa HPV na samoodvzetem brisu obstaja klinično pomembna razlika v tveganju za predrakave spremembe visoke stopnje, glede na predhodno udeležbo v presejalnem programu. Ženske, ki se citološkega presejanja niso udeležile deset let ali več, namesto odloženega ponovnega testiranja potrebujejo takojšnjo kolposkopijo.

Radiol Oncol 2018; 52(4): 413-421.
doi: 10.2478/raon-2018-0025

Intervalni raki debelega črevesa in danke v slovenskem presejalnem programu po negativnem imunokemičnem testu na kri v blatu in primerjava z raki odkritimi v presejanju in med neodzivniki

Novak Mlakar D, Kofol Bric T, Škrjanec AL, Krajc M

Izhodišča. Ocenili smo pojavljanje in značilnosti intervalnih rakov po uporabi imunokemičnega testa na prikrito krvavitev v blatu v presejalnem programu za raka debelega črevesa in danke v Sloveniji. Na ta način smo želeli izračunati občutljivost testa.

Opazovanci in metode. V analizo smo vključili preiskovance v starosti 50 do 69 let, ki smo jih vabili v presejanje od aprila 2011 do decembra 2012. Osebe smo spremljali do naslednjega predvidenega vabljenja v presejalni program, povprečno dve leti. Podatke o intervalnih rakih in rakih med neodzivniki smo pridobili iz Registra raka. Spol, starost opazovanca, leta šolanja ter lokacijo in stadij raka smo primerjali med tremi opazovanimi skupinami. Za izračun občutljivosti presejalnega testa smo uporabili metodo sorazmerne incidenčne stopnje.

Rezultati. Med 502.488 osebami povabljenimi v presejanje smo odkrili 493 rakov po pozitivnem izidu presejalnega testa, 79 intervalnih rakov po negativnem presejalnem testu in 395 rakov med neodzivniki. Delež intervalnih rakov je predstavljal 13,8 %. Pri vseh treh skupinah opazovanih oseb je bil pogosteje odkrit rak pri moških ($p = 0,009$) in pri osebah starejših od 60 let ($p < 0,001$). V primerjavi z raki odkritimi v presejanju in med neodzivniki je bilo intervalnih rakov več med osebami, ki so se šolale 10 let ali več ($p = 0,029$ in $p = 0,001$), imele stadij raka III ($p = 0,027$) in IV ($p < 0,001$) ter rak v desnem delu debelega črevesa ($p < 0,001$). Pri intervalnih rakih je bil bolj pogost stadij I kot pri neodzivnikih ($p = 0,004$). Občutljivost presejalnega testa na prikrito krvavitev je bila 88,45 %.

Zaključki. Intervalni raki se v slovenskem presejalnem programu pojavljajo v pričakovanih deležih ugotovljenih v podobnih programih. S kompletom dveh testerjev na prikrito krvavitev v blatu je dosežena občutljivost testa, ki je med višjimi v primerljivih programih.

Radiol Oncol 2018; 52(4): 422-432.
doi: 10.2478/raon-2018-0043

Dinamično izražanje 11 miRNA v 83 primarnih glioblastomih in recidivih teh glioblastomov ter njegov pomen za zdravljenje, za čas do ponovitve bolezni, preživetje bolnikov in za status gena MGMT

Matos B, Bostjančič E, Matjašič A, Popovič M, Glavač D

Izhodišča. Glioblastom (GBM) je najpogostejši in najbolj maligen podtip glialnih tumorjev. Na njegovo patogenezo poleg številnih genskih sprememb vpliva tudi izražanje miRNA, ki bi lahko bilo tudi vzrok ponovne razrasti tumorja (recidiva) ter razvoja neodzivnosti na prejeto onkološko terapijo. Na podlagi objavljenih raziskav smo izbrali 11 miRNA in analizirali njihovo izražanje v vzorcih GBM. Predpostavili smo, da se izbrane miRNA diferenčno izražajo v novo odkritih in recidivnih GBM ter da so razlike v izražanju statistično značilne in posledica različne oblike onkološkega zdravljenja.

Bolniki in metode. Uporabili smo v formalinu fiksirano in v parafin vklopljeno tumorsko tkivo novo odkritega GBM in pripadajoče tumorske vzorce recidivnih GBM pri 83 bolnikih z GBM. Izbrali smo 11 miRNA (*miR-7*, *miR-9*, *miR-15b*, *miR-21*, *miR26b*, *miR-124a*, *miR-199a*, *let-7a*, *let-7b*, *let-7d* in *let-7f*) in analizirali njihovo izražanje s qPCR. Pri bolnikih, ki so prejemali temozolamid, smo določili status MGMT z uporabo metilspecifične PCR.

Rezultati. Ugotovili smo statistično značilno diferenčno izražanje *miR-7*, *miR-9*, *miR-21*, *miR-26b*, *mirR-124a*, *miR-199a* in *let-7f* v recidivnih tumorskih vzorcih v primerjavi z novoodkritimi vzorci GBM. Pri recidivnih GBM so *miR-15b*, *let-7d* in *let-7f* pokazale statistično značilno diferenčno izražanje, ko smo primerjali oba načina onkološkega zdravljenja. Opazili smo tudi razliko v času do ponovitve bolezni med bolniki, ki so prejemali samo radioterapijo ali pa dodatno še kemoterapijo. Preživetje je bilo daljše pri bolnikih, ki so prejemali kemoterapijo po drugi operaciji, v primerjavi z bolniki, ki te niso prejemali. Izražanje *miR-26b* je bilo v korelaciji s časom do ponovitve bolezni, izražanje *let-7f* pa s preživetjem bolnikov. Izražanje miRNA v tumorskih vzorcih z metiliranim promotorjem gena MGMT ali brez njega ni bilo spremenjeno.

Zaključki. Rezultati naše raziskave kažejo, da analizirane miRNA ne sodelujejo le pri patogenezi novoodkritega GBM, ampak tudi pri njegovi razrasti oziroma recidivu. Izražanje nekaterih miRNA je verjetno odvisno od prejete onkološke terapije, zato bi lahko bile dodatni genetski označevalec za napoved ponovne razrasti tumorja, potencialno pa lahko prispevajo tudi k napovedi rezistence proti onkološki terapiji.

Radiol Oncol 2018; 52(4): 433-442.
doi: 10.2478/raon-2018-0040

Lokalizacija katepsinov K in X in njun pomen za napoved preživetja pri glioblastomu

Breznik B, Limback C, Porčnik A, Blejec A, Koprivnikar Krajnc M, Bošnjak R, Kos J, Van Noorden CJF, Lah TT

Izhodišča. Glioblastom je zelo agresiven tumor centralnega živčnega sistema, za katerega je značilna obsežna invazija rakavih celic v možganovino, kar onemogoča popolno odstranitev tumorja. Cisteinski katepsini B, S, K in L, ki so udeleženi v malignem napredovanju, so prekomerno izraženi tudi v glioblastomu. Ta raziskava prvič dokazuje, da je katepsin X na genskem in proteinskem nivoju prav tako visoko izražen v glioblastomu.

Materiali in metode. Izražanje genov katepsinov K in X smo analizirali z uporabo javno dostopnih transkriptomskih podatkov, ki smo jih primerjali s stopnjo gliomov ter podvrsto glioblastomov. Oceno napovedne vrednosti izražanja mRNA katepsinov K in X smo izvedli s Kaplan-Maierjevo analizo preživetja. Izražanje katepsinov K in X na proteinskem nivoju v tkivih tumorjev smo lokalizirali in semi-kvantitativno ocenili z uporabo imunohistokemije.

Rezultati. Najvišje izražanje genov katepsinov K in X smo ugotovili v gliomih IV. stopnje - glioblastomih, zlasti v mezenhimski podvrsti glioblastomov. Visoko izražanje gena katepsina X, ne pa tudi katepsina K, je bilo povezano z nizko stopnjo preživetja bolnikov. Visoko in heterogeno izražanje proteinov katepsinov K in X smo opazili v tkivih glioblastoma. Katepsina K in X smo lokalizirali v območjih CD133-pozitivnih glioblastomkih matičnih celic, ki smo jih našli v njihovih nišah okoli arteriol, kjer smo zaznali tudi proteina SDF-1a in CD68. Nivo mRNA obeh katepsinov K in X je sovpadal z izražanjem označevalcev glioblastomskih matičnih celic in njihovih niš.

Zaključki. Prisotnost obeh katepsinov v regijah niš glioblastomskih matičnih celic kaže na to, da imata specifično vlogo pri regulaciji zadrževanja glioblastomskih matičnih celic v peri-arteriolarnih nišah. Klinično uporabo teh rezultatov bo potrebno potrditi v nadaljnjih prospektivnih raziskavah.

Radiol Oncol 2018; 52(4): 443-452.
doi: 10.2478/raon-2018-0045

Odziv kronične črevesne vnetne bolezni na zdravljenje z zaviralci dejavnika tumorske nekroze alfa je odvisen od profila dendritičnih celic v vneti črevesni sluznici

Smrekar N, Drobne D, Šmid LM, Ferkolj I, Štabuc B, Ihan A, Kopitar AN

Izhodišča. Dendritične celice uravnavajo procese vnetja in imunske tolerance v črevesni sluznici. Namena raziskave sta bila preučitev vpliva zdravljenja kronične vnetne črevesne bolezni z zaviralci dejavnika tumorske nekroze alfa (TNFa) na črevesne dendritične celice in opredelitev njihove morebitne vloge pri odzivu bolezni na tovrstno zdravljenje.

Bolniki in metode. Tridesetim bolnikom s kronično vnetno črevesno boleznijo (16 s Crohnovo boleznijo in 14 z ulceroznim kolitisom) smo odvzeli bioptične vzorce sluznice debelega črevesa pred in po zdravljenju z zaviralci TNFa (infliximab pri 13 in adalimumab pri 17 bolnikih). S pretočno citometrijo smo v odvzetih vzorcih opredelili deleže fenotipov dendritičnih celic *lamine proprie*. Aktivnost bolezni pred in po pričetku zdravljenja smo ocenjevali endoskopsko.

Rezultati. Pred pričetkom zdravljenja je bil delež konvencionalnih dendritičnih celic v v vneti sluznici višji (7,8 %) kot v nevneti (4,5 %; p = 0,003), delež dendritičnih celic $CD103^+$ je bil v vneti sluznici nižji (47,1 %) kot v nevneti (57,3 %; p=0.03). Po 12 tednih zdravljenja je delež konvencionalnih dendritičnih celic v vneti sluznici upadel s 7,8 % na 4,5 % (p = 0,014), delež dendritičnih celic $CD103^+$ pa je ostal nespremenjen. 18 od 30 bolnikov (60 %) se je na zdravljenje v prvih 12 tednih odzvalo. V vneti sluznici teh bolnikov je bil pred zdravljenjem delež konvencionalnih dendritičnih celic pomembno višji kot pri tistih, ki se na zdravljenje niso odzvali (9,16 % proti 4,4 % p < 0,01), višja pa je bila tudi izraženost HLA-DR (MFI 12152 proti 8837, p = 0,038).

Zaključek. Delež konvencionalnih dendritičnih celic v vneti sluznici bolnikov s kronično vnetno črevesno boleznijo nad 7 % napoveduje dober odziv na zdravljenje z zaviralci TNFa.

Radiol Oncol 2018; 52(4): 453-460.
doi: 10.2478/raon-2018-0038

Lokoregionalna kontrola bolezni po perkutanem obsevanju pri 91 bolnikih z diferenciranim rakom ščitnice in tumorskim stadijem pT4. Izkušnje posamičnega inštituta

Bešić N, Dremelj M, Pilko G

Izhodišča. Lokoregionalna ponovitev bolezni je pogosta pri bolnikih z lokalno napredovalim diferenciranim rakom ščitnice. Namen raziskave je bil ugotoviti, kako pogosto dosežemo lokoregionalno kontrolo bolezni po perkutani radioterapiji vratu in mediastinuma pri bolnikih z diferenciranim rakom ščitnice in tumorskim stadijem pT4.

Bolniki in metode. Zdravili smo 91 bolnikov (47 moških, 44 žensk, srednja starost 61 let) z diferenciranim rakom ščitnice. Perkutana radioterapija vratu in mediastinuma je bila del kombiniranega zdravljenja zaradi tumorskega stadija bolezni pT4 (63 primerov pT4a, 28 primerov pT4b) v obdobju od leta 1973 do leta 2015. Zbrali smo podatke o kliničnih dejavnikih, histopatoloških izvidih in ponovitvi bolezni. Izračunali smo dolžino preživetja brez bolezni, specifično preživetje glede raka ščitnice in celokupno preživetje bolnikov.

Rezultati. Srednja vrednost velikosti tumorja je bila 5 cm (razpon 1–30 cm). Od 91 bolnikov je imelo 23 oddaljene in 38 regionalne zasevke. V 70 % primerov je bila opravljena totalna ali skoraj totalna tiroidektomija, v 14 % lobektomija, v 2 % subtotalna tiroidektomija in v 30 % disekcija vratnih bezgavk. 13 % bolnikov ni bilo zdravljenih s kirurškim posegom. Vsi bolniki so bili zdravljeni s perkutano radioterapijo, 39 pa tudi s kemoterapijo. Ablacijo ostanka ščitnice z radiojodom je imelo 90 %, zdravljenje z radiojodom pa 40 % bolnikov. Ponovitev bolezni smo ugotovili pri 29/64 bolnikih brez perzistentne bolezni. Lokoregionalno ponovitev bolezni je imelo 16 bolnikov, oddaljene zasevke je dobilo 13 bolnikov. Petletno preživetje brez bolezni je bilo 64 %, desetletno preživetje brez bolezni pa 48 %.

Zaključki. Večina bolnikov z diferenciranim rakom ščitnice in stadijem bolezni pT4, ki so bili zdravljeni s perkutano radioterapijo v območju vratu in mediastinuma kot del kombiniranega zdravljenja, je imela dolgotrajno lokoregionalno kontrolo bolezni.

Radiol Oncol 2018; 52(4): 461-467.
doi: 10.2478/raon-2018-0042:

Slikovno vodena brahiterapija z visoko hitrostjo doze in volumetrična modulirana ločna terapija pri raku glave in vratu. Primerjalna analiza dozimetričnih kazalcev za tarčni volumen in kritične organe

Akiyama H, Pesznyák C, Béla D, Ferenczi Ö, Major T, Polgár C, Takácsi-Nagy Z

Izhodišča. V raziskavi smo želeli dozimetrično primerjati slikovno vodeno brahiterapijo z visoko hitrostjo doze (IGBT) ter volumetrično modulirano ločno terapijo (VMAT) pri raku glave in vratu. Upoštevali smo konformnost razporeditve doze v planirnem tarčnem volumnu (PTV) in kritične organe (OAR).

Bolniki in metode. Izbrali smo 38 zaporednih bolnikov s tumorji mobilnega dela jezika, ustnega dna in korena jezika, ki so imeli stadij bolezni T1-4 in smo jih zdravili z IGBT. Naredili smo dodatne obsevalne načrte za obsevanje z VMAT, pri čemer smo uporabili iste računalniške tomografske podatke. Primerjali smo parametre različnih OAR in PTV (npr. V98, D0.1cm3, Dpovprečna, ipd.).

Rezultati. Povprečni V98 za PTV pri IGBT in VMAT je bil 90,2 % proti 90,4 % ($p > 0,05$). Povprečna D0.1cm3 za mandibulo je bila 77,0 % proti 85,4 % ($p < 0,05$). Dpovprečna za parotidno žlezo na isti oz. nasprotni strani je bila 4,6 % proti 4,6 % in 3,0 % proti 3,9 % ($p > 0,05$). Dpovprečna za submandibularno žlezo na isti oz. nasprotni strani je bila 16,4 % proti 21,9 % ($p > 0,05$) in 8,2 % proti 16,9 % ($p < 0.05$).

Zaključki. Z obema tehnikama smo dosegli odlično pokritost tarče. Pri IGBT je bila doza na normalna tkiva nižja kot pri VMAT. Rezultati potrjujejo prednost IGBT pri zaščiti različnih OAR in pomembno vlogo te invazivne metode v času novih teleterapevtskih tehnik.

Radiol Oncol 2018; 52(4): 468-474.
doi: 10.2478/raon-2018-0021

Primerjava anteroposteriorne in posteroanteriorne projekcije pri rentgenskem slikanju ledvene hrbtenice

Alukić E, Škrk D, Mekiš N

Izhodišča. Namen raziskave je bil pri velikem številu pacientov obeh spolov ter različne teže in velikosti, primerjati dozo ionizirajočega sevanja in kakovost slike pri rentgenskem slikanju ledvene hrbtenice v AP in PA projekci.

Bolniki in metode. V prvem delu raziskave, ki potekal na antropomorfnem fantomu, smo izmerili velikost slikovnega polja, DAP (dose area product - produkt doze in površine) in efektivno dozo ter pridobili ocene o kakovosti rentgenogramov pri rentgenskem slikanju ledvene hrbtenice v AP in PA projekcijah. Drugi del raziskave smo izvedli na 100 pacientih, ki smo jih naključno razdelili v dve skupini po 50, nato pa slikali prvo skupino v AP in drugo v PA projekciji. Pri vsakem pacientu smo izmerili ITM (indeks telesne mase), velikost slikovnega polja, debelino trebuha, DAP, efektivno dozo in ocenili kakovost slike.

Rezultati. Raziskava na fantomu ni pokazala statistično značilnih razlik med velikostjo slikovnega polja, DAP in kakovostjo slik, vendar je bila izračunana efektivna doza pri uporabi PA projekcije v primerjavi z AP projekcijo manjša za 25 % ($p = 0,008$). Pri pacientih med obema skupinama nismo ugotovili statistično značilnih razlik med ITM in velikostjo polja. Pri uporabi PA projekcije je bila debelina trebuha manjša za 10 % ($p < 10^{-3}$), DAP za 27 % ($p = 0.009$) in efektivna doza za 53 % ($p < 10^{-3}$). Med ocenami slik, narejenih v AP in PA projekciji, ni bilo statistično značilnih razlik.

Zaključki. Rezultati so pokazali, da je uporaba PA projekcije priporočljiva metoda izbora pri rentgenskem slikanju ledvene hrbtenice.

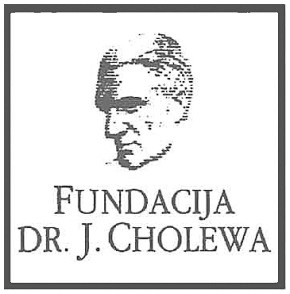

Fundacija "Docent dr. J. Cholewa"
je neprofitno, neinstitucionalno in nestrankarsko
združenje posameznikov, ustanov in organizacij, ki želijo
materialno spodbujati in poglabljati raziskovalno
dejavnost v onkologiji.

Dunajska 106
1000 Ljubljana

IBAN: SI56 0203 3001 7879 431

Activity of "Dr. J. Cholewa" Foundation for Cancer Research and Education - a report for the final quarter of 2017

Dr. Josip Cholewa Foundation for cancer research and education continues with its planned activities in the final quarter of 2018. Its primary focus remains the provision of grants, scholarships, and other forms of financial assistance for basic, clinical and public health research in the field of oncology. In parallel, it also makes efforts to provide financial and other support for the organisation of congresses, symposia and other forms of meetings to spread the knowledge about prevention and treatment of cancer, and finally about rehabilitation for cancer patients. In Foundation's strategy, the spread of knowledge should not be restricted only to the professionals that treat cancer patients, but also to the patients themselves and to the general public.

The Foundation continues to provide support for »Radiology and Oncology«, a quarterly scientific magazine with a respectable impact factor that publishes research and review articles about all aspects of cancer. The magazine is edited and published in Ljubljana, Slovenia. »Radiology and Oncology« is an open access journal available to everyone free of charge. Its long tradition represents a guarantee for the continuity of international exchange of ideas and research results in the field of oncology for all in Slovenia that are interested and involved in helping people affected by many different aspects of cancer.

The Foundation will continue with its activities in the future, especially since the problems associated with cancer affect more and more people in Slovenia and elsewhere. Ever more treatment that is successful reflects in results with longer survival in many patients with previously incurable cancer conditions. Thus adding many new dimensions in life of cancer survivors and their families.

Viljem Kovač M.D., Ph.D.

Borut Štabuc, M.D., Ph.D.

Tomaž Benulič, M.D.

Andrej Plesničar, M.D., M.Sc.

ENA SAMA 30-MINUTNA INFUZIJA ZAGOTOVI CELOVITO ZDRAVLJENJE ABSSSI [1]

Enostavno odmerjanje

Odrasli pacienti z ABSSSI: 1500 mg z enkratnim infundiranjem ali 1000 mg prvi teden, naslednji teden pa 500 mg.

Xydalba™ dalbavancin

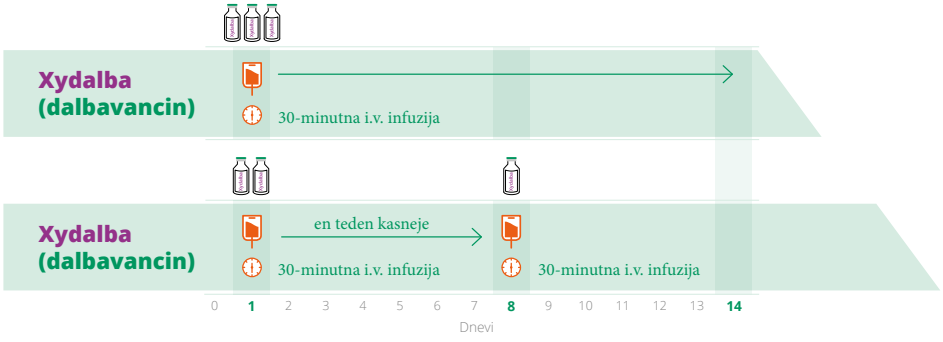

ANGELINI

Skrajšan povzetek glavnih značilnosti zdravila

Xydalba™ 500 mg prašek za koncentrat za raztopino za infundiranje

Za to zdravilo se izvaja dodatno spremljanje varnosti. Tako bodo hitreje na voljo nove informacije o njegovi varnosti. Zdravstvene delavce naprošamo, da poročajo o katerem koli domnevnem neželenem učinku zdravila.

Sestava: Ena viala vsebuje dalbavancinijev klorid, kar ustreza 500 mg dalbavancina. Po rekonstituciji en ml vsebuje 20 mg dalbavancina. Razredčena raztopina za infundiranje mora imeti končno koncentracijo od 1 do 5 mg/ml dalbavancina. **Terapevtske indikacije:** Zdravilo Xydalba je indicirano za zdravljenje akutnih bakterijskih infekcij kože in kožnih struktur (ABSSSI) pri odraslih. Pozornost je treba nameniti uradnim navodilom o ustrezni uporabi protibakterijskih zdravil. **Odmerjanje in način uporabe:** Odmerjanje: *Priporočeni odmerek in trajanje zdravljenja pri odraslih:* Priporočeni odmerek dalbavancina pri odraslih pacientih z akutno bakterijsko infekcijo kože in kožnih struktur (ABSSSI) je 1500 mg z enkratnim infundiranjem 1500 mg ali 1000 mg prvi teden, naslednji teden pa 500 mg. *Starejše osebe:* Prilagoditev odmerka ni potrebna. *Okvara delovanja ledvic:* Pri pacientih z blago ali zmerno okvaro delovanja ledvic prilagoditve odmerka niso potrebne (kreatininski očistek ≥ 30 do 79 ml/min). Pri pacientih, ki redno prejemajo hemodializo (3-krat tedensko), prilagoditve odmerka niso potrebne, dalbavancin se lahko uporablja ne glede na čas hemodialize. Pri pacientih s kronično okvaro delovanja ledvic, katerih kreatininski očistek je < 30 ml/min in ki ne prejemajo redno hemodialize, je priporočen odmerek dalbavancina zmanjšan na 1000 mg z enkratnim infundiranjem ali 750 mg, ki mu sledi 375 mg v naslednjem tednu. *Okvara delovanja jeter:* Pri pacientih z blago okvaro delovanja jeter (Child-Pugh A) prilagoditev odmerka dalbavancina ni potrebna. Previdnost je potrebna pri predpisovanju dalbavancina pacientom z zmerno ali hudo okvaro delovanja jeter (Child-Pugh B & C), ker ni ustreznih podatkov za določitev primernega odmerjanja. *Otroci:* Varnost in učinkovitost dalbavancina pri otrocih v starosti od rojstva do < 18 let še nista ugotovljeni. Priporočila o odmerjanju ne moremo podati. Način uporabe: Zdravilo Xydalba mora biti rekonstituirano in potem še razredčeno pred dajanjem intravenske infuzije, ki traja 30 minut. **Kontraindikacije:** Preobčutljivost na zdravilno učinkovino ali katerokoli pomožno snov. **Posebna opozorila in previdnostni ukrepi:** Preobčutljivostne reakcije: Posebej pozorno se mora zdravilo Xydalba uporabljati pri pacientih, za katere je znano, da so preobčutljivi na druge glikopeptide, saj se lahko pojavi navzkrižna preobčutljivost. Če se pojavi alergijska reakcija na zdravilo Xydalba, je treba njegovo uporabo prekiniti in uvesti ustrezno terapijo za alergijsko reakcijo. Driska zaradi bakterije *Clostridium difficile:* Kolitis, povezan s protibakterijskimi zdravili, in psevdomembranski kolitis sta bila zabeležena pri uporabi skoraj vseh antibiotikov in sta lahko blaga pa vse do smrtno ogrožajoča. Zato je pri pacientih z drisko med ali po zdravljenju z dalbavancinom pomembno upoštevati tudi to diagnozo. V takšnih okoliščinah je treba razmisliti o prekinitvi zdravljenja z dalbavancinom in uvesti podporne ukrepe skupaj z jemanjem posebnega zdravila proti bakteriji *Clostridium difficile.* Takih pacientov nikoli ne smemo zdraviti z zdravili, ki zavirajo peristaltiko. Reakcije, povezane z infuzijo: Zdravilo Xydalba se uporablja z intravenskim infundiranjem, ki traja skupaj 30 minut, da se zmanjša tveganje za z infuzijo povezano reakcijo. Hitre intravenske infuzije glikopeptidnih protibakterijskih zdravil lahko povzročijo reakcijo, ki je podobna "sindromu rdečeličneža", z rdečico na zgornjem delu telesa, z urtikarijo, pruritusom in/ali izpuščajem. S prekinitvijo ali upočasnitvijo infundiranja lahko te reakcije izginejo. Okvara delovanja ledvic: Podatki o učinkovitosti in varnosti dalbavancina pri pacientih s kreatininskim očistkom, manjšim od 30 ml/min, so omejeni. Na podlagi simulacij je prilagoditev odmerjanja potrebna pri pacientih s kronično okvaro delovanja ledvic, katerih kreatininski očistek je manjši od 30 ml/min in ki redno ne prejemajo hemodialize. Mešane okužbe: Pri mešanih okužbah, kjer obstaja sum na Gram-negativne bakterije, se morajo pacienti zdraviti tudi z ustreznim protibakterijskim zdravilom oz. zdravili, proti Gram-negativnim bakterijam. Neobčutljivi organizmi: Uporaba antibiotikov lahko pospeši prekomerno rast neobčutljivih mikroorganizmov. Če pride med zdravljenjem do superinfekcije, je treba ustrezno ukrepati. Omejitev kliničnih podatkov: Podatki o varnosti in učinkovitosti dalbavancina pri uporabi več kot dveh odmerkov (v razmiku enega tedna) so omejeni. V večjih preskušanjih pri akutnih bakterijskih infekcijah kože in kožnih struktur (ABSSSI) so bile vrste zdravljenih infekcij omejene samo na celulitis/šen, abscese in okužbe ran. Izkušenj z dalbavancinom pri zdravljenju pacientov s hudo oslabljenim imunskim sistemom ni. **Medsebojno delovanje z drugimi zdravili in druge oblike interakcij:** Dalbavancin se ne presnavlja z encimi CYP in vitro, zato sočasni CYP induktorji ali inhibitorji malo verjetno vplivajo na farmakokinetiko dalbavancina. Ni znano, ali je dalbavancin substrat za prenašalce jetrnega privzema in efluksa. Uporaba skupaj z inhibitorji teh prenašalcev lahko poveča izpostavljenost dalbavancinu. Primeri takšnih inhibitorjev prenašalcev so okrepljeni inhibitorji proteaze, verapamil, kinidin, itrakonazol, klaritromicin in ciklosporin. Pričakovana je majhna verjetnost interakcije dalbavancina z zdravili, ki se presnavljajo z encimi CYP, saj ni niti inhibitor niti induktor encimov CYP *in vitro.* Podatki o dalbavancinu kot inhibitorju CYP2C8 niso na voljo. Ni znano, ali je dalbavancin inhibitor prenašalcev. Povečane izpostavljenosti substratom prenašalcev, občutljivim na inhibicijo aktivnosti prenašalcev, kot so statini in digoksin, ni mogoče izključiti, če so kombinirani z dalbavancinom. **Plodnost, nosečnost in dojenje:** Nosečnost: O uporabi dalbavancina pri nosečnicah ni podatkov. Študije na živalih so pokazale vpliv na sposobnost razmnoževanja. Uporaba zdravila Xydalba med nosečnostjo ni priporočljiva, razen kadar je to nujno. Dojenje: Ni znano, ali se dalbavancin izloča v mleko pri človeku. Potrebno je sprejeti odločitev o nadaljevanju/prekinitvi dojenja ali o nadaljevanju/prekinitvi zdravljenja z zdravilom Xydalba, pri tem pa pretehtati koristi dojenja za otroka in koristi zdravljenja za doječo žensko. Plodnost: Študije na živalih so pokazale zmanjšano plodnost. Potencialno tveganje za ljudi ni znano. **Neželeni učinki:** Pogosti: glavobol, navzea, driska. Občasni: vulvovaginalna glivična okužba, okužba sečil, glivična okužba, kolitis zaradi razrasta *Clostridium difficile,* oralna kandidiaza, anemija, trombocitoza, eozinofilija, levkopenija, nevtropenija, zmanjšan apetit, insomnia, dizgevzija, omotica, vročinski oblivi, flebitis, kašelj, zaprtost, bolečine v trebuhu, dispepsija, neprijeten občutek v trebuhu, bruhanje, pruritus, urtikarija, izpuščaj, vulvovaginalni pruritus, z infuzijo povezana reakcija, zvišana laktat-dehidrogenaza v krvi, zvišana alanin-aminotransferaza, zvišana aspartat-aminotransferaza, zvišana raven sečne kisline v krvi, neobičajni rezultati testa jetrne funkcije, zvišane vrednosti transaminaz, zvišane vrednosti alkalne fosfataze v krvi, zvišano število krvnih ploščic, zvišana telesna temperatura, zvišana raven jetrnih encimov, zvišane vrednosti gama-glutamil transferaze. Redki: anafilaktoidna reakcija, bronhospazem. **Način in režim predpisovanja in izdaje:** H - Zdravilo se izdaja le na recept, uporablja pa se samo v bolnišnicah. **Imetnik dovoljenja za promet:** Allergan Pharmaceuticals International Ltd., Clonshaugh Industrial Estate, Coolock, Dublin 17, Irska. **Datum zadnje revizije besedila:** 01/2017. **Predstavnik imetnika dovoljenja za promet z zdravilom:** Angelini Pharma d.o.o., Koprska ulica 108A, 1000 Ljubljana.

Pred predpisovanjem se seznanite s celotnim Povzetkom glavnih značilnosti zdravila.
Samo za strokovno javnost. Datum priprave informacije: maj 2018

Vir:

1. Xydalba™ (dalbavancin), Povzetek glavnih značilnosti zdravila, 30. 1. 2017

PR/ANGSI/DAL/2018/001

PRVA REGISTRIRANA TERAPIJA V 2. LINIJI ZA ZDRAVLJENJE ADENOKARCINOMA ŽELODCA ALI GASTRO-EZOFAGEALNEGA PREHODA[1]

CYRAMZA®
(ramucirumab)

UKREPAJTE ZDAJ

USPOSOBLJENI ZA SPREMEMBE, ZA NEPRIMERLJIVE IZKUŠNJE

Skrajšan povzetek glavnih značilnosti zdravila

▼ Za to zdravilo se izvaja dodatno spremljanje varnosti. Tako bodo hitreje na voljo nove informacije o njegovi varnosti. Zdravstvene delavce naprošamo, da poročajo o katerem koli domnevnem neželenem učinku zdravila.

Cyramza 10 mg/ml koncentrat za raztopino za infundiranje

En mililiter koncentrata za raztopino za infundiranje vsebuje 10 mg ramucirumaba. Ena 10-mililitrska viala vsebuje 100 mg ramucirumaba. **Terapevtske indikacije** Zdravilo Cyramza je v kombinaciji s paklitakselom indicirano za zdravljenje odraslih bolnikov z napredovalim rakom želodca ali adenokarcinomom gastro-ezofagealnega prehoda z napredovalo boleznijo po predhodni kemoterapiji, ki je vključevala platino in fluoropirimidin. Monoterapija z zdravilom Cyramza je indicirana za zdravljenje odraslih bolnikov z napredovalim rakom želodca ali adenokarcinomom gastro-ezofagealnega prehoda z napredovalo boleznijo po predhodni kemoterapiji s platino ali fluoropirimidinom, za katere zdravljenje v kombinaciji s paklitakselom ni primerno. Zdravilo Cyramza je v kombinaciji s shemo FOLFIRI indicirano za zdravljenje odraslih bolnikov z metastatskim kolorektalnim rakom (mCRC), z napredovanjem bolezni ob ali po predhodnem zdravljenju z bevacizumabom, oksaliplatinom in fluoropirimidinom. Zdravilo Cyramza je v kombinaciji z docetakselom indicirano za zdravljenje odraslih bolnikov z lokalno napredovalim ali metastatskim nedrobnoceličnim pljučnim rakom, z napredovanjem bolezni po kemoterapiji na osnovi platine. **Odmerjanje in način uporabe** Zdravljenje z ramucirumabom morajo uvesti in nadzirati zdravniki z izkušnjami v onkologiji. Odmerjanje *Rak želodca in adenokarcinom gastro-ezofagealnega prehoda* Priporočeni odmerek ramucirumaba je 8 mg/kg 1. in 15. dan 28-dnevnega cikla, pred infuzijo paklitaksela. Priporočeni odmerek paklitaksela je 80 mg/m^2 in se daje z intravenskim infundiranjem, ki traja približno 60 minut, 1., 8. in 15. dan 28-dnevnega cikla. Pred vsakim infundiranjem paklitaksela je treba pri bolnikih pregledati celotno krvno sliko in izvide kemičnih preiskav krvi, da se oceni delovanje jeter. Priporočeni odmerek ramucirumaba kot monoterapije je 8 mg/kg vsaka 2 tedna. *Kolorektalni rak* Priporočeni odmerek ramucirumaba je 8 mg/kg vsaka 2 tedna, dan z intravensko infuzijo pred dajanjem sheme FOLFIRI. Pred kemoterapijo je treba bolnikom odvzeti kri za popolno krvno sliko. *Nedrobnocelični pljučni rak (NSCLC)* Priporočeni odmerek ramucirumaba je 10 mg/kg na 1. dan 21-dnevnega cikla, pred infuzijo docetaksela. Priporočeni odmerek docetaksela je 75 mg/m^2, dan z intravensko infuzijo v približno 60 minutah na 1. dan 21-dnevnega cikla. *Premedikacija* Pred infundiranjem ramucirumaba je priporočljiva premedikacija z antagonistom histaminskih receptorjev H1. Način uporabe Po redčenju se zdravilo Cyramza daje kot intravenska infuzija v približno 60 minutah. Zdravila ne dajajte v obliki intravenskega bolusa ali hitre intravenske injekcije. Da boste dosegli zahtevano trajanje infundiranja približno 60 minut, največja hitrost infundiranja ne sme preseči 25 mg/minuto, saj morate sicer podaljšati trajanje infundiranja. Bolnika je med infundiranjem treba spremljati glede znakov reakcij, povezanih z infuzijo, zagotoviti pa je treba tudi razpoložljivost ustrezne opreme za oživljanje. **Kontraindikacije** Pri bolnikih z NSCLC je ramucirumab kontraindiciran, kjer gre za kavitacijo tumorja ali prepletenost tumorja z glavnimi žilami. **Posebna opozorila in previdnostni ukrepi** Trajno prekinite zdravljenje z ramucirumabom pri bolnikih, pri katerih se pojavijo resni arterijski trombembolični dogodki, gastrointestinalne perforacije, krvavitev stopnje 3 ali 4, če zdravstveno pomembne hipertenzije ni mogoče nadzirati z antihipertenzivnim zdravljenjem ali če se pojavi fistula, raven beljakovin v urinu > 3 g/24 ur ali v primeru nefrotskega sindroma. Pri bolnikih z neuravnano hipertenzijo zdravljenja z ramucirumabom ne smete uvesti, dokler oziroma v kolikor obstoječa hipertenzija ni uravnana. Pri bolnikih s ploščatoceličnо histologijo obstaja večje tveganje za razvoj resnih pljučnih krvavitev. Če se pri bolniku med zdravljenjem razvijejo zapleti v zvezi s celjenjem rane, prekinite zdravljenje z ramucirumabom, dokler rana ni povsem zaceljena. V primeru pojava stomatitisa je treba takoj uvesti simptomatsko zdravljenje. Pri bolnikih, ki so prejemali ramucirumab in docetaksel za zdravljenje napredovalega NSCLC z napredovanjem bolezni po kemoterapiji na osnovi platine, so opazili trend manjše učinkovitosti z naraščajočo starostjo. **Medsebojno delovanje z drugimi zdravili in druge oblike interakcij** Med ramucirumabom in parlitakselom niso opazili medsebojnega delovanja. **Plodnost, nosečnost in dojenje** Ženskam v rodni dobi je treba svetovati, naj se izogn ejo zanositvi med zdravljenjem z zdravilom Cyramza in jih je treba seznaniti z možnim tveganjem za nosečnost in plod. Ni znano, ali se ramucirumab izloča v materino mleko. **Neželeni učinki** *Zelo pogosti (≥ 1/10)* nevtropenija, levkopenija, trombocitopenija, hipoalbuminemija, hipertenzija, epistaksa, gastrointestinalne krvavitve, stomatitis, driska, proteinurija, utrujenost/astenija, periferni edem, bolečina v trebuhu. *Pogosti (≥ 1/100 do < 1/10)* hipokaliemija, hiponatriemija, glavobol. **Rok uporabnosti** 3 leta **Posebna navodila za shranjevanje** Shranjujte v hladilniku (2 °C–8 °C). Ne zamrzujte. Vialo shranjujte v zunanji ovojnini, da zagotovite zaščito pred svetlobo. **Pakiranje** 2 viali z 10 ml **IMETNIK DOVOLJENJA ZA PROMET Z ZDRAVILOM** Eli Lilly Nederland B.V., Papendorpseweg 83, 3528 BJ Utrecht, Nizozemska **DATUM ZADNJE REVIZIJE BESEDILA** 25.01.2016
Režim izdaje: Predpisovanje in izdaja zdravila je le na recept, zdravilo pa se uporablja samo v bolnišnicah.

Pomembno obvestilo:

Pričujoče gradivo je namenjeno **samo za strokovno javnost**. Zdravilo Cyramza se izdaja le na recept, zdravilo pa se uporablja samo v bolnišnicah. Pred predpisovanjem zdravila Cyramza vas vljudno prosimo, da preberete celotni Povzetek glavnih značilnosti zdravila Cyramza. Podrobnejše informacije o zdravilu Cyramza in o zadnji reviziji besedila Povzetka glavnih značilnosti zdravila so na voljo na sedežu podjetja Eli Lilly (naslov podjetja in kontaktni podatki spodaj) in na spletni strani European Medicines Agency (EMA): www.ema.europa.eu. in na spletni strani European Commission http://ec.europa.eu/health/documents/community-register/html/alfregister.htm.

Eli Lilly farmacevtska družba, d.o.o., Dunajska cesta 167, 1000 Ljubljana, telefon: (01) 5800 010, faks: (01) 5691 705

Referenca: 1. https://pharmaphorum.com/news/lilly-s-cyramza-approved-in-eu-for-stomach-cancer/?epoch=1505121044344

PP-RB-SI-0002, 17.11.2017.

Lilly

Literatura:
1. Povzetek glavnih značilnosti zdravila Perjeta, dostopano maja 2018 na http://www.ema.europa.eu/docs/sl_SI/document_library/EPAR_-_Product_Information/human/002547/WC500140980.pdf

Samo za strokovno javnost.

Perjeta/Herceptin - opozorila za nosečnice in bolnice, ki bi lahko zanosile

- Uporabi zdravila Herceptin se je med nosečnostjo treba izogibati, razen v primerih, ko pričakovana korist za mater upravičuje tveganje za plod. Uporaba zdravila Perjeta med nosečnostjo in pri ženskah v rodni dobi, ki ne uporabljajo kontracepcije, ni priporočljiva. Podatkov o uporabi zdravil Perjeta/Herceptin pri nosečnicah je malo in varna uporaba zdravil Perjeta/Herceptin med nosečnostjo in dojenjem ni bila raziskana/dokazana.
- Podatkov o vplivu na plodnost za zdravili Herceptin/Perjeta ni oz. so omejeni.
- V obdobju po prihodu zdravila Herceptin na trg so pri nosečnicah, ki so prejemale zdravilo Herceptin, poročali o primerih motenj v rasti plodovih ledvic in/ali njihovem delovanju v povezavi z oligohidramnijem, od katerih so bili nekateri povezani s smrtno hipoplazijo pljuč pri plodu.
- Pred uvedbo zdravljenja z zdravili Perjeta/Herceptin preverite, ali je bolnica morda noseča. Ženske, ki so v rodni dobi, morajo uporabljati učinkovito kontracepcijo med zdravljenjem z zdravili Perjeta/Herceptin ter vsaj še 6 mesecev po prejemu zadnjega odmerka zdravila Perjeta oz. vsaj še 7 mesecev po koncu zdravljenja z zdravilom Herceptin.
- Bolnice, ki zanosijo med zdravljenjem z zdravili Perjeta/Herceptin ali v 6 mesecih po prejemu zadnjega odmerka zdravila Perjeta oz. v 7 mesecih po prejemu zadnjega odmerka zdravila Herceptin, je treba spremljati glede oligohidramnija.
- Ni znano, ali se pri ljudeh zdravilo Herceptin izloča v materino mleko. Ker se humani IgG izloča v materino mleko, potencialni škodljivi vpliv na otroka pa ni znan, ženske ne smejo dojiti med zdravljenjem z zdravilom Herceptin in še 7 mesecev po zadnjem odmerku zdravila. Pri zdravilu Perjeta se je treba odločiti o prenehanju dojenja ali prenehanju zdravljenja.

Poudarjeno varnostno poročanje za morebitne primere nosečnosti ob izpostavljenosti zdravilu Perjeta/Herceptin.

Če se zdravili Perjeta/Herceptin uporabljata med nosečnostjo ali če bolnica zanosi med zdravljenjem ali v 6 mesecih po prejemu zadnjega odmerka zdravila Perjeta oz. 7 mesecih po zadnjem odmerku zdravila Herceptin, vas prosimo, da to takoj sporočite podjetju Roche farmacevtska družba d.o.o. (na e-naslov: slovenia.drugsafety@roche.com ali po telefonu na številko 01 3602 606).

Prosili vas bomo za dodatne informacije o izpostavljenosti zdravilома Perjeta/Herceptin med nosečnostjo in v prvem letu otrokovega življenja. Informacije bodo podjetju Roche omogočile bolje razumevanje varnosti uporabe zdravil Herceptin / Perjeta in s tem bodo ustrezno obveščeni tudi regulatorni organi, zdravstveni delavci in bolniki.

Ime zdravila: Perjeta 420 mg koncentrat za raztopino za infundiranje **Kakovostna in količinska sestava:** Ena 14-ml viala koncentrata vsebuje 420 mg pertuzumaba s koncentracijo 30 mg/ml. Po razredčitvi vsebuje en ml raztopine približno 3,02 mg pertuzumaba v začetnem odmerku in približno 1,59 mg pertuzumaba v vzdrževalnem odmerku. **Terapevtske indikacije:** Metastatski rak dojk: Zdravilo Perjeta je v kombinaciji s trastuzumabom in docetakselom indicirano za zdravljenje odraslih bolnikov z metastatskim HER2-pozitivnim rakom dojk ali z lokalno, neoperabilno ponovitvijo raka dojk, ki pred tem še niso prejeli anti-HER2 terapije ali kemoterapije za metastatsko bolezen. Neoadjuvantno zdravljenje raka dojk: Zdravilo Perjeta je v kombinaciji s trastuzumabom in kemoterapijo indicirano za neoadjuvantno zdravljenje odraslih bolnikov s HER2-pozitivnim, lokalno napredovanim, vnetnim rakom dojk ali zgodnjim stadijem raka dojk z visokim tveganjem za ponovitev. **Odmerjanje in način uporabe:** Zdravljenje z zdravilom Perjeta lahko uvede le zdravnik, ki ima izkušnje z uporabo zdravil proti raku. Zdravilo Perjeta lahko daje samo zdravstveni delavec, ki zna ukrepati v primeru anafilaksije, in ga daje v okolju, kjer je na voljo vsa nujno potrebna medicinska oprema za oživljanje. Odmerjanje: Bolniki, zdravljeni z zdravilom Perjeta, morajo imeti HER2-pozitivni tumor, imunohistokemično opredeljen kot 3+ in/ali razmerje pri ***in situ hibridizaciji*** (ISH) ≥ 2,0, opredeljeno z validiranim testom. Priporočen začetni uvajalni odmerek pertuzumaba je 840 mg v 60-minutni intravenski infuziji, ki mu sledi vzdrževalni odmerek 420 mg vsake 3 tedne, dan v 30 do 60 minutah. Zdravila je treba dajati zaporedoma, ne smemo jih mešati v isto infuzijsko vrečko. Zdravilo Perjeta in trastuzumab lahko damo v katerem koli vrstnem redu. Če bolnik prejema docetaksel, ga je treba dati po zdravilu Perjeta in trastuzumabu. Po vsaki infuziji zdravila Perjeta in pred začetkom katere koli nadaljnje infuzije trastuzumaba ali docetaksela je priporočljivo 30-do 60-minutno opazovalno obdobje. ***Metastatski rak dojk:*** Bolnike je treba z zdravilom Perjeta in trastuzumabom zdraviti do napredovanja bolezni ali pojava neobvladljivih toksičnih učinkov. ***Neoadjuvantno zdravljenje raka dojk:*** Pri neoadjuvantnem zdravljenju, ki predstavlja del zdravljenja zgodnjega raka dojk, je treba zdravilo Perjeta dajati 3 do 6 ciklov v kombinaciji s trastuzumabom in kemoterapijo. Po operaciji morajo bolniki prejeti adjuvantno zdravljenje s trastuzumabom do zaključka 1-letnega zdravljenja. ***Prilagoditev odmerka:*** Odmerkov zdravila Perjeta ni priporočljivo zmanjševati. Bolniki lahko med obdobji reverzibilne mielosupresije, povzročene s kemoterapijo, nadaljujejo z zdravljenjem, vendar jih je v tem času treba skrbno spremljati zaradi zapletov, ki jih lahko povzroči nevtropenija. Odmerkov trastuzumaba ni priporočljivo zmanjševati. Če se ukine zdravljenje s trastuzumabom, je treba ukiniti tudi zdravljenje z zdravilom Perjeta. Če se ukine zdravljenje z docetakselom, se lahko zdravljenje z zdravilom Perjeta in trastuzumabom nadaljuje do napredovanja bolezni ali pojava neobvladljivih toksičnih učinkov pri metastatskem raku. ***Disfunkcija levega prekata:*** Zdravljenje z zdravilom Perjeta in trastuzumabom je treba prekiniti za vsaj 3 tedne, če nastopi kar koli od navedenega: znaki in simptomi, ki kažejo na kongestivno srčno popuščanje; iztisni delež levega prekata (LVEF) pade pod 40 %, ali je LVEF 40- do 45-%, in je vrednost padla za ≥ 10 odstotnih točk glede na vrednosti pred začetkom zdravljenja. ***Posebne populacije:*** Za bolnike, starejše od 65 let, prilagajanje odmerka zdravila Perjeta ni potrebno. Pri bolnikih z blago do zmerno okvaro ledvic prilagajanje odmerka pertuzumaba ni potrebno. Varnost in učinkovitost zdravila Perjeta pri bolnikih z okvaro jeter nista raziskani. Varnost in učinkovitost zdravila Perjeta pri otrocih in mladostnikih, mlajših od 18 let, nista raziskani. Način uporabe: Zdravilo Perjeta se daje v intravenski infuziji, ki pa ne sme biti hitra. Zdravila se ne sme dajati v obliki bolusa. ***Infuzijske reakcije:*** Če se razvije infuzijska reakcija, se hitrost infuzije upočasni ali infundiranje prekine. Ko simptomi izzvenijo, lahko z infundiranjem nadaljujemo. **Kontraindikacije:** Preobčutljivost na učinkovino ali katero koli pomožno snov. **Posebna opozorila in previdnostni ukrepi:** ***Sledljivost:*** Za izboljšanje sledljivosti bioloških zdravil je treba zaščiteno ime in številko serije danega zdravila jasno zabeležiti. ***Disfunkcija levega prekata (vključno s kongestivnim srčnim popuščanjem):*** Med uporabo zdravil, ki zavirajo aktivnost HER2, med katere spada tudi zdravilo Perjeta, so poročali o zmanjšanju LVEF. Pri bolnikih, ki so predhodno prejemali antracikline ali bili obsevani v predelu prsnega koša, lahko obstaja večje tveganje za znižanje LVEF. V obdobju neoadjuvatnega zdravljenja je bila incidenca LVD večja v skupinah, zdravljenih z zdravilom Perjeta, kot pri tistih, ki zdravila Perjeta niso prejemali. Pred uvedbo zdravila Perjeta je treba oceniti vrednost LVEF in jo nato med zdravljenjem z zdravilom Perjeta tudi spremljati ter zagotoviti, da LVEF ostaja znotraj normalnih vrednosti, ki veljajo za ustanovo. Pred uporabo zdravila Perjeta skupaj z antraciklinom je treba skrbno razmisliti o srčnem tveganju in ga pretehtati glede na zdravstvene potrebe posameznega bolnika. Na podlagi farmakološkega delovanja pertuzumaba in antraciklinov je mogoče pričakovati večje tveganje za srčno toksičnost ob sočasni uporabi teh učinkovin v primerjavi z zaporedno uporabo, čeprav tega v študiji TRYPHAENA ni bilo opaziti. ***Infuzijske reakcije:*** Priporoča se skrbno opazovanje bolnika med prvo infuzijo in še 60 minut po njej ter med vsako naslednjo infuzijo zdravila Perjeta in še 30 do 60 minut po njej. Če se pojavi pomembna infuzijska reakcija, je treba hitrost infuzije zmanjšati ali jo prekiniti in uporabiti ustrezna zdravila. Bolnike je treba pregledati in jih natančno nadzirati, dokler znaki in simptomi povsem ne izginejo. Pri bolnikih s hudo infuzijsko reakcijo je treba razmisliti o trajnem prenehanju uporabe zdravila. ***Preobčutljivostne reakcije/anafilaksija:*** Bolnike je treba skrbno opazovati glede preobčutljivostnih reakcij. V kliničnih preskušanjih z zdravilom Perjeta so opazili hudo preobčutljivost, vključno z anafilaksijo. Zdravila za zdravljenje take reakcije kot tudi oprema za nujne primere morajo biti na voljo za takojšnjo uporabo. Zdravilo Perjeta je treba dokončno ukiniti v primeru preobčutljivostne reakcije stopnje 4 po merilih NCI-CTCAE, bronhospazma ali akutnega respiratornega distresnega sindroma. ***Febrilna nevtropenija:*** Pri bolnikih, ki se zdravijo z zdravilom Perjeta, trastuzumabom in docetakselom, obstaja večje tveganje za nastanek febrilne nevtropenije v primerjavi z bolniki, ki se zdravijo s placebom, trastuzumabom in docetakselom, še posebej med prvimi 3 cikli zdravljenja. V študiji CLEOPATRA pri metastatskem raku dojk je bilo najmanjše število nevtrofilcev podobno pri bolnikih, zdravljenih z zdravilom Perjeta, in bolnikih, ki so prejemali placebo. Večja incidenca febrilne nevtropenije pri bolnikih, ki so prejemali zdravilo Perjeta, je bila povezana z večjo incidenco mukozitisa in diareje pri teh bolnikih. Smotrno je razmisliti o podpornem zdravljenju mukozitisa in diareje. ***Diareja:*** Pertuzumab lahko izzove hudo diarejo. V primeru pojava hude diareje je treba uvesti antidiaroike in razmisliti o prekinitvi zdravljenja s pertuzumabom, če ne dosežemo izboljšanja stanja. Ko je diareja uravnana, lahko zdravljenje s pertuzumabom ponovno uvedemo. **Medsebojno delovanje z drugimi zdravili in druge oblike interakcij:** Pri 37 bolnikih, ki so bili vključeni v podštudijo ključnega randomiziranega preskušanja CLEOPATRA pri metastatskem raku dojk, niso opazili medsebojnega farmakokinetičnega delovanja med pertuzumabom in trastuzumabom in tudi ne med pertuzumabom in docetakselom. Tudi farmakokinetična populacijska analiza ni pokazala medsebojnega delovanja med pertuzumabom in trastuzumabom ali med pertuzumabom in docetakselom. Štiri študije so ocenjevale vpliv pertuzumaba na farmakokinetiko sočasno danih citotoksičnih zdravil: docetaksela, gemcitabina, erlotiniba in kapecitabina. Med pertuzumabom in navedenimi zdravili niso ugotovili nobenih farmakokinetičnih medsebojnih delovanj. **Neželeni učinki:** ***Zelo pogosti neželeni učinki:*** okužba zgornjih dihal, nazofaringitis, febrilna nevtropenija, nevtropenija, levkopenija, anemija, preobčutljivost/anafilaktična reakcija, infuzijska reakcija/sindrom sproščanja citokinov, zmanjšanje teka, nespečnost, periferna nevropatija, glavobol, dizgevzija, kašelj, diareja, bruhanje, stomatitis, navzea, zaprtje, dispepsija, alopecija, izpuščaj, bolezni nohtov, bolečina v mišicah, bolečina v sklepu, mukozitis/vnetje sluznic, bolečina, edem, zvišana telesna temperatura, utrujenost in astenija. ***Pogosti neželeni učinki:*** paronihija, periferna senzorična nevropatija, omotica, povečano solzenje, disfunkcija levega prekata (vključno s kongestivnim srčnim popuščanjem), plevralni izliv, dispneja, pruritus, suha koža in mrzlica. Poročanje o domnevnih neželenih učinkih: Poročanje o domnevnih neželenih učinkih zdravila po izdaji dovoljenja za promet je pomembno. Omogoča namreč stalno spremljanje razmerja med koristmi in tveganji zdravila. Od zdravstvenih delavcev se zahteva, da poročajo o katerem koli domnevnem neželenem učinku zdravila na: Javna agencija Republike Slovenije za zdravila in medicinske pripomočke, Sektor za farmakovigilanco, Nacionalni center za farmakovigilanco, Slovenčeva ulica 22, SI-1000 Ljubljana, Tel: +386 (0)8 2000 500, Faks: +386 (0)8 2000 510, e-pošta: **h-farmakovigilanca@jazmp.si,** spletna stran: **www.jazmp.si.** Za zagotavljanje sledljivosti zdravila je pomembno, da pri izpolnjevanju obrazca o domnevnih neželenih učinkih zdravila navedete številko serije biološkega zdravila. **Režim izdaje zdravila:** H. **Imetnik dovoljenja za promet:** Roche Registration GmbH, Emil-Barell-Strasse 1, 79639 Grenzach-Wyhlen, Nemčija. **Verzija:** 1.0/18. **Informacija pripravljena:** maj 2018.

Ime zdravila: Herceptin 150 mg prašek za koncentrat za raztopino za infundiranje in Herceptin 600 mg raztopina za injiciranje v viali **Kakovostna in količinska sestava: Herceptin 150 mg prašek za koncentrat za raztopino za infundiranje (v nad. Herceptin i.v.):** ena viala vsebuje 150 mg trastuzumaba. Pripravljena raztopina zdravila Herceptin vsebuje 21 mg/ml trastuzumaba. **Herceptin 600 mg raztopina za injiciranje v viali (v nad. Herceptin s.c.):** ena 5-mililitrska viala vsebuje 600 mg trastuzumaba. Trastuzumab je humanizirano monoklonsko protitelo IgG1, pridobljeno iz suspenzijske celične kulture sesalcev. **Terapevtske indikacije: Metastatski rak dojk** Zdravilo Herceptin je indicirano za zdravljenje odraslih bolnikov s HER2 pozitivno metastatsko obliko raka dojk: a) kot monoterapija za zdravljenje tistih bolnikov, ki so za svojo metastatsko bolezen predhodno že prejemali najmanj dve liniji kemoterapije. Predhodna kemoterapija mora vsebovati vsaj en antraciklinski in taksanski derivat, razen če bolniki za takšno zdravljenje niso bili primerni. Bolniki s hormonsko odvisnimi tumorji, pri katerih je bolezen napredovala po predhodnem hormonskem zdravljenju, razen če bolniki za takšno zdravljenje niso bili primerni. b) v kombinaciji s paklitakselom za zdravljenje tistih bolnikov, ki še niso prejemali kemoterapije za metastatsko bolezen in za katere antraciklini niso primerni. c) v kombinaciji z docetakselom za zdravljenje tistih bolnikov, ki še niso prejemali kemoterapije za metastatsko bolezen. d) v kombinaciji z zaviralcem aromataze za zdravljenje bolnic v postmenopavzi z metastatsko obliko raka dojk s pozitivnimi hormonskimi receptorji, ki predhodno niso bile zdravljene s trastuzumabom. **Zgodnji rak dojk** Zdravilo Herceptin je indicirano za zdravljenje odraslih bolnikov z zgodnjo obliko HER2-pozitivnega raka dojk: a) po operaciji, kemoterapiji (neoadjuvantni ali adjuvantni) in radioterapiji (če je primerno); b) po adjuvantni kemoterapiji z doksorubicinom in ciklofosfamidom, v kombinaciji s paklitakselom ali docetakselom; c) v kombinaciji z adjuvantno kemoterapijo z docetakselom in karboplatinom; d) v kombinaciji z neoadjuvantno kemoterapijo, čemur sledi adjuvantno zdravljenje z zdravilom Herceptin, za lokalno napredovalo (tudi vnetno) bolezen kot tumorje > 2 cm v premeru. Zdravilo Herceptin se uporablja le za bolnike z metastatskim ali zgodnjim rakom dojk, katerih tumorji imajo ali čezmerno izražen HER2 ali amplifikacijo gena HER2, določeno s točno in validirano metodo. **Metastatski rak želodca** (le za Herceptin i.v.) Zdravilo Herceptin je v kombinaciji s kapecitabinom ali 5-fluorouracilom in cisplatinom indicirano za zdravljenje bolnikov s HER2-pozitivnim metastatskim adenokarcinomom želodca ali gastroezofagealnega prehoda, ki še niso prejemali zdravil za zdravljenje raka za metastatsko bolezen. Zdravilo Herceptin se uporablja le za bolnike z metastatskim rakom želodca, katerih tumorji imajo čezmerno izražen HER2, definiran kot IHC2+ z nadaljnjim potrditvenim SISH ali FISH rezultatom ali kot IHC3+. Treba je uporabljati točne in validirane metode. **Odmerjanje in način uporabe:** Pred začetkom zdravljenja je potrebno testiranje na HER2. Pomembno je preveriti ovojnino zdravila in zagotoviti, da bolnik prejme pravilno obliko, kot mu je bila predpisana. Intravenska oblika zdravila Herceptin ni namenjena subkutani aplikaciji in se lahko daje le z intravensko infuzijo. Subkutana oblika zdravila Herceptin ni namenjena intravenski aplikaciji in se lahko daje le s subkutano injekcijo. Za preprečitev napak pri dajanju zdravila je pomembno preveriti nalepke na vialah in tako zagotoviti, da je pripravljeno in uporabljeno zdravilo Herceptin (trastuzumab) in ne zdravila Kadcyla (trastuzumab emtanzin). **Odmerjanje Herceptin i.v.:** ***Metastatski rak dojk: 3-tedenski režim:*** *Uvajalni odmerek:* 8 mg/kg telesne mase. ***Vzdrževalni odmerek:*** 6 mg/kg telesne mase po 3 tednih od prejema uvajalnega odmerka, in nato v tritedenskih razmakih. ***Tedenski režim:*** *Uvajalni odmerek:* 4 mg/kg telesne mase. ***Vzdrževalni odmerek:*** 2 mg/kg telesne mase, z začetkom en teden po uvajalnem odmerku. ***Zgodnji rak dojk: 3-tedenski režim:*** *Uvajalni odmerek:* 8 mg/kg telesne mase. ***Vzdrževalni odmerek:*** 6 mg/kg telesne mase po 3 tednih od prejema uvajalnega odmerka, in nato v tritedenskih razmakih. ***Tedenski režim:*** Pri tedenskem režimu (uvajalni odmerek 4 mg/kg telesne mase, nato 2 mg/kg telesne mase svak teden) se zdravilo Herceptin daje sočasno s paklitakselom po kemoterapiji z doksorubicinom in ciklofosfamidom. ***Metastatski rak želodca: 3-tedenski režim:*** *Uvajalni odmerek:* 8 mg/kg telesne mase. ***Vzdrževalni odmerek:*** 6 mg/kg telesne mase po 3 tednih od prejema uvajalnega odmerka, in nato v tritedenskih razmakih. ***Trajanje zdravljenja:*** Bolnike z metastatskim rakom dojk ali metastatskim rakom želodca je treba z zdravilom Herceptin zdraviti do napredovanja bolezni. Bolnike z zgodnjim rakom dojk je treba z zdravilom Herceptin zdraviti 1 leto ali do ponovitve bolezni, kar nastopi prej. **Način uporabe:** Uvajalni odmerek zdravila Herceptin se daje kot 90-minutna intravenska infuzija. Zdravila ne smemo dajati kot hitro intravensko infuzijo ali bolus. Infuzijo mora dajati zdravstveno osebje, usposobljeno za ukrepanje ob anafilaksiji; na voljo mora biti oprema za urgentno ukrepanje. Bolniki morajo biti pod nadzorom vsaj šest ur po začetku prve infuzije in dve uri po začetku nadaljnjih infuzij zaradi nevarnosti pojava simptomov, kot so zvišana telesna temperatura, mrzlica in drugi simptomi, povezani z infundiranjem. Prekinitev ali upočasnitev hitrosti dajanja infuzije lahko pomaga pri nadzoru teh simptomov. Ko simptomi izginejo, lahko z infuzijo nadaljujemo. Če je bolnik uvajalni odmerek dobro prenašal, lahko nadaljnje odmerke dajemo kot 30-minutne infuzije. **Odmerjanje Herceptin s.c.:** Priporočeni odmerek zdravila Herceptin v subkutani obliki je 600 mg ne glede na bolnikovo telesno maso. ***Trajanje zdravljenja:*** Bolnike z metastatskim rakom dojk je treba z zdravilom Herceptin zdraviti do napredovanja bolezni. Bolnike z zgodnjim rakom dojk je treba z zdravilom Herceptin zdraviti 1 leto ali do ponovitve bolezni, kar nastopi prej. ***Izpuščeni odmerki:*** Če je bolnik izpustil odmerek zdravila Herceptin v subkutani obliki, mu je treba dati naslednji (izpuščeni) 600-mg odmerek čim prej. Interval med zaporednima odmerkoma zdravila Herceptin v subkutani obliki ne sme biti krajši od treh tednov. ***Način uporabe:*** Odmerek 600 mg moramo dati izključno s subkutano injekcijo v 2 do 5 minutah vsake tri tedne. Bolniki morajo biti pod nadzorom šest ur po prvem injiciranju zdravila in dve uri po nadaljnjih aplikacijah zaradi možnosti znakov in simptomov reakcij, povezanih z aplikacijo zdravila. **Zmanjšanje odmerka (obe obliki):** Med kliničnimi preskušanji niso zmanjševali odmerka zdravila Herceptin. Bolniki lahko nadaljujejo zdravljenje tudi med obdobji reverzibilne mielosupresije, ki je posledica kemoterapije, vendar pa jih je v tem času treba skrbno spremljati zaradi zapletov nevtropenije. Če odstotek iztisnega deleža levega prekata (LVEF) pade za ≥ 10 točk od začetne vrednosti IN pod 50 %, zdravljenje prekinemo in ponovno opravimo meritev LVEF v približno treh tednih. Če se LVEF ne izboljša ali pride do nadaljnjega zmanjšanja ali se razvije simptomatsko kongestivno srčno popuščanje, je potreben resen razmislek o prekinitvi zdravljenja z zdravilom Herceptin, razen če je korist za posameznega bolnika večja od tveganja. Vse take bolnike je treba napotiti na pregled h kardiologu in jih spremljati. **Kontraindikacije:** Preobčutljivost za trastuzumab, murine beljakovine ali katerokoli pomožno snov; pri bolnikih, ki imajo hudo dispnejo v mirovanju zaradi komplikacij napredovale maligne bolezni, ali pri tistih, ki potrebujejo zdravljenje s kisikom. **Posebna opozorila in previdnostni ukrepi:** ***Sledljivost:*** Za izboljšanje sledljivosti bioloških zdravil je treba zaščiteno ime in številko serije uporabljenega zdravila jasno zabeležiti. ***Motnje v delovanju srca*** Pri bolnikih, ki so se zdravili z zdravilom Herceptin, obstaja večje tveganje za pojav kongestivnega srčnega popuščanja ali asimptomatične motnje v delovanju srca. Te neželene učinke so opazili pri bolnikih, ki so prejemali zdravilo Herceptin v monoterapiji ali v kombinaciji s paklitakselom ali docetakselom, zlasti po kemoterapiji z antraciklini. Previdnost je potrebna tudi pri zdravljenju bolnikov s povečanim srčnim tveganjem. Vsem kandidatom za zdravljenje z zdravilom Herceptin, posebno tistim, ki smo jih predhodno zdravili z antraciklini in ciklofosfamidom, moramo pred zdravljenjem pregledati delovanje srca, vključno z anamnezo in fizičnim pregledom, EKG, ehokardiogramom in/ali radioizotopsko ventrikulografijo ali magnetnoresonančnim slikanjem. Vse nadaljnje kardiološke preglede, je treba med zdravljenjem ponoviti vsake 3 mesece in vsakih 6 mesecev po končanem zdravljenju do 24 mesecev po prejemu zadnjega odmerka. Če je mogoče, se po prekinitvi zdravljenja z zdravilom Herceptin do 7 mesecev izogibamo zdravljenju z antraciklini. Če bolnika zdravimo z antraciklini, je treba skrbno spremljati delovanje njegovega srca. Med zdravljenjem je treba nadzorovati delovanje srca pri vseh bolnikih. Za bolnike z asimptomatičnimi motnjami v delovanju srca je koristen pogostejši nadzor. Pri bolnikih s kontinuiranim upadanjem funkcije levega prekata, ki ostajajo asimptomatični, naj zdravnik razmisli o ukinitvi zdravljenja z zdravilom Herceptin, če klinična korist ni bila opazna. Če odstotek LVEF pade za ≥ 10 točk od začetne vrednosti IN pod 50 %, zdravljenje prekinemo in ponovno opravimo meritev LVEF v približno treh tednih. Če se LVEF ne izboljša ali pride do nadaljnjega zmanjšanja ali se razvije simptomatsko srčno popuščanje, je potreben resen razmislek o prekinitvi zdravljenja z zdravilom Herceptin, razen če je korist za posameznega bolnika večja od tveganja. Vse take bolnike je treba napotiti na pregled h kardiologu in jih spremljati. Če se med zdravljenjem z zdravilom Herceptin razvije simptomatsko srčno popuščanje, ga zdravimo s standardnimi zdravili za kongestivno srčno popuščanje. ***Metastatski rak dojk*** Pri zdravljenju metastatskega raka dojk kombinacije zdravila Herceptin in antraciklinov ne smemo dajati sočasno. Pri bolnikih z metastatskim rakom dojk, ki so se predhodno zdravili z antraciklini, pri zdravljenju z zdravilom Herceptin tveganje za motnje v delovanju srca še vedno obstaja, le da je manjše kot pri sočasni uporabi. ***Zgodnji rak dojk*** Pri bolnikih, ki prejemajo kemoterapijo z antraciklini, je priporočljivo nadaljnje spremljanje delovanja srca, ki ga je treba izvajati letno do 5 let po zadnjem dajanju zdravila Herceptin ali dlje, če LVEF stalno pada. Bolniki z anamnezo miokardnega infarkta, angino pektoris, ki jo je treba zdraviti, anamnezo kongestivnega srčnega popuščanja, LVEF < 55 %, drugimi kardiomiopatijami, srčno aritmijo, ki jo je treba zdraviti, klinično pomembno boleznijo srčnih zaklopk, slabo uravnano hipertenzijo in hemodinamsko efektivno perikardialno efuzijo niso bili vključeni v adjuvantna in neoadjuvantna ključna preskušanja zgodnjega raka dojk z zdravilom Herceptin. Zato za te bolnike zdravljenja ne moremo priporočiti. ***Adjuvantno zdravljenje*** Pri adjuvantnem zdravljenju raka dojk zdravila Herceptin in antraciklinov ne smemo dajati sočasno. Pri bolnikih z zgodnjim rakom dojk so opazili povišanje incidence simptomatskih in asimptomatskih neželenih učinkov, povezanih s srcem, ko so zdravilo Herceptin (v intravenski obliki) dajali po kemoterapiji, ki je vsebovala antraciklin v primerjavi s sočasnim dajanjem z neantraciklinskim režimom, ki je vseboval docetaksel in karboplatin. Povišanje incidence je bilo izrazitejše pri sočasnem dajanju zdravila Herceptin (v intravenski obliki) in taksanov kot pri zaporednem dajanju zdravila Herceptin (v intravenski obliki) po taksanih. ***Neoadjuvantno-adjuvantno zdravljenje*** Pri bolnikih z zgodnjim rakom dojk, ki so primerni za neoadjuvantno-adjuvantno zdravljenje, se zdravilo Herceptin uporablja sočasno z antraciklini le pri bolnikih, ki še niso bili zdravljeni s kemoterapijo, in to samo pri shemah z majhnimi odmerki antraciklinov. Če so se bolniki v neoadjuvantnem zdravljenju sočasno zdravili z majhnimi odmerki antraciklinov v celoti in zdravilom Herceptin, potem jim po operaciji ne smemo dati dodatne citotoksične kemoterapije. Kliničnih izkušenj pri bolnikih, starejših od 65 let, je malo. ***Reakcije, povezane z infuzijo, in preobčutljivost (Herceptin i.v.)*** Poročali so o resnih reakcijah, povezanih z infuzijo zdravila Herceptin, vključno z dispnejo, hipotenzijo, piskanjem, hipertenzijo, bronhospazmom, supraventrikularno tahiaritmijo, zmanjšano saturacijo arterijske krvi s kisikom, anafilaksijo, dihalno stisko, urtikarijo in angioedemom. Za zmanjšanje tveganja pojava teh neželenih učinkov lahko uporabimo premedikacijo. Če se pojavi infuzijska reakcija, je potrebno infundiranje zdravila Herceptin prekiniti ali upočasniti njegovo hitrost in bolnika nadzorovati, dokler vsi simptomi ne izzvenijo. Lahko jih zdravimo z analgetikom/antipiretikom ali antihistaminikom. Pri večini bolnikov so simptomi izzveneli in so z infundiranjem zdravila Herceptin nadaljevali. Resne reakcije so uspešno zdravili s podpornim zdravljenjem, kot so kisik, beta agonisti in kortikosteroidi. Poročali so tudi o primerih začetnega izboljšanja, ki mu je sledilo klinično poslabšanje, in zapoznelih reakcij s hitrim kliničnim poslabšanjem. ***Reakcije, povezane z aplikacijo (Herceptin s.c.)*** Znano je, da se pri dajanju subkutane oblike zdravila Herceptin pojavijo reakcije, povezane z aplikacijo. Za zmanjšanje tveganja pojava reakcij, povezanih z aplikacijo, lahko uporabimo premedikacijo. Čeprav o resnih neželenih reakcijah, povezanih z aplikacijo v kliničnih preskušanjih subkutane oblike zdravila Herceptin niso poročali, je potrebna previdnost, saj so te povezane z intravensko obliko. Bolnike je treba zaradi pojava reakcij, povezanih z aplikacijo, opazovati šest ur po prvem injiciranju in dve uri po nadaljnjih injiciranjih. Pri bolnikih, ki imajo dispnejo v mirovanju zaradi komplikacij napredovale maligne bolezni in soobolenja, obstaja večje tveganje za reakcije, povezane z aplikacijo, s smrtnim izidom. Zato takih bolnikov ne smemo zdraviti z zdravilom Herceptin. ***Pljučni zapleti*** V obdobju po prihodu zdravila na trg so pri uporabi zdravila Herceptin v intravenski obliki poročali o hudih pljučnih zapletih. Poleg tega so poročali o primerih intersticijske bolezni pljuč, akutnem respiratornem distresnem sindromu, pljučnici, pnevmonitisu, plevralnem izlivu, dihalni stiski, akutnem pljučnem edemu in respiratorni insuficienci. Med dejavnike tveganja, povezane z intersticijsko boleznijo pljuč, spada predhodno ali sočasno zdravljenje z drugimi zdravili z delovanjem na novotvorbe, za katere je znana povezava s to boleznijo, kot so taksani, gemcitabin, vinorelbin in zdravljenje z obsevanjem.Ti učinki se lahko pojavijo kot del infuzijske reakcije ali pa nastopijo kasneje. Pri bolnikih, ki imajo dispnejo v mirovanju zaradi komplikacij napredovale maligne bolezni in soobolenj, obstaja večje tveganje pljučnih zapletov. Zato takih bolnikov ne smemo zdraviti z zdravilom Herceptin. Pozorno je treba spremljati znake pnevmonitisa, še posebno pri bolnikih, ki se sočasno zdravijo s taksani. **Medsebojno delovanje z drugimi zdravili in druge oblike interakcij:** Formalnih študij medsebojnega delovanja niso izvedli. V kliničnih preskušanjih niso opazili klinično pomembnega medsebojnega delovanja med zdravilom Herceptin in zdravili, ki so jih bolniki jemali sočasno. **Neželeni učinki:** Med najbolj resnimi in/ali pogostimi neželenimi učinki, o katerih so poročali pri uporabi zdravila Herceptin (intravenske in subkutane oblike), so motnje v delovanju srca, infuzijske reakcije oz. reakcije povezane z aplikacijo, hematotoksičnost (še posebno nevtropenija), okužbe in pljučni neželeni učinki. ***Zelo pogosti neželeni učinki*** zdravila Herceptin, ki se pojavijo pri več kot 1 od 10 bolnikov, so: okužba, nazofaringitis, febrilna nevtropenija, anemija, nevtropenija, zmanjšano število belih krvnih celic/levkopenija, trombocitopenija, zmanjšanje telesne mase/izguba telesne mase, anoreksija, nespečnost, tremor, omotica, glavobol, parestezija, disgevzija, konjunktivitis, povečano solzenje, znižanje krvnega tlaka, zvišanje krvnega tlaka, nereden srčni utrip, palpitacije, trepetanje srca, zmanjšanje iztisnega deleža, vročinski oblivi, piskanje, dispneja, kašelj, epistaksa, kronična, diareja, bruhanje, navzea, otekanje ustnic, bolečina v trebuhu, dispepsija, zaprtje, stomatitis, eritem, izpuščaj, otekanje obraza, alopecija, spremembe na nohtih, sindrom palmarno-plantarne eritrodisestezije, artralgija, napetost mišic, mialgija, astenija, bolečina v prsnem košu, mrzlica, utrujenost, gripi podobni simptomi, reakcija, povezana z infundiranjem, bolečina, pireksija, vnetje sluznic in periferni edem. Poročanje o domnevnih neželenih učinkih: Poročanje o domnevnih neželenih učinkih zdravila po izdaji dovoljenja za promet je pomembno. Omogoča namreč stalno spremljanje razmerja med koristmi in tveganji zdravila. Od zdravstvenih delavcev se zahteva, da poročajo o katerem koli domnevnem neželenem učinku zdravila na: Javna agencija Republike Slovenije za zdravila in medicinske pripomočke, Sektor za farmakovigilanco, Nacionalni center za farmakovigilanco, Slovenčeva ulica 22, SI-1000 Ljubljana, Tel: +386 (0)8 2000 500, Faks: +386 (0)8 2000 510, e-pošta: **h-farmakovigilanca@jazmp.si,** spletna stran: **www.jazmp.si.** Za zagotavljanje sledljivosti zdravila je pomembno, da pri izpolnjevanju obrazca o domnevnih neželenih učinkih zdravila navedete številko serije biološkega zdravila. **Režim izdaje zdravila:** H. **Imetnik dovoljenja za promet:** Roche Registration GmbH, Emil-Barell-Strasse 1, 79639 Grenzach-Wyhlen, Nemčija. **Verzija: 2.0/18. Informacija pripravljena:** maj 2018

PM-0028-2018-OMN

AMGEN®

ZA ZDRAVILOM KANJINTI® STOJI STROKOVNO ZNANJE DRUŽBE AMGEN, KI VLIVA ZAUPANJE IN ZAGOTAVLJA ZANESLJIVOST.

Za več informacij o zdravilu
KANJINTI® (trastuzumab) družbe Amgen, obiščite:
amgenbiosimiliars.eu/KANJINTI

KANJINTI®
(trastuzumab)
Za intravensko uporabo

SEDAJ NA VOLJO

Zdravilo KANJINTI® vsebuje učinkovino trastuzumab in je indicirano za zdravljenje HER2-pozitivnega metastatskega raka dojke, HER2-pozitivnega zgodnjega raka dojke in HER2-pozitivnega metastatskega adenokarcinoma želodčnega ali gastroezofagealnega prehoda.[2]

KANJINTI 150 mg in 420 mg prašek za koncentrat za raztopino za infundiranje – SKRAJŠAN POVZETEK GLAVNIH ZNAČILNOSTI ZDRAVILA
Samo za strokovno javnost. Pred predpisovanjem si preberite celoten Povzetek glavnih značilnosti zdravila.
▼ Za to zdravilo se izvaja dodatno spremljanje varnosti. Poročati je potrebno o vseh domnevnih neželenih učinkih zdravila. **SESTAVA ZDRAVILA:** Ena viala vsebuje 150 mg ali 420 mg trastuzumaba, humaniziranega monoklonskega protitelesa IgG1, pridobljenega iz suspenzijske celične kulture sesalcev (ovarijske celice kitajskega hrčka) in očiščenega z afinitetno ter ionsko izmenjalno kromatografijo, ki vključuje specifično virusno inaktivacijo ter postopke odstranjevanja. Pripravljena raztopina zdravila KANJINTI vsebuje 21 mg/ml trastuzumaba. **TERAPEVTSKE INDIKACIJE:** Rak dojk. Metastatski rak dojk: Zdravljenje odraslih bolnikov s HER2-pozitivno metastatsko obliko raka dojk: (1) kot monoterapija za zdravljenje tistih bolnikov, ki so za svojo metastatsko bolezen predhodno že prejemali najmanj dve liniji kemoterapije. Predhodna kemoterapija mora vsebovati vsaj en antraciklinski in taksanski derivat, razen če bolniki za takšno zdravljenje niso bili primerni. Bolniki s hormonsko odvisnimi tumorji, pri katerih je bolezen napredovala po predhodnem hormonskem zdravljenju, razen če za takšno zdravljenje niso bili primerni; (2) v kombinaciji s paklitakselom za zdravljenje tistih bolnikov, ki še niso prejemali kemoterapije za metastatsko bolezen in za katere antraciklini niso primerni; (3) v kombinaciji z docetakselom za zdravljenje tistih bolnikov, ki še niso prejemali kemoterapije za metastatsko bolezen; (4) v kombinaciji z zaviralcem aromataze za zdravljenje bolnic v postmenopavzi z metastatsko obliko raka dojk s pozitivnimi hormonskimi receptorji, ki predhodno niso bile zdravljene s trastuzumabom. Zgodnji rak dojk: Zdravljenje odraslih bolnikov z zgodnjo obliko HER2-pozitivnega raka dojk: (1) po operaciji, kemoterapiji (neoadjuvantni ali adjuvantni) in radioterapiji (če je primerno); (2) po adjuvantni kemoterapiji z doksorubicinom in ciklofosfamidom, v kombinaciji s paklitakselom ali docetakselom; (3) v kombinaciji z adjuvantno kemoterapijo z docetakselom in karboplatinom; (4) v kombinaciji z neoadjuvantno kemoterapijo, čemur sledi adjuvantno zdravljenje z zdravilom KANJINTI, za lokalno napredovalo (tudi vnetno) bolezen ali tumorje > 2 cm v premeru. Zdravilo KANJINTI se uporablja le za bolnike z metastatskim ali zgodnjim rakom dojk, katerih tumorji imajo ali čezmerno izražen HER2 ali amplifikacijo gena HER2, določeno s točno in validirano metodo. Metastatski rak želodca: V kombinaciji s kapecitabinom ali 5fluorouracilom in cisplatinom indicirano za zdravljenje odraslih bolnikov s HER2-pozitivnim metastatskim adenokarcinomom želodca ali gastroezofagealnega prehoda, ki še niso prejemali zdravil za zdravljenje raka za metastatsko bolezen. Zdravilo KANJINTI se uporablja le za bolnike z metastatskim rakom želodca, katerih tumorji imajo čezmerno izražen HER2, definiran kot IHC2+ z nadaljnjim potrditvenim SISH ali FISH rezultatom ali kot IHC3+. Treba je uporabljati točne in validirane metode. **ODMERJANJE IN NAČIN UPORABE:** Pred začetkom zdravljenja je potrebno testiranje na HER2. Zdravljenje z zdravilom KANJINTI mora vpeljati zdravnik z izkušnjami s citotoksično kemoterapijo. Zdravilo lahko daje le zdravstveno osebje. Intravenska oblika zdravila KANJINTI ni namenjena subkutani aplikaciji in se lahko daje le z intravensko infuzijo. Za preprečitev napak pri dajanju zdravila je pomembno preveriti nalepke na vialah in tako zagotoviti, da je pripravljeno in uporabljeno zdravilo KANJINTI (trastuzumab) in ne trastuzumab emtanzin. Odmerjanje. Metastatski rak dojk: Štedenski režim: Priporočen polnitveni odmerek je 8 mg/kg telesne mase. Priporočen vzdrževalni odmerek je 6 mg/kg telesne mase po 3 tednih od prejema polnitvenega odmerka, in nato v tritedenskih razmakih. Tedenski režim: Priporočen polnitveni odmerek zdravila KANJINTI je 4 mg/kg telesne mase. Priporočen tedenski vzdrževalni odmerek zdravila KANJINTI je 2 mg/kg telesne mase, z začetkom en teden po polnitvenem odmerku. Odmerjanje v kombinaciji s paklitakselom ali docetakselom: V ključnih študijah (H0648g, M77001) so paklitaksel ali docetaksel dali en dan po polnitvenem odmerku trastuzumaba (za odmerek glejte Povzetek glavnih značilnosti zdravila za paklitaksel ali docetaksel) in takoj po nadaljnjih odmerkih trastuzumaba, če je bolnik predhoden odmerek trastuzumaba dobro prenašal. Odmerjanje v kombinaciji z zaviralcem aromataze: V ključni študiji (BO16216) so trastuzumab in anastrozol dajali od 1. dne dalje. Časovnih omejitev glede dajanja trastuzumaba in anastrozola ni bilo (za odmerjanje glejte Povzetek glavnih značilnosti zdravila za anastrozol ali druge zaviralce aromataz). Zgodnji rak dojk: Štedenski in tedenski režim: Pri štedenskem režimu je priporočen polnitveni odmerek zdravila KANJINTI 8 mg/kg telesne mase. Priporočen vzdrževalni odmerek zdravila KANJINTI je 6 mg/kg telesne mase po 3 tednih od prejema polnitvenega odmerka, in nato v tritedenskih razmakih. Pri tedenskem režimu (polnitveni odmerek 4 mg/kg telesne mase, nato 2 mg/kg telesne mase vsak teden) se zdravilo KANJINTI daje sočasno s paklitakselom po kemoterapiji z doksorubicinom in ciklofosfamidom. Glejte poglavje 5.1 celotnega Povzetka glavnih značilnosti zdravila za odmerjanje v kombinaciji s kemoterapijo. Metastatski rak želodca: Štedenski režim: Priporočen polnitveni odmerek je 8 mg/kg telesne mase. Priporočen vzdrževalni odmerek je 6 mg/kg telesne mase po 3 tednih od prejema polnitvenega odmerka, in nato v tritedenskih razmakih. Rak dojk in rak želodca: Trajanje zdravljenja: Bolnike z metastatskim rakom dojk ali metastatskim rakom želodca je treba z zdravilom KANJINTI zdraviti do napredovanja bolezni. Bolnike z zgodnjim rakom dojk je treba z zdravilom KANJINTI zdraviti 1 leto ali do ponovitve bolezni, kar nastopi prej. Podaljšanje zdravljenja zgodnjega raka dojk na več kot eno leto ni priporočljivo. Zmanjšanje odmerka: Med kliničnimi preskušanji niso zmanjševali odmerka trastuzumaba. Bolniki lahko nadaljujejo zdravljenje tudi med obdobji reverzibilne mielosupresije, ki je posledica kemoterapije, vendar pa jih je v tem času treba skrbno spremljati zaradi zapletov nevtropenije. Za zmanjšanje odmerka ali odlog dajanja paklitaksela, docetakselaali zaviralca aromataze glejte njihove Povzetke glavnih značilnosti zdravila. **Če odstotek iztisnega deleža levega prekata (LVEF) pade za** ≥ 10 točk od začetne vrednosti IN pod 50 %, zdravljenje prekinemo in ponovno opravimo meritev LVEF v približno treh tednih. Če se LVEF ne izboljša ali pride do nadaljnjega zmanjšanja ali se razvije simptomatsko kongestivno srčno popuščanje, je potreben resen razmislek o prekinitvi zdravljenja z zdravilom KANJINTI, razen če je korist za posameznega bolnika večja od tveganja. Vse take bolnike je treba napotiti na pregled h kardiologu in jih spremljati. Izpuščeni odmerki: **Če je bolnik izpustil odmerek zdravila** KANJINTI za en teden ali manj, mu je treba običajni vzdrževalni odmerek (tedenski režim: 2 mg/kg; štedenski režim: 6 mg/kg) dati čim prej. Ne čakamo do naslednjega planiranega cikla. Nadaljnje vzdrževalne odmerke dajemo 7 ali 21 dni zatem, odvisno od režima odmerjanja (tedenskega ali 3-tedenskega). **Če je bolnik izpustil odmerek zdravila** KANJINTI za več kot en teden, mu je treba čim prej ponovno dati polnitveni odmerek zdravila KANJINTI v približno 90 minutah (tedenski režim: 4 mg/kg; štedenski režim: 8 mg/kg). Nadaljnje vzdrževalne odmerke zdravila KANJINTI (tedenski režim: 2 mg/kg; štedenski režim: 6 mg/kg) dajemo od 7 ali 21 dni zatem, odvisno od režima odmerjanja (tedenskega ali štedenskega). Posebne skupine bolnikov: Podrobnejših farmakokinetičnih študij pri starejših bolnikih in tistih z ledvično ali jetrno okvaro niso opravili. Farmakokinetična analiza skupin ni pokazala vplivov starosti in ledvične okvare na razpoložljivost trastuzumaba. Pediatrična populacija: Uporaba trastuzumaba pri pediatrični populaciji ni smiselna. Način uporabe: Zdravilo KANJINTI je samo za intravensko uporabo. Polnitveni odmerek se daje kot 90-minutna intravenska infuzija. Uporaba zdravila kot hitra intravenska infuzija ali bolus je prepovedana. Intravensko infuzijo zdravila KANJINTI mora dajati zdravstveno osebje, usposobljeno za ukrepanje ob anafilaksiji; na voljo mora biti oprema za urgentno ukrepanje. Bolniki morajo biti pod nadzorom vsaj šest ur po začetku prve infuzije in dve uri po začetku nadaljnjih infuzij zaradi nevarnosti pojava simptomov, kot so zvišana telesna temperatura, mrzlica in drugi simptomi, povezani z infundiranjem. Prekinitev ali upočasnitev hitrosti dajanja infuzije lahko pomaga pri nadzoru teh simptomov. Ko simptomi izginejo, lahko z infuzijo nadaljujemo. **Če je bolnik** polnitveni odmerek dobro prenašal, lahko nadaljnje odmerke dajemo kot 30minutne infuzije. Za navodila glede rekonstitucije zdravila KANJINTI v intravenski obliki pred dajanjem glejte celoten Povzetek glavnih značilnosti zdravila. **KONTRAINDIKACIJE:** Preobčutljivost za trastuzumab, murine beljakovine ali katero koli pomožno snov, navedeno v celotnem Povzetku glavnih značilnosti zdravila. Pri bolnikih, ki imajo hudo dispnejo v mirovanju zaradi komplikacij napredovale maligne bolezni, ali pri tistih, ki potrebujejo zdravljenje s kisikom. **POSEBNA OPOZORILA IN PREVIDNOSTNI UKREPI:** Sledljivost: Za izboljšanje sledljivosti bioloških zdravil je treba zaščiteno ime in številko serije uporabljenega zdravila jasno zabeležiti. Testiranje na HER2 mora biti opravljeno v specializiranem laboratoriju, ki lahko zagotavlja ustrezno validacijo postopka testiranja. Motnje v delovanju srca, Splošne opombe: Pri bolnikih, ki so se zdravili z zdravilom KANJINTI, obstaja večje tveganje za pojav kongestivnega srčnega popuščanja (NYHA razred IIIV) ali asimptomatične motnje v delovanju srca. Te teženje učinke so opazili pri bolnikih, ki so prejemali trastuzumab v monoterapiji ali v kombinaciji s paklitakselom ali docetakselom, zlasti po kemoterapiji z antraciklini (doksorubicinom ali epirubicinom). Previdnost je potrebna tudi pri zdravljenju bolnikov s povečanim srčnim tveganjem, npr. hipertenzijo, dokumentirano koronarno arterijsko boleznijo, kongestivnim srčnim popuščanjem, LVEF < 55 %, starejših bolnikih. Vsi kandidati za zdravljenje z zdravilom KANJINTI, posebno tisti, ki so se predhodno zdravili z antraciklini in ciklofosfamidom, morajo opraviti osnovni pregled srca, vključno z anamnezo in fizičnim pregledom, elektrokardiogramom (EKG), ehokardiogramom in/ali radioizotopsko ventrikulografijo ali magnetnoresonančnim slikanjem. Spremljanje lahko olajša razpoznavo bolnikov, pri katerih se pojavijo motnje v delovanju srca. Preglede srca, enake kot je bil osnovni, je treba med zdravljenjem ponoviti vsake 3 mesece in vsakih 6 mesecev po končanem zdravljenju do 24 mesecev po prejemu zadnjega odmerka zdravila KANJINTI. Pred odločitvijo za zdravljenje z zdravilom KANJINTI je treba skrbno pretehtati razmerje med koristjo in tveganjem. Trastuzumab je lahko po prenehanju zdravljenja z zdravilom KANJINTI v krvnem obtoku prisoten do 7 mesecev glede na populacijsko farmakokinetično analizo vseh razpoložljivih podatkov. Pri bolnikih, ki prejemajo antracikline po prenehanju zdravljenja z zdravilom KANJINTI, lahko obstaja večje tveganje za motnje v delovanju srca. Če je mogoče, se po prekinitvi zdravljenja z zdravilom KANJINTI do 7 mesecev izogibamo zdravljenju z antraciklini. Če bolnika zdravimo z antraciklini, je treba skrbno spremljati delovanje njegovega srca. Pri bolnikih, pri katerih so po osnovnem pregledu odkrili kardiovaskularne težave, je treba razmisliti o celovitem kardiološkem pregledu. Med zdravljenjem je treba nadzorovati delovanje srca pri vseh bolnikih (npr. vsakih 12 tednov), kar olajša razpoznavo bolnikov, pri katerih se pojavijo motnje v delovanju srca. Za bolnike z asimptomatičnimi motnjami v delovanju srca je koristen pogostejši nadzor (npr. vsakih 6 do 8 tednov). Pri bolnikih s kontinuiranim upadanjem funkcije levega prekata, ki ostajajo asimptomatični, naj zdravnik razmisli o ukinitvi zdravljenja z zdravilom KANJINTI, če klinična korist ni bila opazna. **Če odstotek LVEF pade za** ≥ 10 točk od začetne vrednosti IN pod 50 %, zdravljenje prekinemo in ponovno opravimo meritev LVEF v približno treh tednih. Če se LVEF ne izboljša ali pride do nadaljnjega zmanjšanja ali se razvije simptomatsko srčno popuščanje, je potreben resen razmislek o prekinitvi zdravljenja z zdravilom KANJINTI, razen če je korist za posameznega bolnika večja od tveganja. Vse take bolnike je treba napotiti na pregled h kardiologu in jih spremljati. **Če se med zdravljenjem z zdravilom** KANJINTI razvije simptomatsko srčno popuščanje, ga zdravimo s standardnimi zdravili za kongestivno srčno popuščanje. To vključuje zaviralec angiotenzinskih konvertaze ali zaviralec angiotenzinskih receptorjev in antagonist receptorjev beta. Metastatski rak dojk: Pri zdravljenju metastatskega raka dojk kombinacije zdravila KANJINTI in antraciklinov ne smemo dajati sočasno. Pri bolnikih z metastatskim rakom dojk, ki so se predhodno zdravili z antraciklini, pri zdravljenju z zdravilom KANJINTI tveganje za motnje v delovanju srca še vedno obstaja, le da je manjše kot pri sočasni uporabi zdravila KANJINTI in antraciklinov. Zgodnji rak dojk: Pri bolnikih z zgodnjim rakom dojk je treba pregled srca, kot je bil opravljen pred zdravljenjem, ponoviti vsake 3 mesece med zdravljenjem in vsakih 6 mesecev po končanem zdravljenju do 24 mesecev po zadnjem dajanju zdravila KANJINTI. Pri bolnikih, ki prejemajo kemoterapijo z antraciklini, je priporočljivo nadaljnje spremljanje, ki ga je treba izvajati letno do 5 let po zadnjem dajanju zdravila KANJINTI ali dlje, če iztisni delež levega prekata (LVEF) stalno pada. Bolniki z anamnezo miokardnega infarkta, angino pektoris, ki jo je treba zdraviti, anamnezo kongestivnega srčnega popuščanja ali prisotnim kongestivnim srčnim popuščanjem (NYHA razred IIIV), LVEF < 55 %, drugimi kardiomiopatijami, srčno aritmijo, ki jo je treba zdraviti, klinično pomembno boleznijo srčnih zaklopk, slabo uravnano hipertenzijo (hipertenzijo, ki bi bila primerno nadzorovana s standardnim zdravljenjem) in hemodinamsko efektivno perikardialno efuzijo niso bili vključeni v adjuvantna in neoadjuvantna ključna preskušanja zgodnjega raka dojk s trastuzumabom. Zato za te bolnike zdravljenja ne moremo priporočiti. Adjuvantno zdravljenje: Pri adjuvantnem zdravljenju raka dojk zdravila KANJINTI in antraciklinov ne smemo dajati sočasno. Neoadjuvantno-adjuvantno zdravljenje: Pri bolnikih z zgodnjim rakom dojk, ki so primerni za neoadjuvantno-adjuvantno zdravljenje, se zdravilo KANJINTI uporablja sočasno z antraciklini le pri bolnikih, ki še niso bili zdravljeni s kemoterapijo, in to samo pri shemah z majhnimi odmerki antraciklinov (največ kumulativni odmerek doksorubicina 180 mg/m² ali epirubicina 360 mg/m²). **Če so se bolniki v neoadjuvantnem zdravljenju sočasno zdravili z majhnimi odmerki antraciklinov v celoti in zdravilom** KANJINTI, potem jim po operaciji ne smemo dati dodatne citotoksične kemoterapije. V drugih primerih odločitev za potrebo po dodatni citotoksični kemoterapiji temelji na dejavnikih posameznika. Reakcije, povezane z infuzijo, in preobčutljivost: Za zmanjšanje tveganja pojava neželenih učinkov lahko uporabimo premedikacijo. Večina teh učinkov se pojavi med ali v 2,5 urah po začetku prvega infundiranja. Če se pojavi infuzijska reakcija, je potrebno infundiranje zdravila KANJINTI prekiniti ali upočasniti njegovo hitrost in bolnika nadzorovati, dokler vsi simptomi ne izzvenijo. Lahko jih zdravimo z analgetikom/antipiretikom, kot je meperidin ali paracetamol, ali antihistaminikom, kot je difenhidramin. Pri večini bolnikov so simptomi izzveneli in so z infundiranjem trastuzumaba nadaljevali. Resne reakcije so uspešno zdravili s podpornim zdravljenjem, kot so kisik, beta agonisti in kortikosteroidi. Pri bolnikih, ki imajo dispnejo v mirovanju zaradi komplikacij napredovale maligne bolezni in sobolenja, obstaja večje tveganje infuzijske reakcije s smrtnim izidom. Zato takih bolnikov ne smemo zdraviti z zdravilom KANJINTI. Bolnike je treba opozoriti na možnost poznega pojava simptomov in jim svetovati, da takoj obvestijo svojega zdravnika, če se ti simptomi pojavijo. Pljučni zapleti: Med dejavnike tveganja, povezane z intersticijsko boleznijo pljuč, spada predhodno ali sočasno zdravljenje z drugimi zdravili z delovanjem na novotvorbe, za katere je znana povezava s to boleznijo, kot so taksani, gemcitabin, vinorelbin in zdravljenje z obsevanjem. Ti učinki se lahko pojavijo kot del infuzijske reakcije ali pa nastopijo kasneje. Pri bolnikih, ki imajo dispnejo v mirovanju zaradi komplikacij napredovale maligne bolezni in sobolenj, obstaja večje tveganje pljučnih zapletov. Zato takih bolnikov ne smemo zdraviti z zdravilom KANJINTI. Pozorno je treba spremljati znake pnevmonitisa, še posebno pri bolnikih, ki se sočasno zdravijo s taksani. **INTERAKCIJE:** Formalnih študij medsebojnega delovanja niso izvedli. V kliničnih preskušanjih niso opazili klinično pomembnega medsebojnega delovanja med trastuzumabom in zdravili, ki so jih bolniki jemali sočasno. Za učinek trastuzumaba na farmakokinetiko drugih zdravil z delovanjem na novotvorbe in za učinek zdravil z delovanjem na novotvorbe na farmakokinetiko trastuzumaba glejte celoten Povzetek glavnih značilnosti zdravila KANJINTI. Sočasno dajanje anastrazola ni imelo vpliva na farmakokinetiko trastuzumaba. **PLODNOST, NOSEČNOST IN DOJENJE: Ženskam v rodni dobi je treba svetovati, naj med zdravljenjem z zdravilom** KANJINTI ter še 7 mesecev po zaključku zdravljenja uporabljajo učinkovito kontracepcijo. Uporabi zdravila KANJINTI med nosečnostjo se moramo izogibati, razen v primerih, ko pričakovana korist za mater upravičuje tveganje za plod. Ženske, ki zanosijo, je treba opozoriti na možnost poškodbploda. Če se noseča ženska zdravi z zdravilom KANJINTI ali če bolnica zanosi med zdravljenjem z zdravilom KANJINTI ali v obdobju 7 mesecev po prejemu zadnjega odmerka zdravila KANJINTI, je zaželeno, da jo skrbno spremlja multidisciplinarna ekipa. Ker se humani IgG1 izloča v materino mleko, potencialni škodljivi vplivi na otroka pa ni znan, naj ženske ne dojijo med zdravljenjem z zdravilom KANJINTI in še 7 mesecev po zadnjem odmerku. Podatkov o vplivu na plodnost ni. **POVZETEK NEŽELENIH UČINKOV:** Zelo pogosti (≥ 1/10): okužba, nazofaringitis, febrilna nevtropenija, anemija, nevtropenija, zmanjšano število belih krvnih celic/levkopenija, trombocitopenija, zmanjšanje telesne mase/izguba telesne mase, anoreksija, nespečnost, tremor, omotica, glavobol, parestezija, disgevzija, konjunktivitis, povečano solzenje, znižanje krvnega tlaka, zvišanje krvnega tlaka, neredna srčni utrip, palpitacije, trepetanje srca, zmanjšanje iztisnega deleža, vročinski oblivi, piskanje, dispneja, kašelj, epistaksa, rinoreja, diareja, bruhanje, navzea, otekanje ustnic, bolečina v trebuhu, dispepsija, zaprtje, stomatitis, eritem, izpuščaj, otekanje obraza, alopecija, spremembe na nohtih, sindrom palmarno-plantarne eritrodisestezije, artralgija, napetost mišic, mialgija, astenija, bolečina v prsnem košu, mrzlica, utrujenost, gripi podobni simptomi, reakcija, povezana z infundiranjem, bolečina, pireksija, vnetje sluznic, periferni edem. Pogosti (≥ 1/100 do < 1/10): nevtropenična sepsa, cistitis, herpes zoster, gripa, sinuzitis, okužba kože, rinitis, okužba zgornjih dihal, okužba sečil, erizipel, celulitis, faringitis, preobčutljivost, anksioznost, depresija, nenormalno razmišljanje, periferna nevropatija, hipertonija, somnolenca, ataksija, suhe oči, (kongestivno) srčno popuščanje, supraventrikularna tahiaritmija, kardiomiopatija, hipotenzija, vazodilatacija, pljučnica, astma, motnje delovanja pljuč, plevralni izliv, hemoroidi, suha usta, hepatocelularna poškodba, hepatitis, napetost in bolečina v predelu jeter, akne, suha koža, ekhimoza, hiperhidroza, makulopapulozni izpuščaj, pruritus, lomljenje nohtov, dermatitis, artritis, bolečina v hrbtu, bolečina v kosteh, mišični krči, bolečina v vratu, bolečina v okončini, motnje delovanja ledvic, vnetje dojk/mastitis, neugodje, edem, kontuzija. Občasni (≥ 1/1.000 do < 1/100): sepsa, gluhost, perikardialni izliv, urtikarija. Redki (≥ 1/10.000 do < 1/1.000): pareza, pnevmonitis, zlatenica. Neznana pogostnost: napredovanje maligne neoplazme, predvanje neoplazme, hipoprotrombinemija, imunska trombocitopenija, anafilaktična reakcija, anafilaktični šok, hiperkaliemija, možganski edem, edem papile vidnega živca, retinalna krvavitev, kardiogeni šok, perikarditis, bradikardija, galop, pljučna fibroza, dihalna stiska, odpoved dihal, pljučni infiltrati, akutni pljučni edem, akutni respiratorni distresni sindrom (ARDS), bronhospazem, hipoksija, zmanjšana saturacija s kisikom, edem grla, ortopneja, pljučni edem, intersticijska pljučna bolezen, jetrna odpoved, angioedem, membranski glomerulonefritis, glomerulonefropatija, ledvična odpoved, oligohidramnij, renalna hipoplazija, pulmonalna hipoplazija. **FARMACEVTSKI PODATKI:** Zdravila ne smemo mešati ali redčiti z drugimi zdravili, razen s tistimi, ki so omenjena v poglavju 6.6 celotnega Povzetka glavnih značilnosti zdravila. Zdravila KANJINTI ne redčite z raztopinami glukoze, ker le-te povzročajo agregacijo beljakovin. Po rekonstituciji s sterilno vodo za injekcije je pripravljena raztopina fizikalno in kemično stabilna 48 ur pri temperaturi od 2°C - 8°C. Raztopino, ki ostane, je treba zavreči. Raztopine zdravila KANJINTI za intravensko infundiranje so v polivinilkloridnih, polietilenskih ali polipropilenskih vrečkah, ki vsebujejo raztopino 9 mg/ml (0,9 %) natrijevega klorida za injiciranje, fizikalno in kemično stabilne 24 ur pri temperaturah, ki ne presežejo 30 °C. Z mikrobiološkega stališča je rekonstituirano raztopino in zdravilo KANJINTI raztopino za infundiranje treba uporabiti takoj. Shranjujte v hladilniku (2°C - 8°C). Ne zamrzujte. Med zdravilom KANJINTI in polivinilkloridnimi, polietilenskimi ali polipropilenskimi vrečkami inkompatibilnosti niso opazili. **NAČIN IN REŽIM PREDPISOVANJA TER IZDAJE ZDRAVILA:** Predpisovanje in izdaja zdravila je le na recept s posebnim režimom – H. **IMETNIK DOVOLJENJA ZA PROMET Z ZDRAVILOM:** Amgen Europe B.V., Minervum 7061, NL-4817 ZK Breda, Nizozemska. Dodatna pojasnila lahko dobite v lokalni pisarni: Amgen zdravila d.o.o., Šmartinska 140, SI-1000 Ljubljana. **DATUM ZADNJE REVIZIJE BESEDILA:** 14. september 2018. **DATUM PRIPRAVE INFORMACIJE:** November 2018. Podrobne informacije o zdravilu so objavljene na spletni strani Evropske agencije za zdravila http://www.ema.europa.eu. **LITERATURA: 1.** http://www.amgenbiosimilars.eu/ (zadnjič dostopano: oktober 2018). **2.** Povzetek glavni značilnosti zdravila KANJINTI®, Amgen. **HER2** = humani epidermalni rastni faktor 2.

SLHR-SL-P-BIO-1018-068770a

Zdravilo za predhodno že zdravljene bolnike z mKRR

Več časa za trenutke, ki štejejo

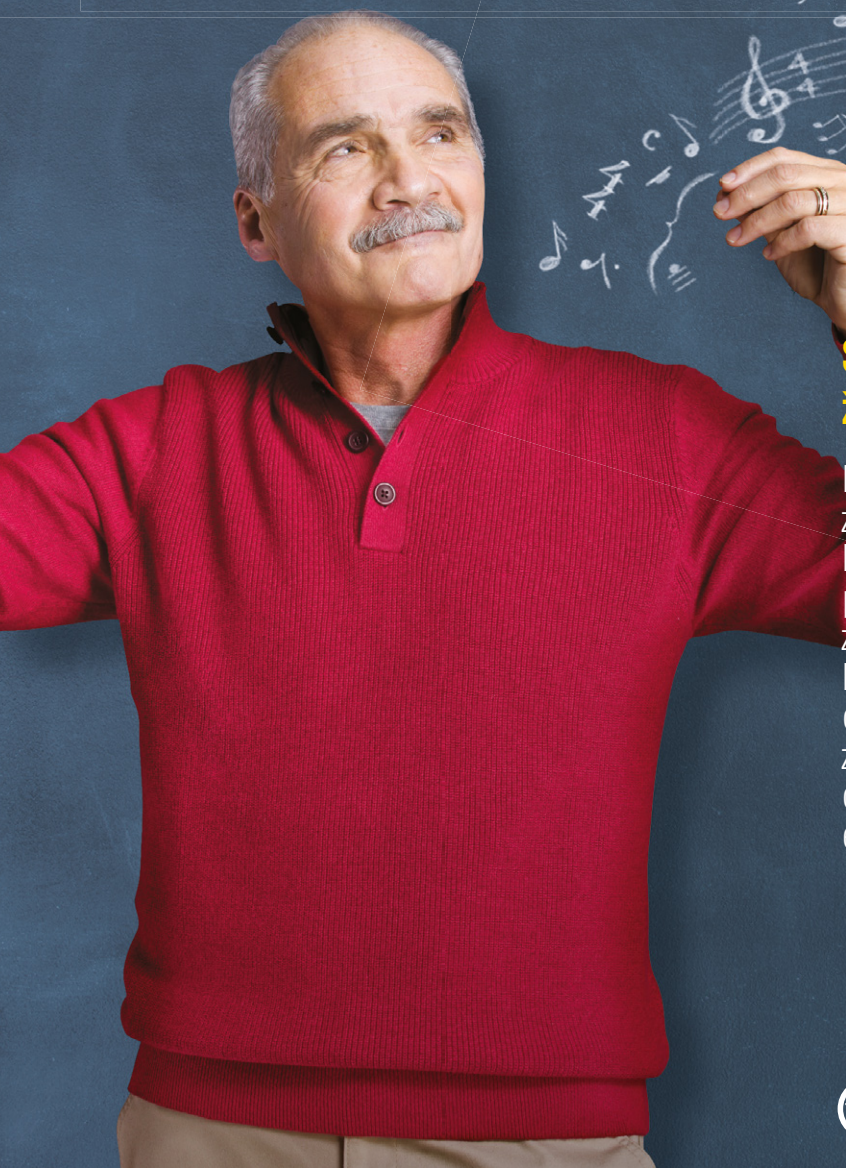

▼Lonsurf®
trifluridin/tipiracil

Spremeni zgodbo predhodno že zdravljenih bolnikov z mKRR

LONSURF® (trifluridin/tipiracil) je indiciran za zdravljenje odraslih bolnikov z metastatskim kolorektalnim rakom (mKRR), ki so bili predhodno že zdravljeni ali niso primerni za zdravljenja, ki so na voljo. Ta vključujejo kemoterapijo na osnovi fluoropirimidina, oksaliplatina in irinotekana, zdravljenje z zaviralci žilnega endotelijskega rastnega dejavnika (VEGF) in zaviralci receptorjev za epidermalni rastni dejavnik (EGFR).

Družba Servier ima licenco družbe Taiho za zdravilo Lonsurf®.
Pri globalnem razvoju zdravila sodelujeta obe družbi in ga tržita na svojih določenih področjih.

TAIHO PHARMACEUTICAL CO., LTD.

SERVIER

Skrajšan povzetek glavnih značilnosti zdravila: Lonsurf 15 mg/6,14 mg filmsko obložene tablete in Lonsurf 20 mg/8,19 mg filmsko obložene tablete

▼Za to zdravilo se izvaja dodatno spremljanje varnosti. **SESTAVA*: Lonsurf 15 mg/6,14 mg:** Ena filmsko obložena tableta vsebuje 15 mg trifluridina in 6,14 mg tipiracila (v obliki klorida). **Lonsurf 20 mg/8,19 mg:** Ena filmsko obložena tableta vsebuje 20 mg trifluridina in 8,19 mg tipiracila (v obliki klorida). **TERAPEVTSKE INDIKACIJE*:** Zdravilo Lonsurf je indicirano za zdravljenje odraslih bolnikov z metastatskim kolorektalnim rakom, ki so bili predhodno že zdravljeni ali niso primerni za zdravljenja, ki so na voljo. Ta vključujejo kemoterapijo na osnovi fluoropirimidina, oksaliplatina in irinotekana, zdravljenje z zaviralci žilnega endotelijskega rastnega dejavnika (VEGF - Vascular Endothelial Growth Factor) in zaviralci receptorjev za epidermalni rastni dejavnik (EGFR - Epidermal Growth Factor Receptor). **ODMERJANJE IN NAČIN UPORABE*:** Priporočeni začetni odmerek zdravila Lonsurf pri odraslih je 35 mg/m^2/odmerek peroralno dvakrat dnevno na 1. do 5. dan in 8. do 12. dan vsakega 28-dnevnega cikla zdravljenja, najpozneje 1 uro po zaključku jutranjega in večernega obroka. Odmerjanje, izračunano glede na telesno površino, ne sme preseči 80 mg/odmerek. Možne prilagoditve odmerka glede na varnost in prenašanje zdravila: dovoljena so največ 3 zmanjšanja odmerka na najmanjši odmerek 20 mg/m^2 dvakrat dnevno. Potem ko je bil odmerek zmanjšan, povečanje ni dovoljeno. **KONTRAINDIKACIJE*:** Preobčutljivost na zdravilni učinkovini ali katero koli pomožno snov. **OPOZORILA IN PREVIDNOSTNI UKREPI*:** Supresija kostnega mozga: Pred uvedbo zdravljenja, pred vsakim ciklom zdravljenja in po potrebi je treba pregledati celotno krvno sliko. Zdravljenja ne smete začeti, če je absolutno število nevtrofilcev < 1,5 x 10^9/l, če je število trombocitov < 75 x 10^9/l ali če se je pri bolniku zaradi predhodnih zdravljenj pojavila klinično pomembna nehematološka toksičnost 3. ali 4. stopnje, ki še traja. Bolnike je treba skrbno spremljati zaradi morebitnih okužb, uvesti je treba ustrezne ukrepe, kot je klinično indicirano. Toksičnost za prebavila: Potrebna je uporaba antiemetikov, antidiaroikov ter drugih ukrepov, kot je klinično indicirano. Če je potrebno, prilagodite odmerke. Ledvična okvara: Zdravilo Lonsurf ni primerno za uporabo pri bolnikih s hudo ledvično okvaro ali končno stopnjo ledvične okvare. Bolnike z zmerno ledvično okvaro je treba zaradi hematološke toksičnosti bolj pogosto spremljati. Jetrna okvara: Uporaba zdravila Lonsurf pri bolnikih z obstoječo zmerno ali hudo jetrno okvaro ni priporočljiva. Proteinurija: Pred začetkom zdravljenja in med njim je priporočljivo spremljanje proteinurije z urinskimi testnimi lističi. Pomožne snovi: Zdravilo vsebuje laktozo. **INTERAKCIJE*:** Zdravila, ki medsebojno delujejo z nukleozidnimi prenašalci CNT1, ENT1 in ENT2, zaviralci OCT2 ali MATE1, substrati humane timidin-kinaze (npr. zidovudinom), hormonskimi kontraceptivi. **PLODNOST*, NOSEČNOST IN DOJENJE*:** Ni priporočljivo. **KONTRACEPCIJA*:** Ženske in moški morajo uporabljati učinkovito metodo kontracepcije med zdravljenjem in do 6 mesecev po zaključku zdravljenja. **VPLIV NA SPOSOBNOST VOŽNJE IN UPRAVLJANJA S STROJI*:** Med zdravljenjem se lahko pojavijo utrujenost, omotica ali splošno slabo počutje. **NEŽELENI UČINKI*:** *Zelo pogosti:* nevtropenija, levkopenija, anemija, trombocitopenija, zmanjšan apetit, diareja, navzea, bruhanje, utrujenost. *Pogosti:* okužba spodnjih dihal, okužba zgornjih dihal, febrilna nevtropenija, limfopenija, monocitoza, hipoalbuminemija, nespečnost, disgevzija, periferna nevropatija, omotica, glavobol, vročinski oblivi, dispneja, kašelj, bolečina v trebuhu, zaprtje, stomatitis, bolezni ustne votline, hiperbilirubinemija, sindrom palmarne plantarne eritrodisestezije, izpuščaj, alopecija, pruritus, suha koža, proteinurija, pireksija, edem, vnetje sluznice, splošno slabo počutje, zvišanje jetrnih encimov, zvišanje alkalne fosfataze v krvi, zmanjšanje telesne mase. *Občasni:* septični šok, infekcijski enteritis, pljučnica, okužba žolčevoda, gripa, okužba sečil, vnetje dlesni, herpes zoster, tinea pedis, kandidiaza, bakterijska okužba, okužba, bolečina zaradi raka, pancitopenija, granulocitopenija, monocitopenija, eritropenija, levkocitoza, dehidracija, hiperglikemija, hiperkaliemija, hipokaliemija, hipofosfatemija, hipernatriemija, hiponatriemija, hipokalciemija, protin, anksioznost, nevrotoksičnost, disestezija, hiperestezija, hipoestezija, sinkopa, parestezija, pekoč občutek, letargija, zmanjšana ostrina vida, zamegljen vid, diplopija, katarakta, konjunktivitis, suho oko, vrtoglavica, neugodje v ušesu, angina pektoris, aritmija, palpitacije, embolija, hipertenzija, hipotenzija, pljučna embolija, plevralni izliv, izcedek iz nosu, disfonija, orofaringealna bolečina, epistaksa, hemoragični enterokolitis, krvavitev v prebavilih, akutni pankreatitis, ascites, ileus, subileus, kolitis, gastritis, refluksni gastritis, ezofagitis, moteno praznjenje želodca, abdominalna distenzija, analno vnetje, razjede v ustih, dispepsija, gastroezofagealna refluksna bolezen, proktalgija, bukalni polip, krvavitev dlesni, glositis, parodontalna bolezen, bolezen zob, siljenje na bruhanje, flatulenca, slab zadah, hepatotoksičnost, razširitev žolčnih vodov, luščenje kože, urtikarija, preobčutljivostne reakcije na svetlobo, eritem, akne, hiperhidroza, žulj, bolezni nohtov, otekanje sklepov, artralgija, bolečina v kosteh, mialgija, mišično-skeletna bolečina, mišična oslabelost, mišični krči, bolečina v okončinah, občutek teže, ledvična odpoved, neinfektivni cistitis, motnje mikcije, hematurija, levkociturija, motnje menstruacije, poslabšanje splošnega zdravstvenega stanja, bolečina, občutek spremembe telesne temperature, kseroza, zvišanje kreatinina v krvi, podaljšanje intervala QT na elektrokardiogramu, povečanje mednarodnega umerjenega razmerja (INR), podaljšanje aktiviranega parcialnega tromboplastinskega časa (aPTČ), zvišanje sečnine v krvi, zvišanje laktatne dehidrogenaze v krvi, znižanje celokupnih proteinov, zvišanje C-reaktivnega proteina, zmanjšan hematokrit. *Post-marketinške izkušnje:* pri bolnikih, zdravljenih z zdravilom Lonsurf na Japonskem, so poročali o primerih intersticijske bolezni pljuč. **PREVELIKO ODMERJANJE*:** Neželeni učinki, o katerih so poročali v povezavi s prevelikim odmerjanjem, so bili v skladu z uveljavljenim varnostnim profilom. Glavni pričakovani zaplet prevelikega odmerjanja je supresija kostnega mozga. **FARMAKODINAMIČNE LASTNOSTI*:** *Farmakoterapevtska skupina:* zdravila z delovanjem na novotvorbe, antimetaboliti, oznaka ATC: L01BC59. Zdravilo Lonsurf sestavljata antineoplastični timidinski nukleozidni analog, trifluridin, in zaviralec timidin-fosforilaze (TPaze), tipiracilijev klorid. Po privzemu v rakave celice timidin-kinaza fosforilira trifluridin. Ta se v celicah nato presnovi v substrat deoksiribonukleinske kisline (DNA), ki se vgradi neposredno v DNA ter tako preprečuje celično proliferacijo. TPaza hitro razgradi trifluridin in njegova presnova po peroralni uporabi je hitra zaradi učinka prvega prehoda, zato je v zdravilo vključen zaviralec TPaze, tipiracilijev klorid. **PAKIRANJE*:** 20 filmsko obloženih tablet. **NAČIN PREDPISOVANJA IN IZDAJE ZDRAVILA:** Rp/ Spec. **Imetnik dovoljenja za promet:** Les Laboratoires Servier, 50, rue Carnot, 92284 Suresnes cedex, Francija. **Številka dovoljenja za promet z zdravilom:** EU/1/16/1096/001 (Lonsurf 15 mg/6,14 mg), EU/ 1/16/1096/004 (Lonsurf 20 mg/8,19 mg). **Datum zadnje revizije besedila: avgust 2017. * Pred predpisovanjem preberite celoten povzetek glavnih značilnosti zdravila. Celoten povzetek glavnih značilnosti zdravila in podrobnejše informacije so na voljo pri: Servier Pharma d.o.o., Podmilščakova ulica 24, 1000 Ljubljana, tel: 01 563 48 11, www.servier.si.**

Datum priprave informacije: februar 2018.
LNF17/18C2AD2 Samo za strokovno javnost.

Instructions for authors

The editorial policy

Radiology and Oncology is a multidisciplinary journal devoted to the publishing original and high quality scientific papers and review articles, pertinent to diagnostic and interventional radiology, computerized tomography, magnetic resonance, ultrasound, nuclear medicine, radiotherapy, clinical and experimental oncology, radiobiology, radiophysics and radiation protection. Therefore, the scope of the journal is to cover beside radiology the diagnostic and therapeutic aspects in oncology, which distinguishes it from other journals in the field.

The Editorial Board requires that the paper has not been published or submitted for publication elsewhere; the authors are responsible for all statements in their papers. Accepted articles become the property of the journal and, therefore cannot be published elsewhere without the written permission of the editors.

Submission of the manuscript

The manuscript written in English should be submitted to the journal via online submission system Editorial Manager available for this journal at: **www.radioloncol.com**.

In case of problems, please contact Sašo Trupej at **saso.trupej@computing.si** or the Editor of this journal at **gsersa@onko-i.si**

All articles are subjected to the editorial review and when the articles are appropriated they are reviewed by independent referees. In the cover letter, which must accompany the article, the authors are requested to suggest 3-4 researchers, competent to review their manuscript. However, please note that this will be treated only as a suggestion; the final selection of reviewers is exclusively the Editor's decision. The authors' names are revealed to the referees, but not vice versa.

Manuscripts which do not comply with the technical requirements stated herein will be returned to the authors for the correction before peer-review. The editorial board reserves the right to ask authors to make appropriate changes of the contents as well as grammatical and stylistic corrections when necessary. Page charges will be charged for manuscripts exceeding the recommended length, as well as additional editorial work and requests for printed reprints.

Articles are published printed and on-line as the open access (**https://content.sciendo.com/raon**).

All articles are subject to 700 EUR + VAT publication fee. Exceptionally, waiver of payment may be negotiated with editorial office, upon lack of funds.

Manuscripts submitted under multiple authorship are reviewed on the assumption that all listed authors concur in the submission and are responsible for its content; they must have agreed to its publication and have given the corresponding author the authority to act on their behalf in all matters pertaining to publication. The corresponding author is responsible for informing the coauthors of the manuscript status throughout the submission, review, and production process.

Preparation of manuscripts

Radiology and Oncology will consider manuscripts prepared according to the Uniform Requirements for Manuscripts Submitted to Biomedical Journals by International Committee of Medical Journal Editors (www.icmje.org). The manuscript should be written in grammatically and stylistically correct language. Abbreviations should be avoided. If their use is necessary, they should be explained at the first time mentioned. The technical data should conform to the SI system. The manuscript, excluding the references, tables, figures and figure legends, must not exceed 5000 words, and the number of figures and tables is limited to 8. Organize the text so that it includes: Introduction, Materials and methods, Results and Discussion. Exceptionally, the results and discussion can be combined in a single section. Start each section on a new page, and number each page consecutively with Arabic numerals.

The Title page should include a concise and informative title, followed by the full name(s) of the author(s); the institutional affiliation of each author; the name and address of the corresponding author (including telephone, fax and E-mail), and an abbreviated title (not exceeding 60 characters). This should be followed by the abstract page, summarizing in less than 250 words the reasons for the study, experimental approach, the major findings (with specific data if possible), and the principal conclusions, and providing 3-6 key words for indexing purposes. Structured abstracts are required. Slovene authors are requested to provide title and the abstract in Slovene language in a separate file. The text of the research article should then proceed as follows:

Introduction should summarize the rationale for the study or observation, citing only the essential references and stating the aim of the study.

Materials and methods should provide enough information to enable experiments to be repeated. New methods should be described in details.

Results should be presented clearly and concisely without repeating the data in the figures and tables. Emphasis should be on clear and precise presentation of results and their significance in relation to the aim of the investigation.

Discussion should explain the results rather than simply repeating them and interpret their significance and draw conclusions. It should discuss the results of the study in the light of previously published work.

Charts, Illustrations, Images and Tables

Charts, Illustrations, Images and Tables must be numbered and referred to in the text, with the appropriate location indicated. Charts, Illustrations and Images, provided electronically, should be of appropriate quality for good reproduction. Illustrations and charts must be vector image, created in CMYK color space, preferred font "Century Gothic", and saved as .AI, .EPS or .PDF format. Color charts, illustrations and Images are encouraged, and are published without additional charge. Image size must be 2.000 pixels on the longer side and saved as .JPG (maximum quality) format. In Images, mask the identities of the patients. Tables should be typed double-spaced, with a descriptive title and, if appropriate, units of numerical measurements included in the column heading. The files with the figures and tables can be uploaded as separate files.

References

References must be numbered in the order in which they appear in the text and their corresponding numbers quoted in the text. Authors are responsible for the accuracy of their references. References to the Abstracts and Letters to the Editor must be identified as such. Citation of papers in preparation or submitted for publication, unpublished observations, and personal communications should not be included in the reference list. If essential, such material may be incorporated in the appropriate place in the text. References follow the style of Index Medicus, DOI number (if exists) should be included.

All authors should be listed when their number does not exceed six; when there are seven or more authors, the first six listed are followed by "et al.". The following are some examples of references from articles, books and book chapters:

Dent RAG, Cole P. In vitro maturation of monocytes in squamous carcinoma of the lung. *Br J Cancer* 1981; **43:** 486-95. doi: 10.1038/bjc.1981.71

Chapman S, Nakielny R. *A guide to radiological procedures*. London: Bailliere Tindall; 1986.

Evans R, Alexander P. Mechanisms of extracellular killing of nucleated mammalian cells by macrophages. In: Nelson DS, editor. *Immunobiology of macrophage.* New York: Academic Press; 1976. p. 45-74.

Authorization for the use of human subjects or experimental animals

When reporting experiments on human subjects, authors should state whether the procedures followed the Helsinki Declaration. Patients have the right to privacy; therefore the identifying information (patient's names, hospital unit numbers) should not be published unless it is essential. In such cases the patient's informed consent for publication is needed, and should appear as an appropriate statement in the article. Institutional approval and Clinical Trial registration number is required. Retrospective clinical studies must be approved by the accredited Institutional Review Board/Committee for Medical Ethics or other equivalent body. These statements should appear in the Materials and methods section.

The research using animal subjects should be conducted according to the EU Directive 2010/63/EU and following the Guidelines for the welfare and use of animals in cancer research (Br J Cancer 2010; 102: 1555 – 77). Authors must state the committee approving the experiments, and must confirm that all experiments were performed in accordance with relevant regulations.

These statements should appear in the Materials and methods section (or for contributions without this section, within the main text or in the captions of relevant figures or tables).

Transfer of copyright agreement

For the publication of accepted articles, authors are required to send the License to Publish to the publisher on the address of the editorial office. A properly completed License to Publish, signed by the Corresponding Author on behalf of all the authors, must be provided for each submitted manuscript.

The non-commercial use of each article will be governed by the Creative Commons Attribution-NonCommercial-NoDerivs license.

Conflict of interest

When the manuscript is submitted for publication, the authors are expected to disclose any relationship that might pose real, apparent or potential conflict of interest with respect to the results reported in that manuscript. Potential conflicts of interest include not only financial relationships but also other, non-financial relationships. In the Acknowledgement section the source of funding support should be mentioned. The Editors will make effort to ensure that conflicts of interest will not compromise the evaluation process of the submitted manuscripts; potential editors and reviewers will exempt themselves from review process when such conflict of interest exists. The statement of disclosure must be in the Cover letter accompanying the manuscript or submitted on the form available on **www.icmje.org/coi_disclosure.pdf**

Page proofs

Page proofs will be sent by E-mail to the corresponding author. It is their responsibility to check the proofs carefully and return a list of essential corrections to the editorial office within three days of receipt. Only grammatical corrections are acceptable at that time.

Open access

Papers are published electronically as open access on **https://content.sciendo.com/raon**, also papers accepted for publication as E-ahead of print.

XALKORI® – 1. linija zdravljenja napredovalega, ALK pozitivnega nedrobnoceličnega pljučnega raka[1]

ALK = anaplastična limfomska kinaza

BISTVENI PODATKI IZ POVZETKA GLAVNIH ZNAČILNOSTI ZDRAVILA

XALKORI 200 mg, 250 mg trde kapsule

▼ Za to zdravilo se izvaja dodatno spremljanje varnosti. Tako bodo hitreje na voljo nove informacije o njegovi varnosti. Zdravstvene delavce naprošamo, da poročajo o kateremkoli domnevnem neželenem učinku zdravila. Glejte poglavje 4.8 povzetka glavnih značilnosti zdravila, kako poročati o neželenih učinkih.

Sestava in oblika zdravila: Ena kapsula vsebuje 200 mg ali 250 mg krizotiniba. **Indikacije:** Monoterapija za: - prvo linijo zdravljenja odraslih bolnikov z napredovalim nedrobnoceličnim pljučnim rakom (NSCLC – *Non-Small Cell Lung Cancer*), ki je ALK (anaplastična limfomska kinaza) pozitiven; - zdravljenje odraslih bolnikov s predhodno zdravljenim, napredovalim NSCLC, ki je ALK pozitiven; - zdravljenje odraslih bolnikov z napredovalim NSCLC, ki je ROS1 pozitiven. **Odmerjanje in način uporabe:** Zdravljenje mora uvesti in nadzorovati zdravnik z izkušnjami z uporabo zdravil za zdravljenje rakavih bolezni. Preverjanje prisotnosti ALK in ROS1: Pri izbiri bolnikov za zdravljenje je treba pred zdravljenjem opraviti točno in validirano preverjanje prisotnosti ALK ali ROS1. Odmerjanje: Priporočeni odmerek je 250 mg dvakrat na dan (500 mg na dan), bolniki pa morajo zdravilo jemati brez prekinitev. Če bolnik pozabi vzeti odmerek, ga mora vzeti takoj, ko se spomni, razen če do naslednjega odmerka manjka manj kot 6 ur. V tem primeru bolnik pozabljenega odmerka ne sme vzeti. *Prilagajanja odmerkov:* Glede na varnost uporabe zdravila pri posameznem bolniku in kako bolnik zdravljenje prenaša, utegne biti potrebna prekinitev in/ali zmanjšanje odmerka pri bolnikih, ki se zdravijo s krizotinibom 250 mg peroralno dvakrat na dan (za režim zmanjševanja odmerka glejte poglavje 4.2 v povzetku glavnih značilnosti zdravila). Za prilagajanje odmerkov pri *hematološki in nehematološki toksičnosti* (povečanje vrednosti AST, ALT, bilirubina; ILD/pnevmonitis; podaljšanje intervala QTc, bradikardija, bolezni oči) glejte preglednici 1 in 2 v poglavju 4.2 povzetka glavnih značilnosti zdravila. *Okvara jeter:* Pri zdravljenju pri bolnikih z okvaro jeter je potrebna previdnost. Pri blagi okvari jeter prilagajanje začetnega odmerka ni priporočeno, pri zmerni okvari jeter je priporočeni začetni odmerek 200 mg dvakrat na dan, pri hudi okvari jeter pa 250 mg enkrat na dan (za merila glede klasifikacije okvare jeter glejte poglavje 4.2 v povzetku glavnih značilnosti zdravila). *Okvara ledvic:* Pri blagi in zmerni okvari prilagajanje začetnega odmerka ni priporočeno. Pri hudi okvari ledvic (ki ne zahteva peritonealne dialize ali hemodialize) je začetni odmerek 250 mg peroralno enkrat na dan; po vsaj 4 tednih zdravljenja se lahko poveča na 200 mg dvakrat na dan. *Starejši bolniki (≥ 65 let):* Prilagajanje začetnega odmerka ni potrebno. *Pediatrična populacija:* Varnost in učinkovitost nista bili dokazani. Način uporabe: Kapsule je treba pogoltniti cele, z nekaj vode, s hrano ali brez nje. Ne sme se jih zdrobiti, raztopiti ali odpreti. Izogibati se je treba uživanju grenivk, grenivkinega soka ter uporabi šentjanževke. **Kontraindikacije:** Preobčutljivost na krizotinib ali katerokoli pomožno snov. **Posebna opozorila in previdnostni ukrepi:** Določanje statusa ALK in ROS1: Pomembno je izbrati dobro validirano in robustno metodologijo, da se izognemo lažno negativnim ali lažno pozitivnim rezultatom. Hepatotoksičnost: V kliničnih študijah so poročali o hepatotoksičnosti, ki jo je povzročilo zdravilo (vključno s primeri s smrtnim izidom). Delovanje jeter, vključno z ALT, AST in skupnim bilirubinom, je treba preveriti enkrat na teden v prvih 2 mesecih zdravljenja, nato pa enkrat na mesec in kot je klinično indicirano. Ponovitve preverjanj morajo biti pogostejše pri povečanjih vrednosti stopnje 2, 3 ali 4. Intersticijska bolezen pljuč (ILD)/pnevmonitis: Lahko se pojavi huda, življenjsko nevarna ali smrtna ILD/pnevmonitis. Bolnike s simptomi ILD/pnevmonitisa je treba spremljati, zdravljenje pa prekiniti ob sumu na ILD/pnevmonitis. Podaljšanje intervala QT: Opažali so podaljšanje intervala QTc. Pri bolnikih z obstoječo bradikardijo, podaljšanjem intervala QTc v anamnezi ali predispozicijo zanj, pri bolnikih, ki jemljejo antiaritmike ali druga zdravila, ki podaljšujejo interval QT, ter pri bolnikih s pomembno obstoječo srčno boleznijo in/ali motnjami elektrolitov je treba krizotinib uporabljati previdno; potrebno je redno spremljanje EKG, elektrolitov in delovanja ledvic; preiskavi EKG in elektrolitov je treba opraviti čimbližje uporabi prvega odmerka, potem se priporoča redno spremljanje. Če se interval QTc podaljša za 60 ms ali več, je treba zdravljenje s krizotinibom začasno prekiniti in se posvetovati s kardiologom. Bradikardija: Lahko se pojavi simptomatska bradikardija (lahko se razvije več tednov po začetku zdravljenja); izogibati se je treba uporabi krizotiniba v kombinaciji z drugimi zdravili, ki povzročajo bradikardijo; pri simptomatski bradikardiji je treba prilagoditi odmerek. Srčno popuščanje: Poročali so o hudih, življenjsko nevarnih ali smrtnih neželenih učinkih srčnega popuščanja. Bolnike je treba spremljati glede pojavov znakov in simptomov srčnega popuščanja in ob pojavu simptomov zmanjšati odmerjanje ali prekiniti zdravljenje. Nevtropenija in levkopenija: V kliničnih študijah so poročali o nevtropeniji, levkopeniji in febrilni nevtropeniji; spremljati je treba popolno krvno sliko (pogostejše preiskave, če se opazijo abnormalnosti stopnje 3 ali 4 ali če se pojavi povišana telesna temperatura ali okužba). Perforacija v prebavilih: V kliničnih študijah so poročali o perforacijah v prebavilih, v obdobju trženja pa o smrtnih primerih perforacij v prebavilih. Krizotinib je treba pri bolnikih s tveganjem za nastanek perforacije v prebavilih uporabljati previdno; bolniki, pri katerih se razvije perforacija v prebavilih, se morajo prenehati zdraviti s krizotinibom; bolnike je treba poučiti o prvih znakih perforacije in jim svetovati, naj se nemudoma posvetujejo z zdravnikom. Vplivi na ledvice: V kliničnih študijah so opazili zvišanje ravni kreatinina v krvi in zmanjšanje očistka kreatinina. V kliničnih študijah in v obdobju trženja so poročali tudi o odpovedi ledvic, akutni odpovedi ledvic, primerih s smrtnim izidom, primerih, ki so zahtevali hemodializo in hiperkaliemiji stopnje 4. Vplivi na vid: V kliničnih študijah so poročali o izpadu vidnega polja stopnje 4 z izgubo vida. Če se na novo pojavi huda izguba vida, je treba zdravljenje prekiniti in opraviti oftalmološki pregled. Če so motnje vida trdovratne ali se poslabšajo, je priporočljiv oftalmološki pregled. Histološka preiskava, ki ne nakazuje adenokarcinoma: Na voljo so le omejeni podatki pri NSCLC, ki je ALK in ROS1 pozitiven in ima histološke značilnosti, ki ne nakazujejo adenokarcinoma, vključno s ploščatoceličnim karcinomom (SCC). **Medsebojno delovanje z drugimi zdravili in druge oblike interakcij:** Izogibati se je treba sočasni uporabi z močnimi zaviralci CYP3A4, npr. atazanavir, ritonavir, kobicistat, itrakonazol, ketokonazol, posakonazol, vorikonazol, klaritromicin, telitromicin in eritromicin (razen če morebitna korist za bolnika odtehta tveganje, v tem primeru je treba bolnike skrbno spremljati glede neželenih učinkov krizotiniba), ter grenivko in grenivkinim sokom, saj lahko povečajo koncentracije krizotiniba v plazmi. Izogibati se je treba sočasni uporabi z močnimi induktorji CYP3A4, npr. karbamazepin, fenobarbital, fenitoin, rifampicin in šentjanževka, saj lahko zmanjšajo koncentracije krizotiniba v plazmi. Učinek zmernih induktorjev CYP3A4, npr. efavirenz in rifabutin, še ni jasen, zato se je treba sočasni uporabi s krizotinibom izogibati. Zdravila, katerih koncentracije v plazmi lahko krizotinib spremeni (midazolam, alfentanil, cisaprid, ciklosporin, derivati ergot alkaloidov, fentanil, pimozid, kinidin, sirolimus, takrolimus, digoksin, dabigatran, kolhicin, pravastatin: sočasni uporabi s temi zdravili se je treba izogibati oziroma izvajati skrben klinični nadzor; bupropion, efavirenz, peroralni kontraceptivi, raltegravir, irinotekan, morfin, nalokson, metformin, prokainamid). Zdravila, ki podaljšujejo interval QT ali ki lahko povzročijo Torsades de pointes (antiaritmiki skupine IA (kinidin, disopiramid), antiaritmiki skupine III (amiodaron, sotalol, dofetilid, ibutilid), metadon, cisaprid, moksifloksacin, antipsihotiki) – v primeru sočasne uporabe je potreben skrben nadzor intervala QT. Zdravila, ki povzročajo bradikardijo (nedihidropiridinski zaviralci kalcijevih kanalčkov (verapamil, diltiazem), antagonisti adrenergičnih receptorjev beta, klonidin, gvanfacin, digoksin, meflokin, antiholinesteraze, pilokarpin) – krizotinib je treba uporabljati previdno. **Plodnost, nosečnost in dojenje:** Ženske v rodni dobi se morajo izogibati zanositvi. Med zdravljenjem in najmanj 90 dni po njem je treba uporabljati ustrezno kontracepcijo (velja tudi za moške). Zdravilo lahko škoduje plodu in se ga med nosečnostjo ne sme uporabljati, razen če klinično stanje matere ne zahteva takega zdravljenja. Matere naj se med jemanjem zdravila dojenju izogibajo. Zdravilo lahko zmanjša plodnost moških in žensk. **Vpliv na sposobnost vožnje in upravljanja strojev:** Lahko se pojavijo simptomatska bradikardija (npr. sinkopa, omotica, hipotenzija), motnje vida ali utrujenost; potrebna je previdnost. **Neželeni učinki:** Najresnejši neželeni učinki so bili hepatotoksičnost, ILD/pnevmonitis, nevtropenija in podaljšanje intervala QT. Najpogostejši neželeni učinki (≥ 25 %) so bili motnje vida, navzea, diareja, bruhanje, edem, zaprtje, povečane vrednosti transaminaz, utrujenost, pomanjkanje apetita, omotica in nevropatija. Ostali zelo pogosti (≥ 1/10 bolnikov) neželeni učinki so: nevtropenija, anemija, levkopenija, disgevzija, bradikardija, bolečina v trebuhu in izpuščaj. **Način in režim izdaje:** Predpisovanje in izdaja zdravila je le na recept, zdravilo pa se uporablja samo v bolnišnicah. Izjemoma se lahko uporablja pri nadaljevanju zdravljenja na domu ob odpustu iz bolnišnice in nadaljnjem zdravljenju. **Imetnik dovoljenja za promet:** Pfizer Europe MA EEIG, Boulevard de la Plaine 17, 1050 Bruxelles, Belgija. **Datum zadnje revizije besedila:** 23.10.2018.

Pred predpisovanjem se seznanite s celotnim povzetkom glavnih značilnosti zdravila.

Vir: 1. Povzetek glavnih značilnosti zdravila Xalkori, 23.10.18

XALKORI® ▼
KRIZOTINIB

XAR-03-18 Samo za strokovno javnost

Pfizer Luxembourg SARL, GRAND DUCHY OF LUXEMBOURG, 51, Avenue J.F. Kennedy, L-1855,
Pfizer podružnica Ljubljana, Letališka cesta 29a, 1000 Ljubljana

Radiology and Oncology | Ljubljana | Slovenia | https://content.sciendo.com/raon

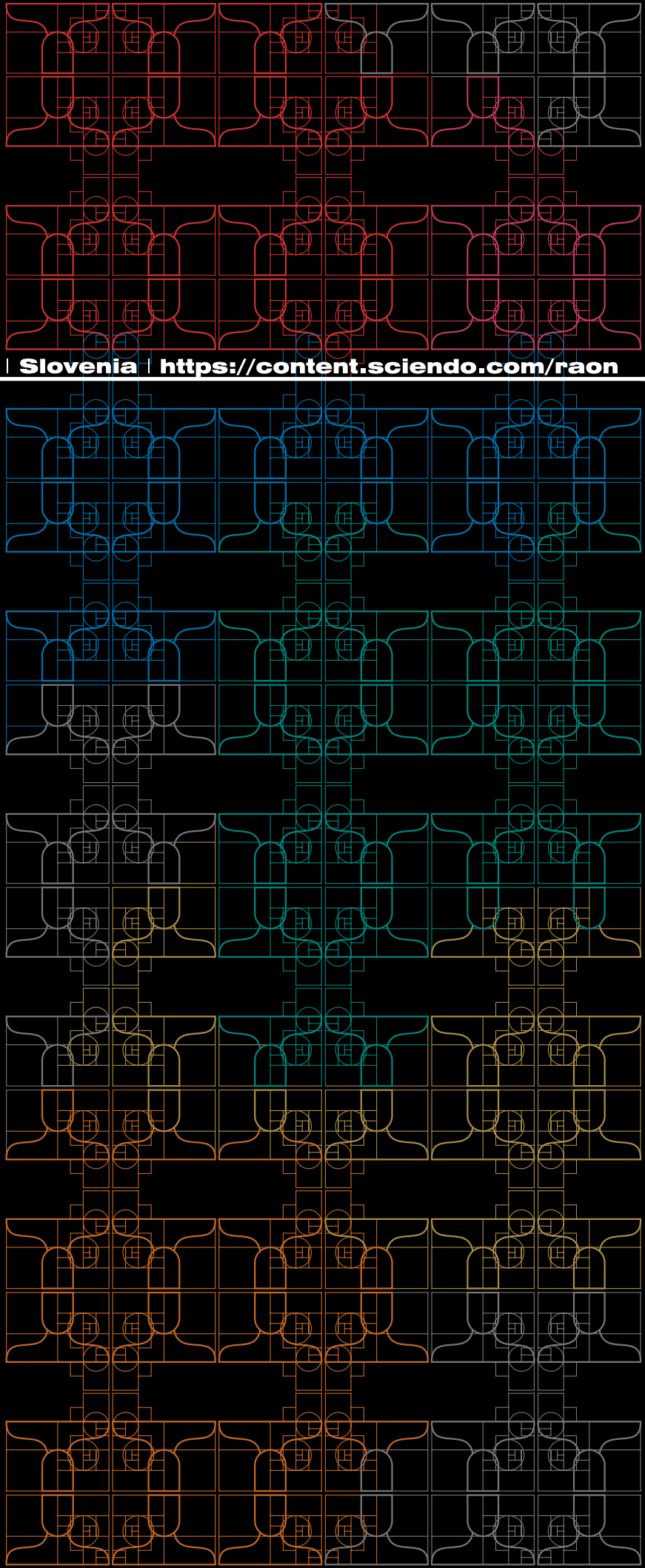

ISSN 1318 - 2099